P_4 Activation by Late-Transition Metal Complexes[†,‡]

Maria Caporali, Luca Gonsalvi, Andrea Rossin, and Maurizio Peruzzini*

Istituto di Chimica dei Composti Organometallici, Consiglio Nazionale delle Ricerche (ICCOM-CNR), Via Madonna del Piano 10, 50019 Sesto Fiorentino (Firenze), Italy

Received October 23, 2009

Contents

1. Introduction

The coordination chemistry of white phosphorus is nowadays a mature discipline, which during the last four decades has reached a deep understanding of the mechanisms governing the metal-mediated activation of this unique and highly reactive molecule. The birth certificate of this story dates back to 1970 when the synthesis of $[RhCl(PPh_3)_2(\eta^2\text{-}P_4)]$ together with other rhodium and iridium species was reported by Ginsberg and Lindsell as a short communication in *Transactions of the New York Academy of Sciences*.[1,2] Immediately, this seminal discovery motivated intense research activity worldwide. Worth mentioning among the pioneers in this area are the groups led by Markó in Veszprem, Hungary; Dahl in Madison, Wisconsin, U.S.A.; and Sacconi in Florence, Italy. While the first two demonstrated that fragments deriving from P_4 degradation could be stabilized as ligands in the coordination sphere of cobalt carbonyl[3] and cyclopentadienyl derivatives,[4] Sacconi first succeeded in coordinating the intact tetrahedral P_4 molecule to a metal,[5] obtaining the Ni(0) complex $[(\kappa^3\text{-}P,P,P\text{-}NP_3)Ni(\eta^1\text{-}P_4)]$, and in fully characterizing a vast family of *cyclo*-P_3 late transition metal derivatives spanning from iron to osmium.[6]

In the following decade, the development of the isolobal concept[7] and its application to organometallic and main group chemistry paved the way to the synthesis of an incredible variety of polyphosphorus architectures where CH, CH_2, and CH_3 fragments in acyclic and cyclic hydrocarbons could be formally replaced by naked P atoms and substituted PH and PH_2 units, respectively. Spectacular examples of organometallic phosphorus topologies ruled by the isolobal relationship can be found in the systematic work done in Kaiserslautern by Scherer and his co-workers who applied the isolobal P ↔ C−H relation to the synthesis of a myriad of polycyclic phosphorus species mimicking benzene and other arenes. Landmarks in this area were the discovery of the *cyclo*-P_6 ligand stabilized as internal layer in the triple-decker dimolybdenum complex $[\{Cp^*Mo\}_2(\mu,\eta^{6:6}\text{-}P_6)]$[8] and the pentaphosphaferrocene derivative $[\{Cp^*Fe\}(\eta^5\text{-}P_5)]$.[9] These species, within the loose boundaries of the isolobal concept, may be considered as the all-phosphorus analogues of benzene and cyclopentadienyl anion, respectively. The intriguing analogy between hydrocarbon species and organophosphorus compounds has been reviewed in the successful book "*Phosphorus: The Carbon Copy*" published by Wiley in 1998.[10] In the last two decades, several reviews have also appeared covering different aspects of transition metal-mediated white phosphorus activation. These include specific surveys addressing the formation of P−H[11] and P−C species[12] as well as some general reviews targeting the synthesis and the characterization of transition metal complexes incorporating naked phosphorus atoms and units as ligands.[13−17]

The importance of studying the coordination chemistry of elemental phosphorus by late (and early) transition metal complexes also stems from the need to replace the current technology for the production of organophosphorus derivatives. This reaction, which is of great industrial relevance, is still based on the chlorination of white phosphorus followed by the reaction of PCl_3, PCl_5, or $POCl_3$ with the

[†] This contribution is dedicated to our colleague and friend Prof. Piero Stoppioni on occasion of his 65th birthday and in recognition of his outstanding achievements in the field of white phosphorus activation.
[‡] Note: In figures showing X-ray crystal structures, H atoms are generally omitted for clarity unless specified.
* To whom correspondence should be addressed. E-mail: mperuzzini@iccom.cnr.it.

10.1021/cr900349u
Published on Web 02/19/2010

Maria Caporali was born in Arezzo, Italy, in 1973. She got her degree in Chemistry in 1998 at the University of Florence, with a thesis on the synthesis and characterization of dendrimers. During the period 2000−2003, she developed her Ph.D. at the University of Florence working on rhodium-catalyzed hydroformylation. Soon after, she joined the group of Prof. P.W.N.M. van Leeuwen at the Technical University of Eindhoven (NL) as postdoctoral fellow, working on palladium-catalyzed carbon monoxide−ethene copolymerization. In 2006 she moved back to Italy, and since then she is working as postdoctoral associate at ICCOM-CNR in Florence. Her main research interests focus on the activation and functionalization of white phosphorus mediated by transition metal complexes and organic compounds.

Luca Gonsalvi was born in Parma, Italy, in 1968. In 1994 he obtained his Degree in Chemistry at the University of Parma (Italy) with a final project under the supervision of G. Predieri and A. Tiripicchio. From 1996 to 1999, he did his Ph.D. research at the University of Sheffield (U.K.) with A. Haynes and P. M. Maitlis. From 1999 to 2001, he was postdoctoral associate at Delft University of Technology (NL) in the group of R. A. Sheldon then joined ICCOM-CNR as staff researcher. He was awarded the Turner Prize for Chemistry of The University of Sheffield (2000) and the CNR Young Researchers Career Development Prize for 2005. His research interests include catalysis in water, transition metal hydrides, white phosphorus chemical activation, and hydrogen storage materials. He has authored more than 50 articles in peer-reviewed journals, filed 1 patent, and presented his work at more than 80 conferences and symposia.

Andrea Rossin was born in Biella, Northern Italy, in 1974. He got his degree with full marks in Inorganic Chemistry in 1999 at the University of Turin, with a thesis on the IR and Raman study of organometallics containing aromatic C_xH_y rings. In 2001−2004, he developed his Ph.D. work on experimental and computational studies of transition metal boryl ($M-BR_2$) and borylene ($M{=}BR$) complexes at Cardiff University (Wales, U.K.). In 2005, he took part in Marie Curie RTN network AQUACHEM as postdoctoral associate at the Universitat Autònoma de Barcelona (Barcelona, Spain), dealing with DFT studies of homogeneous catalysis in aqueous media. From 2006 he is a postdoctoral associate at ICCOM-CNR. His research interests focus on hydrogen storage, Metal Organic Frameworks (MOFs), and transition metal hydrides and their reactivity with ammonia−borane.

Maurizio Peruzzini was born in Florence, Italy, in 1955. After his "Laurea" cum laude (University of Florence 1979, supervisors L. Sacconi and P. Stoppioni), he moved to ICCOM-CNR in 1986, where he is currently Research Director. He was awarded the Nasini Gold Medal of the Inorganic Chemistry Division of Italian Chemical Society in 1993 in recognition of his contribution to the chemistry of nonclassical hydrides. He is currently Chair of the Division of Inorganic Chemistry of SCI. Together with R. Poli he edited the book "Recent Advances on Hydride Chemistry". He has been the coordinator of several international projects and is responsible for FIRENZE HYDROLAB (an integrated laboratory on hydrogen as energy carrier). His research interests are primarily in the field of organometallic chemistry and catalysis, white phosphorus activation, and hydrogen storage materials. He has authored over 280 papers and patents.

desired organic molecule, i.e., alcohols, amines, etc.[18] The use of the extremely toxic and corrosive chlorine gas, and the generation of large amounts of hydrochloric acid, makes the oxidative phosphorylation of white phosphorus quite distant from the paradigm of a sustainable and environmentally friendly process, which represents the target of any modern chemical manufacturing. A tantalizing alternative to this procedure might be developed within the coordination polyhedron of a metal catalyst capable in a first step of coordinating and activating white phosphorus before combining the activated MP_x species with the organic substrate to form the organophosphorus compound. A requisite to bring about the not yet accomplished *catalytic functionalization of white phosphorus* is the deep understanding of the processes that take place at the metal center when these kind of species are allowed to react with P_4. Although the targeted catalytic process is still far from being achieved, important steps have been moved to reach this goal, showing that both P−H and P−C bonds can be easily formed from early transition metal-mediated white phosphorus activation.[11−17] An important contribution in this field has been given during the past years by, among other authors, Cummins and co-workers, who focused on the use of Mo and Nb precursors to mediate the activation of white phosphorus toward the assembly of novel P−P bonds (see also section 5.3).[16d−f] Recent breakthroughs have been also reported by Bertrand and co-workers who used metal-free NHC and CAAC

reagents to form organophosphorus derivatives via direct stoichiometric P_4 activation.[19]

This review intends to provide a comprehensive view of the chemistry occurring when white phosphorus is reacted with late transition metal complexes. In contrast, the many intriguing results dealing with P_4 activation by either early transition metal systems or main-group elements are not covered.[20] The emphasis of this article is to review the papers dealing with transition metal polyphosphorus species, which were published between 1970 and the end of 2008. However, some addition of more recent literature published in year 2009 is occasionally present.

Apart from metals belonging to groups from 8 to 10, which represent the largest part of the compounds subject of this review, we have expanded the coverage to include also the very few known polyphosphorus complexes with manganese and rhenium (d^6 ions) as well as those dealing with coinage metals. The chemistry of copper and silver halides as Lewis acids with preformed metal complexes incorporating naked P_x units has been briefly explored, and interesting examples of activated polyphosphorus species have been reported. Such results, mainly due to the elegant work by Scheer and co-workers, have inspired the synthesis of 1D, 2D, and even 3D coordination polymers in which a variety of preformed L_nMP_x units may behave as suitable platforms to build extraordinary polyphosphorus assemblies.

The development of this last topic projected toward the synthesis of nanostructured phosphido materials together with the dream to functionalize catalytically white phosphorus justify the momentum of research in this area and represent a genuine challenge for inorganic chemists active in both catalysis and material science.

2. Group 7 Metals

Complexes of group 7 transition metals containing white phosphorus or fragments deriving from its activation are extremely scarce and practically limited to a few rhenium derivatives. In fact, while no technetium species is known, manganese derivatives are also virtually neglected apart from a few $CpMn(CO)_2$ adducts coordinating to P-lone pair in polyphosphorus ligands. Likewise, if one excludes a few $Re(CO)_5$ adducts coordinated to naked phosphorus atoms in L_nP_x species, the few complexes of rhenium containing bare phosphorus assemblies are limited to Re(I) complexes where the metal atom exhibits the d^6 electronic configuration similar to Fe(II) and Ru(II) ions, which are involved in a large number of metal complexes coordinating polyphosphorus, P_x, species (see sections 3.1 and 3.2).

2.1. Manganese

Although not directly related to processes dealing with white phosphorus activation, the two manganese complexes containing a single naked phosphorus atom (phosphido) of formula $[Cp^*(CO)_2Mn{=}P{=}Mn(CO)_2Cp^*]Y$ species (Y = OTf, (**1**); PF_6, (**2**)] are worth mentioning here.[21] These organometallic cumulenes were prepared by Huttner et al. in 1988 via hydride abstraction from the starting material $[\{Cp^*(CO)_2Mn\}_2(\mu,\eta^{1:1}\text{-PH})]$ using strong electrophiles such as MeOTf or CPh_3PF_6 in DCM at RT (Scheme 1).

The presence of the unusual Mn=P=Mn bonding type is confirmed by both UV−vis (λ_{max} shift from 522 to 411 nm in passing from the starting material to the products) and

Scheme 1

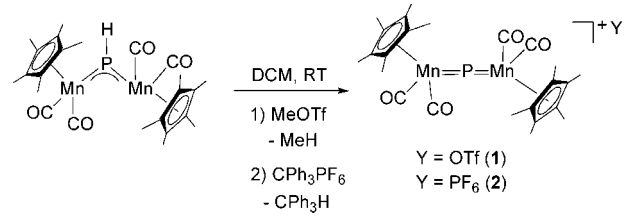

Scheme 2

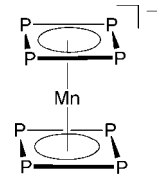

3

Scheme 3

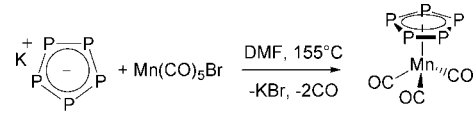

4

from the large ^{31}P NMR highfield shift on passing from phosphinidene ($\delta_P = 816$) to phosphacumulene ($\delta_P = 172$).

Theoretical studies on the equilibrium geometries, energies, and MOs composition and aromaticity/antiaromaticity of the sandwich-type structure $[Mn(\eta^4\text{-}P_4)_2]^-$ (**3**) (Scheme 2) have been carried out by DFT methods at the B3LYP//6-311G* level of theory. The analyzed Mn(III) d^4 structure adopts the sandwich-type D_{4h} eclipsed conformation as the lowest-energy conformer, and its P_4 rings exhibit both σ and π antiaromaticity.[22] The structure of **3** has been compared with several other 3d-transition metal anions $[M(\eta^4\text{-}P_4)_2]^{n-}$ (M = Ti, V, Cr, Fe, Co, Ni).

The mixed carbonyl-P_5 manganese complex $[(\eta^5\text{-}P_5)Mn(CO)_3]$ (**4**, Scheme 3) was prepared in 1991 by Baudler and co-workers, by heating the potassium salt of the pentaphosphacyclopentadienide ion, KP_5, with $Mn(CO)_5Br$ in DMF.[23] Proof of identity was given by the occurrence of a ^{31}P NMR singlet at 126.7 ppm, falling in the typical range of pentaphosphametallocenes, and by the observation of two ν(CO) bands in the IR spectrum that are related to the piano-stool C_{3v} symmetry. Some debate on the nature of **4** has risen through the scientific community, since several attempts of reproducing these results by different groups failed so far.

2.2. Rhenium

The first stable *tetrahedro*-tetraphosphorus complex ever reported was the rhenium derivative $[(triphos)Re(CO)_2(\eta^1\text{-}P_4)]OTf$ (**5**) obtained by the straightforward reaction of P_4 with the Re(I) species $[(triphos)Re(CO)_2(OTf)]$ in DCM at RT (Scheme 4).[24] Further addition of 1 equiv of the rhenium precursor to **5** in DCM produced the dinuclear compound $[\{(triphos)Re(CO)_2\}_2(\mu,\eta^{1:1}\text{-}P_4)\}](OTf)_2$ (**6**), the first example of a bridging tetrahedral P_4 ligand. Although crystals suitable for an X-ray diffraction analysis could not be grown, the presence of the intact P_4 tetrahedron and the ligand hapticity were confirmed by a detailed ^{31}P NMR analysis.

The reaction of $[Cp^*Re(CO)_2]_2$ with P_4 at low temperature (−18 °C) in toluene led to the Re_2P_2 butterfly complex

Scheme 4

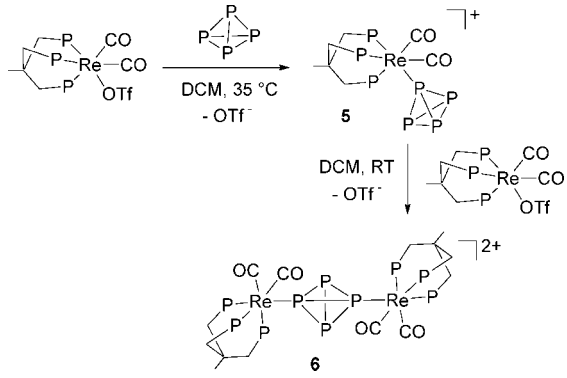

Scheme 5

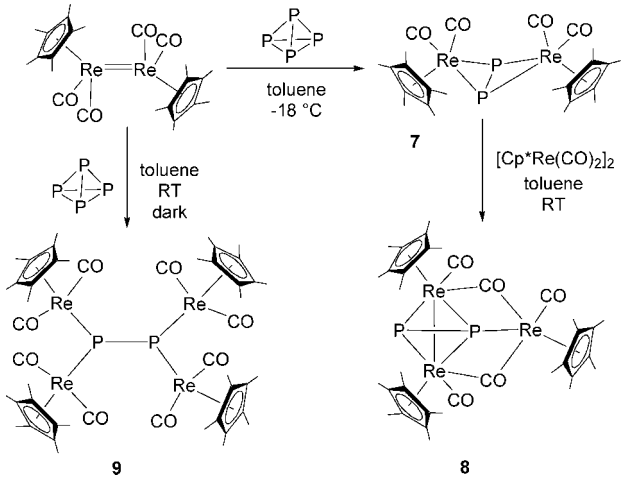

[{Cp*(CO)$_2$Re}$_2$(μ,$\eta^{2:2}$-P$_2$)] (**7**) (Scheme 5).[25] The yellow complex was characterized by single-crystal X-ray diffraction (Figure 1). The P≡P fragment (d_{P-P} = 2.032 Å) is coordinated side-on to both rhenium centers, mimicking the coordination mode of diphenylacetylene in [{Co$_2$(CO)$_6$}-(CPh≡CPh)]. It acts as a four-electron donor, bridging two metal centers, as expected given the isolobal analogy between the P_2 ligand and acetylene. Complex **7** easily adds further [Cp*Re(CO)$_2$]$_2$ at RT in toluene to give the trinuclear species [{Cp*(CO)Re}$_3$(μ-CO)$_2$(μ,$\eta^{2:2:1}$-P$_2$)] (**8**) which was characterized by NMR and MS only (Scheme 5).

If the P_4 addition is carried out at room temperature in the dark, the main species obtained (in ca. 40% yield) is the photolabile tetranuclear complex [{Cp*(CO)$_2$Re}$_4$(μ,$\eta^{1:1:1:1}$-P$_2$)] (**9**), with an end-on diphosphinidene ligand bonded to four rhenium atoms.[26] In **9**, the P_2 moiety can be formulated as an eight-electron donor, being a complex-stabilized form of the unusual mesomeric form **B** of the P_2 molecule (Scheme 6). Remarkably, on passing from **9** to **8**, the P−P separation decreases from 2.226 Å (typical of a single P−P bond) to 2.032 Å (suggesting a bond order close to 2).

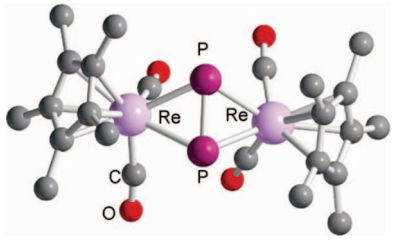

Figure 1. Molecular structure of [{Cp*(CO)$_2$Re}$_2$(μ,$\eta^{2:2}$-P$_2$)] (**7**), adapted from ref 25.

Scheme 6

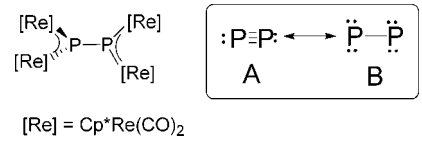

[Re] = Cp*Re(CO)$_2$

Scheme 7

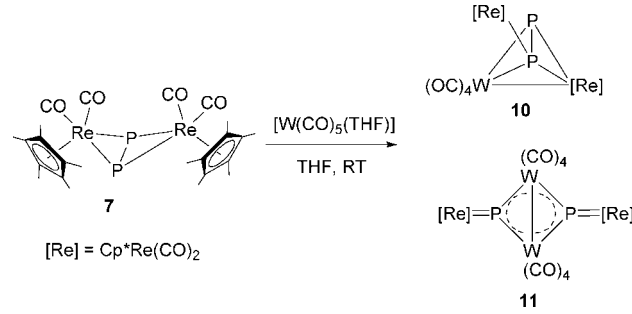

[Re] = Cp*Re(CO)$_2$

The reactivity of **7** with Lewis acids such as tungsten-containing fragments was also studied by Scherer and co-workers. Thus, treatment of **7** in THF with excess [W(CO)$_5$(THF)] led to a mixture of two interesting species that could be separated after chromatographic workup (Scheme 7).[26] The minor product (29%) corresponds to the heterobimetallic derivative **10**, representing the first structurally characterized example of a transformation of the M_2P_2 butterfly framework into a (chiral) M_2P_2 tetrahedrane geometry, as confirmed by single-crystal XRD studies and ^{31}P NMR spectroscopy with two doublets at δ_P = −87.7 and −188.7, showing tungsten satellites and $^1J_{(W,P)}$ = 35/22 Hz. The other product, [{Cp*Re(CO)$_2$}$_2$({W(CO)$_4$}$_2$)(μ_3,$\eta^{1:1:1}$-P)$_2$](W−W) (**11**), obtained in slightly higher yield (34%), originates from the formal split of the diphosphido ligand in **7** into two unconnected P-atoms, exhibiting a large downfield shifted ^{31}P NMR resonance δ = 885, which are held together by a bridging W$_2$(CO)$_8$ fragment. The nice crystal structure of this intriguing tetrametallic $Re_2W_2P_2$ planar complex is shown in Figure 2. Remarkable metrical data include the very short P−Re distance ($d_{P=Re}$ = 2.245 Å) and the presence of a single bond between the two tungsten atoms (d_{W-W} = 3.0523 Å).

Reaction of **9** with 0.1 M HCl aqueous solution in toluene at RT gives, after prolonged standing, the μ-P(OH) hydroxyphosphinidene species **12**, which was characterized as a bridging ligand between two Cp*Re(CO)$_2$ fragments by XRD, IR, and NMR analyses (Scheme 8).[27]

Although not involving directly white phosphorus activation, it is worth mentioning that the one-pot reaction of [Cp*Re(CO)$_2$]$_2$ with Bu^{t}C≡P in THF at RT, followed by in

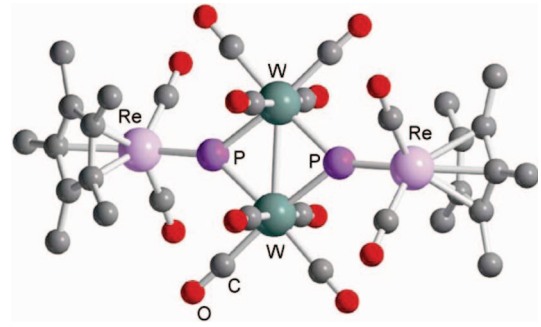

Figure 2. Molecular structure of [{Cp*Re(CO)$_2$}$_2$({W(CO)$_4$}$_2$)-(μ_3,$\eta^{1:1:1}$-P)$_2$](W−W) (**11**), adapted from ref 26.

Scheme 8

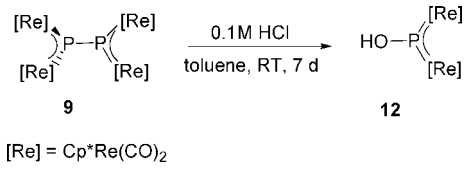

Scheme 9

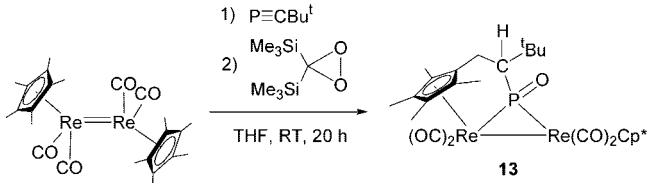

situ oxidation using the siloxirane $(Me_3Si)_2O_2$, affords the dinuclear rhenium complex **13**. The XRD analysis disclosed in **13** the presence of a chiral phosphinidene oxide ligand bridging between the two unequivalent rhenium atoms (Scheme 9).[28]

3. Group 8 Metals

3.1. Iron

The chemistry of iron with white phosphorus and ligands derived thereof is largely dominated by the derivatives of the pentaphosphaferrocene species [Cp*Fe(η^5-P_5)] (**14**) prepared by Scherer and co-workers in 1987.[9] Starting from this beautiful example of the validity of the isolobal relationship between P atoms and CH methyne fragments, a rich and spectacular chemistry has been developed with remarkable perspectives and potentialities toward 1D- and 2D-coordination polymers as well as to supramolecular chemistry and material science (section 3.1.3). Much less represented are the compounds containing the tetraphosphorus ligand, either intact or differently activated, as well as species featuring more than four phosphorus atoms, although some intriguing examples of unusual polyphosphorus topologies have been reported.

3.1.1. Iron Complexes Containing P_4 and P_n Ligands Resulting from the Degradation of the P_4 Tetrahedron (n < 4)

The first example of white phosphorus activation in the presence of an iron complex was described by Schmid and Kempny[29] in 1977, who reported on the reaction of P_4 with [$Fe_2(CO)_9$] (Scheme 10). The reaction, carried out in benzene at room temperature, afforded the monomeric diamagnetic complex {[$Fe(CO)_4]_3(P_4)$} (**15**), where a single tetraphosphorus ligand is proposed bridging three iron centers. According to Mössbauer spectroscopy, complex **15** contains either penta- and hexacoordinated Fe atoms in 1:2 ratio, while the four phosphorus atoms are equivalent in the ^{31}P NMR spectrum, suggesting a dynamic behavior with the $Fe(CO)_4$ groups freely switching between bridging and terminal position onto the tetraphosphorus unit. The reaction temperature played an important role in determining the final product. Thus, heating the mixture of [$Fe_2(CO)_9$] and white phosphorus in benzene to 70 °C yielded a polymeric compound containing diphosphorus units $[(CO)_3FeP_2]_n$ (**16**). The preparation of **16** could also be accomplished in two other different ways, as shown in Scheme 10, i.e., by either

Scheme 10

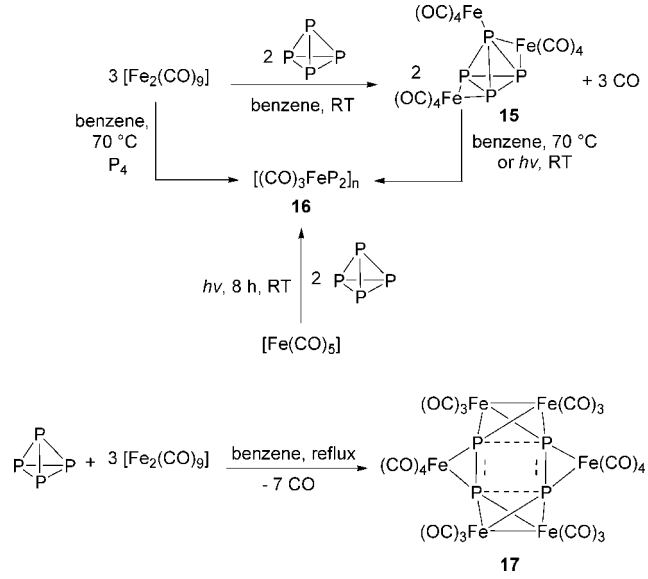

warming or UV irradiating **15** in benzene or by reaction of [$Fe(CO)_5$] with P_4 in the same solvent. The Mössbauer spectrum of **16** shows equivalent Fe atoms in an octahedral environment. However, since no X-ray data is available for **15** and **16**, there are still many doubts about the accuracy of structural attribution for such compounds. A few years later, the reaction of P_4 with [$Fe_2(CO)_9$] in benzene was reinvestigated by Scheer et al. at a slightly higher temperature (80 °C). Under these conditions, **16** was not obtained, but the novel iron cluster, [{$Fe(CO)_4(\mu_5$-$\eta^{2:1:1:1:1}$-$P_2)$}$_2${μ-$Fe_2(CO)_6$}$_2$] (**17**), was isolated in a very low yield,[30] deriving from formal cleavage of four P−P bonds followed by formation of two separated diphosphorus units. The crystal structure of **17** was determined by X-ray diffraction analysis, showing a very elongated rectangular tetraphosphorus unit that bridges the [$Fe(CO)_4$] groups on its shorter sides [$d_{(P-P)ave}$ = 2.137 Å] while two di-iron [$Fe_2(CO)_6$] groups are sitting on the longer sides [$d_{(P-P)ave}$ = 2.603 Å] of the rectangle as shown in Figure 3.

Coordination of intact elemental phosphorus to iron has been reported by Peruzzini et al.,[31] who described a family of exceptionally thermally and air stable Fe(II) and Ru(II) complexes [Cp*M(L_2)(η^1-P_4)]Cl, [M = Fe, L_2 = 1/2 Ph_2-$PCH_2CH_2PPh_2$ (**18**); M = Ru, L = PEt_3 (**19**), L_2 = 1/2 $Ph_2PCH_2CH_2PPh_2$ (**20**)] (Scheme 11). The iron complex was prepared by the straightforward reaction of white phosphorus with a suitable iron precursor such as [Cp*Fe(L_2)Cl] in THF or DCM at RT following the easy

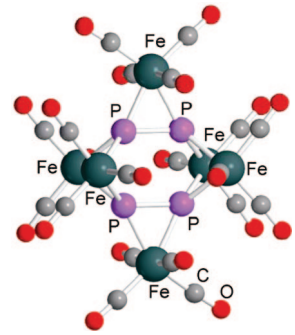

Figure 3. X-ray crystal structure of [{$Fe(CO)_4(\mu_5$-$\eta^{2:1:1:1:1}$-$P_2)$}$_2${μ-$Fe_2(CO)_6$}$_2$] (**17**); adapted from ref 30.

Scheme 11

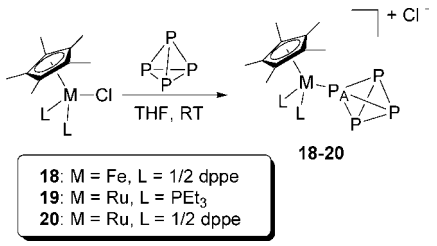

displacement of the chloride ligand without the need for any chloride scavenger. Addition of salts containing less coordinating anions ($NaBPh_4$, NH_4PF_6, etc.) in THF/MeOH mixture afforded the corresponding salt.

Complexes **18**−**20**, which contain the intact P_4 molecule coordinated as a *tetrahedro*-η^1-P_4 ligand, were characterized by spectroscopic and X-ray crystallographic measurements. The $^{31}P\{^1H\}$ NMR spectrum was particularly informative, showing the expected AM_3 pattern for the coordinated P_4 ligand with the metalated P_A atom resonating at a significantly lower field with respect to elemental phosphorus ($\delta P_{A(\mathbf{18})} = -299.54$), with a downfield coordination chemical shift as great as 227 ppm.

The solid-state structure of **18**, crystallized as tetraphenylborate salt, was determined by X-ray diffraction methods at low temperature. The coordination cation (Figure 4) contains the tetraphosphorus ligand end-on coordinated to the iron atom and slightly deformed upon coordination with respect to the free tetrahedron.[31,32]

The rich and interesting chemistry of this class of compounds has been developed more on the related ruthenium derivatives than on **18** and, therefore, will be discussed in section 3.2, dedicated to ruthenium complexes.

Much less controllable is the reaction of white phosphorus with iron organometallic fragments when it is carried out under forcible reaction conditions, i.e., at high temperature in high boiling point solvents or under photolytic (UV) irradiation. Either thermally or photochemically activated, these reactions give rise to many products that, being without any thermodynamic control, frequently encompass multiple reaction mechanisms. These result in different P_x-containing species depending on the level of degradation of the phosphorus tetrahedron as well as on the bonding properties of the resulting P_x fragments. Additional complications may arise from the direct involvement of the ancillary ligands in assembling the final reaction products (P−C, P−H, and P−heteroatom bond formation).

The photochemical activation of white phosphorus was studied by Scherer et al. who investigated in detail the reaction of the iron cyclopentadienyl dicarbonyl dimeric complex, $[Cp''Fe(CO)_2]_2$, with cyclopentadienyl ligands bearing sterically demanding substituents such as *tert*-butyl groups, (Cp″ = 1,3-di-*tert*-butylcyclopentadienyl).[33] The photolytic reaction affords different products that are related to each other by progressive P−P bond breaking and/or CO loss depending on the reaction conditions (solvent, irradiation time, and temperature). Although the reaction cannot be selectively directed toward the formation of a specific derivative, all the possible iron complexes with general formula $[Cp''_2Fe_2P_4(CO)_{4-n}]$ are generated in a reaction sequence entailing progressive CO loss and sequential harmonized evolution of the tetraphosphorus topology. Scheme 12 illustrates the reaction cascade progressively stripping the iron complex from its carbonyl ligands. Thus, at the first stage, the reaction affords the P_4^{2-} butterfly-type complex $[\{Cp''Fe(CO)_2\}_2(\mu,\eta^{1:1}\text{-}P_4)]$ (**21**) via single P−P bond cleavage of the white phosphorus tetrahedron without CO loss ($n = 0$). Initial decarbonylation affords $[\{Cp''Fe(CO)_2\}_2\{Cp''Fe(CO)\}(\mu,\eta^{1:2}\text{-}P_4)]$ (**22**, $n = 1$), where one iron fragment has inserted into a P−P bond while the butterfly geometry for P_4 is essentially unchanged. Subsequent photochemical elimination of CO produces complex $[\{Cp''Fe\}\{Cp''Fe(CO)_2\}(\mu,\eta^{4:1}\text{-}P_4)]$ (**23**) where the P_4 moiety is a flat cyclic ligand ($n = 2$). Decarbonylation of the second iron fragment promotes its insertion into a P−P bond of the P_4 square, giving rise to an almost planar five-membered tetraphosphaferrole ring, which is the most intriguing structural motif of $[\{Cp''Fe\}\{\eta^5\text{-}P_4Fe(CO)Cp''\}]$ (**24**, $n = 3$). Finally, loss of the last CO ligand causes an internal rearrangement of the FeP_4 cycle, which eventually affords the totally decarbonylated complex $[\{Cp''Fe\}_2(\mu,\eta^{4:4}\text{-}P_4)]$ (**25**), in which an opened tetraphosphabutadiene-like P_4-chain bridges two equivalent {Cp″Fe} moieties. All of the complexes were separated in low to moderate yields by column chromatography and characterized by ^{31}P NMR spectroscopy. Complexes **23** and **25** were also authenticated by X-ray diffraction analysis, which confirmed the preservation of the P-topology in both cases and in agreement with the solution structure postulated on the basis of NMR data.

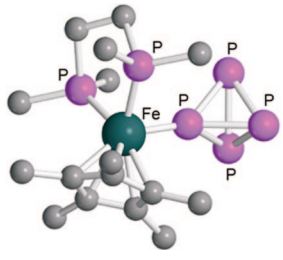

Figure 4. X-ray crystal structure of $[Cp^*Fe(dppe)(\eta^1\text{-}P_4)]^+$, (**18**); only *ipso*-carbons of phenyl rings shown; adapted from ref 31.

There are few examples of butterfly-type complexes other than **21**. In particular, the related $[\{Cp^*Fe(CO)_2\}_2(\mu,\eta^{1:1}\text{-}P_4)]$ (**26**) was briefly described, forming in low yield and moderate purity from either the diphosphenyl iron complexes[34,35] $[Cp^*Fe(CO)_2(P{=}PR)]$ (R = Cp*) and $[\{Cp^*Fe(CO)_2\}(P{=}P)]$ or by cothermolysis of white phosphorus and $[Cp''Fe(CO)_2]_2$.[36]

A much more complete study on this class of compounds was provided a few years later by Scherer and co-workers, who reported on the thermal activation of P_4 in the presence of the dinuclear iron complex $[\{Cp'''Fe(CO)_2\}]$, in which the presence of the more sterically demanding 1,2,4-$C_5H_2Bu^t_3$ coligand allows a better control of the reaction.[37] Thus, a short-time thermal reaction (toluene, 110 °C, 2 min) selectively afforded the complex $[\{Cp'''Fe(CO)_2\}_2(\mu,\eta^{1:1}\text{-}P_4)]$ (**27**) in high yield. Further thermolysis of **27** in decalin at 190 °C for 3 h started demolitive/reaggregation processes, which gave, after chromatographic workup, a 1:1 mixture of the pentaphosphaferrocene complex, $[Cp'''Fe(\eta^5\text{-}P_5)]$ (**28**) (see section 3.1.2) and the *cisoid* tetraphosphabutadiene complex $[\{Cp'''Fe\}_2(\mu,\eta^{4:4}\text{-}P_4)]$ (**29**) similar to **25**. Scheme 13 illustrates this chemistry, suggesting that the open-edged *exo*-*exo*-P_4 species may work as the starting platform for more complicated structural elaborations.

When the thermal reaction of **27** in boiling decalin is stopped after 45 min, the new diphosphadiferratetrahedrane $[\{Cp'''Fe\}_2(\mu\text{-}CO)(\mu,\eta^{2:2}\text{-}P_2)]$ (**30**) is obtained in 18% yield, together with **28** (12%) and **29** (44%) (Scheme 13).[38] The

Scheme 12

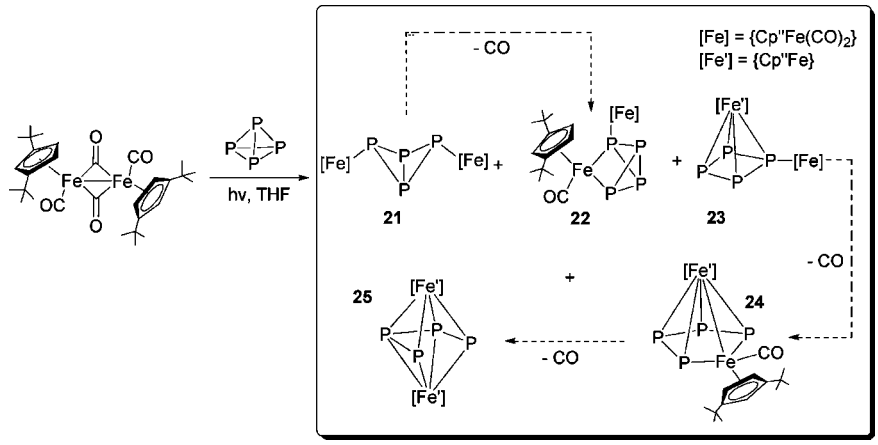

Scheme 13

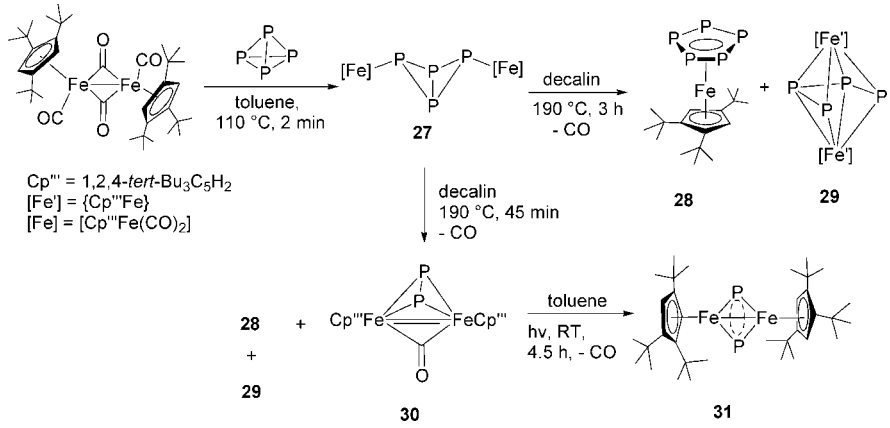

new cluster **30** contains a Fe−Fe double bond (d_{Fe-Fe} = 2.3944 Å), while a genuine P_2 unit (d_{P-P} = 2.064 Å) completes the tetrahedrane polyhedron (Figure 5). Under UV irradiation, the P_2 unit of **30** splits in two bent μ-P ligands with further elimination of CO to afford the very unusual compound [{Cp‴Fe}$_2$(μ,$\eta^{1:1}$-P)$_2$] (**31**). The unusual bonding situation in complex **31** is confirmed by the abnormal downfield shift of the ^{31}P NMR resonance of the phosphido ligands (δ_P = 1406.9). The crystal structure analysis (see Figure 6) confirmed the presence of a planar rhombic Fe_2P_2 arrangement of the complex core in **31**.

The thermal reaction of [{Cp^{R}Fe(CO)$_2$}$_2$(μ,$\eta^{1:1}$-P$_4$)] [**27**: Cp^R = 1,2,4-Bu$^t_3$C$_5$H$_2$ (Cp‴), **32**: Cp^R = C$_5$Pr$^i_5$ (Cp^{Pr5})] with diphenylacetylene at 110 °C in toluene for prolonged time afforded the 1,2,3-triphosphaferrocene complexes [Cp^{R}Fe(η^5-P$_3$C$_2$Ph$_2$)] [Cp^R = Cp‴ (**33**), Cp^{Pr5} (**34**)] in moderate yields (Scheme 14).[39] Complexes **33** and **34** contain the 1,2,3-triphospholyl ligand, which likely forms by coupling of a diphenylacetylene molecule with a P_3 unit originated from the butterfly molecule **27**. In the case of the isopropyl derivative **32**, the formation of the expected sandwich complex **34** is accompanied by a side-product in approximately 10% yield. X-ray crystallography showed that this additional species is the astonishing trinuclear iron cluster [{(Cp^{Pr5})$_3$Fe$_3$(CO)$_4$}P$_{11}$] (**35**) featuring a unique P_{11} ligand.[39] The crystal structure analysis (see Figure 7) shows that the P_{11} structural motif in **35** may be interpreted as deriving from the P_8P_2 substructure found in the Hittorf's violet phosphorus by insertion of single P atom into one P−P bond of the P_8-subunit.[40] Later on, the P_4Fe_2 butterfly was reacted with HC≡CPh to form 1,2,3-triphosphaferrocenes, a class of compounds that is described in detail in section 3.1.2.

The occurrence of fragments identical to those existing in Hittorf's monoclinic phosphorus allotrope, such as that found in **35**, was not unprecedented as the cage-like P_8-subunit of violet phosphorus was first recognized in the beautiful tetrametallic complex [Cp$^{Me}_4$Fe$_4$(CO)$_6$P$_8$] (**36**) prepared by Dahl and co-workers by cophotolysis of [Cp^{Me}Fe(CO)$_2$]$_2$ and P_4 in toluene at RT (Scheme 15).[41] Further reaction of **36** in THF with iron carbonyls capable of generating in situ the

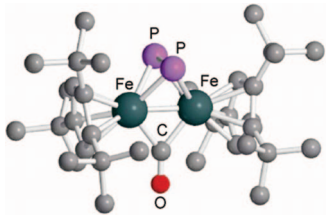

Figure 5. X-ray crystal structure of [{Cp‴Fe}$_2$(μ-CO)(μ,$\eta^{2:2}$-P$_2$)], (**30**); adapted from ref 38.

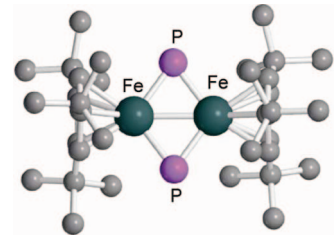

Figure 6. X-ray crystal structure of [{Cp‴Fe}$_2$(μ,$\eta^{1:1}$-P)$_2$], (**31**); adapted from ref 38.

Scheme 14

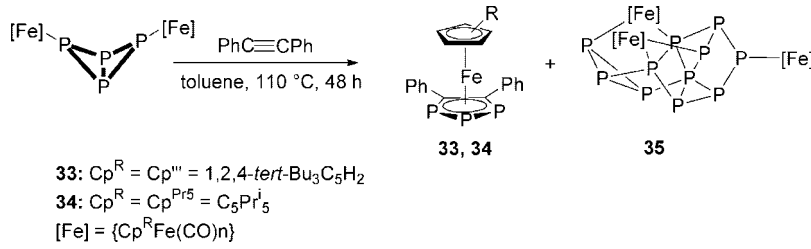

33: $Cp^R = Cp''' = 1,2,4\text{-}tert\text{-}Bu_3C_5H_2$
34: $Cp^R = Cp^{Pr5} = C_5Pr^i_5$
[Fe] = {$Cp^RFe(CO)n$}

carbene-like fragment $Fe(CO)_4$ afforded the higher nuclearity cluster $[Cp^{Me}{}_4Fe_6(CO)_{13}P_8]$ (**37**).

Compounds **36** and **37** were characterized in the solid state by X-ray diffraction analysis, which confirmed in both structures the presence of the novel octaphosphorus topology (P_8^{4-} cage anion). Apart from being one of the alternating structural motifs of Hittorf's allotrope,[42] the cuneane topology described by Dahl was previously known from the work of Baudler and co-workers, who briefly described the highly thermally unstable alkyl derivatives of formula P_8R_4 (R = Me, Et, Pr^i)[43] and mentioned the mass spectrometric detection of the tetrahydride P_8H_4.[44] A view of the crystal structure of **36** is presented in Figure 8.

The 1,2,3-trisphospholyl ligand found in complexes **33** and **34**[39] belongs to the rich family of polyphospholyl ligands, $[(CH)_{5-n}P_n]^-$ ($0 \le n \le 5$), which may be considered as formally deriving from the cyclopentadienyl ligand C_5H_5 by progressive replacement of each CH group with isolobal P atoms. The discovery of Scherer's pentaphosphaferrocene complex **14**,[9] which represented a real breakthrough in the coordination chemistry of naked phosphorus ligands, disclosed also the existence of the broad family of η^5-polyphospholyl complexes. All the members of this intriguing family of ligands have been synthesized and properly stabilized as six-electron donor ligands in ferrocenyl based moieties where the $[(CH)_{5-n}P_n]^-$ ring replaces one Cp ligand of ferrocene. Scheme 16 shows the sketches of these complexes.

The many synthetic procedures leading to species **A**−**E** and the chemistry of these complexes have been reviewed by Mathey and Nixon.[45] In particular, Mathey published in 1977 the seminal report on the synthesis of the **A**-type phospholylferrocene derivative $[CpFe(\eta^5\text{-}PC_4R_2H_2)]$ (**38**) (R = H or Me) by reaction of $[\{CpFe(CO)_2\}_2]$ with 1-phenylphospholes[10] as shown in Scheme 17, and later described the first examples of **B1**-type species $[CpFe(\eta^5\text{-}P_2C_3Et_2H)]$ (**39**) obtained by displacement of the arene ligand from the complex $[Fe(\eta^5\text{-}C_5H_5)(\eta^6\text{-}1,4\text{-}Me_2C_6H_4)][PF_6]$ in the presence of 1,2-diphospholide ion, prepared by reduction of the appropriate chloro precursor at ambient temperature,[46] as shown in Scheme 17.

More troublesome was the synthesis of the other polyphospholylferrocenes (types **B2**, **C2**, and **D**, Scheme 16) that required the use of phosphalkynes, P≡CR, as key reagents to assemble the appropriate di- and triphospholyl rings.[47] Particularly elusive were the tetraphosphaferrocene complexes (**D**). The route for these derivatives was eventually opened by Scheer et al.,[48] who elegantly designed a synthetic strategy encompassing the use of the phosphalkyne $Bu^tC{\equiv}P$, and the phosphorus reservoir provided by the bicyclotetraphosphine complex **27**. The reaction in boiling toluene for prolonged time (see Scheme 18) gave a mixture of products that were separated by chomatography. The main products were the novel complex **39**, containing the targeted 1,2,3,4-tetraphospholyl ligand, and complex **40** characterized by 1,2,4-triphosphospholyl ligand (the known class of 1,2,4-triphosphaferrocene derivatives).[47a] Additional products formed in very poor yield (ca. 2%) were the intriguing complex **41**, which represents the first coordination compound bearing a triphosphallyl P_3-bridged ligand, and the known pentaphosphaferrocene **14** (see section 3.1.2).

The molecular structure of the tetraphosphaferrocene derivative is presented in Figure 9, showing the almost

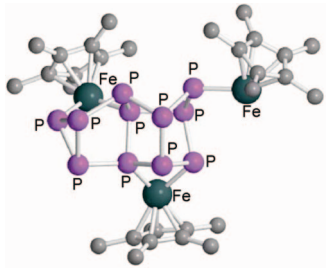

Figure 7. X-ray crystal structure of $[\{(Cp^{Pr5})_3Fe_3(CO)_4\}P_{11}]$ (**35**); carbonyl ligands omitted for clarity; only secondary carbons from Pr^i substituents shown; adapted from ref 39.

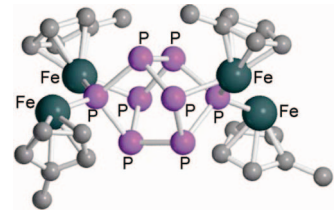

Figure 8. X-ray crystal structure of $[Cp^{Me}{}_4Fe_4(CO)_6P_8]$ (**36**); carbonyl ligands omitted for clarity; adapted from ref 41.

Scheme 15

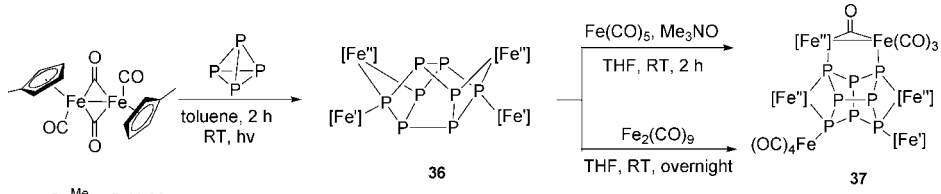

$Cp^{Me} = C_5H_4Me$
[Fe'] = {Cp'Fe(CO)$_2$}
[Fe"] = {Cp'Fe(CO)}

Scheme 16

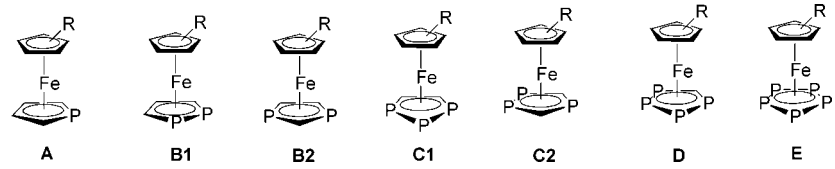

Scheme 17

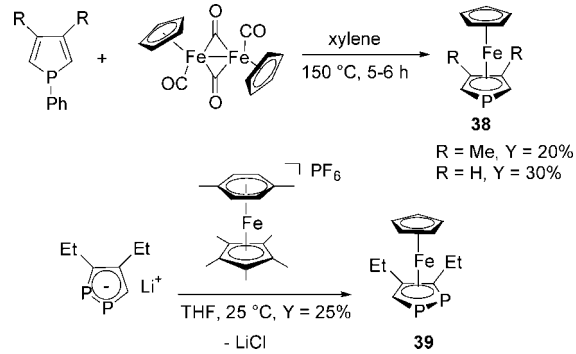

Scheme 18

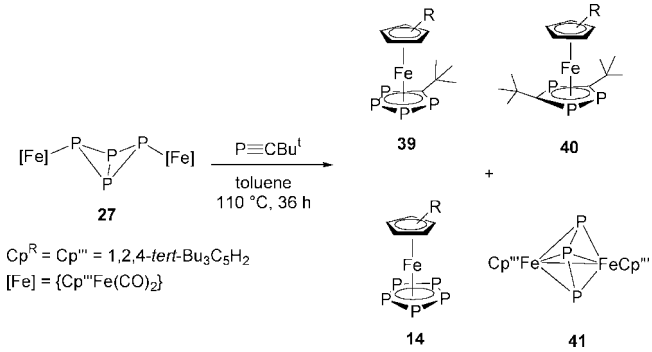

perfectly planar arrangement of the two five-membered rings. Remarkably, both P−C (1.763 Å) and P−P (2.115 Å) bonds in the tetraphospholyl ring are at intermediate values between single and double bonds, indicating some extent of aromaticity in the ring.

The molecular structure of **41** was determined by X-ray crystallography (Figure 10), showing a linear phosphallylic unit sitting on the Fe−Fe axis. The open P_3 ligand exhibits a P−P separation of 2.141 Å, which is in between genuine P−P single and double bonds. The bonding scheme in **41** was also investigated by DFT methods, and the topological analysis of the electronic charge density suggested that a staggered conformation of the *tert*-butyl groups is necessary to minimize steric repulsions.

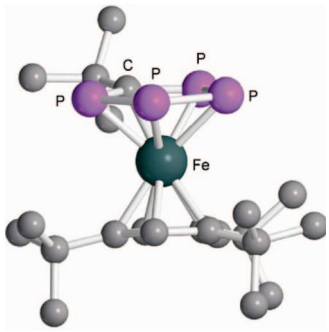

Figure 9. X-ray crystal structure of [Cp‴Fe(η^5-P_4CBu^t)] (**39**); adapted from ref 48.

cyclo-P_3 iron complexes are very rare and, to the best of our knowledge, limited to the Fenske's cluster [(Cp*Fe)$_3${(η^3-P_3)Fe}P_6] (**42**)[49] and to the Sacconi's heterometallic triple-decker [{(triphos)Co}(μ,$\eta^{3:3}$-*cyclo*-P_3){Fe(etriphos)}]$(PF_6)_2$ (**43**)[50] containing the tripodal triphosphine ligands MeC-$(CH_2PPh_2)_3$ (triphos) and MeC$(CH_2PEt_2)_3$ (etriphos). Complex **43** has a 30 VE structure and belongs to the well-known family of dinuclear triple-decker sandwich complexes containing the *cyclo*-P_3 or *cyclo*-As_3 units as the internal layer.[14a,51] Complex **43** forms dark blue crystals obtained by reacting the monodecker cobalt species [(triphos)Co(η^3-*cyclo*-P_3)] (**44**) (see section 4.1) with $[Fe(H_2O)_6](BF_4)_2$ in the presence of excess NBu_4PF_6 (Scheme 19).

X-ray diffraction analysis confirmed the expected double confacial octahedral geometry of the dication, proper of the rich family of Sacconi's triple-decker species without any significant deviation ascribable to the presence of two different tripodal triphosphines (triphos on cobalt and etriphos on iron) as external layers of the complex (Figure 30 in section 4.1).

By cophotolysis of white phosphorus with [{Cp*Fe-$(CO)_2$}$_2$], Dahl[52] obtained the bimetallic diphosphido complex [{Cp*Fe(μ,$\eta^{2:2}$-P_2)}$_2$] (**45**) bearing two μ,$\eta^{2:2}$-P_2 units each acting as formal 4-electron donors toward the two 13-electron {Cp*Fe} fragments (Scheme 20). The presence of an Fe−Fe single bond was proven by X-ray structure analysis showing a d_{Fe-Fe} = 2.59 Å. The germane species [{Cp*Co-(μ,$\eta^{2:2}$-P_2)}$_2$] (**46**) was also described by Dahl at the same time and will be discussed later (see section 4.1).

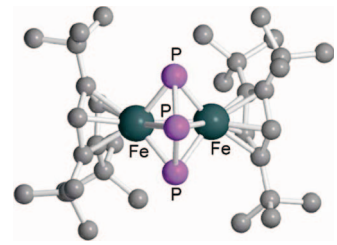

Figure 10. X-ray crystal structure of [{Cp‴Fe}$_2$(μ,$\eta^{2:2}$-P_3)] (**41**); adapted from ref 48.

Scheme 19

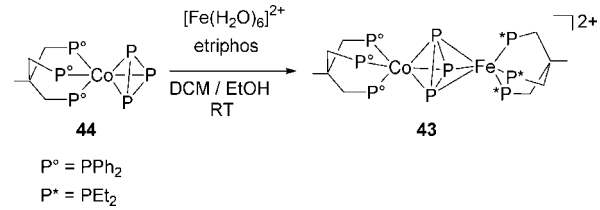

Scheme 20

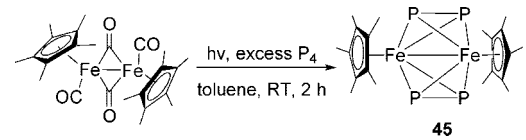

Scheme 21

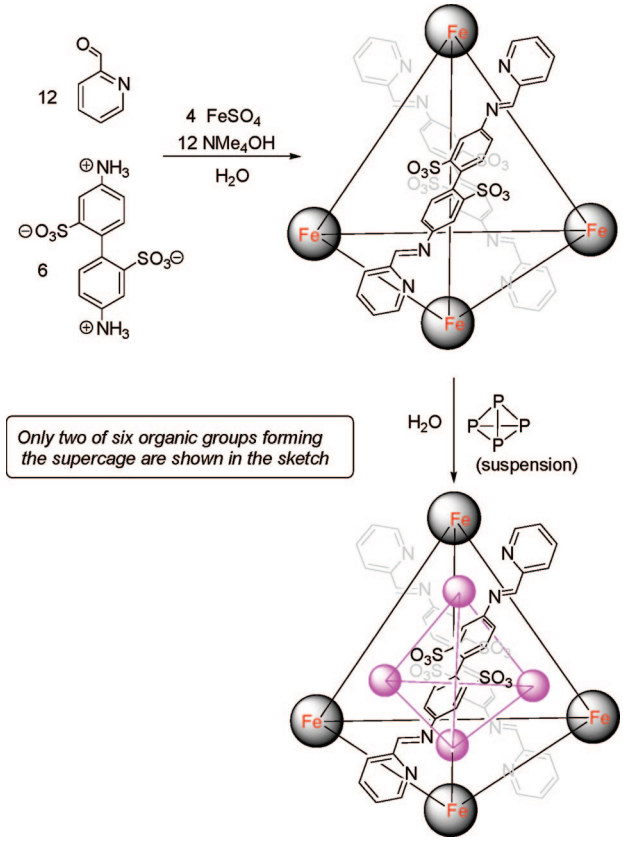

Before closing this section, we think it appropriate to mention briefly a recent report by Nitschke and co-workers describing the encapsulation of white phosphorus into a self-assembled iron cage behaving as supermolecular container of the tetrahedral P_4 molecule.[53] Thus, the aqueous-phase reaction of 1-pyridinaldehyde with the zwitterionic 4,4′-diaminobiphenyl-2,2′-disulfonic acid in the presence of iron sulfate and a base, easily and spontaneously assembles a tetrahedral tetrairon supercage, which is highly soluble in water and able to incorporate in its internal cavity a variety of hydrophobic guest molecules,[54] including white phosphorus.[53] Once encapsulated in the cage, P_4 becomes hydrosoluble and indefinitely stable to air oxidation. The inclusion compound of tetraphosphorus is likely stabilized by van der Waals interactions with the hydrophobic phenylene rings upholstering the inside cavity of the supercage with no direct bonding interaction with the iron centers. Scheme 21 provides a sketch of this intriguing host−guest chemistry.

3.1.2. Synthesis, Coordination Chemistry, and Reactivity of Pentaphosphaferrocene

The discovery of pentaphosphaferrocene [Cp*Fe(η^5-P_5)] (**14**), the cognate compound of ferrocene where a Cp* ligand has been replaced by a *cyclo*-P_5 unit, may be considered a landmark in the chemistry of naked P-atoms and units.[9] Its fascinating chemistry has largely attracted the interest of academic research in the past two decades, and already in the late 1980s, many publications appeared dealing with the synthesis of this new ligand, its coordination ability toward transition metals such as Fe, Ni, Rh, Mn, Cr, or Mo, and the study of its redox properties and reactivity.[14]

The preparation of the pentaphosphacyclopentadienide ion, P_5^- (**47**), as sodium, NaP_5, or lithium salt, LiP_5, was reported

Scheme 22

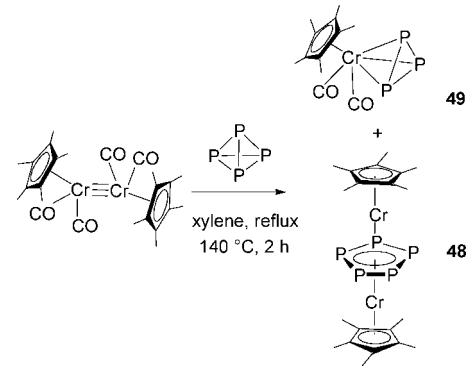

by Baudler et al.[55−57] upon cleavage of white phosphorus with sodium in diglyme or with lithium dihydrogen phosphide in THF at low temperature, respectively. The yield was increased by running the reaction between sodium and P_4 in the presence of crown ethers.[57] The alkaline salts of P_5^- could not be isolated in the solid state as their solutions were very sensitive to oxidation and underwent a rearrangement with formation of heavier polyphosphides while attempting concentration of the solutions. Therefore, the complete characterization of the *cyclo*-P_5 anion was carried out in solution and not in the solid state. In particular, IR and UV studies pointed out that **47** exhibits a planar pentatomic ring, characterized by a 6π-electron system resembling the cyclopentadienide ion, confirming the aromatic character of the P_5^- anion. In keeping with a structure where all phosphorus bonds are equal, solutions of *cyclo*-P_5 in THF-d_8 show a narrow singlet in the ^{31}P NMR spectrum (δ = 467.2). Recently, a new method for preparing the pentaphospholide ion has been reported in the patented literature using metallic sodium and white phosphorus under the conditions of phase-transfer catalysis.[58]

The chemistry of *cyclo*-P_5 shares many properties with that of the well-known $C_5H_5^-$ anion, with the most outstanding similarity being the largely developed coordination chemistry of **47**, which recalls that of Cp anion. Thus, a large number of triple-decker and sandwich complexes have been synthesized in which the *cyclo*-P_5 is η^5-bonded to one or two metal atoms as for the corresponding metallocene derivatives. The first triple-decker complex, [{Cp*Cr}$_2$-(μ,$\eta^{5:5}$-P_5)] (**48**), containing the *cyclo*-P_5 unit bridging two chromium centers via double penta-hapto coordination (Scheme 22), was published in 1986 by Scherer et al.[59] This unexpected and remarkable new complex was isolated, together with [Cp*Cr(CO)$_2$(η^3-P_3)] (**49**), as reddish-black crystals after chromatographic workup from the straightforward reaction of the precursor [{Cp*Cr(CO)$_2$}$_2$](Cr≡Cr) with P_4 in boiling xylene for 2 h.

The crystal structure of **48** (see Figure 11) shows the presence of three planar, parallel five-membered rings confirming the triple-decker structure proposed on the basis of electron spin resonance spectroscopy (ESR) data and MO calculations.

The synthesis of **48** confirmed that *cyclo*-P_5 can be stabilized as bridging ligand in mixed-valence triple-decker complexes and paved the way to the development of ferrocene analogues containing this intriguing ligand. Cp-like coordination of *cyclo*-P_5 to the iron(II) ion was first discovered by Scherer and Brück,[9,60] who obtained the 1,2,3,4,5-pentaphosphaferrocene, [Cp*Fe(η^5-P_5)] (**14**), in poor yield (11%), as green, air stable crystals by prolonged

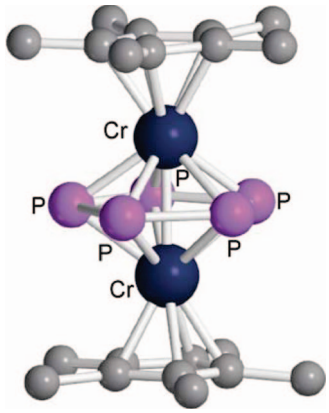

Figure 11. X-ray crystal structure of [{Cp*Cr}$_2$(μ,$\eta^{5:5}$-P$_5$)] (**48**); adapted from ref 59.

Scheme 23

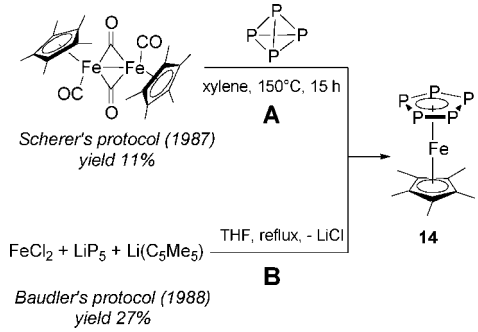

cothermolysis of white phosphorus with [Cp*Fe(CO)$_2$]$_2$ in xylene (Scheme 23, path A).[61]

Scherer's protocol illustrated in Scheme 23 is versatile enough to allow for the preparation of a variety of pentaphosphaferrocenes [Cp^{R}Fe(η^5-P$_5$)] with different Cp^R rings depending on the availability of the dinuclear carbonyl precursor [Cp^{R}Fe(CO)$_2$]$_2$. Thus, repeating the reaction with [Cp^{Et}Fe(CO)$_2$]$_2$ gave the related complex [Cp^{Et}Fe(η^5-P$_5$)] (**50**),[60] while the cothermolysis of [Cp^{R}Fe(CO)$_2$]$_2$ [Cp^R = η^5-C$_5$(CH$_2$Ph)$_5$, (Cp^{bz}); η^5-C$_5$Me$_4$(C$_2$H$_4$SMe), (Cp^S)] with elemental phosphorus gave [Cp^{R}Fe(η^5-P$_5$)] [Cp^R = Cp^S (**51**), Cp^{bz} (**52**)] containing highly functionalized and sterically bulky cyclopentadienyl ligands.[62]

In agreement with the existence of aromaticity in the *cyclo*-P$_5$ anion, the five phosphorus atoms of **14** and **50** are identical in C$_6$D$_6$ solution by ^{31}P NMR [δ_P = 153.0 (**14**); 152.8 (**50**)]. Complex **14** could not be authenticated by X-ray methods; however, because of the high thermal stability (to at least 270 °C), the relatively high volatility,[63] and the high symmetry, it could be studied by gas electron diffraction technique.[64] The resultant molecular structure in the gas phase confirmed that the molecule has a ferrocene-like structure with a C$_{5v}$ symmetry. Both the P$_5$ and Cp* rings are η^5-bonded to the iron ion and in a staggered conformation. The structure of **50** was also studied by X-ray diffraction analysis (Figure 12), confirming the planar arrangement of the cyclo-P$_5$ ring and its staggered disposition with respect to the pentamethylcyclopentadienyl ring.[60]

Soon after the seminal Scherer's report in *Angewandte Chemie*,[9] a slightly better yielding synthesis of **14** was obtained by Baudler et al.[57] through a one-pot procedure starting from LiP$_5$, LiCp*, and anhydrous FeCl$_2$ in refluxing THF (Scheme 23, path B). The synthesis of the naked pentaphospholide anion P$_5^-$, stable in solution under nitrogen

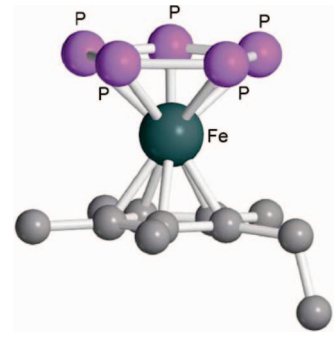

Figure 12. X-ray crystal structure of [Cp^{Et}Fe(η^5-P$_5$)] (**50**); adapted from ref 60.

Scheme 24

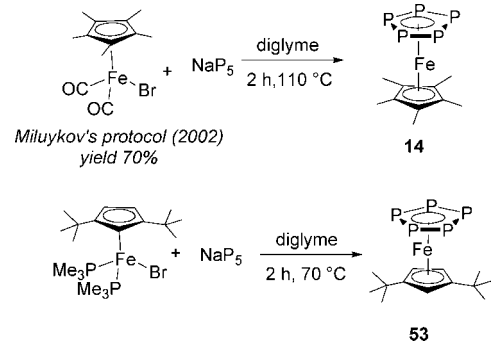

for days, and its successful application to prepare Scherer's pentaphosphaferrocene **14**, made scientists wonder about the possible preparation of [Fe(η^5-P$_5$)$_2$], the all-phosphorus analogue of ferrocene. A first claim about the formation of decaphosphaferrocene from the reaction of FeCl$_2$ and LiP$_5$ in THF could not be further substantiated.[57] Hence, molecular orbital calculations at the extended Hückel molecular orbital level (EHMO) were carried out, exploring different bonding and geometrical possibilities for this system, but in conclusion, high destabilization energy values suggested the isolation of the species [Fe(η^5-P$_5$)$_2$] was very difficult.[65] Moreover, DFT studies carried out by Frunzke et al. pointed out that the Fe-(η^5-P$_5$) bonding in the not yet isolated mixed-sandwich complex [CpFe(η^5-P$_5$)] is much stronger compared to the homoleptic compound [Fe(η^5-P$_5$)$_2$], albeit the latter is still an energy minimum on the potential energy surface.[66] Remarkably, and despite the fact that decaphosphaferrocene is still a dream molecule for synthetic chemists, the preparation of the stable decaphosphatitanocene dianion, [Ti(η^5-P$_5$)$_2$]$^{2-}$, starting from white phosphorus and TiCl$_4$, was recently reported by Ellis et al.[67]

Pure solutions of NaP$_5$, prepared by boiling P$_4$ and sodium in diglyme[58] in the presence of a catalytic amount of dibenzo-18-crown-6 as phase-transfer catalyst, have been used by Miluykov et al. to prepare **14** in excellent yield (Scheme 24).[68] The method involves the use of the half-sandwich iron compound [Cp*Fe(CO)$_2$Br] that, after warming for 2 h with NaP$_5$ in diglyme at 110 °C, gave **14** in 70% yield, much higher than what was obtained by the methods published previously. Using [Cp″Fe(PMe$_3$)$_2$Br], the pentaphosphaferrocene [Cp″Fe(η^5-P$_5$)] (**53**), was obtained in very good yield (ca. 80%).

When trimethylsilyl-substituted cyclopentadienyl iron precursors, namely, [{η^5-1,3-C$_5$H$_3$(SiMe$_3$)$_2$}Fe(PhPMe$_2$)$_2$Br] and [{η^5-1,2,4-C$_5$H$_2$(SiMe$_3$)$_3$}Fe(PhPMe$_2$)$_2$Br], were employed in this reaction, the formation of the pentaphosphaferrocene

Scheme 25

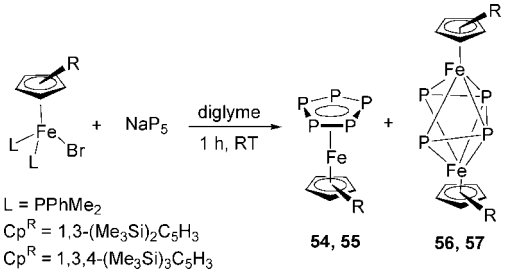

Scheme 26

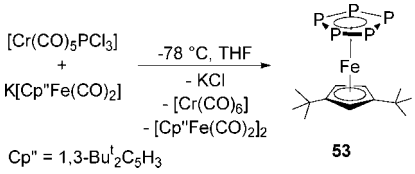

species is accompanied by a secondary product in a ratio dependent on the NaP_5/organoiron stoichiometry.[69] In particular, when NaP_5 is treated with an excess of the half-sandwich iron educt, the searched pentaphosphaferrocenes [$Cp^{Si_2}Fe(\eta^5\text{-}P_5)$] (**54**) [$Cp^{Si_2}$= 1,3-$C_5H_3(SiMe_3)_2$] and [$Cp^{Si_3}Fe(\eta^5\text{-}P_5)$] (**55**) [$Cp^{Si_3}$= 1,2,4-$C_5H_2(SiMe_3)_3$] were obtained in moderate yield (9−12%), and unexpectedly, the major products were the triple-decker complexes [$(Cp^{Si_2})_2Fe(\mu,\eta^{4:4}\text{-}P_4)$] (**56**) and [$(Cp^{Si_3})_2Fe(\mu,\eta^{4:4}\text{-}P_4)$] (**57**), containing as the middle deck a tetracoordinated tetraphosphorus fragment. The related tetraphosphabutadiene complex [{Cp‴-Fe}$_2(\mu,\eta^{4:4}\text{-}P_4)$] (**29**) was prepared by cothermolysis of P_4 and [Cp‴$Fe(CO)_2]_2$.[33]

The crystal structure of **56** shows that the P_4 skeleton has a trapezoidal shape, with two short ($d_{(P-P)ave}$ = 2.091 Å) and one long (d_{P-P} = 2.436 Å) P−P bond, suggesting the P_4 fragment acts as a $\mu,\eta^{4:4}$-tetraphosphabutadiene ligand, bridging the two iron centers as shown in Scheme 25.

Because of the high thermodynamic stability of **14** and related species, it is not surprising that ferrocene-like complexes with the *cyclo*-P_5 ligand could be obtained starting from phosphorus sources different from the P_5^- anion and the white phosphorus molecule. As an example, the pentaphosphaferrocene derivative [Cp″$Fe(\eta^5\text{-}P_5)$] (**53**), bearing two bulky *tert*-butyl substituents on the cyclopentadienyl ring, was prepared by Scheer and co-workers[70,71] by treating [$Cr(CO)_5(PCl_3)$] (a P_1-building block) with K[Cp″$Fe(CO)_2$] at low temperature (Scheme 26).

The electron-transfer properties of **14** have been carefully detailed by Geiger and Winter.[72] The redox properties are similar to those of ferrocene, giving monoelectronic oxidation/reduction steps. However, both the 17-electron cation [Cp*$Fe(\eta^5\text{-}P_5)]^+$ (**14**+) and the 19-electron anion [Cp*$Fe(\eta^5\text{-}P_5)]^-$ (**14**−) rapidly equilibrate to give dinuclear species that regenerate Fe(0) upon reverse electrolysis. Putative structures for the two coupling reaction products [{Cp*$Fe(\eta^5\text{-}P_5)\}_2]^{2+}$ (**14**++) and [{Cp*$Fe(\eta^5\text{-}P_5)\}_2]^{2-}$ (**14**− −) were proposed on the basis of ligand−ligand coupling (P−P or C−C bond formation) and are shown in Scheme 27.

The pentaphosphaferrocene **14** and its homologues, containing more elaborated Cp^R ligands, are endowed with additional reactivity and behave as adaptable synthetic platforms for bringing about a flourishing chemistry. In particular, interesting studies have been carried out focusing on pentaphosphaferrocene as complex ligand due to the

Scheme 27

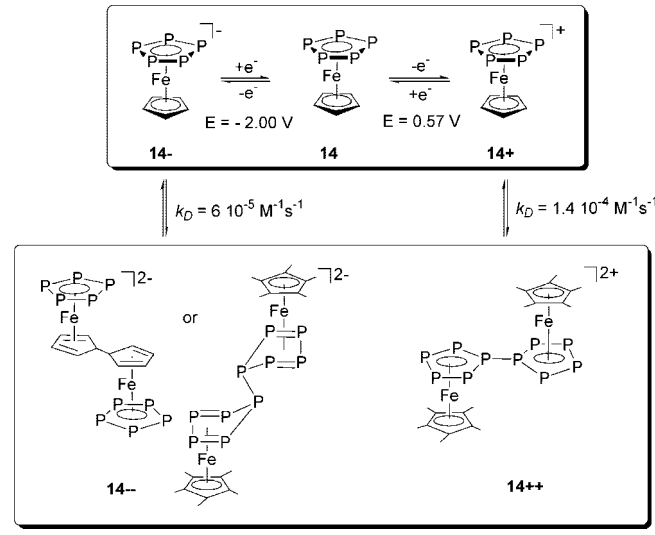

possibility to use one or more of the lone pairs on the P-atoms to coordinate additional metal−ligand fragments or to exploit the aromatic electron system to π-coordinate a second metal moiety.[73] As an example of the first intriguing additional bonding possibility, Scheme 28 highlights the reaction of [Cp*$Fe(\eta^5\text{-}P_5)$] with the highly reactive species [$Cr(CO)_5$-(THF)], which affords the trimetallic complex [Cp*$Fe(\eta^5\text{-}P_5)\{Cr(CO)_5\}_2$] (**58**). Likewise, the reaction of **14** with [$Cp(CO)_2Mn(THF)$] gives mixtures of the polymetallic complexes [Cp*$Fe(\eta^5\text{-}P_5)\{Mn(CO)_2Cp\}_n$] [$n$ = 1−4, (**59**−**62**)]. In complexes **58**−**62**, one or more phosphorus atoms of the *cyclo*-P_5 ring are 1,3-exocoordinated by P-lone pairs to two [$Cr(CO)_5$] units (**58**) or up to four organomanganese [$CpMn(CO)_2$] groups. The structure of **58** is presented in Figure 13, showing the trimetallic coordination of the *cyclo*-P_5 with the two [$Cr(CO)_5$] bent away from the pentaphosphorus plane.

Exocyclic coordination of different transition metal fragments was also accomplished for a variety of phospholyl complexes, which may use the lone pair on the P-atom(s) to bind coordinatively unsaturated metal moieties. In this regard, a brief mention should be given here to the bonding properties shown by the 1,2,3-triphosphaferrocene complexes [$Cp^RFe(\eta^5\text{-}P_3C_2Bu^t_2)$] ($Cp^R$ = Cp (**63**),[47] Cp‴ (**64**)[48] toward a variety of fragments including [$M(CO)_5$] (M = Cr, Mo, W), [Cp*Rh(CO)], [$CpRe(CO)_3Br$], and [$PtCl_2(PR_3)$] (R = Me, Et, Ph).[74,75]

The synthesis of **48** (see above) has shown that the *cyclo*-P_5 ligand in phosphametallocenes may be used to build up triple-decker sandwich complexes where it behaves as the internal deck of the complex. Intrigued by this possibility, the reactivity of **14** and **50** with [$CpFe(\eta^6\text{-}C_6H_6)$]$PF_6$, having a photolabile arene ligand, was shown to afford straightforwardly the cationic

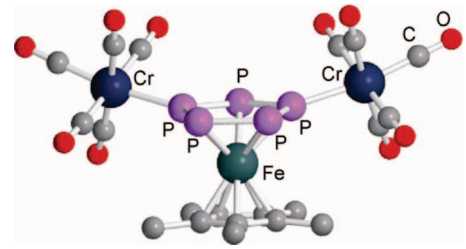

Figure 13. X-ray crystal structure of [Cp*$Fe(\eta^5\text{-}P_5)\{Cr(CO)_5\}_2$] (**58**); adapted from ref 73.

Scheme 28

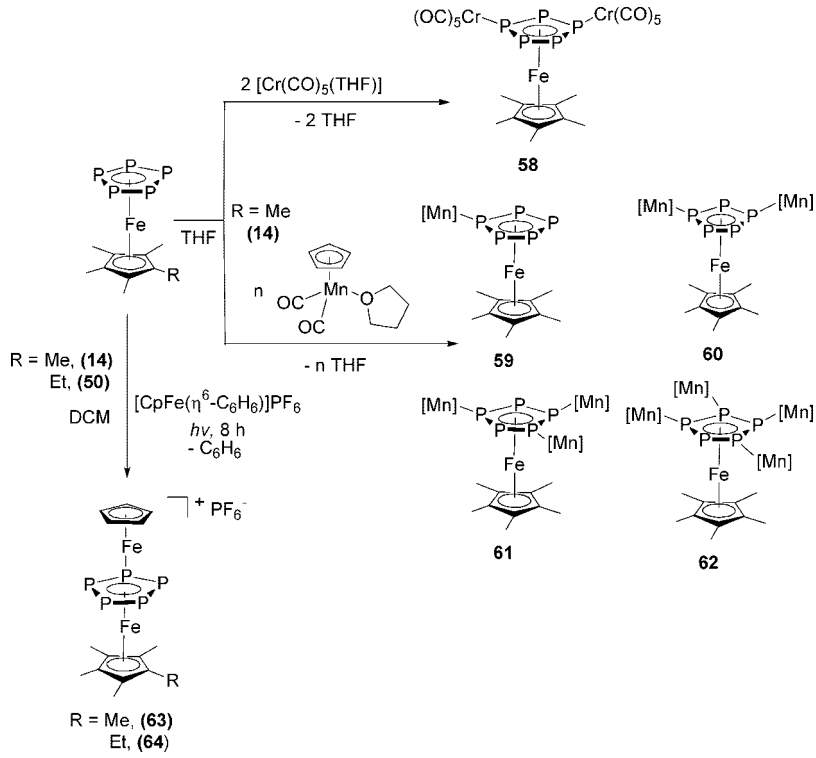

30-VE triple-decker complexes, $[CpFe(\mu,\eta^{5:5}\text{-}P_5)FeCp^R)]PF_6$ [Cp^R = Cp* (**65**); Cp^{Et} (**66**)] (Scheme 28).[73]

A straightforward approach to the synthesis of triple-decker complexes of iron and ruthenium containing a central pentaphosphorus cyclic ligand has been discovered later by Kudinov.[76,77] This synthetic route exploits the stacking reaction between coordinatively unsaturated transition metal fragments and sandwich complexes. In particular, (see Scheme 29) the cophotolysis at room temperature of the pentaphospharutenocene, [Cp*Ru(η^5-P_5)] (**67**), the Ru(II) analogue of **14**, with the fragment $[CpFe(\eta^6\text{-}C_6H_6)]^+$ afforded the mixed iron−ruthenium triple-decker complex $[CpFe(\mu,\eta^{5:5}\text{-}P_5)RuCp^*]^+$ (**68**) identical to **65**. The preparation of a family of FeFe, RuRu, and mixed FeRu triple-decker complexes of the type $[Cp^*M(\mu,\eta^{5:5}\text{-}P_5)M'Cp^*]^+$ was accomplished by taking advantage of the labile acetonitrile complex $[Cp^*Fe(MeCN)_3]^+$ since the permethylated fragment $[Cp^*Fe]^+$ cannot be obtained from the highly stable benzene complex $[Cp^*Fe(\eta^6\text{-}C_6H_6)]^+$. The interesting complex $[\{Cp^*Ru\}_2(\mu,\eta^{5:5}\text{-}P_5)]^+$ (**69**) was also prepared by refluxing in ethanol the ruthenium dimer $[Cp^*RuCl_2]_2$ with **14**. By refluxing **68** in acetonitrile for 10 h, a nucleophilic degradation occurred with selective elimination of the $[CpFe]^+$ fragment and formation of the pentaphospharuthenacene [Cp*Ru(η^5-P_5)] (**67**).

Only the CpFe-containing complexes were reactive in this process; probably the steric hindrance of the Cp* ring disfavors the nucleophilic attack at the metal center coordinated to it. The structurally related mixed Mo/Fe dimer $[CpFe(\mu,\eta^{5:5}\text{-}P_5)\{Mo(C_7H_7)\}]BF_4$ (**70**) was also obtained from the reaction of **14** with $[(C_7H_7)Mo(MeCN)_3]BF_4$ in acetone at RT (Scheme 29).[78]

π-Bonding of the *cyclo*-P_5 ligand in **14** also could be exploited toward $M(CO)_3$ moieties (M = Cr, Mo).[79] As a result, neutral 30-VE triple-decker complexes containing *cyclo*-P_5 as the middle deck were prepared by treatment of [Cp*Fe(η^5-P_5)] with $[M(CO)_3(NCMe)_3]$ (M = Cr, Mo) in

Scheme 29

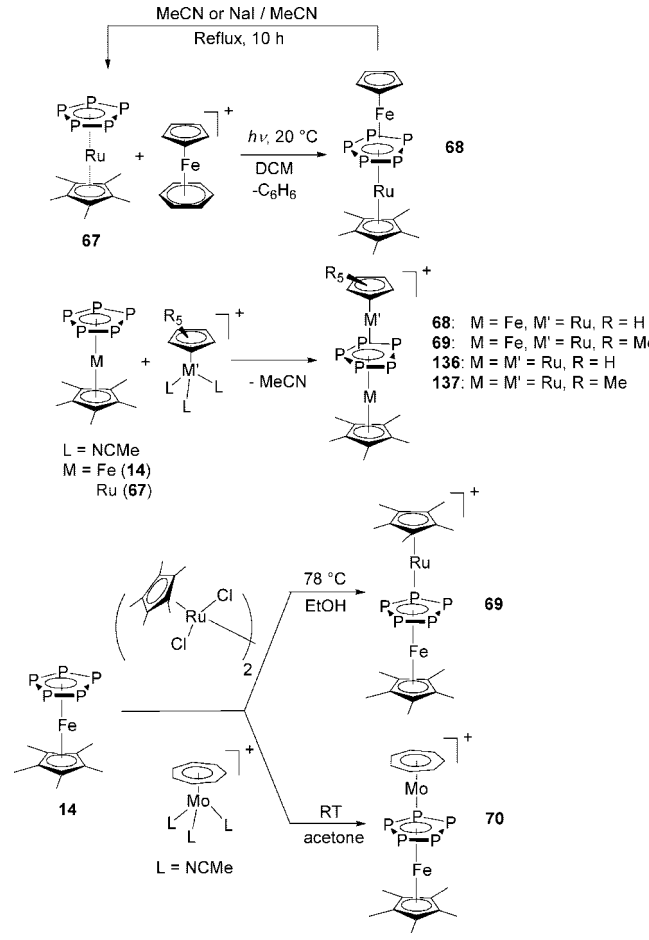

Scheme 29

DCM at RT. The new mixed complexes $[Cp^*Fe(\eta^{5:5}\text{-}P_5)\text{-}M(CO)_3]$ [M = Cr (**71**); Mo (**72**)] were characterized by

Scheme 30

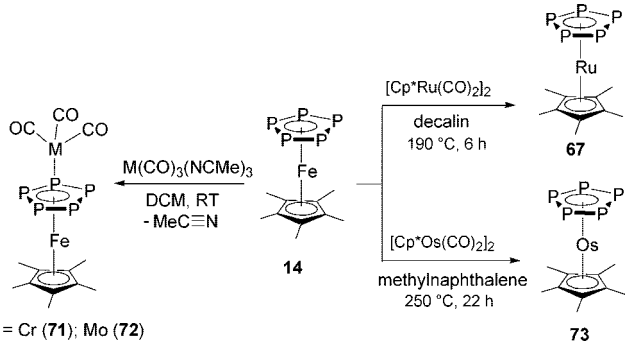

standard spectroscopic methods and, for the molybdenum derivative only, also by X-ray structural analysis. Scheme 30 highlights this synthesis, which could be extended to tungsten only for the pentaarsaferrocene analogue of **14**, i.e., [Cp*Ru(η^5-As_5)].

Ruthenium and osmium complexes analogous to **14**, i.e., [Cp*Ru(η^5-P_5)] (**67**) and [Cp*Os(η^5-P_5)] (**73**), could be prepared by intramolecular *cyclo*-P_5 transfer from the iron complex to the heavier metal center by cothermolysis of **14** with [{Cp*M$(CO)_2$}$_2$] (M = Ru, Os).[80] The reaction requires high boiling solvents and prolonged reaction times and was therefore carried out at 190 °C in decalin for 6 h in the case of ruthenium (yield 63%) and at 250 °C for 22 h in the case of osmium (yield 9%) (Scheme 30) (see sections 3.2 and 3.3).

In all the reactions described above, the *cyclo*-P_5 unit remains intact and its planar arrangement is not modified during the reaction even if very harsh conditions are applied.[73,80] However, the possibility to disaggregate or activate the pentaphosphorus ring cannot be discarded. In fact, many reactions encompassing this chemistry, which often proceed without any selection of the many available reaction pathways, have been reported. Thus, simply replacing [{Cp*Ru$(CO)_2$}$_2$] with [{Cp″Ru$(CO)_2$}$_2$] in the thermal reaction described in Scheme 30 (decalin, 190 °C, 16 h) does not afford only the *cyclo*-P_5 transfer derivative, [Cp″Ru(η^5-P_5)] (**74**), produced only in ca. 9% yield, but gives a great number of products that could be separated by column chromatography (Scheme 31).[81] ^{31}P NMR spectroscopy and X-ray crystallography have helped to characterize these new derivatives, which, apart from pentaphospharutenocene **74**, include the triangulated homo- and heterotrimetallic dodecahedral clusters [{Cp″Ru$}_3P_5$] (**75**), [{Cp″Ru$}_2${Cp*Fe$}P_5$] (**76**), and [{Cp*Fe$}_2${Cp″Ru$}P_5$] (**77**) and the tetrametallic compounds [{Cp″Ru$}_3${Cp*Fe$}P_4$] (**78**) and [{Cp″Ru$}_2P_4$] (**79**). X-ray crystallographic studies show that the P_5 ligand originally present in **14** was partially disaggregated in all the ruthenium and the mixed iron−ruthenium clusters. In particular, it appears that, in the distorted M_2M' P_5-triangulated dodecahedra of **76** and **77**, the P_5 unit in the educt species has been split into $\eta^{3:2:2}$-P_3 and $\eta^{3:2}$-P_2 fragments still held together by a single P−P bond. Complete breakage of the P_5 topology has occurred in the tetraphosphorus complex **78** where two orthogonally arranged P_2 ligands are connecting the four metal atoms. A similar structural pattern has been found in the dodecahedral cluster [{Cp″Fe$}_4$(μ,$\eta^{1:2:2:1}$-P_2)$_2$] (**80**), which was generated by cothermolysis of [Cp″Fe$(CO)_2$]$_2$ with white phosphorus at high temperature.[82]

Mixed metal complexes featuring a *cyclo*-P_5 opening were also obtained from the reaction of **14** with early transition

Scheme 31

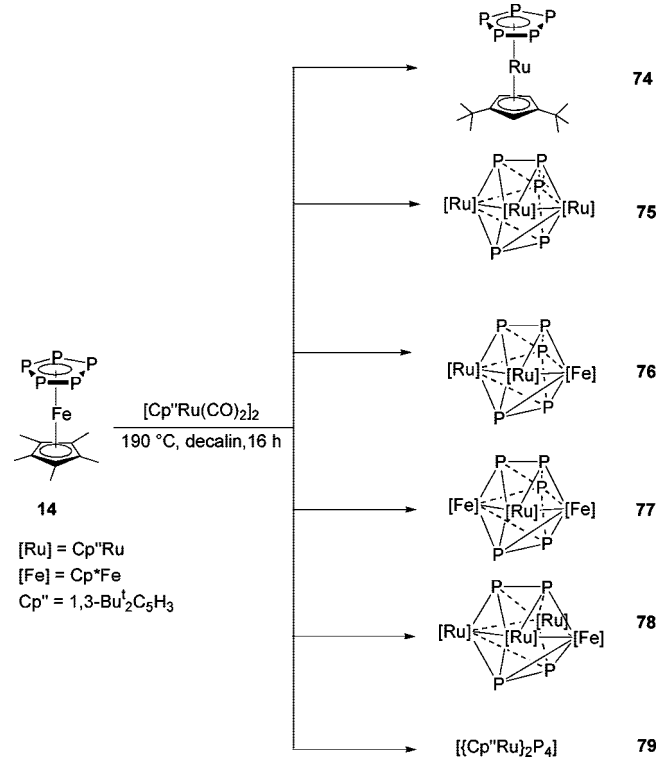

organometallic fragments such as [Cp″Ta$(CO)_4$].[83] Thus, after prolonged cothermolysis in boiling decaline, the new bimetallic complex [Cp*Fe(μ,$\eta^{4:3}$-P_5)(TaCp″)] (**81**) was obtained (Scheme 32). Complex **81** bears a fully decarbonylated half tantalocene fragment inserted into the *cyclo*-P_5 ligand, which therefore opens to form a folded P_5 chain. The dinuclear complex [Cp*Fe($\mu-\eta^{5:1}$-P_5){Cp″Ta$(CO)_3$}] (**82**), generated after short-time photolysis in the same solvent, is the precursor of **81** and contains the *cyclo*-P_5 ligand coordinated terminally to the [Cp″Ta$(CO)_3$] fragment. Further thermal elimination of CO from **82** eventually resulted in the cleavage of a P−P bond of the *cyclo*-P_5, leading to **81**.

The thermolysis of [Cp″Ta$(CO)_4$] with elemental phosphorus in boiling decalin afforded the trinuclear cluster [(Cp″Ta$)_3$(μ_3-P_4)(μ_3-P_2)] (**83**) that, after reaction with [$Fe_2(CO)_9$] at RT, gave the $FeTa_3$ cluster [(Cp″Ta$)_3$(μ_3,$\eta^{3:2}$-P_2)(μ_4,$\eta^{4:3:3:1}$-P_4{Fe$(CO)_4$})] (**84**) (Scheme 32).[84]

Reducing the time of cothermolysis of **14** with [Cp″Ta$(CO)_4$] in boiling decalin gave, apart from **81**, an equilibrium mixture of the two cubanes [(Cp*Fe)(Cp″Ta$)_2$-(P_5)] (**85**) and [(Cp*Fe)(Cp″Ta$)_2$(P_4)(P_1)] (**86**), both exhibiting a $FeTa_2P_5$-framework but distinct arrangements, i.e., an open P_5 chain in **85** and two distinct subunits, P_4/P_1 in **86**.[85] A small amount (ca. 3%) of **83** is formed together with [(Cp″Ta$)_4$(P_3)$_2$] (**87**) (Scheme 33). The equilibrium between **85** and **86** may be selectively shifted toward the P_5-moiety by coordination to one P-vertex of the cubane of the {Mo$(CO)_5$} fragment by reaction of either **85** or **86** with [Mo$(CO)_5$(THF)]. This exclusively affords [(Cp*Fe)-(Cp″Ta$)_2$(P_5){Mo$(CO)_5$}] (**88**), consisting of a cubane-like polyhedron featuring the open P_5 chain.

The cleavage of the acyclic P_5 ligand in the heterodinuclear complex [(Cp*Fe)(Cp″Ta)(P_5)] (**81**) was accomplished by reaction at RT with [Cp″Ta$(CO)_2$(COD)], as shown in Scheme 33.[85] The new product **89**, isolated in high yield, derives from the formal insertion of a {Cp″Ta$(CO)_2$} unit

Scheme 32

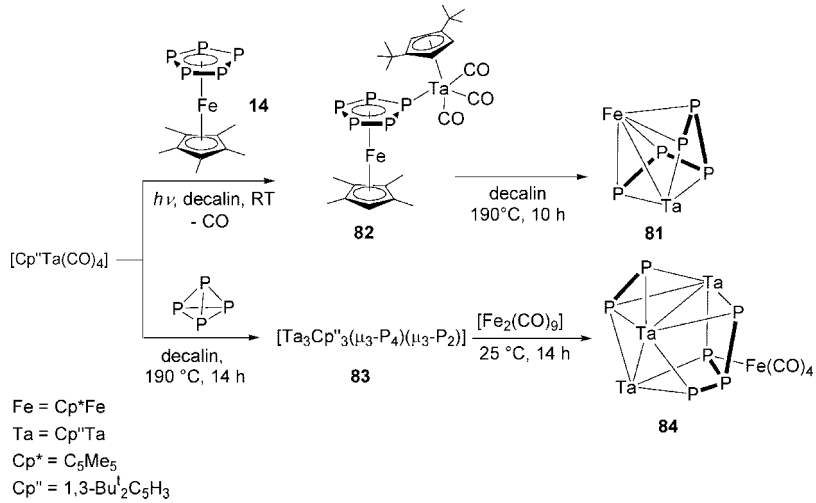

Scheme 33

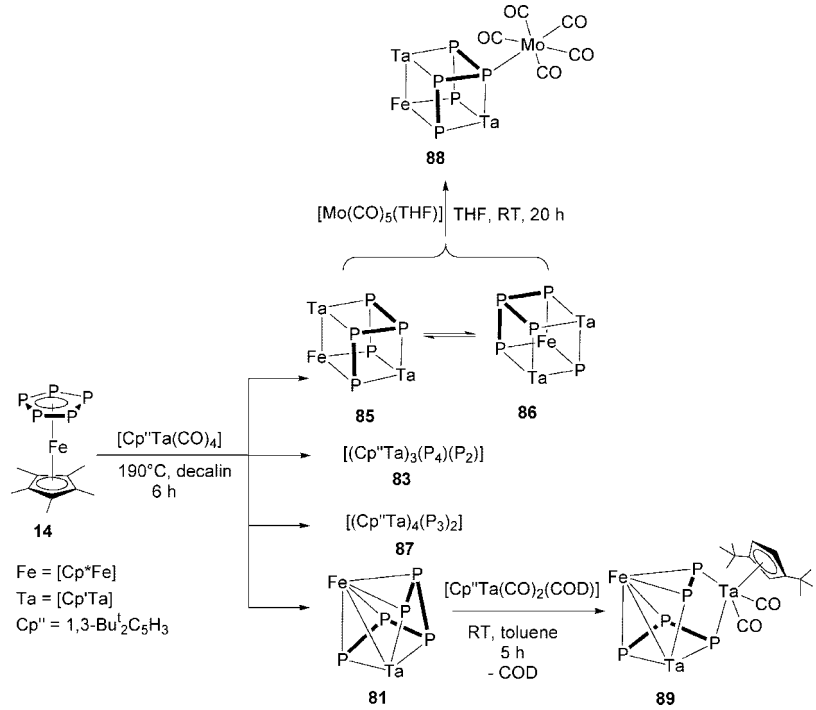

into the P_5 chain of **81**, providing a trinuclear species containing separated P_3 and P_2 ligands bridged by the added tantalum moiety. Figure 14 shows the nice trinuclear cluster of **89**.

The thermolysis of **14** with 1 and 2 equiv of the iridium binuclear complex [{Cp*Ir(CO)}$_2$] afforded the new compounds [(Cp*Fe)(μ_3,$\eta^{4:1:1}$-P_5){Cp*Ir(CO)}$_2$] (**90**) and the pentanuclear $FeIr_4$ cluster **91**, respectively.[83] Both compounds resulted from the unexpected opening of the *cyclo*-P_5 moiety, with loss of the π aromaticity. Complex **90** shows a planar folded envelope structure while a new bent phosphorus chain is assembled in compound **91** (see Scheme 34). Remarkably, the pentanuclear complex **91** may be generated from **90** by reaction with a second equivalent of the iridium precursor at RT.

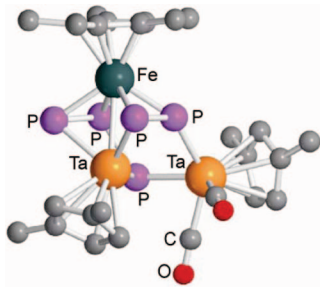

Figure 14. X-ray crystal structure of [(Cp*Fe)(Cp″Ta){Cp″Ta-(CO)$_2$}(P$_3$)(P$_2$)] (**89**); only secondary carbons of Pr^i substituents shown; adapted from ref 85.

Replacing the dinuclear [{Cp*Ir(CO)}$_2$] species with the 16-VE fragment [Cp*Ir(CO)$_2$] afforded, after reaction with **14** under UV light irradiation, a mixture of the mixed complexes [(Cp*Fe)(μ,$\eta^{5:1}$-P_5){Cp*Ir(CO)}] (**92**) and [(Cp*Fe)(μ,$\eta^{5:2}$-P_5)-{Cp*Ir(CO)}] (**93**) (see Scheme 35).[86] While the former species contains the iridium fragment η^1-coordinated to one P-atom of the pentaphosphaferrocene complex, the bonding mode of the latter complex consists of a new sandwich structure with the μ,$\eta^{5:2}$ coordination mode for the cyclo-P_5 moiety (Figure 15). The P−P bond, which has undergone

Scheme 34

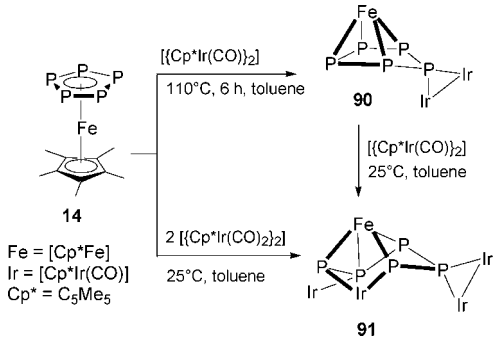

Scheme 35

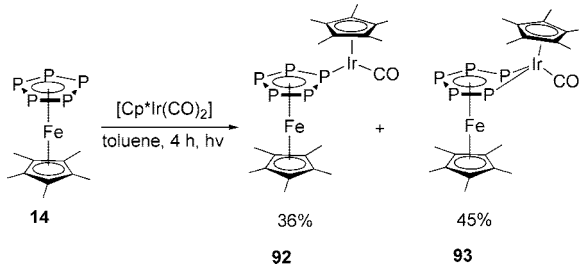

the formal insertion of the {Cp*Ir(CO)$_2$} unit, lengthens considerably, passing from 2.096 Å ($d_{(P-P)ave}$ in **50**) to 2.36 Å. The other four P atoms remain almost coplanar with the Cp* ring while the dihedral angle of the butterfly-type Fe−P1−P2−Ir subunit opens to 158.5°.

The cothermolysis of **14** with the organomolybdenum complex [Cp*Mo(CO)$_3$CH$_3$] gave a new heterodinuclear complex [{Cp*Mo(CO)}($\mu,\eta^{2:2}$-P$_2$)$_2${FeCp*}] (**94**) bearing two P$_2$ ligands bridging the two metal centers (Scheme 36). Subsequent reaction with white phosphorus resulted in the formal transfer of a further P$_2$ unit to [{Cp*Mo(CO)}(μ−$\eta^{2:2}$-P$_2$)$_2${FeCp*}] and afforded the heterobimetallic heaxaphosphorus fully decarbonylated cluster [Cp*$_2$MoFeP$_6$]

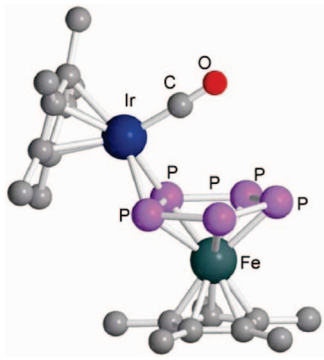

Figure 15. X-ray crystal structure of [(Cp*Fe)($\mu,\eta^{5:2}$-P$_5$){Cp*Ir(CO)}] (**93**); adapted from ref 86.

Scheme 36

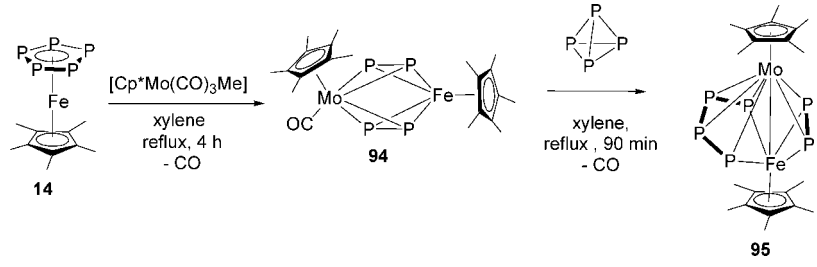

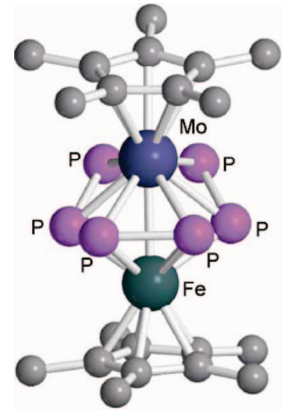

Figure 16. X-ray crystal structure of [{Cp*Mo}($\mu,\eta^{4:2}$-P$_4$)($\mu,\eta^{2:2}$-P$_2$){FeCp*}] (**95**); adapted from ref 87.

(**95**).[87] X-ray diffraction analysis (Figure 16) pointed out that the new P$_6$ moiety was constituted by two separated $\mu,\eta^{4:2}$-P$_4$ and $\mu,\eta^{2:2}$-P$_2$ ligands, then assigning to **95** the formula [{Cp*Mo}($\mu,\eta^{4:2}$-P$_4$)($\mu,\eta^{2:2}$-P$_2$){FeCp*}]. A detailed analysis of bond distances and angles, suggested that the $\mu,\eta^{2:2}$-P$_2$ can be regarded as a 2e$^-$ donor ligand, while the $\mu,\eta^{4:2}$-P$_4$ can be considered as a 6e$^-$ donor tetraphosphabutene ligand, i.e., formally a P$_4^{4-}$ ion. An intermetallic Mo−Fe bond (2.7646 Å) completes the dimetalladiphosphatetrahedrane substructure.

In addition, [{Cp*Mo(CO)}($\mu,\eta^{2:2}$-P$_2$)$_2${FeCp*}] (**94**) under suitable thermal conditions may revert into **14**, forming also the intriguing triple-decker complex [{Cp*Mo}$_2$($\mu,\eta^{6:6}$-P$_6$)] (**96**),[87] which was first described by Scherer and co-workers in 1985.[8] The importance of this latter complex lies in the stabilization of the six-membered *cyclo*-P$_6$ ligand, the so-called hexaphosphabenzene, a molecule which represents the all-phosphorus counterpart of benzene and does not exist in the free state.

The pentaphosphaferrocene **14** has been also used as a suitable P-source for achieving a variety of cobalt complexes (section 4.1).[88] Here only those containing both cobalt and iron will be detailed. Thus, the cothermolysis of **14** and [Cp^{R}Co(CO)$_2$] (Cp^R = Cp^{Bu}, Cp″) at 190 °C in decalin (Scheme 37) afforded a variety of clusters, some of them incorporating iron. These mixed Co/Fe compounds are [{Cp*Fe}{Cp^{Bu}CoP$_4$}{FeCp*}] (**97**), a triple-decker *closo*-cluster with a CoP$_4$ middle deck and [{Cp*Fe}{Cp″Co}$_2$(P$_4$)(P)] (**98**), a trinuclear cubane exhibiting a P$_4$/P$_1$ arrangement similar to the mixed Fe/Ta complex **86** described above.

The oxidation of compound [{Cp*Fe}{Cp″Co}$_2$(P$_4$)(P)] (**98,** Figure 17) at room temperature with atmospheric oxygen afforded the novel tetranuclear cluster [{Cp*Fe}{Cp″Co}$_3$(P$_2$O)(PO)(P$_2$)] (**99**) as shown in Scheme 37.[89] The most remarkable structural feature of **99** is the presence of the P$_2$O ligand, the phosphorus analogue of N$_2$O, that has been

Scheme 37

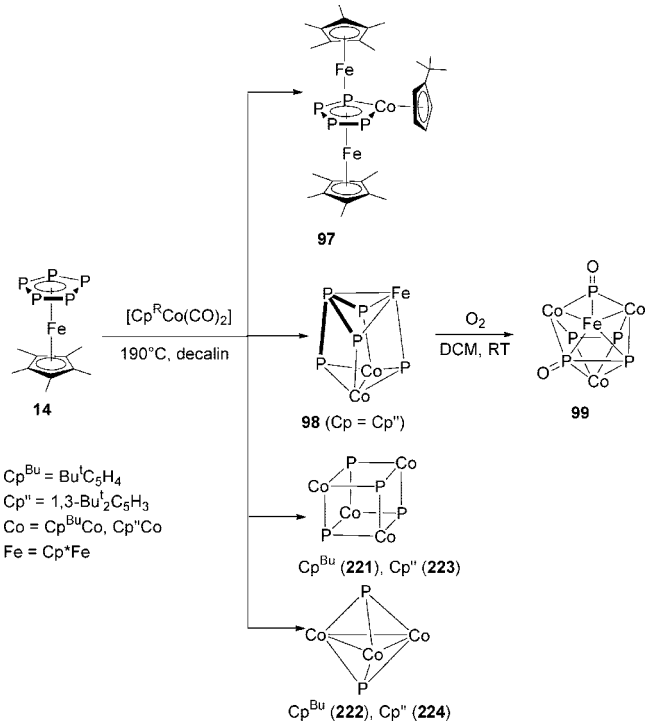

stabilized in this complex through coordination to the cobalt and iron centers.[90] Free P_2O is indeed highly unstable, and it has been generated from P_2 (P_4) and ozone and characterized at low temperature in a matrix by IR and UV-vis spectroscopy.[91] Ab initio calculations[92] showed that for P_2O the linear form is more stable than the three-membered ring structure. In agreement with ^{31}P NMR spectrum, the P_2O ligand in **99** is not separated into a μ_3-PO and μ_3-P ligand, but it is coordinated as a $\eta^{1:2:2:1}$-P_2O ligand.

Replacing the mononuclear cobalt complex $[Cp^RCo(CO)_2]$ with the dinuclear cobalt species $[\{Cp^RCo(\mu\text{-}CO)\}_2]$ (Cp^R = Cp^{Bu}, Cp″) in the thermal or photochemical reaction with the pentaphosphaferrocenyl derivative **50** led to the new tetranuclear $FeCo_3$ cluster $[Cp^{Et}Fe(\mu_4,\eta^{5:2:2:1}\text{-}P_5)\{Cp''Co(CO)\}\{Co_2Cp_2''(\mu\text{-}CO)\}]$ (Co−Co, **100**) in which a still intact *cyclo*-P_5 ligand is engaged in the novel and unique $\mu_4,\eta^{5:2:2:1}$ coordination mode shown in Scheme 38.[88] The crystal structure of **100** is shown in Figure 18.

3.1.3. Polymers and Supramolecular Assemblies Based on the Pentaphosphaferrocene Building Block

The chemistry of *cyclo*-P_5 ring in pentaphosphaferrocenyl complexes shows an extremely rich and diverse reactivity

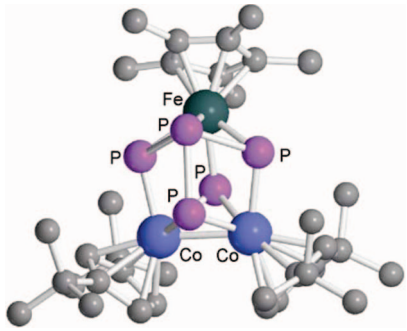

Figure 17. X-ray crystal structure of $[\{Cp^*Fe\}\{Cp''Co\}_2(P_4)(P)]$ (**98**); adapted from ref 89.

Scheme 38

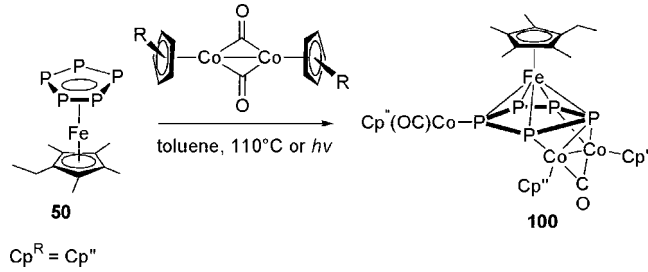

and encompasses a variety of coordination modes that have been highlighted in section 3.1.2. Besides its capacity to form cationic triple-decker complexes, to undergo P_5-transfer reactions, there are several examples of reactions in which the *cyclo*-P_5 ring expands its coordination ability, either remaining intact or being cleaved. In the latter case, the P_5 topology may still be preserved by forming a pentaphosphorus chain or may be lost, affording compounds featuring separated P_4/P_1 and P_3/P_2 fragments. Further possibilities may be envisaged, and some of them have been recently explored by Scheer and co-workers, who have provided the first confirmatory evidence[93] about the use of *cyclo*-P_5 as a suitable ligand to build up novel 1D and 2D inorganic polymers by the previously unknown 1,2-ligation and 1,3,4-ligation modes.[94] This fascinating and largely unpredictable chemistry has been developed mostly on the reaction with different coinage metal salts, particularly copper and silver halides and pseudohalides.

The first examples of these polymeric species were obtained by the reaction of $[Cp^*Fe(\eta^5\text{-}P_5)]$ with CuX (X = Cl, Br, I) in DCM/CH_3CN at RT. The following crystalline materials suitable for being investigated by X-ray diffraction analysis were isolated: $[CuCl\{Cp^*Fe(\eta^{5:1:1}\text{-}P_5)\}]_\infty$ (**101**), $[CuX\{Cp^*Fe(\eta^{5:1:1:1}\text{-}P_5)\}]_\infty$, [X = Br (**102**); X = I (**103**)].[93] The structural analysis showed that **101** is constituted by a linear 1D chain with planar six-membered Cu_2P_4 rings alternated in an orthogonal manner with four-membered $CuCl_2$ rings. The planar *cyclo*-P_5 rings and the six-membered Cu_2P_4 units are coplanar while each Cu(I) center is tetrahedrally coordinated as shown in the Figure 19. The linear chains are separated from each other by interchain π-stacking between Cp* and *cyclo*-P_5 units. Surprisingly, while the reaction with CuCl affords the 1D coordination polymer **101**, the reaction with CuBr and CuI affords the isostructural 2D coordination polymers **102** and **103**; the X-ray crystal structure for **102** is shown in Figure 20. In the latter compound, the Cu(I) centers exhibit a distorted tetrahedral

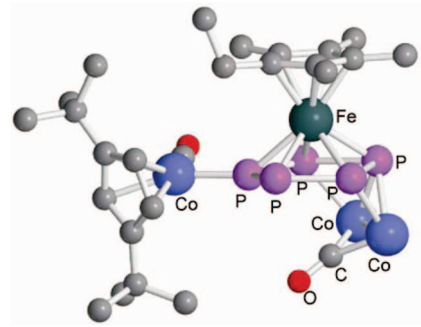

Figure 18. X-ray crystal structure of $[Cp^{Et}Fe(\mu_4,\eta^{5:2:2:1}\text{-}P_5)\{Cp''Co(CO)\}\{(\mu\text{-}CO)Cp_2''Co_2\}]$ (**100**); Cp″ ligands on two Co centers (right-hand side) omitted for clarity; adapted from ref 88.

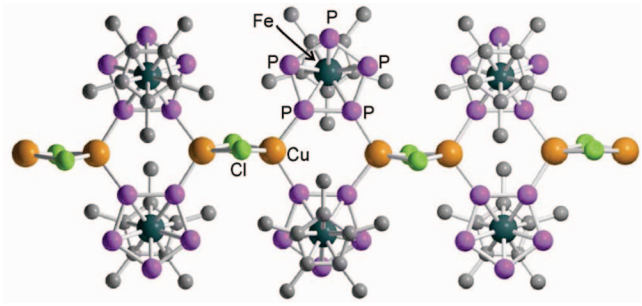

Figure 19. X-ray crystal structure of the 1D chain in [CuCl{Cp*Fe($\eta^{5:1:1}$-P_5)}]$_\infty$ (**101**); adapted from ref 93.

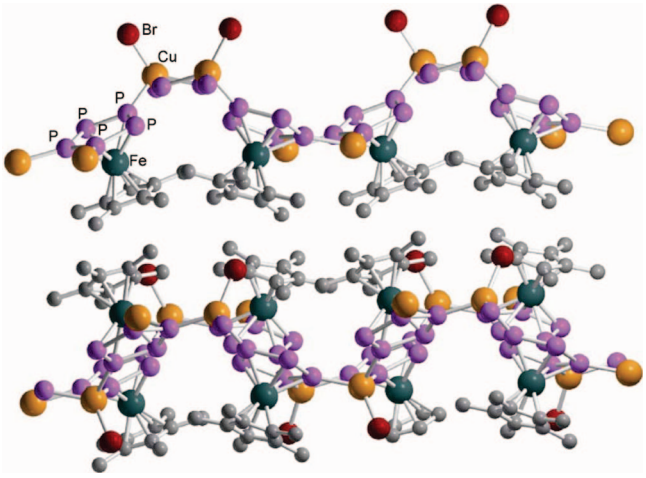

Figure 20. X-ray crystal structure of the 1D chain in [CuBr{Cp*Fe($\eta^{5:1:1:1}$-P_5)}]$_\infty$ (**102**); adapted from ref 93.

geometry being coordinated by one halogen atom and three P atoms, each coming from a different [Cp*Fe(η^5-P_5)] unit. Thus, the new coordination mode $\eta^{5:1:1:1}$ is observed for the *cyclo*-P_5 ring. A further interesting feature of the coordination polymers **101**−**103** is that the P−P bonds belonging to the polymetalated *cyclo*-P_5 ring do not differ significantly from the P−P bonds in **14**. This finding is rather surprising as elongation of the P−P bond lengths and/or distortion of the *cyclo*-P_5 planarity are generally observed upon reaction of [Cp*Fe(η^5-P_5)] with different organometallic fragments.

Polymeric chains based on multimetallic coordination of the *cyclo*-P_5 in [Cp*Fe(η^5-P_5)] also may be assembled with metals other than copper. Particularly remarkable results were obtained using silver salts containing weakly coordinating anions such as the Krossing's anion [Al{$(CF_3)_3CO$}$_4$]$^-$, which conjugates null coordination ability of the perfluoroalkoxy aluminate with bulkiness.[95] Thus, the straightforward reaction of **14** with Ag[Al{$(CF_3)_3CO$}$_4$] in DCM affords dark brown crystals of [Ag{Cp*Fe($\eta^{5:2:1}$-P_5)}$_2$]$_n$[Al{$(CF_3)_3CO$}$_4$]$_n$ (**104**), which in the solid state forms polymeric 1D chains where the intact *cyclo*-P_5 ligand features a new $\eta^{5:2:1}$-bonding mode.[96,31]P NMR analysis and VPO measurements in DCM solution showed that the polymer dissolved, disrupting its polymeric structure, and gave the monomer [Ag{Cp*Fe(η^5-P_5)}$_2$][Al{$(CF_3)_3CO$}$_4$] (**105**). Because low-temperature NMR was not conclusive to assess the solution dynamic behavior, a possible rationalization of the exchange process was obtained from DFT calculations, which pointed to the existence of a dynamic equilibrium between the monocation **105** and polycations, with this latter species becoming prevalent at lower temperatures. Scheme 39 illustrates this interesting chemistry.

The possibility to form polydimensional coordination polymers has been explored also using triphosphaferrocene complexes instead of **14**. Thus, in a recent report, Scheer and co-workers reported on the reactivity of 1,2,4-triphosphaferrocenes [Cp^{R}Fe(η^5-$P_3C_2Bu^t_2$)] (Cp^R = Cp (**63**),[47] Cp‴ (**64**)[48]] with copper(I) chloride.[97] Remarkably, while **63** reacts with CuCl in acetonitrile to give the discrete dimeric complex [{CpFe($\eta^{5:1:1}$-$P_3C_2Bu^t_2$)}{μ-CuCl(MeCN)}]$_2$ (**106**) irrespectively of the stoichiometric ratio used, the bulkier complexes **64** give the dimer [{Cp‴Fe($\eta^{5:1:1}$-$P_3C_2Bu^t_2$)}{μ-CuCl}]$_2$ (**107**) when the reaction is carried out in 1:1 ratio (see Scheme 40). NMR and ESI- analysis confirmed that the dimeric structure authenticated in the solid state is also maintained in solution.

Doubling the amount of CuCl in the reaction with **64** at RT gives the polymeric 1D-complex [{(Cp‴Fe)$_2$(μ,$\eta^{4:4:1:1}$-P_4)}{μ-CuCl(MeCN)}]$_\infty$ (**108**), which results from the unexpected fragmentation/reaggregation of the triphosphacyclopentadienyl ligand and features the interesting $\eta^{4:4}$-coordinated tetraphosphabutadiene ligand. The latter P_4-

Scheme 39

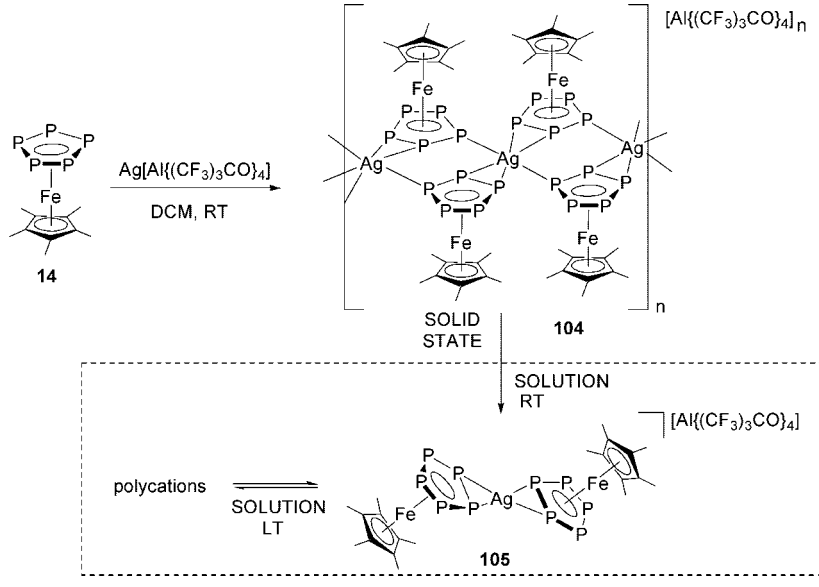

Scheme 40

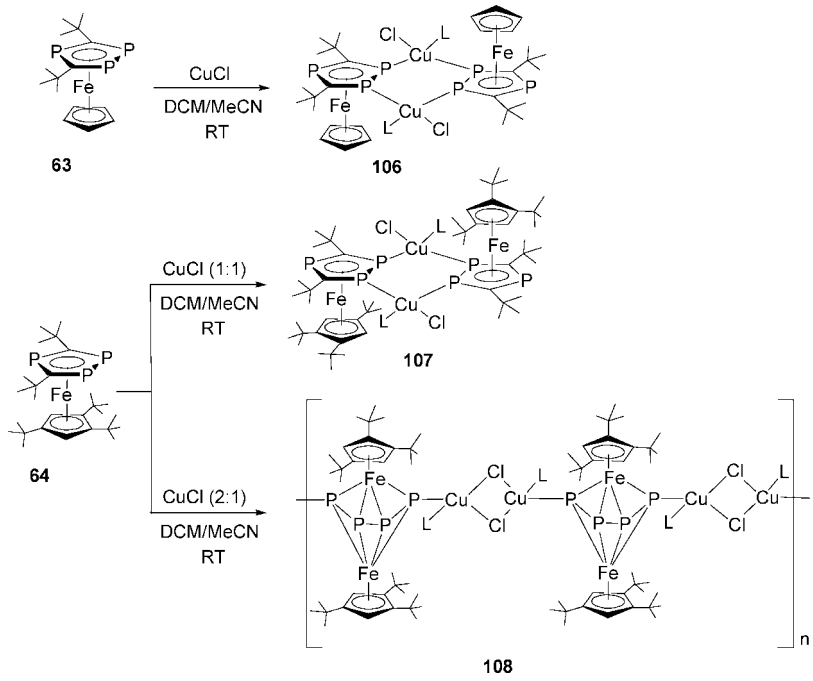

moiety additionally binds to two tetrahedrically coordinated CuCl(MeCN) dimers, forming the scaffold of a polymeric chain supported by bridging chloride ligands.

Taking a step forward in the synthesis of supramolecular assemblies based on the multilinking capabilities of the pentaphosphaferrocene unit toward multiple metal cations, Scheer et al.[98] isolated, from the solution reaction of **14** and CuCl in DCM/CH_3CN at RT after elimination of the crystallized **101**, an entirely new and unexpected inorganic fullerene-like molecule of formula $[\{Cp^*Fe(\eta^{5:1:1:1:1:1}\text{-}P_5)\}_{12}\{CuCl\}_{10}\{Cu_2Cl_3\}_5\{Cu(CH_3CN)_2\}_5]$ (**109**). This black cluster exhibits a spectacular spherical shape, with a fullerene-like structural motif, formed by 90 noncarbon core atoms (Figure 21). All P atoms of the planar *cyclo*-P_5 ring, belonging to the 12 $[Cp^*Fe(\eta^5\text{-}P_5)]$ units, coordinate to CuCl moieties, showing the novel 1,2,3,4,5-coordination mode. Moreover, each copper center further coordinates P atoms of different *cyclo*-P_5 rings, leading to the formation of six-membered Cu_2P_4 rings, giving an alternating array of five- and six-membered rings similar to that found in fullerene.

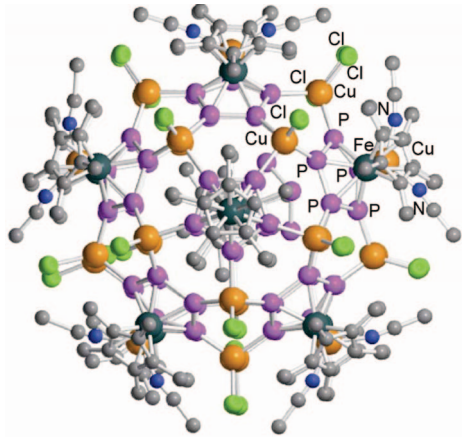

Figure 21. X-ray crystal structure of $[\{Cp^*Fe(\eta^{5:1:1:1:1:1}\text{-}P_5)\}_{12}\{CuCl\}_{10}\{Cu_2Cl_3\}_5\{Cu(CH_3CN)_2\}_5]$ (**109**). Atom color code: Fe, olive; Cu, gold; P, purple; Cl, pale green; N, blue; C, gray. Adapted from ref 98.

Remarkably, the outside diameter of the inorganic fullerene-like molecule is about 21.3 Å, i.e., three times larger than that of C_{60}.

The unexpected synthesis of **109** stimulated the search for other spherical giant molecules formed completely by heteroatoms and based on the powerful abilities of the pentaphosphaferrocene assembly to create a network via multibonding interaction with copper(I) ions. An in-depth study of the reactions of **14** and **50** with CuBr showed that, depending on the stoichiometry of the reagents and the concentration of the solution, it is possible to drive the reaction toward the exclusive formation of soluble spherical fullerene-like nanoballs[99] without producing any insoluble coordination 1D or 2D polymer.[93] Then, the reaction of either **14** or **50** with CuBr in MeCN/DCM mixture at RT gave only the spherical cage compound $[\{Cp^RFe(\eta^{5:1:1:1:1:1}\text{-}P_5)\}_{12}\{CuBr\}_{10}\{Cu_2Br_3\}_5\{Cu(CH_3CN)_2\}_5]$ ($Cp^R = Cp^*$, **110**, Cp^{Et} = **111**), analogous to the CuCl-based species **109**. The cluster **111** has an inside diameter of 12.9 Å and an outside diameter of 23.7 Å. The internal size of the nanoball suggests the intriguing possibility to host an appropriate molecule. This fascinating hypothesis was proved by crystallographic studies on **111**, which confirmed the existence of an encapsulated molecule of **50** within the inner cavity of the nanocluster.[100] This further intriguing discovery raised the question whether the pentaphosphaferrocene molecules were fortuitously incorporated in the inner cavity of the nanoball or whether a 5-fold symmetry molecule is required to activate molecular recognition processes, eventually resulting in the formation of the supramolecular aggregate **111**. This working hypothesis was empirically verified by adding pure fullerene C_{60} to the reaction mixture of $[Cp^*Fe(\eta^5\text{-}P_5)]$ and CuCl under dilute conditions, as it has the appropriate size and symmetry to be incorporated as an endohedral molecule in nanocluster **109**. In keeping with this expectation, the exclusive formation of black crystals of the soluble supramolecular species of composition $C_{60}@[Cu_{26}Cl_{26}(H_2O)_2\{Cp^*Fe(\eta^5\text{-}P_5)\}_{13}(CH_3CN)_9]$ (**112**) was observed.[101] The cluster **112** exhibits an inorganic coating, consisting of 99 inorganic core atoms

resulting from the aggregation of building blocks such as pentaphosphaferrocene molecules and CuCl units, and likely forms via a template synthesis driven by molecular recognition elementary steps.

From this result, it was hypothesized that larger spherical heteroatomic molecules with fullerene topology could be accessible only using larger guest molecules through a template-controlled aggregation reaction. A beautiful substantiation of this working hypothesis was applied to the *ortho*-carborane $C_2B_{10}H_{12}$, which has proper size and symmetry to be encapsulated into a spherical molecule.[102] Thus, the reaction between **14** and CuCl was attempted in the presence of *o*-$C_2B_{10}H_{12}$, and the first example of carbon-free C_{80} fullerene analogue with icosahedral symmetry was isolated as dark brown crystals of formula $C_2B_{10}H_{12}$@[{Cp*-Fe($\eta^{5:1:1:1:1}$-P_5)}$_{12}$($CuCl)_{20}$] (**113**). This spherical cluster consists of 80 noncarbon atoms and contains 12 five-membered *cyclo*-P_5 and 30 six-membered Cu_2P_4 rings.

3.1.4. Polyphosphorus Ligands, P_x ($x > 5$)

Although not strictly related to the topic of this review, which specifically focuses on white phosphorus activation and coordination chemistry, the inorganic chemistry of phosphorus comprises an impressive variety of polyphosphorus compounds exhibiting different geometries and topologies that, although not directly related to elemental phosphorus,[17a,55] have been used as ligands to coordinate transition metal units including a few ones containing iron. Worth being briefly mentioned here is the chemistry of the Zintl anion, P_7^{3-}, which shows an α-P_4S_3 cage-like structure. Important studies by Fritz et al.[103] showed that the lithium salt Li_3P_7 reacts with [$CpFe(CO)_2Br$] to form the cluster [P_7{$CpFe(CO)_2$}$_3$] (**114**) containing the intact P_7 cage. The structure of **114** was later determined by X-ray crystallography, which confirmed the maintainance of the nortricyclane assembly with three {$CpFe(CO)_2$} moieties coordinated to the three bridging P-atoms of the cage upper rim.[49] The reaction of the neutral $P_7(SiMe_3)_3$ with $FeCl_2$ and LiCp* at −78 °C afforded the new complex [$(Cp^*Fe)_3P_6$][$FeCl_3$-(THF)] (**115**) constituted by [$(Cp^*Fe)_3P_6$]$^+$ cations and [$FeCl_3$(THF)]$^-$ anions. X-ray analysis showed the occurrence of a nine-membered polyhedron reminiscent of $B_9H_9^{2-}$ and consisting of six phosphorus atoms and three iron centers. The P−P separations are different, ranging from 2.268 to 2.498 Å. Carrying out the same reaction at room temperature in THF led to a completely different product, i.e., [$(Cp^*Fe)_3${(η^3-P_3)Fe}P_6] (**42**), which exhibits a different cluster topology and features a *cyclo*-P_3 unit trihapto bonded to a single iron atom. A description of this chemistry is shown in Scheme 41.

Scheme 41

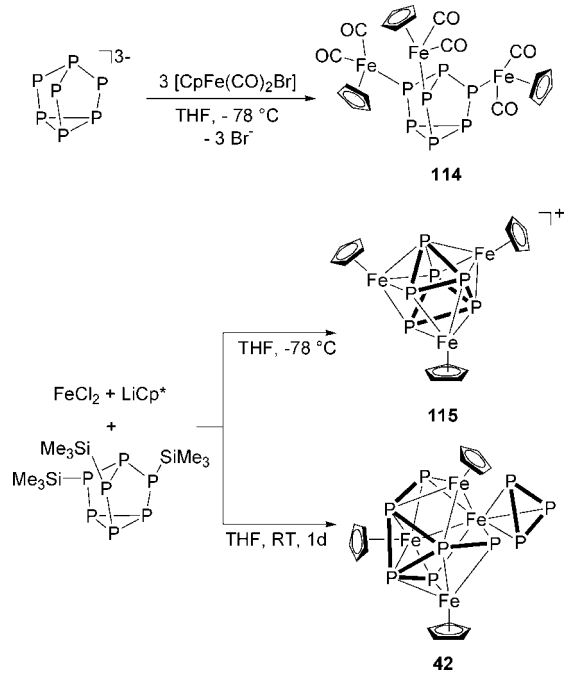

3.2. Ruthenium

The first ruthenium complex bearing an intact P_4 ligand was prepared by Peruzzini et al.[104] by reacting [$Ru(PPh_3)_3Cl_2$] with white phosphorus as shown in Scheme 42. Interestingly, the coordination of P_4 to the metal center causes the displacement of the triphenylphosphine ligands and the subsequent formation of a neutral ruthenium dimer [{$(PPh_3)_2ClRu$}(μ-Cl)$_3${$Ru(PPh_3)_2(\eta^1$-$P_4)$}] (**116**), which is both air- and light-sensitive. The binuclear structure was assigned on the basis of ^{31}P NMR measurements and related simulations, which revealed an octahedral geometry for the

Scheme 42

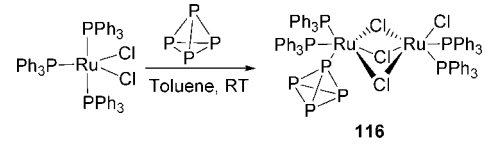

two ruthenium atoms and the preserved tetrahedral geometry for the P_4 moiety η^1-coordinated to one metal.

Coordination of the intact tetraphosphorus molecule was also observed when white phosphorus was allowed to react with mononuclear ruthenium complexes bearing the pentamethylcyclopentadienyl ligand and phosphines more basic then triphenylphosphine, such as PEt_3 or chelating dppe.[31] The chloride ligand was easily displaced by P_4, and the cationic monometallic ruthenium complexes **19** and **20** containing the P_4 molecule as monohapto ligand were isolated. The analogous reaction having iron as the metal center has been discussed previously in section 3.1.1; see Scheme 11. The reactivities of both **19** and **20** were briefly investigated, and the dinuclear heterobimetallic complexes [{$Cp^*Ru(PEt_3)_2$}(μ,$\eta^{1:1}$-P_4){$Re(CO)_2$(triphos)}]$(BPh_4)_2$ (**117**) and [{Cp^*Ru(dppe)}(μ,$\eta^{1:1}$-P_4){$W(CO)_5$}]BPh_4 (**118**) were synthesized by the straightforward reaction of the ruthenium complex with the appropriate metal synthon, {(triphos)-$Re(CO)_2$} or {$W(CO)_5$}, respectively (Scheme 43).[31]

Replacing Cp* with the less basic Cp allowed the synthesis of a variety of complexes endowed with an intriguing reactivity toward nucleophiles, especially water.[105] Thus, using [$CpRu(PPh_3)_2Cl$] as precursor, Stoppioni et al. found that the coordination of white phosphorus to the metal center was feasible only in the presence of a chloride scavenger such as $TlPF_6$ or $AgPF_6$, whereas when working with the more electron-rich complexes [$Cp^*RuCl(L)_2$] shown in Scheme 43, it was not necessary to abstract the chloride ligand. Simple reaction of white phosphorus with [$CpRu(PPh_3)_2Cl$] in THF/DCM at RT readily yielded [$CpRu(PPh_3)_2(\eta^1$-$P_4)$]$^+$ (**119**), which was crystallized as hexafluorophosphate salt from NH_4PF_6. ^{31}P NMR confirmed the

Scheme 43

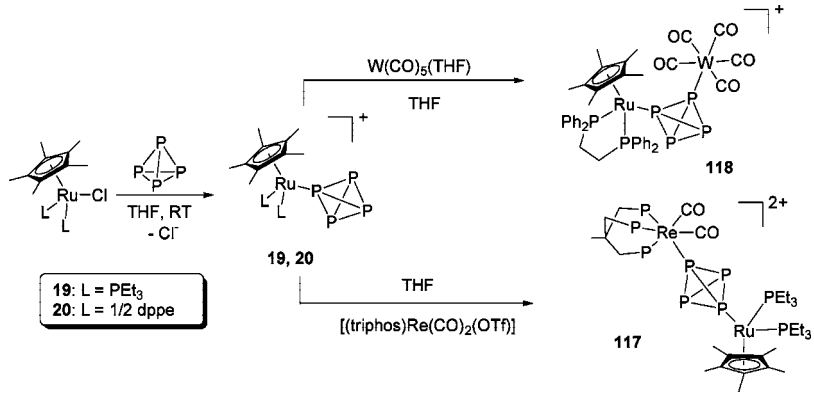

Scheme 44

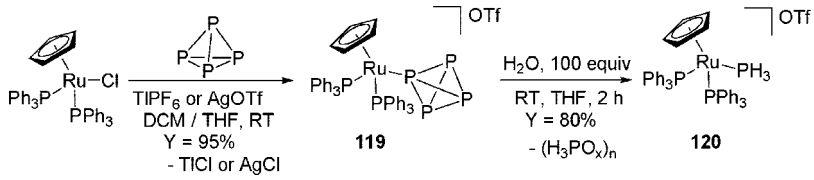

expected structure for the complex, with the intact P_4 molecule coordinated as a *tetrahedro*-η^1-P_4, analogous to the corresponding iron complex **18** shown in Figure 4.

By treatment of **119** with water, the unexpected hydrolysis of the coordinated P_4 moiety was observed taking place in exceedingly mild conditions, as shown in Scheme 44, and affording the phosphine complex $[CpRu(PPh_3)_2(PH_3)]^+$ (**120**) in almost quantitative yield.[105] Considering that white phosphorus is indefinitely stable in water at room temperature, this change of properties of the P_4 molecule after its coordination to the metal center is astonishing. Complex **120** was fully characterized by NMR and X-ray methods, and its nature was confirmed by an independent synthesis using PH_3 gas as reagent. The crystal structure of the complex cation **120** is shown in Figure 22. Formation of a brown precipitate, likely a mixture of polymeric low-valent phosphorus oxyacids, prevents a clear assignment of the reaction stoichiometry.

The study of the hydrolysis of coordinated η^1-P_4 was extended also to complex $[CpRu(dppe)(\eta^1\text{-}P_4)]^+$ (**121**), prepared following the same procedure as for **119**.[106] Interestingly, the easy hydrolysis of the coordinated η^1-P_4 in such a derivative helped with unraveling the reaction mechanism (Scheme 45). Remarkably, the products identified in the reaction mixture after hydrolysis were $[CpRu(dppe)(PH_3)]PF_6$ (**122**) and the new $[CpRu(dppe)\{P(OH)_3\}]PF_6$ (**123**), which contains the unstable $P(OH)_3$ tautomer of

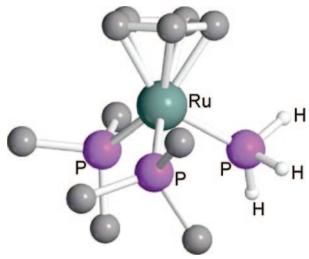

Figure 22. X-ray crystal structure of the cation $[CpRu(PPh_3)_2(PH_3)]^+$ (**120**). Hydrogen atoms, except those of PH_3, omitted for clarity; only *ipso*-carbons of phenyl rings shown. Adapted from ref 105.

Scheme 45

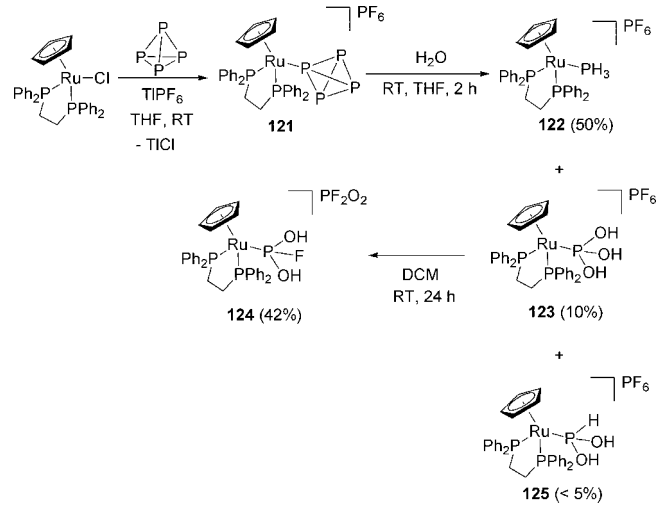

phosphorous acid as a monodentate ligand.[107] On standing at room temperature in DCM, compound **123** easily transforms into the unexpected compound $[CpRu(dppe)\{PF(OH)_2\}](PF_2O_2)$ (**124**) via hydrolysis of the hexafluorophosphate anion and subsequent replacement of one hydroxyl group by fluoride anion in the $P(OH)_3$ coordinated ligand. Complex $[CpRu(dppe)\{PH(OH)_2\}]PF_6$ (**125**), which contains the pyramidal tautomer of the hypophosphorous acid, H_3PO_2, was also observed as a minor product in a few cases in the hydrolyzed solution of **121**.

To confirm the nature of both **123** and **125**, the reaction of $[CpRu(PPh_3)_2Cl]$ in THF with aqueous solutions of the low-valent phosphorus oxyacids, H_3PO_2 and H_3PO_3, was attempted. The direct reaction was straightforward and resulted in the formation of the targeted products $[CpRu(PPh_3)_2\{PH(OH)_2\}]^+$ (**126**) and $[CpRu(PPh_3)_2\{P(OH)_3\}]^+$ (**127**)[108] (Scheme 46), via tautomerization of the tetrahedral acid form into the pyramidal phosphine-like species $PH(OH)_2$ and $P(OH)_3$, respectively. Further reaction with H_3PO_2 and H_3PO_3 resulted in the replacement of a second triphenylphosphine molecule to give $[CpRu(PPh_3)\{PH(OH)_2\}_2]^+$ (**128**) and $[CpRu(PPh_3)\{P(OH)_3\}_2]^+$ (**129**), respectively.

Scheme 46

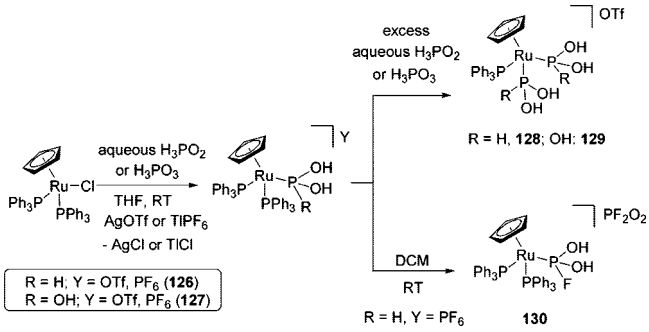

Scheme 47

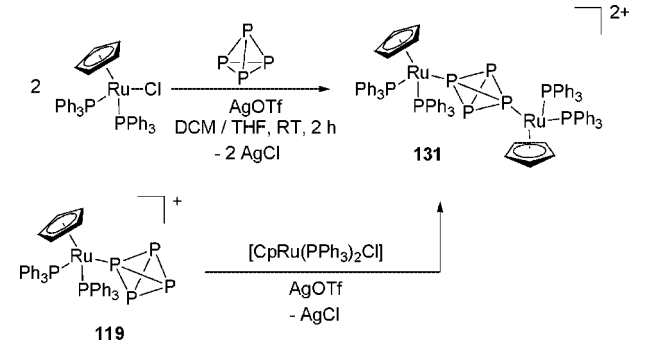

Although extremely rare, tautomeric forms of both hypophosphorus[109] and phosphorus acid[110] have been recently stabilized by coordination to both nickel and palladium clusters.

The hexafluorophosphate salt of **126** in DCM at ambient temperature slowly transforms into $[CpRu(PPh_3)_2\{PF(OH)_2\}]$-$PF_2O_2$ (**130**), whose difluorophosphate anion comes from the hydrolysis of PF_6^- similarly to the previously mentioned ruthenium complex **124**.

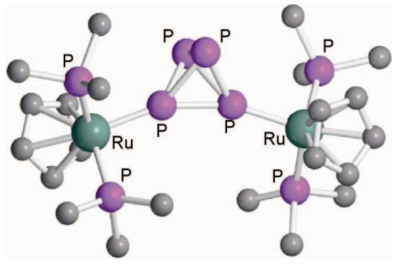

Figure 23. X-ray crystal structure of the complex cation $[\{CpRu(PPh_3)_2\}_2(\mu,\eta^{1:1}\text{-}P_4)]^{2+}$ (**131**); only *ipso*-carbons on phenyl rings shown. Adapted from ref 111.

By reaction of $[CpRu(PPh_3)_2Cl]$ with half equivalent of P_4 in the presence of AgOTf as chloride abstractor, the stable bimetallic complex $[\{CpRu(PPh_3)_2\}_2(\mu,\eta^{1:1}\text{-}P_4)](OTf)_2$ (**131**) was obtained.[111] Complex **131** could also be prepared by coupling complex **119** with the organometallic fragment $\{CpRu(PPh_3)_2\}^+$ as shown in Scheme 47. The structure of the binuclear diruthenium cation was determined by X-ray diffraction analysis (Figure 23).

Remarkably, the bimetallic cation of **131**, which contains the tetrahedral cage of P_4 sandwiched between the two $\{CpRu(PPh_3)_2\}$ fragments, exhibits only minor alterations of the metrical parameters upon double metalation with respect to its monometal precursor **119**. However, the peculiar electronic and steric situation in **131** imparts to the coordinated P_4 moiety a unique reactivity. The hydrolysis of **131** was studied to compare such a process with the behavior of the previously studied mononuclear ruthenium complexes. In the presence of a 100-fold excess of water, **131** is readily hydrolyzed to a complex mixture of products as shown in Scheme 48. Among them is the intriguing diphosphane complex cation $[\{CpRu(PPh_3)_2\}_2(\mu,\eta^{1:1}\text{-}P_2H_4)]^{2+}$ (**132**), which is generated together with other products, such as $[CpRu(PPh_3)_2(PH_3)]^+$ (**120**), $[CpRu(PPh_3)_2\{PH(OH)_2\}]^+$ (**126**), and $[CpRu(PPh_3)_2\{P(OH)_3\}]^+$ (**127**) and free phosphorus acids (ca. 17%). Other minor products are also formed, coming from the disproportionation and the partial degradation of the coordinated P_4 moiety, suggesting the existence of very complicated hydrolysis pathways for the sandwiched P_4 ligand. On the basis of a mechanistic investigation, it was proposed that $[\{CpRu(PPh_3)_2\}_2(\mu,\eta^{1:1}\text{-}P_2H_4)]^{2+}$ forms directly from **131**, rather than by reaggregation of intermediates after formation of transient-free diphosphane P_2H_4. Once generated within the coordination polyhedron supported by the two $\{CpRu(PPh_3)_2\}$ moieties, the labile species P_2H_4, which as a free molecule decomposes at a temperature higher than −30 °C,[112] is stabilized by double metalation at ruthenium and could be characterized by spectroscopic and crystallographic methods (Figure 24).

Further insights into the hydrolysis of the homobimetallic complex **131** were obtained by repeating the reaction with a large excess of water, i.e., 500 equiv instead of 100.[113] In such a case, the reaction was complete in ca. 10 min (Scheme 49), yielding only the novel compound $[\{CpRu(PPh_3)_2\}_2\{\mu,\eta^{1:1}\text{-}PH(OH)PHPH_2\}](OTf)_2$ (**133**, see Figure 25) and an equimolar amount of phosphorous acid, H_3PO_3. The diruthenium complex **133** contains the unknown species 1-hydroxytriphosphane, $PH(OH)PHPH_2$, as bridging ligand sta-

Scheme 48

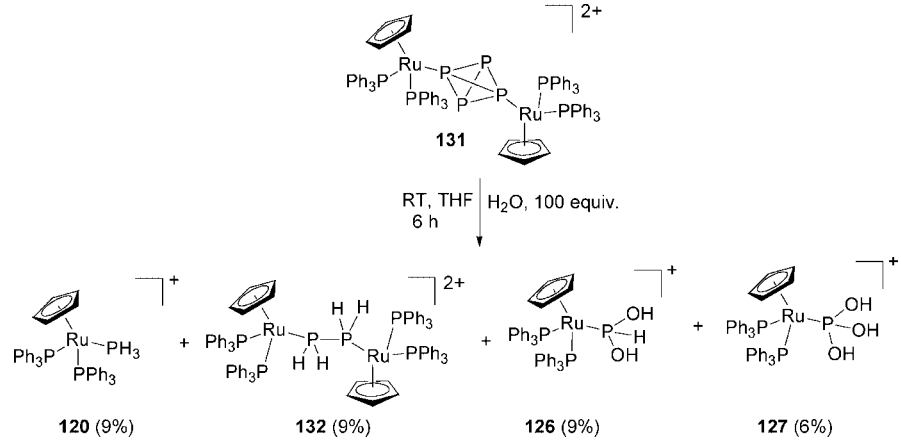

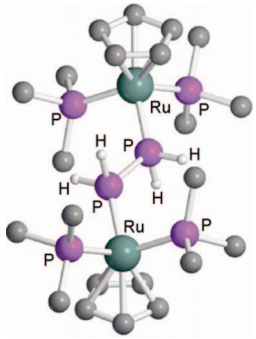

Figure 24. X-ray crystal structure of the complex cation [{CpRu(P-Ph_3)$_2$}$_2$(μ,$\eta^{1:1}$-P_2H_4)]$^{2+}$ (**132**). Hydrogen atoms omitted for clarity, except those of P_2H_4; only *ipso*-carbons on phenyl rings shown. Adapted from ref 111.

bilized in solution at room temperature via coordination to the two ruthenium fragments {CpRu(PPh_3)$_2$}.[114] Interestingly, the new triphosphane species PH(OH)PHPH_2 bridging the two ruthenium atoms contains two stereogenic centers; therefore, complex **133** exists in solution as a mixture of two diastereoisomers, in a ratio of 83% to 17% according to NMR measurements.

It is noteworthy that, while the hydrolysis of free P_4 takes place in alkaline water and gives as final products PH_3 and H_3PO_2, once P_4 is sandwiched between two metal centers as in **133**, the hydrolytic disproportionation follows a different pathway that markedly depends on the amount of water used as far as the nature and the distribution of the final products is concerned (see Schemes 44, 45, 48, and 49).

A further breakthrough in this chemistry was achieved by reacting the dimer **131** with a small excess of water (1:20) and allowing the system to stay for longer times (Scheme 50).[115] Reducing the amount of water, in comparison to the previous experiments, slowed down the reaction rate significantly, and in the final reaction mixture the most abundant species were two ruthenium bimetallic complexes [{CpRu(P-Ph_3)}{μ,$\eta^{2:1}$-P(OH)$_2$PHPHPH(OH)}{CpRu(PPh_3)$_2$}]$^{2+}$ (**134**) and [{CpRu(PPh_3)$_2$}{μ,$\eta^{1:1}$-P_2H_4}{CpRu(PPh_3){P(OH)$_3$}}]$^{2+}$ (**135**). The reaction mixture contains also free phosphorus acid, H_3PO_3 and small amounts of the already described mono- and diruthenium hydrolysis products **120**, **132**, **126**, and **127**.

Complex **134** contains a new phosphorus species, namely, 1,1,4-tris(hydroxyl)tetraphosphane, previously unknown in the literature, which is 1,4-η^2 and 3-η^1-coordinated to the nonequivalent fragments {CpRu(PPh_3)} and [CpRu(PPh_3)-{(POH)$_3$}]. This tetraphosphane species, like PH(OH)PHPH_2 or P_2H_4, is stabilized via coordination to the two ruthenium centers, forming polynuclear Ru_2P_x assemblies ($2 \leq x \leq 4$). Moreover, the interception of the novel species 1,1,4-tris(hydroxyl)tetraphosphane in **134** gives some hints about the mechanism ruling the metal-mediated hydrolysis of **131**. Indeed, the formation of **134** can be rationalized via a stepwise addition of four molecules of water to the P_4 bridging the two ruthenium centers. In this way, the addition of each water molecule causes the selective cleavage of a P−P bond until the observed linear tetraphosphane topology is generated. In the last step, displacement of a triphenylphosphine ligand to one ruthenium center favors the coordination of a PH(OH) unit yielding complex **134**.

In section 3.1.2, the intriguing chemistry of phosphametallocenes has been shown, in particular the rich and fascinating reactivity of pentaphosphaferrocene, [Cp*Fe(η^5-P_5)] (**14**), with half-sandwich complexes of many transition metal species. The related [Cp*Ru(η^5-P_5)] (**67**) is also known, although its chemistry has been much less studied than that of its lighter congener. Scheme 51 shows that the cothermolysis of **14** with [{Cp*Ru(CO)$_2$}$_2$] in decalin at 190 °C for a prolonged time allows the *cyclo*-P_5 ring transfer from iron to ruthenium.[80] In this way, the new pentaphospharutenocene [{Cp*Ru(η^5-P_5)] (**67**) is formed in good yield (63%). Previously, the preparation of **67** was attempted by direct reaction of elemental phosphorus with [Cp*Ru(CO)$_2$-

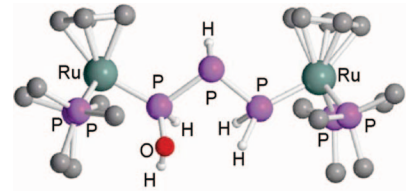

Figure 25. X-ray crystal structure of the cation [{CpRu(P-Ph_3)$_2$}$_2${μ,$\eta^{1:1}$-PH(OH)PHPH_2}] (**133**); only *ipso*-carbons on phenyl rings shown. Adapted from ref 113.

Scheme 50

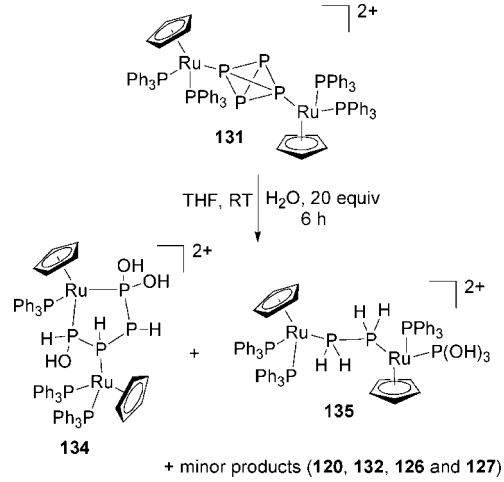

Scheme 51

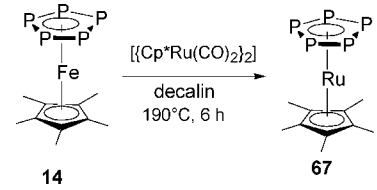

Scheme 49

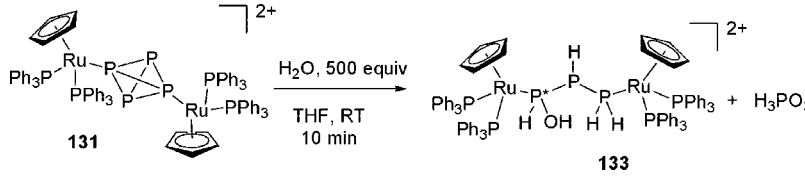

Scheme 52

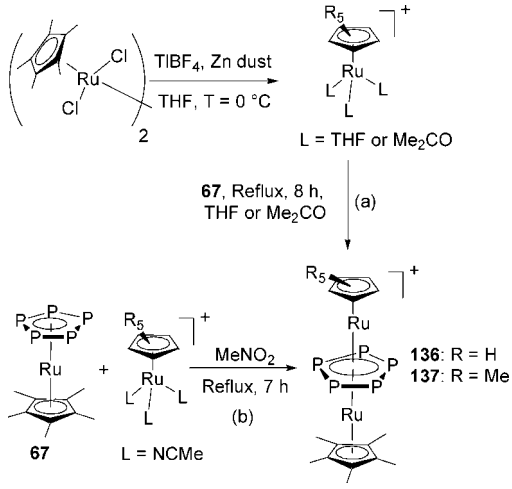

Br] in boiling decalin, but the yield was far too low (16% after 45 h of reaction time).[60] The [Cp″Ru(η^5-P_5)] (**74**) also has been obtained from the cothermolysis of **14** with [{Cp″Ru(CO)$_2$}$_2$] (vide supra, Scheme 30), albeit in modest yield and mixed with several other products.[81] Among these are worth mentioning the diruthenium and triruthenium clusters [{Cp″Ru}$_3$P$_5$] (**75**) and [{Cp″Ru}$_2$P$_4$] (**79**).

Mixed Fe/Ru systems bearing the *cyclo*-P_5 ligand as internal slice in triple-decker complexes, such as [Cp^{R}Fe-(μ,$\eta^{5:5}$-P_5)RuCp*]$^+$ (Cp^R = Cp, **68**; Cp* = **69**)[76] or other Fe/Ru clusters incorporating naked phosphorus units, also have been synthesized and are described in Section 3.1.

Diruthenium triple-decker complexes have been prepared by Kudinov et al.[76] Starting from the half-sandwich complex **67**, the reaction with [CpRu(CH$_3$CN)$_3$]$^+$ in boiling MeNO$_2$ gave complex [{CpRu}$_2$(μ,$\eta^{5:5}$-P_5)] (**136**) in modest yield (41%) as shown in Scheme 52 (path b). The preparation of the Cp* analogue [{Cp*Ru}$_2$(μ,$\eta^{5:5}$-P_5)] (**137**) was accomplished either by using the same procedure or by refluxing [Cp*Ru(solv)$_3$]$^+$ in THF or acetone (solv = THF, Me$_2$CO, Scheme 52, path a). Higher yields were obtained by starting from [Cp*Ru(S)$_3$]$^+$ (S = THF or Me$_2$CO) than from the more commonly used [Cp*Ru(MeCN)$_3$]$^+$ precursor (82% instead of 57%). In all cases, heating was essential to obtain **136** and **137** as pure products, because under milder conditions, complex mixtures are obtained.

Extensive work about the coordination chemistry of phosphorus monoxide PO and diphosphorus oxide P$_2$O has been carried out by Carty and co-workers in the past decade. As already explained in section 3.1, P$_2$O is a highly unstable molecule that has been characterized in matrices and, like its lighter omologue N$_2$O, has a linear structure, which was observed in organometallic compound **99** prepared by Scherer.[89] By studying the open-faced 62-electron cluster [Ru$_4$(CO)$_{12}$(μ_3-PNPr$^i_2$)], it was observed that, by treating this compound with the strong acid HBF$_4$, the hydroxyphosphinidene cluster [Ru$_4$(CO)$_{13}$(μ_3-POH)] (**138a**) was formed as the major product, together with a small amount of the unexpected cluster [{Ru$_4$(CO)$_{13}$}$_2$(μ_6,η^2-P$_2$O)] (**138b**), as shown in Scheme 53.[116] The molecular structure of **138b** obtained by X-ray diffraction shows that the elusive species P$_2$O bridges the two {Ru$_4$(CO)$_{13}$} cluster fragments, assuming a bent POP structure. Moreover, ^{31}P{^{1}H} NMR shows only a singlet resonance at 509 ppm, which is the characteristic region of μ_3-PO ligand.[117] P$_2$O behaves as an 8-electron donor, the equivalent of two 4-electron donor

Scheme 53

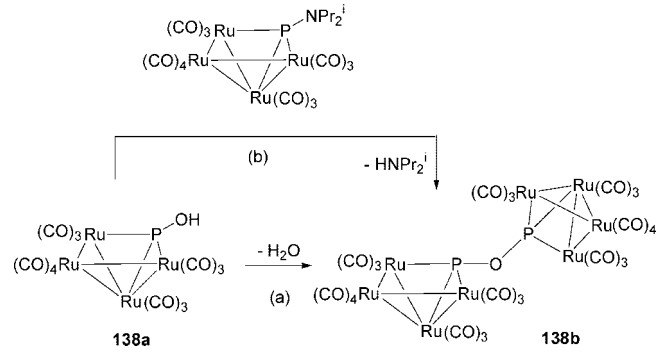

phosphinidene groups. The formation of **138b** has been explained either as deriving from intermolecular condensation of cluster [Ru$_4$(CO)$_{13}$(μ_3-POH)] (Scheme 53, path a) or as being the product of coupling of [Ru$_4$(CO)$_{12}$(μ_3-PNPr$^i_2$)] with [Ru$_4$(CO)$_{13}$(μ_3-POH)] after amine elimination (Scheme 53, path b).

3.3. Osmium

Osmium complexes deriving from the activation of white phosphorus are scarcely represented, and their chemistry has not been practically investigated. Apart from the pentaphosphaosmacene species [Cp*Os(η^5-P_5)] (**73**) obtained like its ruthenium germane via intramolecular *cyclo*-P_5 transfer from **14** to osmium by cothermolysis with [{Cp*Os(CO)$_2$}$_2$],[80] the only other known osmium complex derived from the activation of white phosphorus is the recently prepared [CpOs(PPh$_3$)$_2$(η^1-P$_4$)]OTf (**139**), which contains a tetraphosphorus tetrahedron coordinated to the {CpOs(PPh$_3$)$_2$} moiety.[118] Complex **139** was prepared by reaction of white phosphorus with [CpOs(PPh$_3$)$_2$Cl] in a 1:1 THF/DCM mixture at RT in the presence of silver triflate to remove the coordinated chloride (Scheme 54). Complex **139**, which was authenticated by NMR and X-ray analysis, shares with [CpRu(PPh$_3$)$_2$(η^1-P$_4$)]$^+$ (**119**) most of its chemical properties and similarly undergoes slow hydrolysis in THF, giving free hypophosphorous and phosphorus acids and the cationic species [CpOs(PPh$_3$)$_2$(PH$_3$)]$^+$ (**140**) and [CpOs(PPh$_3$)$_2${P-(OH)$_3$)}]$^+$ (**141**). Other unidentified products complete the hydrolysis reaction.

The solid-state structure of **139** was determined, and a view of the complex cation is given in Figure 26. As expected, the substitution of Os for Ru does not significantly affect the geometry of the cation in **139**, which is similar to that of the ruthenium complex **119**, owing to the similarity in the atomic radii of the two metals.

Scheme 54

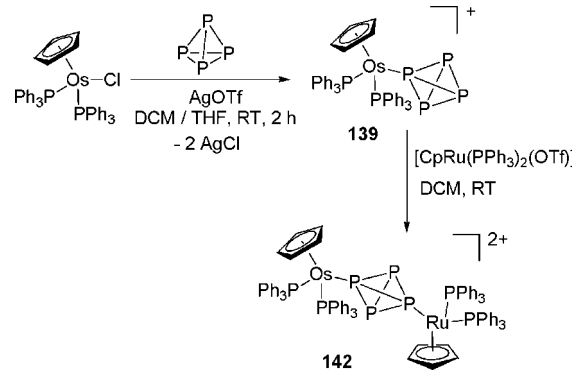

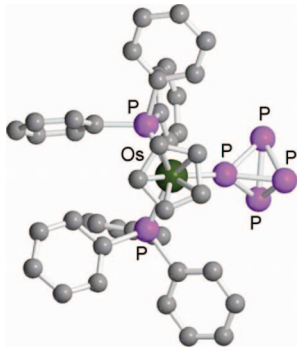

Figure 26. X-ray crystal structure of the cation $[CpOs(PPh_3)_2(\eta^1\text{-}P_4)]^+$(**139**). The hydrogen atoms are omitted for sake of clarity; adapted from ref 118.

The reaction of **139** with the ruthenium complex $[CpRu(PPh_3)_2Cl]$ in DCM yielded the heterodinuclear dimer $[\{CpRu(PPh_3)_2\}\{CpOs(PPh_3)_2\}(\mu,\eta^{1:1}\text{-}P_4)]^{2+}$ (**142**), the first heterodinuclear species containing a bridging tetraphosphorus *tetrahedro*- ligand authenticated by X-ray crystallography. The structure of the dimer resembles that of the diruthenium analogue **131** with disordered occupation of the two metal sites. The hydrolysis of **142** has been briefly investigated and does not deserve additional comments as it parallels that of the homodiruthenium compound **131**.

4. Group 9 Metals

4.1. Cobalt

The first organometallic cobalt complex containing a "naked" phosphorus atom as ligand was reported by Simon and Dahl.[4] The tetrameric Co complex $[\{CpCo(\mu_3\text{-}P)\}_4]$ (**143**) was prepared by refluxing a toluene solution of $[CpCo(CO)_2]$ with a stoichiometric amount of white phosphorus. Black−green, air-stable crystals were isolated, and the corresponding X-ray crystal structure was determined (Figure 27).

Each "naked" phosphorus atom acts as triply bridging ligand to three Co atoms, yielding a cubane-like tetrameric structure isoelectronic to the previously known neutral chalcogen complex $[Cp_4Fe_4S_4]$. The packing of the orthorhombic unit cell is kept together by long-range van der Waals forces. Each Co atom having similar localized environment is coordinated by η^5-Cp ring, three P atoms, and another Co atom with a long contact Co(1)−Co(3) of 3.624(1) Å. The metal−metal interactions, however, weaker than the Co−P bonds, represent the driving force for the substantial deformations from the ideal geometry of the M_4X_4 cluster, taking into account both the minimization of nonbonded repulsions and interorbital electron-pair interactions, finally giving a wider bridging angle. The tetrameric nature of the complex was also confirmed by mass spectrometric data.

Scheme 55

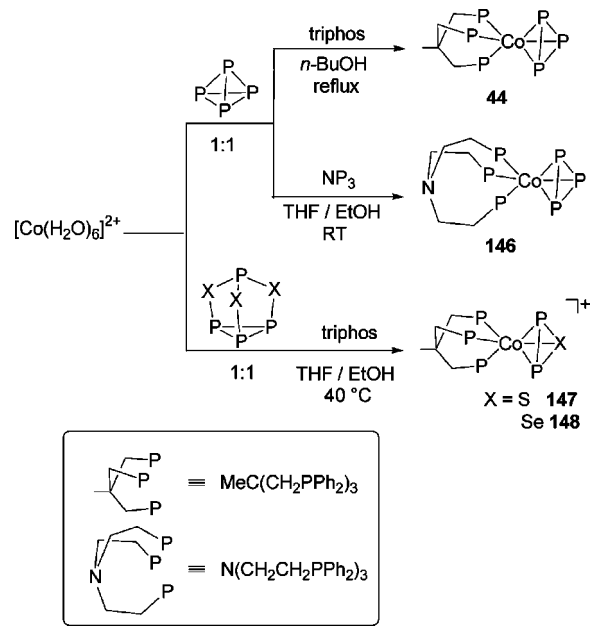

The reactivity of group 9 transition metal complexes stabilized by tripodal polyphosphines with white phosphorus was explored in Florence by Sacconi et al. starting from 1978. From the reaction of $[Co(H_2O)_6](BF_4)_2$ with an excess of white phosphorus in the presence of the ancillary ligand triphos in *n*-BuOH at reflux under nitrogen, the complex $[(triphos)Co(\eta^3\text{-}cyclo\text{-}P_3)]$ (**44**) containing the *cyclo*-triphosphorus unit was obtained (Scheme 55).[6] The corresponding Rh and Ir analogues (**144** and **145**) were obtained later on (see sections 4.2 and 4.3). Orange crystals of **44** are diamagnetic and air-stable also in THF, DCM, and $CH_3CH_2NO_2$ solutions.

The corresponding X-ray crystal structure (Figure 28) shows that the metal is coordinated by three P atoms of the tripodal ligand and the three atoms of the *cyclo*-P_3 unit in a staggered geometric arrangement, with a *cyclo*-P_3-to-Co average distance of 2.301 Å.

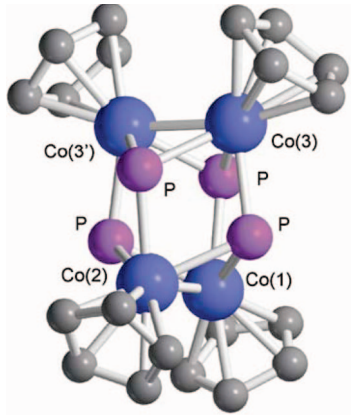

Figure 27. X-ray crystal structure of $[\{CpCo(\mu_3\text{-}P)\}_4]$ (**143**) showing the tetrahedral geometry and Cp coordination. Adapted from ref 4.

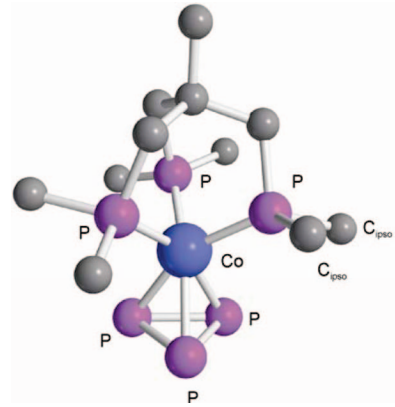

Figure 28. Inner core of complex $[(triphos)Co(\eta^3\text{-}cyclo\text{-}P_3)]$ (**44**) showing *ipso*-carbons only of phenyl rings on triphos; adapted from ref 6.

A similar reactivity was observed by exchanging triphos with the potentially tetradentate tris(2-diphenylphosphinoethyl)amine $N(CH_2CH_2PPh_2)_3$, NP_3, but running the reaction in THF/ethanol at room temperature instead of refluxing *n*-butanol (Scheme 55). The product $[(NP_3)Co(\eta^3\text{-}cyclo\text{-}P_3)]$ (**146**), insoluble in common organic solvents such as THF, benzene, $Cl_2CH_2CH_2Cl_2$, and $CH_3CH_2NO_2$, was isolated as rhombohedral crystals, and the corresponding solid-state structure was obtained.[119] As for **44**, the central atom is hexacoordinate by the three P atoms of NP_3 acting as tridentate tripodal ligand and the η^3-P_3 unit. The Co−P average distances in **146** were found to be remarkably shorter than in **44**, at 2.25 Å, while the P−Co−P angles have a mean value of 102.6°, much larger than that for **44** (54.9°). No significant changes in the *cyclo*-P_3 unit were observed in passing from **44** to **146** (P−P distance 2.14 Å); however, a distinctive shortening of the P−P distance from P_4 to *cyclo*-P_3 (2.14 vs 2.21 Å) was rationalized by partial delocalization of the electron charge of the P_3 fragment to the more electronegative Co(tripod) moiety [tripod = triphos, NP_3]. No Co−N coordination was observed for this complex (Co−N distance at 3.42 Å).

Sandwich complexes featuring three-membered ring structurally and chemically related to *cyclo*-P_3 were prepared by Stoppioni and co-workers from the reaction of the tetraphosphorus trichalcogenides, P_4S_3 and P_4Se_3, with cobalt hydrated salts following the protocol shown in Scheme 55 above.[120] Thus, the thia- and selenadiphosphirene species $[(triphos)Co(\eta^3\text{-}cyclo\text{-}P_2X)]BF_4$ [X = S (**147**), Se (**148**)] could be prepared and completely characterized by spectroscopic and crystallographic methods. The formal replacement of sulfur or selenium for phosphorus in the *cyclo*-P_3 ring accounts for the formation of monocationic species whose chemistry and reactivity, paralleling that of **44**, has been already described.[14a]

An important class of "double-sandwich" complexes of Co and Ni containing bridging *cyclo*-P_3 ligands was described by the Florentine group in the same years.[51,14a,121] Reaction of white phosphorus with $[M(H_2O)_6](BF_4)_2$ and triphos gave complexes of general formula $[\{(triphos)M\}_2(\mu,\eta^{3:3}\text{-}cyclo\text{-}P_3)]Y_n$ [M = Co (**149**), Ni (**150**); Y = BF_4, BPh_4; n = 1, 2) as homobimetallic compounds (Scheme 56). In these complexes, the *cyclo*-P_3 ring system behaves as 3π donor and is able to bridge two metal atom fragments. Heterobimetallic complexes such as $[\{(triphos)Co\}(\mu,\eta^{3:3}\text{-}cyclo\text{-}P_3)\{Ni(triphos)\}](BPh_4)_2$ (**151**) were obtained from the reaction of **44** with $[Ni(H_2O)_6](BF_4)_2$ and 1 equiv of triphos in DCM/EtOH at RT. Anion exchange was performed in situ by adding $NaBPh_4$ to the reaction mixture.[122]

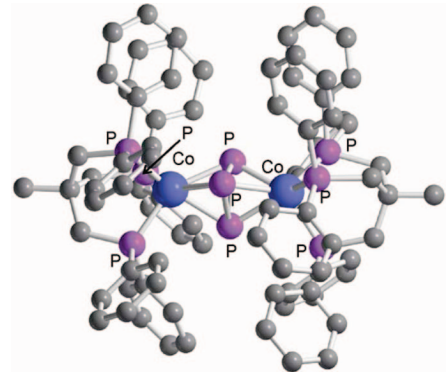

Figure 29. A view of the $[(triphos)Co\text{-}\mu\text{-}(\eta^3\text{-}P_3)Co(triphos)]^+$ cation; adapted from ref 50.

In some cases, X-ray crystal structures of these complexes (and of their *cyclo*-As_3 analogues) including solvent molecules were obtained. The isomorphous complexes $[\{(triphos)Ni\}_2(\mu,\eta^{3:3}\text{-}cyclo\text{-}P_3)](BPh_4)_2 \cdot 2\ Me_2(CO)$ (**150**, see section 5.1) and $[\{(triphos)Co\}(\mu,\eta^{3:3}\text{-}cyclo\text{-}P_3)\{Ni(triphos)\}](BPh_4)_2 \cdot 2\ Me_2(CO)$ (**151**) consist of dinuclear cations where each metal atom is bonded to the three P atoms of triphos and to the three bridging atoms of the *cyclo*-P_3 group, forming a distorted six-coordinate arrangement, the main difference within the series being the degree of skewing between triphos and $\mu,\eta^{3:3}$-P_3 moiety, clearly reflecting the different steric effects imparted in each case by triphos ligand (Figure 29). The M−P(ring) distances range from 2.32 to 2.38 Å, which are longer than those for **44** and **146**, again as an effect of the steric repulsions between two triphos ligands facing each other. The P−P bond lengths within the *cyclo*-P_3 group are slightly longer than for the mononuclear analogues (avg. 2.164 compared to 2.13−2.14 Å). The study was complemented by MO calculations. The role of *cyclo*-triphosphorus *in plane* σ-orbitals in coordinating transition metal fragments was also highlighted later.[123]

Electrochemical studies were also carried out on these sandwich compounds.[124] The 31- and 33-electron dications identified as Co_2P^{2+} and Ni_2P^{2+} were formed as described above and then reacted with $NaBH_4$ to get the singly charged 32- and 34-electron cations by one-electron reduction, respectively. Reversible three-step voltammograms made of a one-electron oxidation and two one-electron reduction processes were obtained using a Pt electrode for Co_2P^+ in

Scheme 56

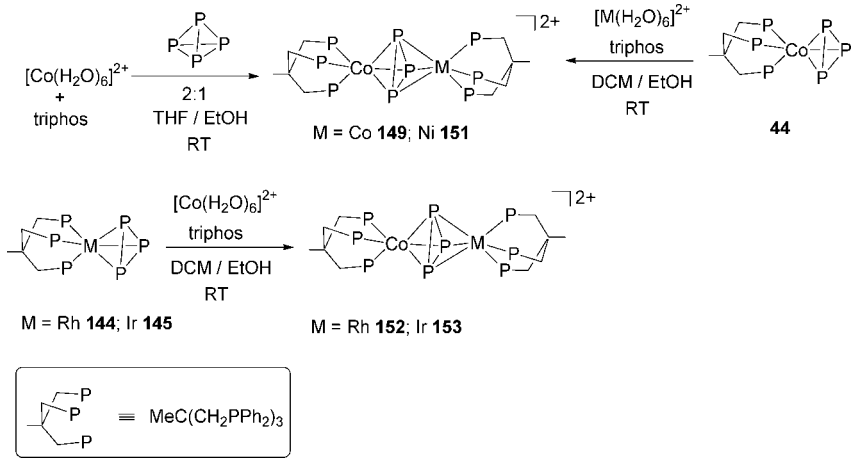

acetonitrile solutions. A bright green solution of diamagnetic Co_2P^{3+} was obtained via bulk oxidation of Co_2P^{2+} at controlled potential. The $E_{1/2}$ values obtained were reported as +0.22 V (Co_2P, +2/+3), −0.47 V (Co_2P, +2/+1), −1.61 V (Co_2P, +1/0) vs $Ag/AgNO_3$ 0.01 M, 0.1 M Et_4NBF_4, 25 °C.

The structural and magnetic properties of triple-decker sandwich complexes comprising triphos and two 4d or 5d metals bridged by *cyclo*-P_3 were studied by Bianchini et al.[125] Precursors [(triphos)M(η^3-*cyclo*-P_3)] (see section 4.2), obtained from the reactions of $[RhCl(C_2H_4)_2]_2$ [M = Rh (**144**)] or $[Ir(CO)Cl(PPh_3)_2]$ [M = Ir (**145**)] with P_4 in the presence of triphos, further react with $[M'(H_2O)_6](BF_4)_2$ [M′ = Co, Ni] to yield the bimetallic complexes of general formula [{(triphos)M}($\mu,\eta^{3:3}$-*cyclo*-P_3){M′(triphos)}]Y_n (Y = BF_4, BPh_4; n = 1, 2) (Scheme 56). Cobalt containing complexes [{(triphos)M}($\mu,\eta^{3:3}$-*cyclo*-P_3){Co(triphos)}]Y_2 (M = Rh, (**152**); M = Ir, (**153**); Y = BF_4, BPh_4) are 1:2 electrolytes, air-stable in the solid state, but unstable in solution. Magnetic moment measurements show that **152** and **153** are paramagnetic with a doublet ground state, whereas the Rh−Ni analogue has a magnetic moment that is dependent on the nature of the counteranion and of the solvent in the lattice, ranging from 1.3−1.6 μ_B at room temperature to 0.7 μ_B at 100 K (see section 5.1). A full study of this class of "triple-decker" sandwich complexes [{(triphos)M_1}($\mu,\eta^{3:3}$-*cyclo*-P_3){M_2(triphos)}]Y_n (M_1 = Co, Ni, Rh; M_2 = Rh, Ir; Y = BF_4, BPh_4; n =1, 2) was later disclosed by the same authors.[126] The solid-state structure of **152**, crystallizing as BPh_4^- salt, shows a distorted geometry around the metal atoms, featuring a Rh−P(ring) distance ranging from 2.31 to 2.48 Å and a Co−P(ring) distance ranging from 2.33 to 2.56 Å. The intermetallic Rh−Co distance was found to be at 3.869(6) Å, excluding any metal−metal interactions between the two centers. Such parameters are indicative of strong metal−ligand interactions in the complex.

Further studies on this class of compounds included the evaluation of steric effects imparted by the substituents on the P atoms of the tripodal ligand. Hence, the phenyl rings of triphos were replaced by ethyl groups by using 1,1,1-tris(diethylphosphinomehyl)ethane, $MeC(CH_2PEt_2)_3$, etriphos. Homo- and heterometal triple-decker complexes bridged by *cyclo*-P_3 with mixed triphosphine ligands of general formula [{(triphos)Co}($\mu,\eta^{3:3}$-*cyclo*-P_3){M(etriphos)}]Y_2 (M = Fe, (**43**); Co, (**154**); Ni, (**155**); Y = PF_6, BPh_4) were then obtained.[50] The presence of the etriphos ligand allowed for the coordination of the Fe(II) cation (see section 3.1.1), which did not occur when the less nucleophilic triphos was used, thus yielding the first 30-electron dinuclear *cyclo*-P_3 complex, which was also characterized in the solid state by X-ray diffraction methods (Figure 30). The synthetic pathway is based on the reaction of **44** with $[M(H_2O)_6](BF_4)_2$ in DCM/EtOH at room temperature in the presence of etriphos and $(Bu_4N)PF_6$ or $NaBPh_4$ salts. The presence of etriphos allows for the solubility of the complexes in chlorinated solvents, acetone and nitroethane. Room-temperature magnetic moments were measured at 0.0 μ_B for **43**, 2.29 μ_B for **154**, and 3.12 μ_B for **155**, respectively, and were found to be temperature-invariant.

The structure of [{(triphos)Co}($\mu,\eta^{3:3}$-*cyclo*-P_3){Fe(etriphos)}]$(PF_6)_2$ (**43**), crystallized as dichloromethane solvate, shows the usual triple-decker arrangement formed by the tripodal ligands and the internal "slice" of bridging *cyclo*-P_3 moiety. Interestingly, it was demonstrated that the size of the coordination polyhedron measured from the M−P and M−M distances increases almost linearly with the number of valence electrons, reflecting the antibonding nature of the orbital occupied by the electrons in excess of 30 in this remarkable series of compounds. Table 1 above summarizes this trend.

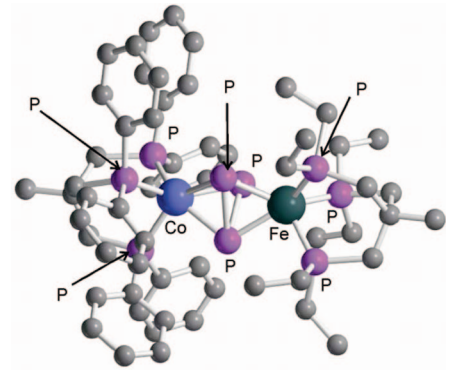

Figure 30. X-ray crystal structure of [{(triphos)Co}($\mu,\eta^{3:3}$-*cyclo*-P_3){Fe(etriphos)}]$^{2+}$ (**43**); adapted from ref 50.

Table 1. Structural Data for the [LM($\mu,\eta^{3:3}$-*cyclo*-P_3)M′L′]$^{2+}$ Complexes (Bond Distances in Å)

M, M′	Co, Fe	Co, Co	Co, Ni	Ni, Ni
VE	30	31	32	33
M−P(L,L′)	2.20[a]	2.23[b]	2.24[b]	2.25[b]
M−P(η^3-P_3)	2.29	2.31	2.33	2.35
M···M′	3.80	3.86	3.93	3.99
P−P(η^3-P_3)	2.23	2.18	2.16	2.16

[a] L = triphos, L′ = etriphos. [b] L, L′ = triphos.

It was also suggested that the shortening of the M···M distances may increase the interactions between the metal orbitals and the orbitals lying in the plane of the *cyclo*-P_3 fragment, with the latter being a doubly degenerate set with essentially lone-pair antibonding character. The various aspects of coordination chemistry, MO studies, electronic spectral data, and magnetic and redox properties of tripodal phosphine based complexes described above was reviewed by Di Vaira and Sacconi.[51]

Within the series of triphos-stabilized monodecker *cyclo*-P_3 complexes, structural characterization in solution has included full $^{31}P\{^1H\}$ NMR spectroscopy of the diamagnetic derivatives. These data are summarized in Table 2. In the representative complex **44**, two featureless resonances are observed at room temperature, becoming more resolved at low temperature, but, however, not being resolved even at −80 °C. The chemical shifts belonging to triphos P atoms decrease on descending each group, and the variation is smaller in absolute value for cationic complexes compared to neutral analogues. Whereas little difference is observed for the chemical shifts belonging to *cyclo*-P_3 resonances, a larger effect is observed for M−P coupling constants (see Table 2).[127]

Although it forms a variety of triple-decker sandwich complexes, either homo- or heterodinuclear, the Sacconi's cobalt *cyclo*-triphosphorus compound **44** is endowed with further interesting reactivity, which may involve exocyclic coordination to one, two, or three P-atoms of the cyclotriphosphorus unit, as well as the involvement of the whole P_3 ring in building supramolecular aggregates. Among the most simple derivatives of [(triphos)Co(η^3-*cyclo*-P_3)], the adducts with coordinatively unsaturated middle transition metal fragments are worth mentioning. As an example of

Table 2. $^{31}P\{^1H\}$ NMR Spectral Data for [(triphos)M(η^3-*cyclo*-P_3)]$^{n+}$ Complexes (n = 0, 1) in CD_2Cl_2, RT

compound	chemical shifts (ppm)[a]		coupling constants (J, Hz)		
	$P_{(cyclo\text{-}P3)}$	$P_{(triphos)}$	P−P	M−$P_{(cyclo\text{-}P3)}$	M−$P_{(triphos)}$
[(triphos)Co(η^3-*cyclo*-P_3)] (**44**)	−276.21 br[b]	38.16 br[c]	n.o.		
[(triphos)Rh(η^3-*cyclo*-P_3)] (**144**)	−261.04 dq[c]	18.65 dq[c]	12	13	138
[(triphos)Ir(η^3-*cyclo*-P_3)] (**145**)	−312.89 q	−11.85 q	13		
[(triphos)Ni(η^3-*cyclo*-P_3)]BF_4 (**105b**)	−132.90 q	4.90 q	11		
[(triphos)Pd(η^3-*cyclo*-P_3)]BF_4(**317**)	−155.66 q	16.33 q	14		
[(triphos)Pt(η^3-*cyclo*-P_3)]BF_4 (**319**)	−217.43 q[d]	−18.58 q[d]	9	171	2476

[a] br, broad; d, doublet; q, quartet. [b] Broadened due to cobalt quadrupole. [c] Each ^{31}P resonance is doubled by coupling with ^{103}Rh (I = 1/2). [d] The ^{31}P resonances are flanked by satellites due to coupling with ^{195}Pt (I = 1/2).

Scheme 57

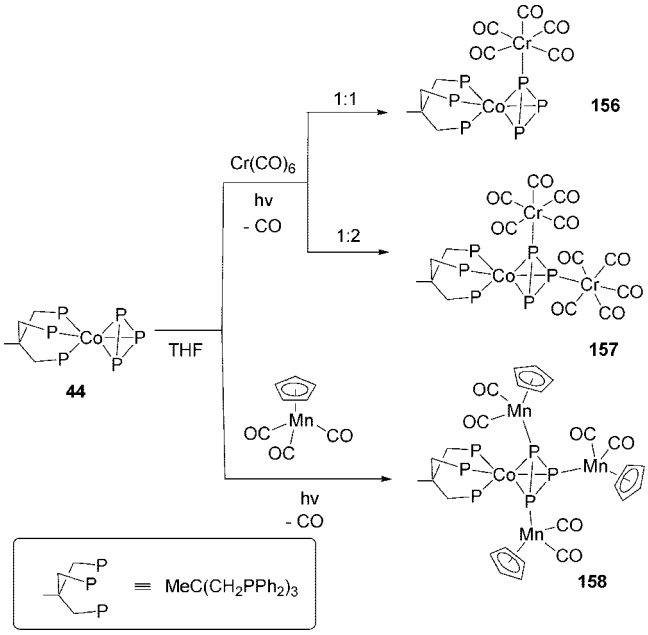

this class of reactions, Sacconi and co-workers showed that, when **44** is reacted with UV photolysed THF solutions of $Cr(CO)_6$, the new bi- and trinuclear heterometallic complexes [{(triphos)Co}(μ,$\eta^{3:1}$-*cyclo*-P_3){$Cr(CO)_5$}] (**156**) and [{(triphos)Co}(μ_3,$\eta^{3:1:1}$-*cyclo*-P_3){$Cr(CO)_5$}$_2$] (**157**) were obtained, depending on the Co/Cr ratio used (Scheme 57).[128] The X-ray crystal strucutre of **157** is shown in Figure 31. The η^3-P_3 moiety is now "sandwiched" between three metal centers but virtually unchanged in its structural parameters [$d_{(P-P)ave}$ = 2.14 Å]. The Cr−P bonds lie out of the plane of the P_3 ring, as deduced from the CrPCo and CrPP angles (ranging from 123.3 to 165.4°, respectively). The Cr−P distances at 2.42 Å suggest that *cyclo*-P_3 behaves as PPh_3 as donor ligand to Cr because these bond lengths are the same as those found in [$Cr(PPh_3)(CO)_5$].[129]

A similar approach was applied to the synthesis of [(triphos)Co(μ_4,$\eta^{3:1:1:1}$-*cyclo*-P_3){$CpMn(CO)_2$}$_3$] (**158**), i.e.,

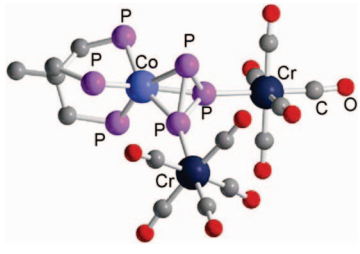

Figure 31. X-ray crystal structure of [{(triphos)Co}(μ_3,$\eta^{3:1:1}$-*cyclo*-P_3){$Cr(CO)_5$}$_2$] (**157**); phenyl groups on triphos omitted for clarity. Adapted from ref 128.

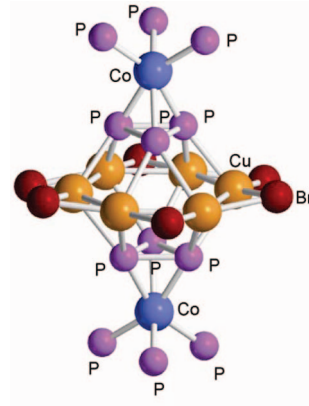

Figure 32. View of the core of [{(triphos)Co(η^3-*cyclo*-P_3)}$_2$($CuBr)_6$] (**162**); adapted from ref 132.

by reaction of **44** with [$CpMn(CO)_3$] in THF under UV light irradiation (Scheme 57). In this compound, each of the three P atoms of the *cyclo*-P_3 ring additionally binds to one $CpMn(CO)_2$ fragment with P−P bond distances in the tetrametalated μ_4,$\eta^{3:1:1:1}$-*cyclo*-P_3 ligand averaged at 2.131 Å, which is slightly shorter than in the parent complex **44**.[130]

A few years later, Stoppioni et al.[131] expanded this series of compounds, showing that other $M'(CO)_5$ fragments (M′ = Mo, W, Re) can coordinate to the *cyclo*-P_3 unit. The new complexes [{(triphos)Co}(μ,$\eta^{3:1}$-P_3){$M(CO)_5$}] [M = Mo, (**159**); W, (**160**)] and [{(triphos)Co}(μ,$\eta^{3:1}$-P_3){$Re(CO)_5$}]-BF_4·C_7H_8 (**161**) were obtained. The related rhodium derivatives will be briefly discussed in section 4.2.

A breakthrough in the reactivity of "naked" phosphorus units and ligands was published soon thereafter by Midollini and co-workers[132] who described the synthesis and the structure of the "super sandwich" complex [{(triphos)Co(η^3-*cyclo*-P_3)}$_2$($CuBr)_6$] (**162**) obtained from the reaction of **44** with CuBr in DCM or $THF/CHCl_3$ for 3 h at 30 °C under nitrogen. A highly unusual Cu_6 hexagonal core was formed, and by resolving the corresponding X-ray crystal structure, it was possible to observe that two symmetry-related [(triphos)Co(η^3-*cyclo*-P_3)] units are kept together by the Cu_6 moiety whose edges are symmetrically bridged by Br atoms. The inner core can be described as a cuboctahedron of Cu and P atoms with two triangular P_3 faces each capped with a (triphos)Co group (Figure 32).

The reactivity of **44** and its higher congeners toward coinage metal salts and complexes was further extended by Stoppioni and co-workers, who discovered new reaction pathways and complex geometries (Scheme 58). Thus, treatment of **44** and **144** with Cu(I) and Ag(I) derivatives such as [$MCl(PPh_3)]_4$, [$Cu(MeCN)_4$]Y (Y = BF_4, PF_6), or AgY (Y = NO_3, ClO_4) afforded the compounds [{(triphos)Co(μ,$\eta^{3:2}$-*cyclo*-P_3)}$_2$M]Y [M = Cu, Y = BF_4, PF_6 (**163**);

Scheme 58

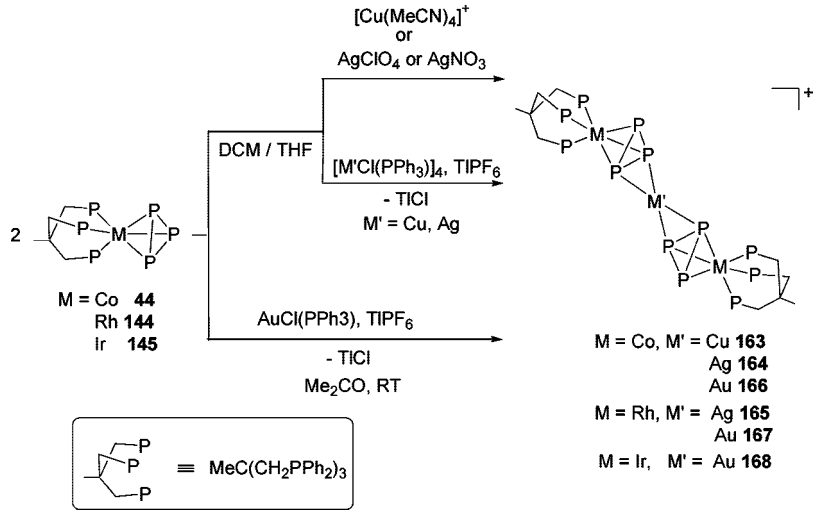

M = Ag, Y = ClO_4, PF_6 (**164**)].[133] The analogous rhodium/silver trinuclear complex, [{(triphos)Rh(μ,$\eta^{3:2}$-*cyclo*-P_3)}$_2$Ag]Y, [Y = OTf, PF_6 (**165**)] was also prepared from **144** and the appropriate silver salt AgY. Trinuclear gold complexes of formula [{(triphos)M(μ,$\eta^{3:2}$-*cyclo*-P_3)}$_2$Au]PF_6 [M = Co (**166**), Rh (**167**), Ir (**168**)] were also prepared for the three isomorphous [{(triphos)M(η^3-*cyclo*-P_3)}] complexes by reaction with gold(I) chloro derivatives in the presence of thallium hexafluorophosphate as chloride scavenger (see section 5.3).[134]

X-ray analysis for [{(triphos)Co(μ,$\eta^{3:2}$-*cyclo*-P_3)}$_2$Cu]PF_6 (**163**) shows that the Cu atom is bridging two {(triphos)Co(η^3-*cyclo*-P_3)} units with a geometry intermediate between distorted tetrahedral and square planar (Figure 33). This was explained by EHMO calculations on the model system [{(PH_3)$_3$Co(μ,$\eta^{3:2}$-*cyclo*-P_3)}$_2$Cu], indicating that the bonding between the Cu atom and the *cyclo*-P_3 moieties is due to the interaction between the empty s and p Cu orbitals and filled orbitals based on the P atoms of the rings. A drift of charge toward the Cu atom and the concomitant antibonding nature of the highest occupied molecular orbital (HOMO) resulting from the interactions between filled orbitals may account for the lengthening of the P−P bonds. Packing forces and steric effects caused by the phenyl rings on triphos could be responsible for the deviation from perfect tetrahedral structure about the Cu atom.

The cyclotriphosphorus unit is endowed with further reactivity than coordination to metal fragments, giving polymetallic complexes. In 1986, Stoppioni and co-workers[135] showed that, when the neutral complexes [(triphos)M(η^3-*cyclo*-P_3)] (M = Co, Rh, Ir) are reacted at 0 °C with either methyl triflate, MeOTf, or the oxonium salt (Me_3O)BF_4 in DCM, the novel methyltriphosphirene unit η^3-MeP_3 is obtained via electrophilic attack (Scheme 59), yielding the novel [(triphos)M(η^3-MeP_3)]Y complexes (M = Co (**169**), Rh (**170**), Ir (**171**); Y = BF_4, OTf).

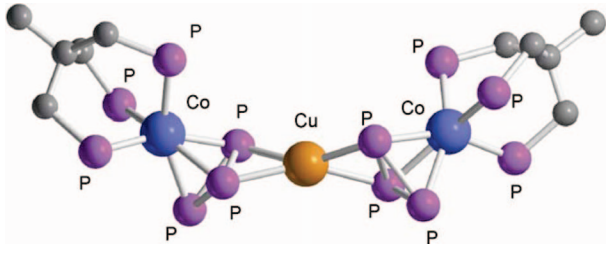

Figure 33. X-ray crystal structure of [{(triphos)Co(μ,$\eta^{3:2}$-*cyclo*-P_3)}$_2$Cu]$^+$ (**163**); phenyl rings on triphos omitted for clarity. Adapted from ref 133.

Scheme 59

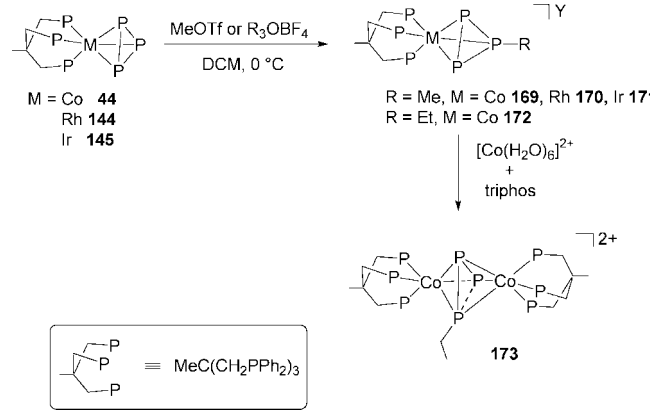

The X-ray crystal structure of **169** (Figure 34) shows that the Co(η^3-*cyclo*-P_3) core has undergone substantial deformation, which the authors attributed to the interactions of HOMO and lowest unoccupied molecular orbital (LUMO) of the Me carbocation with one component of the doubly degenerate set of high-energy occupied orbitals of **44**. The Co−P(Me) bond length was found to be 2.16 Å, much shorter than the other two Co−P distances (2.41 and 2.38 Å, respectively); the P(Me)−P bonds are also shorter than the other P−P bond within the η^3-MeP_3 unit (2.08 vs 2.17 Å).

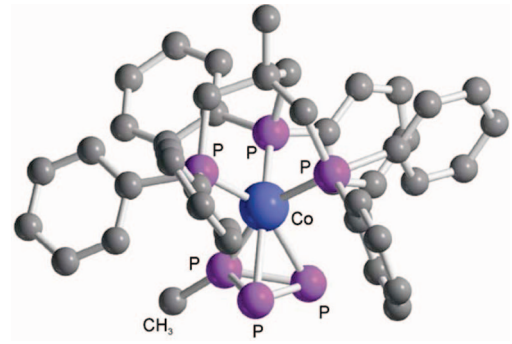

Figure 34. X-ray crystal structure of [(triphos)M(η^3-MeP_3)]$^+$ cation (**169**); adapted from ref 135.

A similar reactivity was reported by Huttner and coworkers, who described the reaction with Et_3OBF_4 yielding the ethyltriphosphirene complex [(triphos)Co(η^3-EtP_3)]BF_4 (**172**). Remarkably, complex **172** reacts with 1 equiv of $[Co(H_2O)]_6^{2+}$ and triphos to give the dication [{(triphos)-Co}$_2$(η^3-EtP_3)]$^{2+}$ (**173**) where a formal analogue of ethyltriphosphazide species is sandwiched between two (triphos)Co moieties.[136] A dynamic scrambling of the three P atoms of the EtP_3 ligand was observed by VT ^{31}P NMR spectroscopy.

Replacing MeOTf with triflic acid as electrophilic reagent in the reaction with **44** affords the unstable compound [(triphos)Co(η^3-P_3H)][$(OTf)_2$·(H_5O_2)] (**174**).[137] The formula was confirmed both by NMR and X-ray crystallography. Room-temperature ^{1}H NMR spectrum shows, apart from the triphos signals, a broad resonance peak at −13.75 ppm, consistent with the presence of one hydride hydrogen. The ^{31}P{^{1}H} NMR spectrum exhibits two broad temperature-invariant resonances at 28.21 (triphos) and −269.49 ppm (P_3), with the latter not affected by proton coupling and shifted at higher field compared to **44** (−276.21 ppm). This effect is rather unexpected if compared with the general downfield shift observed for cationic analogues of **44**, such as **169** described above. The authors suggest that the P_3 core has a structure consisting of a three-centered bond and two "classic" Co−P bonds, the overall interaction of the ring with the metal therefore being smaller than in the parent compound. The absence of P−H coupling was imputed to fast exhange between the Co−P bonds and rotation in solution of the P_3H group. Solid-state structural data, supported by Frontier Molecular Orbital (FMO) energy-matching criteria, confirm the existence of a three-centered Co−H−P bonding situation, where the added proton lies close to the Co−P edges and has similar bonding opportunities to the P_3 group as those available to Me^+ in **169**. The P−P bond lengths within the η^3-P_3 ring are scarcely affected by such a bonding mode. The attempt to rationalize the NMR fluxionality was the subject of further studies.[138] The paths for motion of the proton over the CoP_3 core were investigated by quantum mechanical procedures. It was concluded that several accessible pathways are available, and the one with the hydrogen atom residing in proximity of the metal atom should possess overall lower energies than those with the hydrogen localized on the P_3 far side. Then, the observed NMR fluxionality can be explained by relative rotations of triphos and P_3 core around an axis passing through the metal atom.

In the same study describing **174**, the one-electron oxidation of **44** with $[Cp_2Fe]PF_6$ was reported. The reaction yielded the cationic Co(II) complex [(triphos)Co(η^3-*cyclo*-P_3)]PF_6 (**175**) containing the radical cluster CoP_3^+ (Scheme 60). The electrochemical behavior of **44** was then studied, and the EPR spectrum of **175**, generated both by chemical and electrochemical methods, showed a magnetic moment of 2.2 μ_B at room temperature.

Complex **175** and its Ni isolectronic analogue, [(triphos)Ni(η^3-*cyclo*-P_3)]BF_4 (**150b**, see section 5.1), were reacted with the zerovalent platinum species [Pt(C_2H_4)(PPh_3)$_2$], capable of easily generating the carbene-like fragment Pt(PPh_3)$_2$ after ethene removal.[139] Whereas complex **150b** undergoes insertion of the Pt moiety in the P−P bond of the P_3 ring to yield [(triphos)Ni($\eta^{3:2}$-*cyclo*-P_3){Pt(PPh_3)$_2$}]BPh_4 (**176**, section 5.1), a more complex reaction occurs in the case of **175**, namely, the formation of a P_6 unit deriving from P−P coupling of two opened *cyclo*-P_3 fragments (Scheme

Scheme 60

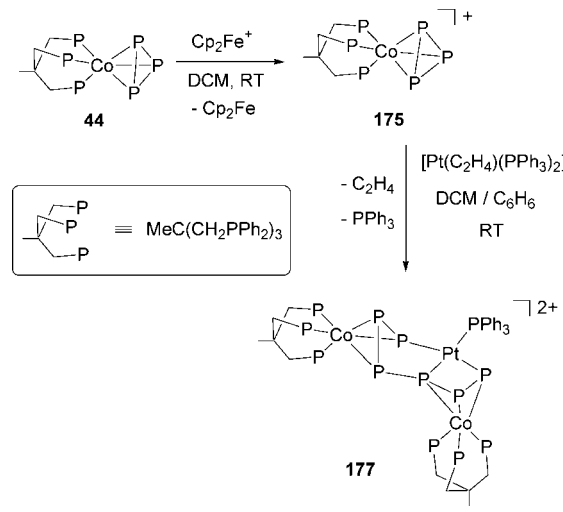

60). The resulting complex [{(triphos)Co}$_2$(μ_3,$\eta^{3:3:3}$-P_6H_2)-{Pt(PPh_3)}](OTf)$_2$ (**177**) was characterized in the solid state and solution, and its X-ray crystal structure is shown in Figure 35. The new P_6 unit is obtained via formal assembly of two [(triphos)Co(η^3-P_3)]$^+$ cations, via formation of a novel P−P bond, and a Pt(PPh_3) fragment, with the latter causing the elongation of the P−P bonds in the P_3 unit coordinated to Co (2.517 and 3.016 Å, respectively). The formation of **177** was explained by a first reaction step involving insertion of Pt(PPh_3)$_2$ into a P−P bond of the P_3 ring, followed by loss of a PPh_3 and final attachment of a second [(triphos)Co(η^3-P_3)]$^+$ cation to the vacant coordination site on Pt via the cyclotriphosphorus ring with simultaneous P−P bond forming between the two CoP_3 moieties.

Other multidentate polyphosphines were used to stabilize transition metal fragments able to activate white phosphorus. The reaction of white phosphorus with the coordinatively unsaturated system [(PP_3)M]$^+$ yields the trigonal bipyramidal [(PP_3)M(η^1-P_4)]$^+$ (M = Co, **178**; Rh, **179**) containing the intact P_4 molecule coordinated to the metal in an end-on fashion. This behavior is in sharp contrast with what was observed in the case of other tetradentate phosphine-based transition metal complexes as, for example, [(NP_3)Rh]$^+$, where the octahedral complex [(NP_3)Rh(η^2-P_4)]$^+$ (**180**) was

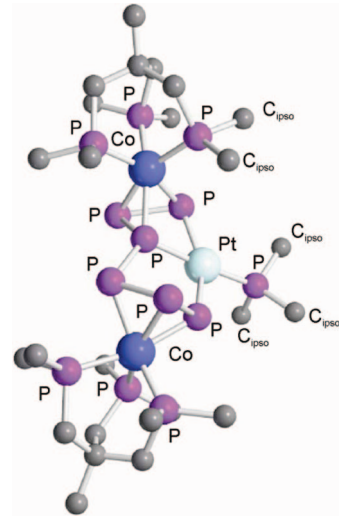

Figure 35. View of the core of the dication [{(triphos)Co}$_2$-(μ_3,$\eta^{3:3:3}$-P_6H_2){Pt(PPh_3)$_2$}]$^{2+}$ (**177**). Only the *ipso*-carbon of each phenyl ring is shown for clarity; adapted from ref 139.

Scheme 61

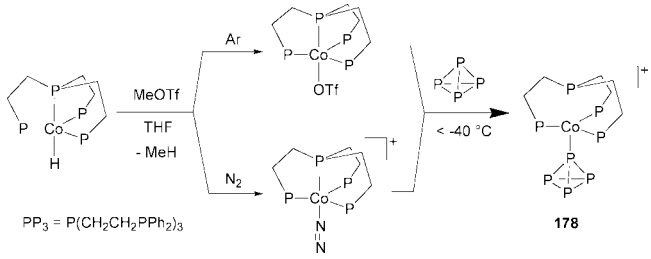

Scheme 62

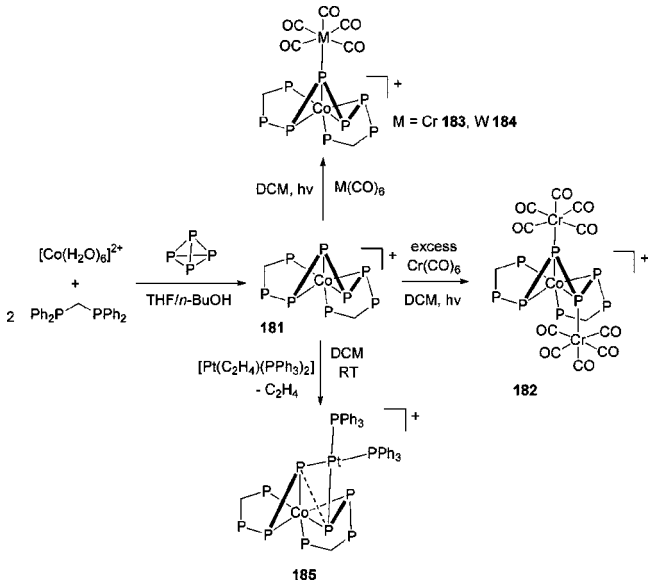

obtained (see section 4.2). In the latter case, a wingtip coordination mode is shown by the activated white phosphorus molecule.[140] The preparation of the tetraphosphorus adduct $[(PP_3)Co(\eta^1\text{-}P_4)]^+$ (**178**) involved the preliminary reaction of $[(PP_3)CoH]$ with MeOTf under argon or nitrogen in THF at RT that yields either the labile green species $[(PP_3)Co(OTf)]$ or the red dinitrogen complex $[(PP_3)Co(N_2)]^+$, respectively (Scheme 61). Cooling to −70 °C and adding an equimolar amount of white phosphorus in THF gave the deep violet η^1-P_4 adduct **178** with $^{31}P\{^1H\}$ NMR signals (THF-d_8 at 233 K) at −333.5 (m) and −472.3 ppm (dm) for the tetraphosphorus ligand coordinated to cobalt complex, showing downfield shifts with respect to the free molecule of white phosphorus. Attempts to isolate the cobalt adduct produced extensive decomposition over −40 °C.

A spectacular activation of the P_4 molecule was shown by Midollini and co-workers,[141] who obtained a functionalization of white phosphorus to η^4-coordinated tetraphosphabutadiene ligand by a Co-mediated process occurring in the presence of a bidentate phosphine (Scheme 62). A solution of white phosphorus in THF was added under nitrogen to a mixture of $[Co(H_2O)_6](BF_4)_2$ in *n*-BuOH in the presence of dppm and refluxed until deep red color developed. Recrystallization from DCM/*n*-BuOH gave dark red crystals of $[Co\{Ph_2PCH_2P(Ph)_2PPPP(Ph)_2CH_2PPh_2\}]BF_4$ (**181**), in which the P_4 tetrahedron was opened by the attack of two dppm ligands, forming a novel overall P_6-open chain ligand (Figure 36).

The P_6 ligand coordinates to the metal through all of the P atoms of the activated P_4 fragment and two of the four P atoms of the dppm ligands, resulting in a highly distorted octahedral coordination about the Co center.

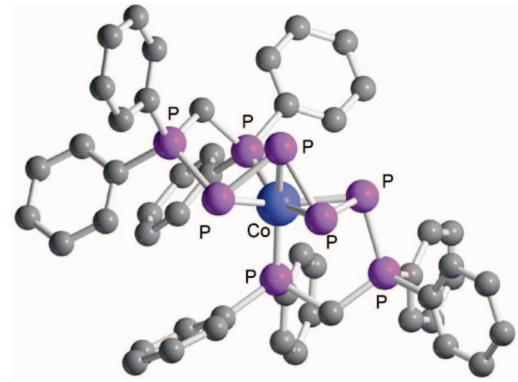

Figure 36. X-ray molecular structure of the $[Co\{Ph_2PCH_2P(Ph)_2PPPP(Ph)_2CH_2PPh_2\}]^+$ cation (**181**); adapted from ref 141.

Scheme 63

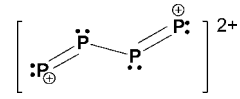

The overall electronic structure within the chain ligand must be considered as delocalized, with the external P−P bonds of the P_4 chain possessing partial double bond character ($d_{(P-P)ave}$ = 2.172 Å) and the central P−P bond slightly elongated ($d_{(P-P)}$ = 2.193 Å). The formation of the P_6 ligand can be assumed to occur upon bielectronic oxidation of the P_4 molecule followed by nucleophilic attack by the dppm P atoms at the positively charged sites of the tetraphosphorus activated chain (Scheme 63).

Midollini's compound **181** is endowed with further reactivity toward unsaturated transition metal fragments such as hexacarbonyl derivatives.[142] Therefore, heterometallic complexes $[\{Co(Ph_2PCH_2P(Ph)_2PPPP(Ph)_2CH_2PPh_2)\}\{Cr(CO)_5\}_2]BF_4$ (**182**) and $[\{Co(Ph_2PCH_2P(Ph)_2PPPP(Ph)_2CH_2PPh_2)\}\{M(CO)_5\}]Y$ (M = Cr, (**183**); W, (**184**); Y = BPh_4, BF_4) were obtained by reaction of **181** with the corresponding $[M(CO)_6]$ precursors under photochemical irradiation in DCM (Scheme 62). X-ray crystal structure determination on the tungsten derivative **184** showed that the cobalt atom maintains the coordination sphere as in the parent compound **181** with the *zigzag* open-chain ligand binding through the four P_4 atoms and two dppm P atoms, whereas one of the internal P atoms of the activated white phosphorus also coordinates to the $W(CO)_5$ moiety.

More recently, Peruzzini and co-workers showed that the reaction of **181** with $[Pt(C_2H_4)(PPh_3)_2]$ at room temperature affords in almost quantitative yield the heterobimetallic complex $[\{Co(\mu,\eta^{1:2:1}\text{-}P{=}P\text{-}PPh_2CH_2PPh_2)_2\}\{Pt(PPh_3)_2\}]BF_4$ (**185**) by elimination of ethene and insertion of the PtL_2 moiety into the central P−P bond of the P_6 ligand of **181** (Scheme 62).[143] The original P_6 *zigzag* chain in **181** has been cleaved, giving two separate P_3 moieties, $RP_5-P_4{=}P_3$ and $RP_9-P_8{=}P_7$, that are nearly identical on the basis of bond length and angles inspection (Figure 37). The reaction has occurred with complete regioselectivity and may be viewed as the formal oxidative cleavage of the internal P−P single bond of the η^4-tetraphosphabutadiene unit, $P^{(+)}-P{=}P-P{=}P-P^{(+)}$. In particular, following the insertion of PtL_2 across P(3)−P(7) bond, the distance changes from 2.197(3) Å in **181** to 2.823(4) Å in **185**, while the P(3)−Co−P(7) angle opens from 57.2(1)° to 74.43(11)°, respectively. The most outstanding feature of the bimetallic adduct **185** is the electronic nature of the two P_3 ligands that can be described

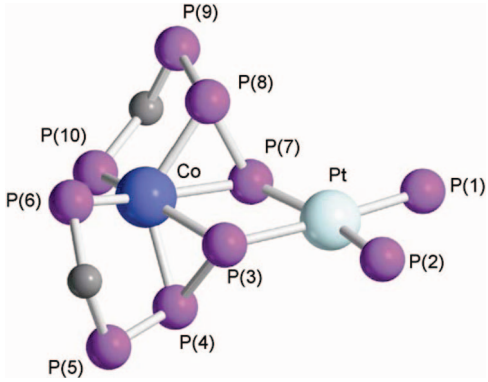

Figure 37. Molecular structure of the $[Co(\mu,\eta^{1:2:1}\text{-}P{=}P{-}PPh_2CH_2PPh_2)_2\{Pt(PPh_3)_2\}]^+$ cation (**185**); phenyl rings omitted for clarity, only *ipso*-carbons shown. Adapted from ref 143.

Scheme 64

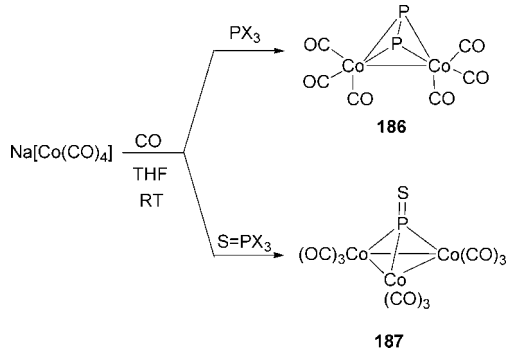

as a zwitterionic diphenyl(alkyl)phosphonium(+)diphosphenide(−) molecule, $RPh_2P^{(+)}{-}P{=}P^{(-)}$ ($R = Ph_2PCH_2$), with the negative charge onto the μ-Co,Pt bridging P-atom and the positive one onto the opposite PPh_2R phosphonium P-atom. The $^{31}P\{^1H\}$ NMR spectrum exhibits a temperature-invariant AA′BB′CC′DD′EE′X splitting pattern (X = ^{195}Pt), and the relatively high value of $^1J_{P7-P8}$ and $^1J_{P3-P4}$ constants (289.6 Hz) matches that found in other diphosphene complexes and supports the partial double bond character of these bonds.

The reactivity of white phosphorus with simple Co carbonyl clusters was explored in detail by Markó and coworkers starting from 1973. In a preliminary communication,[3] the authors reported on the synthesis of diphosphido cobalt carbonyl cluster $[(\mu,\eta^{2:2}\text{-}P_2)\{Co_2(CO)_6\}]$ (**186**) and the monophoshido species $[\{\mu_3,\eta^{1,1,1}\text{-}P(S)\}\{Co_3(CO)_9\}]$ (**187**), which were obtained as air-sensitive oily materials by reacting $Na[Co(CO)_4]$ with either PX_3 or SPX_3 (X = Cl, Br), respectively, in THF at RT under CO. On the basis of the analysis of CO stretching frequencies, the coordination modes of P_2 and P═S naked fragments to Co were hypothesized, as shown in Scheme 64.

In 1976 Vizi-Orosz completed the series of the $[P_n\{Co(CO)_3\}_{4-n}]$ (n =1−3) tetrahedranes by describing the first *cyclo*-P_3 derivative, i.e., $[(\eta^3\text{-}cyclo\text{-}P_3\}Co(CO)_3]$ (**188**) and the monophosphido species $[\{\mu_3\text{-}P\}\{Co_3(CO)_9\}]$ (**189**) from the reaction of $Co_2(CO)_8$ with white phosphorus in *n*-hexane under different conditions (Scheme 65).[144] Such a reaction gave a mixture of all the possible CoP tetrahedranes with ratios depending on the reaction parameters. The best yield of **188** requested high pressure of CO (120 atm) and moderate heating (50 °C). The monophosphido derivative **189** is highly reactive and spontaneously cyclotrimerizes,

Scheme 65

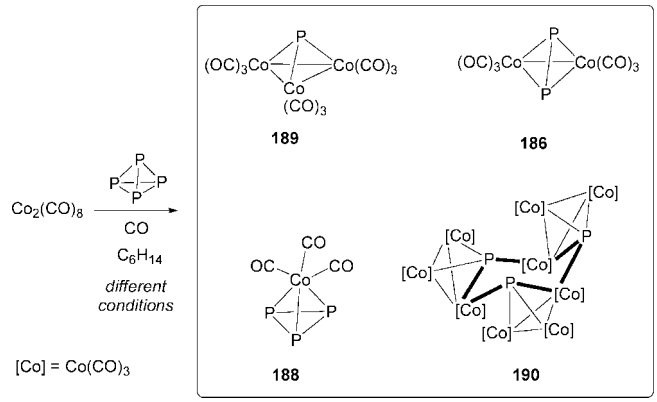

losing three molecules of CO, within a few minutes to afford the dodecacobalt cluster $[P_3Co_9(CO)_{24}]$ (**190**).

The tetrahedrane clusters of the series $[P_n\{Co(CO)_3\}_{4-n}]$ (n =1−3), containing P (**189**), P_2 (**186**), and P_3 (**188**) ligands, were studied in their reactivity with different metal carbonyl compounds behaving as soft Lewis acids.[145] The stabilization of $[\{\mu_3,\eta^{1,1,1}\text{-}P\}\{Co_3(CO)_9\}]$ (**189**) was therefore possible following the reaction with $[Fe(CO)_4(THF)]$ to yield $[\{(CO)_4\text{-}Fe\}(\mu_4,\eta^{1:1:1:1}\text{-}P)\{Co_3(CO)_9\}]$ (**191**), while $[(\mu,\eta^{2:2}\text{-}P_2)\{Co_2(CO)_6\}]$ (**186**) reacted in *n*-hexane with $M(CO)_6$ (M = Cr, Mo, W) under UV irradiation to give a mixture of the tetrametalated phosphido clusters $[\{(CO)_5M\}(\mu_4,\eta^{1:1:1:1}\text{-}P)\{Co_3(CO)_9\}]$ [M = Cr (**192**), Mo (**193**), W (**194**)] together with the cyclotrimer $[P_3Co_9(CO)_{24}]$ (**190**).

Replacement of one or more carbonyl ligands in the *cyclo*-P_3 derivative $[\{\eta^3\text{-}cyclo\text{-}P_3\}Co(CO)_3]$ (**188**) with PBu_3 gave mono- or disubstituted products $[\{\eta^3\text{-}cyclo\text{-}P_3\}\{Co(CO)_2(PBu_3)\}]$ (**195**) and $[\{\eta^3\text{-}cyclo\text{-}P_3\}\{Co(CO)(PBu_3)_2\}]$ (**196**), whereas less basic phosphines did not react.[145]

The first structurally characterized derivative containing a bridging diphosphido ligand, $[\{Co_2(CO)_5(PPh_3)\}(\mu,\eta^{2:2}\text{-}P_2)]$ (**197**) was prepared by Markó by refluxing **186** in benzene with a double amount of PPh_3, and its crystal structure was determined by Dahl (Figure 38).[146] The core of **197** is formed by Co_2P_2 fragment that possesses an idealized C_{2v} geometry. Coordination about each cobalt atom may be described as a distorted tetragonal pyramid with two equatorial carbonyl ligands and two bridging phosphorus atoms at the corners in the basal plane and with either an axial carbonyl ligand or a triphenylphosphine ligand at the apex. The P−P distance in the $\mu,\eta^{2:2}$-P_2 fragment is 2.019(9) Å, which is 0.20 Å shorter than the average P−P single-bond distance of 2.21

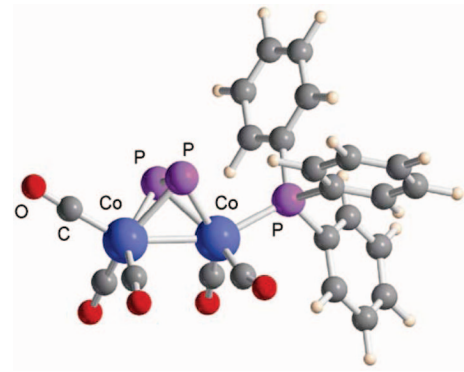

Figure 38. Molecular structure of $[\{Co_2(CO)_5(PPh_3)\}(\mu,\eta^{2:2}\text{-}P_2)]$ (**197**), adapted from ref 146.

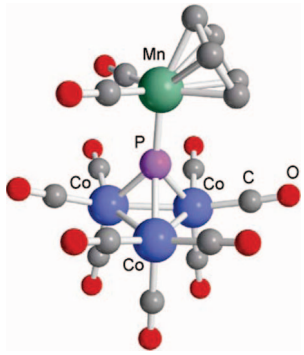

Figure 39. X-ray crystal structure of [{CpMn(CO)$_2$}(μ_4,$\eta^{1:1:1:1}$-P){Co$_3$(CO)$_9$}] (**199**); adapted from ref 150.

reported[147] for P_4 and 0.12 Å longer than the triple-bond distance of 1.893 Å observed for gaseous P_2.[148]

Examples of further reactivity of coordinated diphosphorus (μ-P_2) ligand with metal carbonyl fragments were also reported.[149] Then, starting from [{$Co_2(CO)_5(L)$}(μ,$\eta^{2:2}$-P_2)] [L = CO (**186**), PBu_3 (**195**), PPh_3 (**197**)], reactions with $M(CO)_6$ (M = Cr, Mo, W) or $Fe(CO)_5$ gave mono- or disubstituted products once photochemically activated, also in a stepwise fashion, to yield, for example, Co_2P_2 clusters decorated by two different carbonyl fragments, i.e., [{$Cr(CO)_5$}{$W(CO)_5$}{$Co_2(CO)_5(PBu_3)$}(μ_4,$\eta^{2:2:1:1}$-P_2)] (**198**). The Co_2P_2 tetrahedral core is fully substituted at all tips, either by carbonyl groups (Co) or $M(CO)_5$ fragments (P). The P−P distance for this complex was measured at 2.061 Å.

{Co_3P} tetrahedral clusters of the type shown above for [{μ_3,$\eta^{1,1,1}$-P}{$Co_3(CO)_9$}] (**189**) were also prepared by Huttner and co-workers from the trihalophosphine complexes L_nM-PX_3 [L_nM = $CpMn(CO)_2$, $Cr(CO)_5$, $W(CO)_5$; X = Cl, Br] by treatment with $Co_2(CO)_8$.[150] The reactions were run in THF at moderate temperature, giving the clusters [(L_nM)-(μ_4,$\eta^{1:1:1:1}$-P){$Co_3(CO)_9$}] [L_nM = $CpMn(CO)_2$ (**199**), $Cr(CO)_5$ (**200**), $W(CO)_5$ (**201**)] in moderate yield. In the case of L_nM = $CpMn(CO)_2$, the corresponding X-ray crystal structure was obtained (Figure 39).

Cobalt organometallic coordinatively unsaturated fragments supported by different CpR ancillary ligands have found wide use in the activation of white phosphorus by cobalt derivatives. Often subtle variations of reaction conditions and modest structural modifications have a deep impact on the nature of the final activation product.

Scherer and co-workers[151] showed that the *thermolysis* of a [Cp*Co(μ-CO)]$_2$ in toluene with a 3-fold excess of white phosphorus at 60 °C for 30 min caused release of CO and formation of [Cp*Co(η^2-P_4)(CO)] (**202**). The complex was isolated and purified by column chromatography and characterized also by X-ray diffraction methods, which showed the molecular structure belonging to dark red crystals reported in Figure 40a. The residue from the eluted fraction was heated to 60 °C for further 6 h, and upon recrystallization from toluene/*n*-hexane, complex [{Cp*Co(CO)}$_2$(μ,$\eta^{2:2}$-P_4)] (**203**) was obtained as black crystals (Figure 40b). This interesting reactivity is summarized in Scheme 66 below. The X-ray structures confirm that white phosphorus has been activated by Co, and that one or two edges of the tetrahedron have been opened and coordinated to a Cp*Co(CO) fragment. In the former case, white phosphorus can be formally considered as a P_4^{2-} ligand, whereas in the latter, it is a P_4^{4-} one. P−P distances for the η^2-P_4 fragment for **202** are ranging

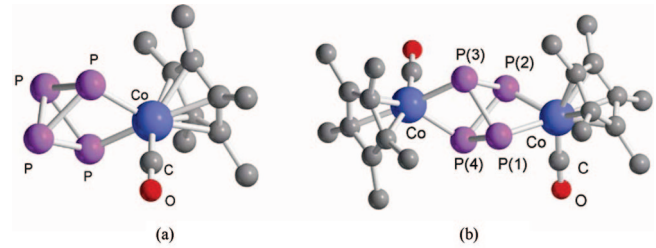

Figure 40. X-ray crystal structure of [Cp*Co(η^2-P_4)(CO)] (**202**) (a) and [{Cp*Co(CO)}$_2$(μ,$\eta^{2:2}$-P_4)] (**203**) (b); adapted from ref 151.

Scheme 66

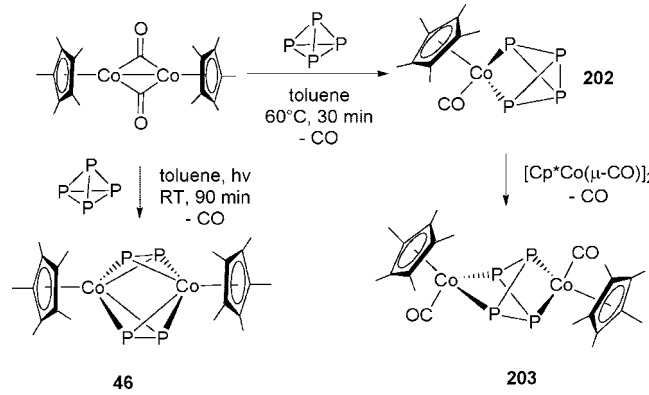

from 2.158(2) to (nonbonding) 2.606(2) Å, comparable to the situation in phosphabicyclobutane derivatives $P_2(PR_2)$ (R = $N(SiMe_3)_2$, $Bu^t_3C_6H_2$). In the case of **203**, the P−P distances are in the range 2.22−2.23 Å, with the nonbonding P(3)···P(4) and P(1)···P(2) being 2.560(2) and 2.597(2) Å, respectively.

Barr and Dahl described the synthesis, bonding features, and chemical and electrochemical reactivity of the related dimetal bridged bisdiphosphide complex [{Cp*Co(μ,$\eta^{2:2}$-P_2)}$_2$] (**46**) and the Fe analogue (**45**; see section 3.1).[52] At variance with Scherer's results, these complexes were obtained via *photolysis* of toluene solutions of [Cp*Co(μ-CO)]$_2$ and [{Cp*Fe(CO)}$_2$(μ-CO)$_2$] with P_4, respectively (Scheme 66). X-ray crystal determination data are also available for **46**, and the corresponding molecular structure is shown in Figure 41. The 36 VE cobalt dimer consists of two 14-electron Cp*Co fragments bridged by two 4-electron donating P_2 ligands that are coordinated in an η^2-fashion. The P−P distances were measured at P(1)−P(2) 2.053(4) and P(3)−P(4) 2.058(4), comparable to those found for [{$Co_2(CO)_5(PPh_3)$}(μ,$\eta^{2:2}$-P_2)] (**197**), while the Co−P distances are all around 2.30 Å, showing a highly symmetrical (pseudo $D_{2\,h}$) structure of the Co_2P_4 core. Cyclic voltammetry shows that the dimer exhibits reversible redox behavior in

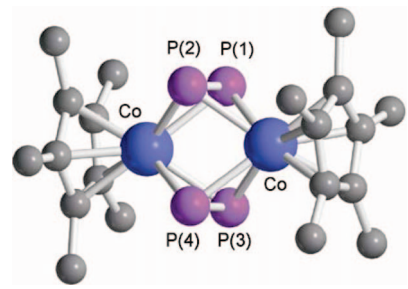

Figure 41. X-ray crystal structure of [{Cp*Co(μ,$\eta^{2:2}$-P_2)}$_2$] (**46**); adapted from ref 52.

Scheme 67

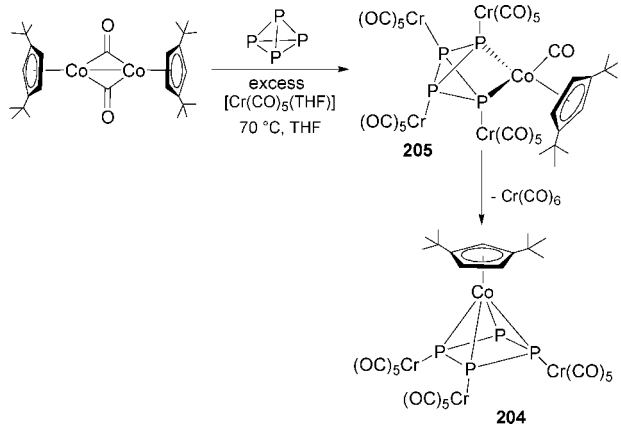

DCM. The laser-desorption FT MS of both **46** and **45** were also reported, confirming the presence of two bridging P_2 ligands in both compounds.[152]

Replacement of Cp* with cyclopentadienyl rings substituted with bulky alkyl groups was thoroughly investigated. In a preliminary communication, Scheer and co-workers showed that the reaction of white phosphorus with [Cp″Co(μ-CO)]$_2$ in 2:1 ratio in THF at 70 °C, carried out in the presence of [Cr(CO)$_5$(THF)] (6-fold excess to Co),[153] yields [Cp″Co(μ_4,$\eta^{4:1:1:1}$-P$_4$){Cr(CO)$_5$}$_3$] (**204**) along with traces of [{Cp″Co(CO)}(μ_4,$\eta^{2:1:1:1:1}$-P$_4$){Cr(CO)$_5$}$_4$] (**205**), as indicated by ^{31}P{^{1}H} NMR studies. The reaction pathway (Scheme 67) is thought to be similar to what was observed for the related [Cp^{Bu}Rh(μ_4,$\eta^{4:1:1:1}$-P$_4$){Cr(CO)$_5$}$_4$] (**206**; see section 4.2),[154] but in the former case, trisubstituted product was preferred because of the steric hindrance caused by the two *tert*-butyl groups on the ring. The X-ray crystal structure of **205** reveals the presence of a surprising square planar *cyclo*-P$_4$ ligand (10 valence-electron donor) capped by a Cp″Co unit and likely stabilized by three P atoms coordinated to Cr(CO)$_5$ fragments. All P−P distances are equivalent within error at 2.142(4) Å and shorter than typical P−P single bonds (2.21 Å). The Co atom is placed above the plane generated by the four P atoms at 1.754 Å distance.

The effect of systematic replacement of Cp protons with Bu^t groups on the reaction pathways of P_4 activation was then explored in detail by studying the three-component reaction of [Cp^{R}Co(μ-CO)$_2$] (Cp^R = Cp, Cp^{Bu}, Cp″, Cp‴) with P_4 in the presence of [Cr(CO)$_5$(THF)] under UV irradiation. The reaction proceeds via the tetrasubstituted-at-P bicyclotetraphosphine intermediate (complex **205** in the case of Cp^R = Cp″).[155,156] Depending on the degree of the Cp-ring substitution, the nature of the final stable product may vary, i.e., the square-based pyramidal complex (complex **204** for Cp^R = Cp″) can be fully substituted by four Cr(CO)$_5$ terminal groups, giving [Cp^{R}Co(μ_4,$\eta^{4:1:1:1:1}$-*cyclo*-P$_4$){Cr(CO)$_5$}$_4$] (Cp^R = Cp (**207**), Cp^{Bu} (**208**), or trisubstituted [Cp^{R}Co(μ_4,$\eta^{4:1:1:1}$-*cyclo*-P$_4$){Cr(CO)$_5$}$_3$] [Cp^R = Cp″ (**209**), Cp‴, (**210**)]. An interesting comparison was made with the related two-component system, i.e., by running the same reactions without [Cr(CO)$_5$(THF)] under UV irradiation, using [Cp″Co(μ-CO)$_2$] as cobalt precursor. The reaction mixture gave a minor amount of violet [{Cp″Co(μ,$\eta^{2:2}$-P$_2$)}$_2$] (**211**), similar to what observed for Cp^R = Cp* (**46**), and a major amount of the new complex [(Cp″Co)(μ_3,$\eta^{4:2:2}$-P$_4$){(Cp″Co)$_2$(μ-CO)}] (**212**), showing a "kite-like" distorted planar P_4 ligand capped by a Cp″Co moiety and a [(Cp″Co)$_2$(CO)](*Co*−*Co*) fragment coordinating three of the four P atoms and lying on the opposite side of the Cp″Co (Scheme 68).

Scheme 68

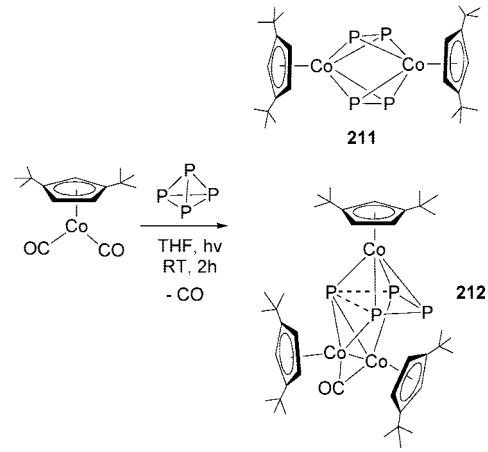

Complex **212** was characterized by X-ray diffractometry (Figure 42) and ^{31}P{^{1}H} NMR spectroscopy, and these data were supported by theoretical analysis of the bonding situation.[156] The ^{31}P{^{1}H} NMR spectrum consists of three groups of signals belonging to an A_2MX spin system, with the P_X atom featuring a highly upfield shifted triplet at −398.6 ppm. The X-ray structure confirms the *quasi*-planar *cyclo*-P$_4$ core and the different disposition of Cp″Co fragments as described above. The Co−Co distance of 2.459(2) Å is consistent with a metal−metal single bond. The P−P bonds are dissimilar with P(3)−P(4) (2.503 Å) much longer than P(3)−P(5) (2.161 Å), with the former being an intermediate distance between a P−P bonding length and a van der Waals contact. Extended Hückel theory (EHT) calculations support the authors' description of the P(3)−P(4) distance as a weak bond rather than a contact.

Following on the study of ring-substitution effects, Scheer and Becker also reported the three-component reaction involving [Cp^{Ph}Co(μ-CO)$_2$]. Under photolytic conditions, in the presence of [Cr(CO)$_5$(THF)] capping reagent, [{Cp^{Ph}Co(μ_4,$\eta^{4:1:1:1}$-*cyclo*-P$_4$)}{Cr(CO)$_5$}$_3$] (**213**) is again formed in a similar way of the Cp″ analogue.[157] By analyzing in details the X-ray crystal structures obtained, it was observed that the angle between the *cyclo*-P$_4$ and Cp^R planes increases from 4 to 9° in the series Cp^R = Cp″ < Cp‴ < Cp^{Ph}. Because of the large steric hindrances present on the cyclopentadienyl

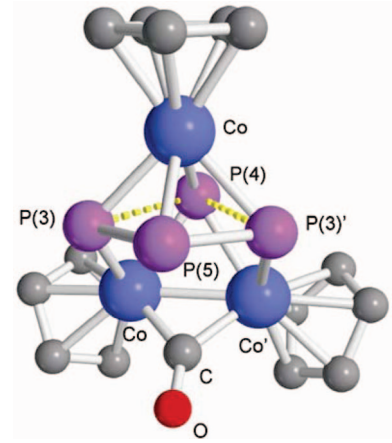

Figure 42. View of the core structure of [(Cp″Co)(μ_3,$\eta^{4:2:2}$-P$_4$){(Cp″Co)$_2$(μ-CO)}] (**212**), with *tert*-butyl groups on Cp″ omitted for clarity; adapted from ref 156.

Scheme 69

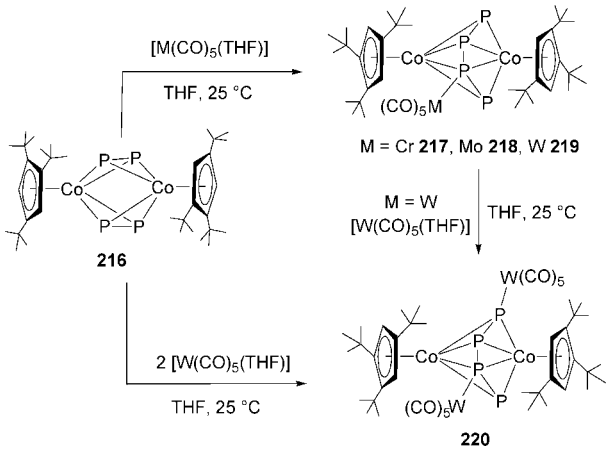

rings, complexes **209** and **213** showed the tendency to lose one $Cr(CO)_5$ group in solution to form the stable complexes *trans*-[{$Cp^RCo(\mu_4,\eta^{4:1:1}$-*cyclo*-$P_4$)]{$Cr(CO)_5$}$_2$] ($Cp^R$ = Cp″ (**214**); Cp^{Ph} (**215**).

An interesting ligand-induced P_2-coupling to form an acyclic P_4 ligand was described by Scherer and co-workers.[158] Terminal coordination of $M(CO)_5$ to [$(Cp'''Co)_2(\mu,\eta^{2:2}$-$P_2)_2$] (**216**), the tris-*tert*-butyl substituted (Cp‴) analogue of **211** and **46**, gives the polynuclear cobalt complexes [{$(Cp'''Co)_2$-($\mu_{(2+n)}$-$\eta^{4:4:1:(1)}$-*cyclo*-P_4)}{$M(CO)_5$}$_n$] [n = 1, M = Cr (**217**), Mo (**218**), W (**219**); n = 2, M = W (**220**)] as shown in Scheme 69. The X-ray crystal structures of **216**, **219**, and **220** were also obtained, confirming the bonding scheme illustrated above. Figure 43 below shows the X-ray crystal structure of the tungsten monoadduct **219**.

Higher nuclearity Co clusters containing bare P atoms and units were obtained by the cothermolysis of [$Cp^RCo(CO)_2$] (Cp^R = Cp^{Bu}, Cp″) with the pentaphosphaferrocene complex [Cp*Fe(η^5-P_5)] (**14**) (see section 3.1.2), carried out in boiling decalin.[88] The reaction, already discussed in the section dedicated to **14** (see Scheme 37) and its rich chemistry, afforded both mixed FeCo clusters (described in section 3.1.2) and cobalt derivatives. The latter examples include [{$Cp^RCo(\mu_3$-P)}$_4$] [Cp^R = Cp^{Bu} (**221**), Cp″ (**224**)], showing a tetragonal antiprismatic structure slightly different from that of the seminal Dahl's derivative [{CpCo(μ_3-P)}$_4$] (**143**), and [{Cp^RCo}$_3$(μ_3-P)}$_2$] [Cp^R = Cp^{Bu} (**223**), Cp″ (**334**)], possessing a trigonal bipyramidal structure where an isosceles

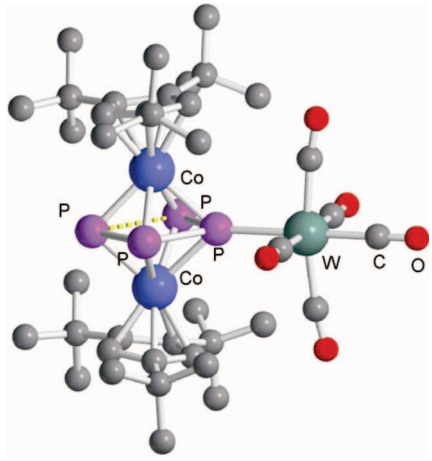

Figure 43. Molecular structure of [{$(Cp'''Co)_2(\mu_3,\eta^{4:4:1}$-$P_4$)}-{$W(CO)_5$}] (**219**); adapted from ref 158.

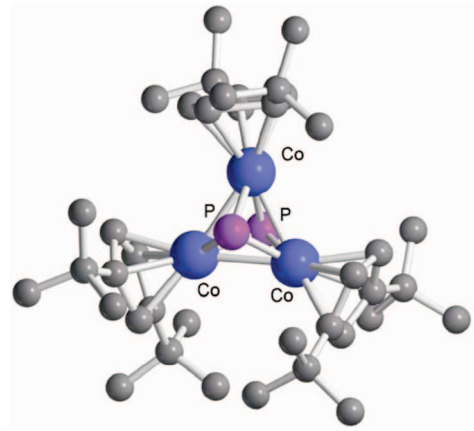

Figure 44. Molecular structure of the Co_3P_2 cluster of [{Cp″Co}$_3$(μ_3-P)}$_2$] (**224**); adapted from ref 88.

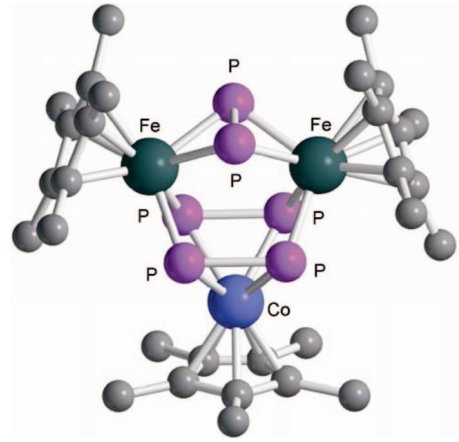

Figure 45. Molecular structure of [$(Cp*Fe)_2(Cp*Co)(\mu,\eta^{2:2}$-$P_2)$-($\mu_3,\eta^{1:2:1}$-$P_2)_2$] (**225**); adapted from ref 159.

triangle of Cp^RCo units is capped by two phosphido ligands occupying the polar positions of the almost regular bipyramid. The elegant structure of **224** is shown in Figure 44.

The similar thermal reaction of **14** with the less sterically encumbered [Cp*Co(μ-CO)]$_2$ precursor gave access to the already mentioned complexes [{Cp*Co($\mu,\eta^{2:2}$-P_2)}$_2$] (**46**) and [{Cp*Fe($\mu,\eta^{2:2}$-P_2)}$_2$] (**45**) as well as to the trinuclear cluster [$(Cp*Fe)_2(Cp*Co)(\mu,\eta^{2:2}$-$P_2)(\mu_3,\eta^{1:2:1}$-$P_2)_2$] (**225**) whose unusual topology was confirmed by single-crystal X-ray diffraction analysis (Figure 45). Further reaction of **225** with [$Mo(CO)_5$(THF)] in THF at RT gave the tetranuclear cluster [$(Cp*Fe)_2(Cp*Co)(P_6)${$Mo(CO)_5$}] (**226**) following a build-up reaction (Scheme 70).[159] The X-ray crystal structure of **226** confirms that the $Mo(CO)_3$ unit is sitting on a face of the nine-vertices polyhedron of **225**.

The influence of bulky substituents on the Cp ring on the aggregation patterns of activated P_4-derived fragments has been the subject of deeper investigations by Scherer's group using the {Cp‴Co} moiety as the standard. The reaction of [$Cp'''Co(\mu$-CO)$_2$] with white phosphorus was carried out under both thermolytic and photolytic conditions as shown in Scheme 71.[160] The presence of three *tert*-butyl arms on the Cp ring caused a spectacular diversity of the reaction products and allowed the stabilization of new unexpected polyphosphorus topologies resulting from reaggregation processes of fragments derived from P_4. The species isolated after chromatographic workup include novel P_8 and P_{12} ligands binding three {Cp‴Co} moieties in cluster complexes such as [$(Cp'''Co)_3P_8$] (**227**) and [$(Cp'''Co)_3P_{12}$] (**228**). In

Scheme 70

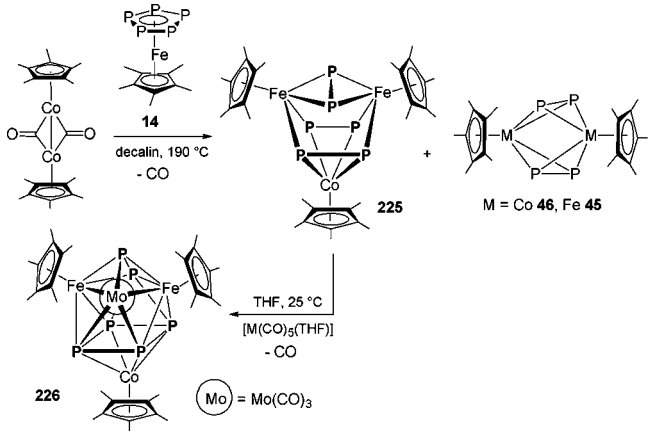

these complexes, the P_n ligands form P_5-P_3 and P_5-P_7 arrangements that are reminiscent of Hittorf's violet phosphorus. Complex $[(Cp'''Co)_4P_{10}]$ (**229**), which also formed in traces in the thermolytic reaction, was generated in slightly higher yield (13%) after prolonged thermolysis of **216** in decalin (10 days at 190 °C!). The decaphosphorus species **229** exhibits a P_5-P_5 structure similar to that found in $[(Cp''Rh)_4P_{10}]$ (**230**) (see section 4.2).[161] Remarkably, **229** could also be generated from a refluxing decalin solution of the P_8 complex **227** together with the P_4 dimer **216**, suggesting that the P_{10} unit in **229** could be assembled via a [2 + 2]-cycloaddition of P_2 to the P_8 unit. The X-ray structure of the related $[(Cp^{Si_2}Co)_4P_{10}]$ cluster was determined by X-ray methods; see below.[162]

The $^{31}P\{^1H\}$NMR pattern of **227** consists of a ABMM′XX′Y_2 complex spin system that was resolved by computer simulation. The network of P−P connectivities was unraveled by a perusal of homonuclear $^{31}P,^{31}P$-COSY45 2D-NMR spectroscopy, which allowed the construction of the conformation of the P_8 skeleton in solution. Similarly, it was possible to assign the P_{12} and P_{10} solution structures of **228** and **229**.

The oxidation of naked P-atoms belonging to polyphosphorus ligands in pnictido metal clusters is a well-developed reaction as generally the formation of oxidized polyphosphorus units, P=X (X = O, S, Se, Te) bears additional stabilization to the system. An illustrative example of this concept is the Marko's $[\{\mu_3,\eta^{1,1,1}\text{-P(S)}\}\{Co_3(CO)_9\}]$ (**187**) where the presence of the sulfur atom of the μ_3-coordinated thiophosphido ligand imparts high stability to the Co_3P

Scheme 71

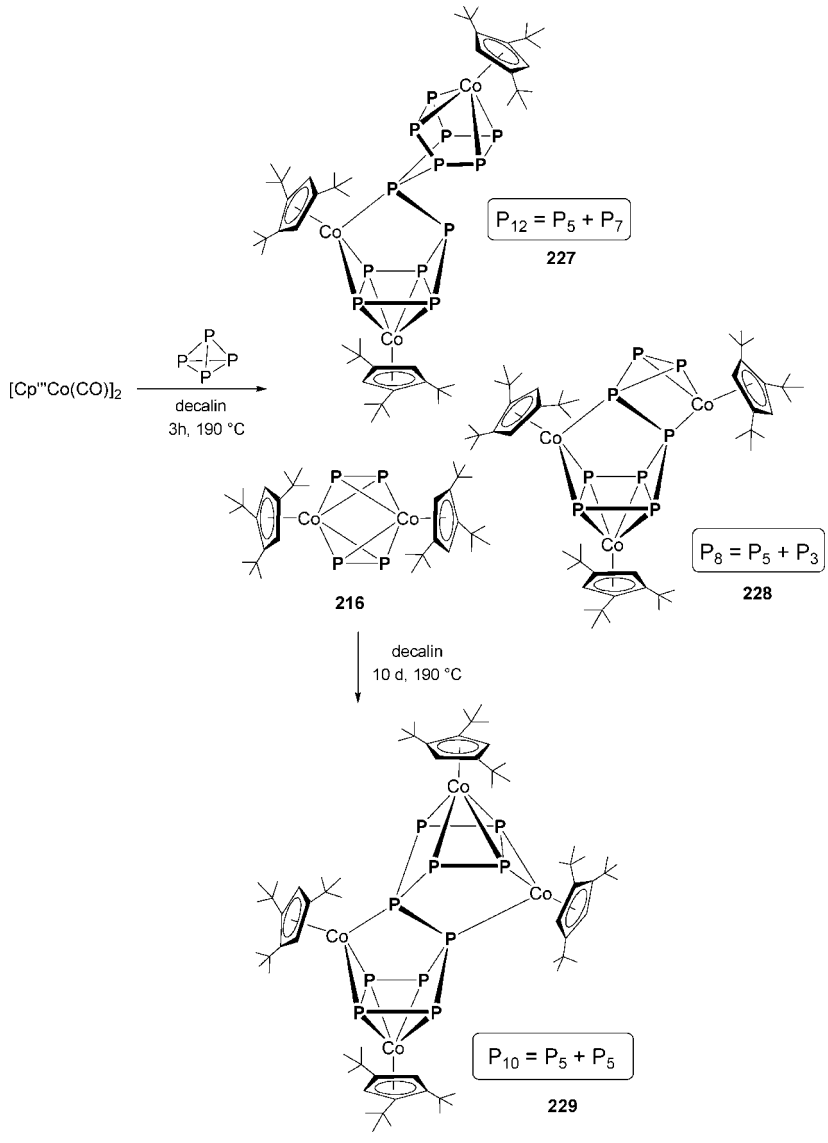

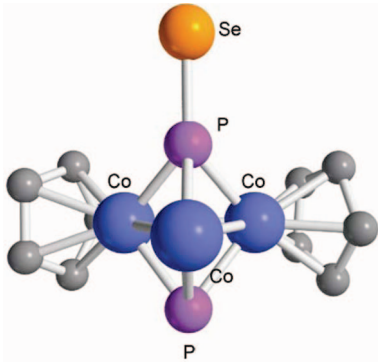

Figure 46. Molecular structure of [{Cp″Co}$_3$(μ_3-P)(μ_3-P = Se)] (**231**). For Cp″ ligands, one is omitted, and for the other, two *tert*-butyl groups are omitted for clarity. Adapted from ref 163.

Scheme 72

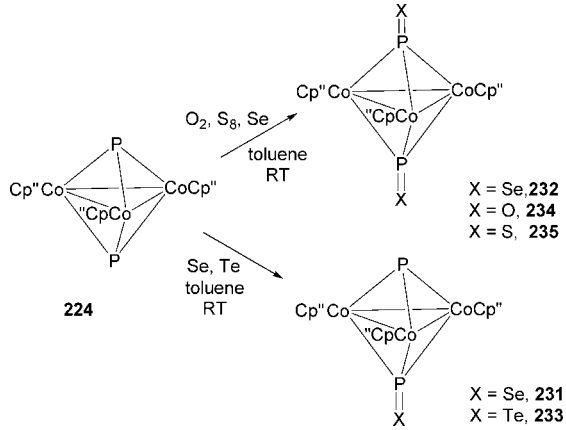

cluster.[3] Later on this chemistry was fully exploited by Scherer and co-workers, who first reported on the oxidation of the known trigonal bipyramidal diphosphido cluster [{Cp″Co}$_3$(μ_3-P)}$_2$][163,164] (**224**) with gray selenium at 20 °C in toluene to give a mixture of the oxidation products [{Cp″Co}$_3$(μ_3-P)(μ_3-P═Se)}] (**231**) and [{Cp″Co}$_3$(μ_3-P═Se)}$_2$] (**232**). The X-ray crystal structure of **231** shows a trigonal bipyramidal Co_3P_2 core capped by one μ_3-P═Se group (Figure 46).

The results on oxidation chemistry of Co clusters supported by the μ_3-P atoms were extended to chalcogens other than selenium with the use of other oxidants, namely, O_2, S_8, and Te.[165] The room-temperature oxidation of **224** with the whole series of chalcogens gave the mono-oxidized products [{Cp″Co}$_3$(μ_3-P)(μ_3-P═X)] (X = Se, **231**; Te, **233**) and the bis-oxidized [{Cp″Co}$_3$(μ_3-P═X)$_2$] (X = Se, **232;** O, **234**; S, **235**) according to Scheme 72. The novel P_4Se ligand present in the trinuclear complex [(Cp*Fe)$_2$(Cp″Co)$_2$-(μ_3,$\eta^{3:2:2}$-P_4Se)(μ_3-P)] (**236**) was generated by the reaction of [{Cp*Fe}{Cp″Co}$_2$(μ_3,$\eta^{3:2:2}$-P_4)(μ_3-P)] (**98**, see section 3.1.2) with gray Se at 0 °C (Scheme 73). Complexes **234** and **235** were also characterized by X-ray crystal structure determination, displaying as expected a trigonal bipyramidal core as the parent compound. Remarkably, whereas the starting compound **224** shows a $^{31}P\{^1H\}$ NMR resonance at 1058.7 ppm (C_6D_6), a large upfield shift is observed for **232** (581.9 ppm) and **231** (530.5 ppm).

The substitution pattern on the Cp ring was not limited to alkyl groups. Ligand 1,3-bis(trimethylsilyl)cyclopentadienyl (Cp^{Si_2}) was also used by Scherer et al. to prepare [$Cp^{Si_2}Co(CO)_2$], which was then reacted thermally or photochemically with white phosphorus.[162] Also in this case, the

Scheme 73

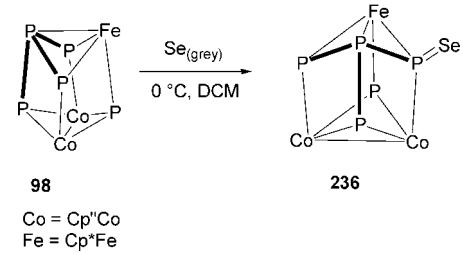

Scheme 74

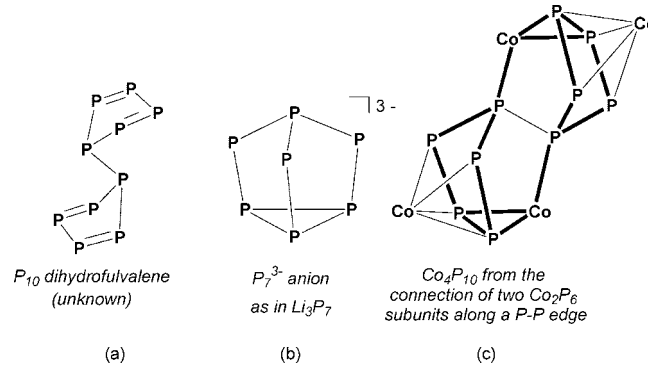

two activation methods gave different P-assemblies. Thus, the cothermolysis of white phosphorus in xylene at 140 °C for 72 h in the presence of [$Cp^{Si_2}Co(CO)_2$] (Co/P = 1:7) gave in unusually high yield (87%) the tetranuclear olive-green complex [($Cp^{Si_2}Co)_4P_{10}$] (**237**) that shares with **229** and **230** the remarkable P_{10} topology (see Scheme 71).[160,161] On the other hand, the photochemical activation in THF at room temperature for 14 h of the same component mixture, albeit in a Co/P = 1:2 ratio, behaves similarly to the Cp″Co system[156] (see Scheme 68) giving complexes [($Cp^{Si_2}Co$)-(μ_3,$\eta^{4:2:2}$-P_4)}{($Cp^{Si_2}Co)_2$(μ-CO)}] (**238**), [{$Cp^{Si_2}Co$(μ,$\eta^{2:2}$-P_2)}$_2$] (**239**), and traces of other species. For all three compounds, the corresponding X-ray crystal structures were obtained. The structures of both **238** and **239** do not differ substantially for the Cp″ analogues (vide supra), with only a slightly more pronounced kite-like deformation found in **238**. Double-bond character can be attributed to the P−P bond distance (2.053−2.054 Å) of the P_2 side-on coordinated units in **239**.

The P_5−P_5 topology is part of the Co_4P_{10} framework and has been in principle compared to the structure of either P_{10} dyhydrofulvalene (sketch (a) in Scheme 74) or to the known Zintl anion Li_3P_7 (sketch (b)) by replacing one basal P atom by the {$CoCp^{Si_2}$} unit. The connection of two Co_2P_6 (sketch (c)) subunits with a common P−P edge formally gives the P_{10} skeleton of **237**.

The lithium salt Li_3P_7 containing the cage-like Zintl anion P_7^{3-} and its neutral trimethylsilyl derivative, $P_7(SiMe_3)_3$, were used by Fenske and co-workers[166] as building blocks for the synthesis of polynuclear transition metal complexes incorporating naked P units (Scheme 75).[49,167] In particular, the reaction of $P_7(SiMe_3)_3$ at room temperature in THF with [Cp*CoCl]$_2$, generated in situ from Cp*Li and $CoCl_2$, yielded the trinuclear cluster [(Cp*Co)$_3$(μ,$\eta^{2:2}$$P_2$)($\mu_3$,$\eta^{2:2:2}$-$P_2$)$_2$] (**240**).

Complex **240**, formally the Co analogue of Scherer's As complex [(Cp*Co)$_3$(As_2)$_3$],[168] is composed of three {Cp*Co} units bridged by three P_2 units, two of which are μ_3,$\eta^{2:2:2}$-bridges and one of which is a μ,$\eta^{2:2}$-bridge. The analysis of the bond lengths for the three P_2 units in the crystallographi-

Scheme 75

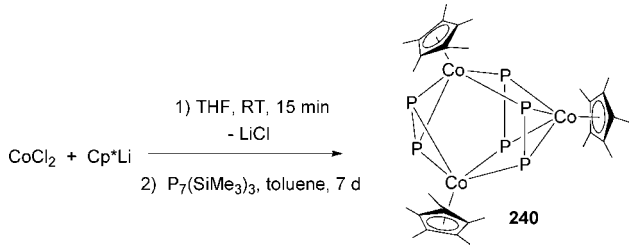

cally authenticated structure of **240** is interesting (Figure 47). The P−P separations range from 2.047 Å [P(1)−P(2)] to 2.172 Å [P(3)−P(4)] and 2.171 Å [P(5)−P(6)]. While the P(1)−P(2) bond length is unusually short, possible weak interactions can be present between P(3) and P(6) at 2.554 Å, P(4) and P(5) at 2.523 Å.

Although not directly deriving from white phosphorus activation, it is worth mentioning for the sake of completeness the synthesis and characterization of complexes deriving from the reaction of the chlorophosphinidene complex [{$W(CO)_5$}$_2$PCl] with K[$Co(CO)_4$], as part of the synthetic procedures leading to "naked" P atoms being incorporated in cluster assemblies (Scheme 76).[169] When the reaction is carried out at −78 °C in THF, it yields the novel complexes [{$W(CO)_4Co_2(CO)_6$}{μ_3-$PW(CO)_5$}$_2$] (**241**) and [{$W(CO)_3Co_3(CO)_6$}{μ_3-$PW(CO)_5$}$_3$] (**242**) along with the known complexes [$Co_2(CO)_6${$\mu,\eta^{2:2}$-$PW(CO)_5$}$_2$] (**243**) and [$Co_3(CO)_9${μ_3-$PW(CO)_5$}] (**244**), which were previously obtained by room-temperature reactions, namely, [{$W(CO)_5$}$_2$PCl] with K[$Co(CO)_4$] and [$W(CO)_5(PH_3)$] with $Co_2(CO)_8$, respectively.[170] The X-ray crystal structures of **281** and **242** were also obtained (Figure 48).

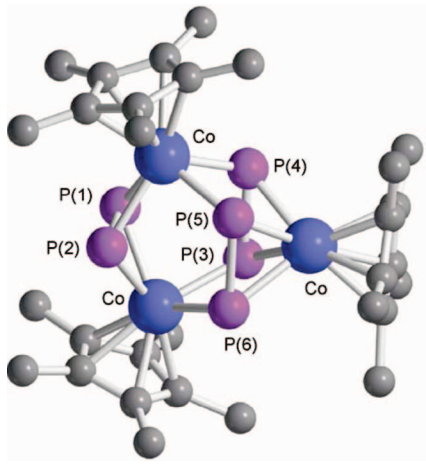

Figure 47. Molecular structure of [$(Cp^*Co)_3(\mu,\eta^{2:2}P_2)(\mu_3,\eta^{2:2:2}$-$P_2)_2$] (**240**); adapted from ref 49.

The molecular structure of **241** shows a *cyclo*-Co_2P_2 core [torsion angle Co−P−P−Co at 16.52°] capped by a $W(CO)_4$ group and the remaining P-lone pairs coordinating a $W(CO)_5$ fragment, to generate an overall *nido* structure. The P−$W(CO)_4$ distances are 2.430 and 2.439 Å, respectively, shorter than the average W−P distance (2.604 Å) found for example in [$W(CO)_4${$\mu_5,\eta^{4:1:1:1:1}$-P_4[$W(CO)_5$]$_4$}].[171] The structure of **242** shows instead a tetrahedral WCo_3 core in which each Co_2W face is bridged by a P atom. The lone pairs of the three "naked" P atoms are each further coordinated to a $W(CO)_5$ fragment. The Co−Co bonds are in the average for this class of P-capped Co_3 clusters at ca. 2.580 and 2.545 Å, respectively. Complex **241** decomposes in a two-step pathway in the temperature range 65−165 °C, as determined by thermogravimetric analysis, leaving a stable sample of formal composition {$Co_3P(CO)_3$} by loss of CO and $W(CO)_5$.

4.2. Rhodium

The coordination chemistry of elemental phosphorus to rhodium was virtually unexplored until 1970, when the first report on the synthesis of [$RhCl(PPh_3)_2(\eta^2$-$P_4)$] (**245**) by Ginsberg and Lindsell appeared in the literature.[1] The authors report on the characterization of several monomeric complexes containing an intact P_4 molecule bonded to a rhodium atom. The compounds of general formula [$RhCl(L)_2(P_4)$] [L = PPh_3 (**245**), $AsPh_3$ (**246**), P(*p*-Tol)$_3$ (**247**), P(*m*-Tol)$_3$ (**248**)] were obtained from the reaction of either the appropriate trisarylphosphine or arsine rhodium halide with white phosphorus in DCM or diethyl ether at −78 °C (Scheme 77). Interestingly, whereas CO easily displaced P_4 to generate the known *trans*-[$Rh(CO)Cl(L)_2$], neither ethene nor dihydrogen were observed to react with this class of compounds. Although reactions between complexes [$MCl(L)_3$] (M = Rh; L = $P(OPh)_3$, $PEtPh_2$, or PMe_2Ph) and P_4 also occur under similar conditions, the products could not be isolated as the complete removal of residual solvent led to decomposition.

Complex **245** and its congeners are moderately air-sensitive yellow or orange solids stable under dinitrogen or *vacuum*. They are soluble in DCM, chloroform, and in some cases in aromatic solvents, being stable below −20 °C. In the case of L = PPh_3, the dihapto- nature of P_4 bonding was clarified at first by ^{31}P NMR spectroscopy[172] and later by X-ray crystal structure determination[173] supported by theoretical calculations. Chemical shift values range from −278.3

Scheme 76

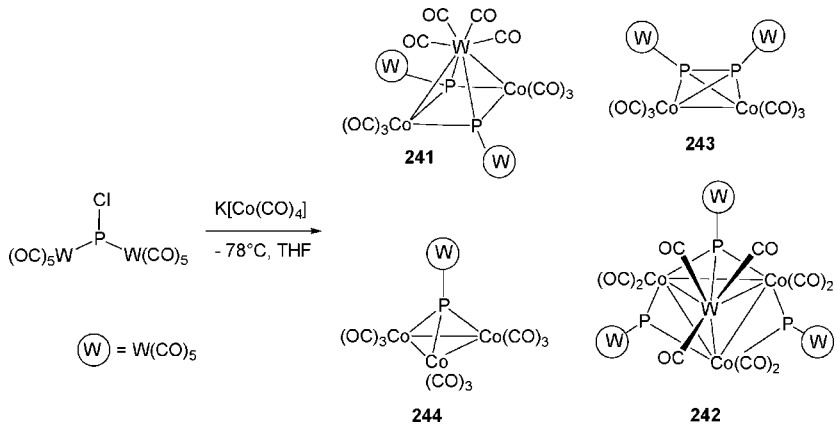

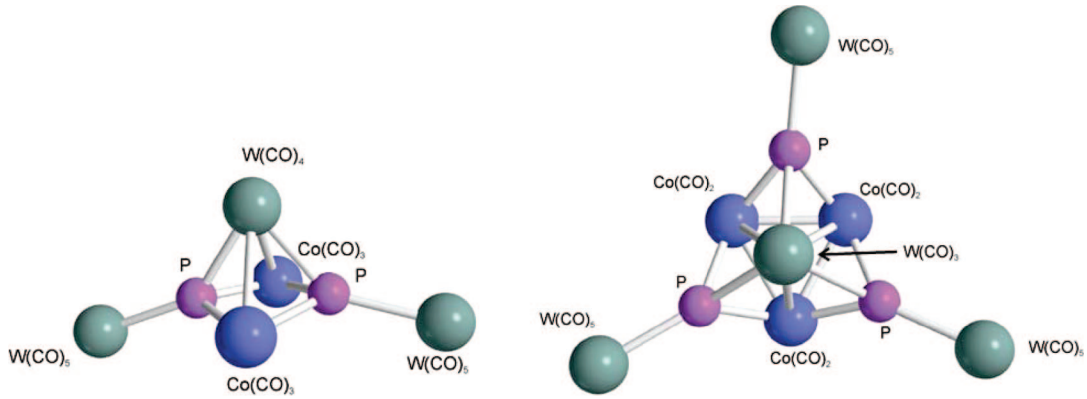

Figure 48. Views of the core structures of $[\{W(CO)_4Co_2(CO)_6\}\{\mu_3\text{-}PW(CO)_5\}_2]$ (**241**, left) and $[\{W(CO)_3Co_3(CO)_6\}\{\mu_3\text{-}PW(CO)_5\}_3]$ (**242**, right); carbonyl ligands omitted for clarity. Adapted from ref 169.

Scheme 77

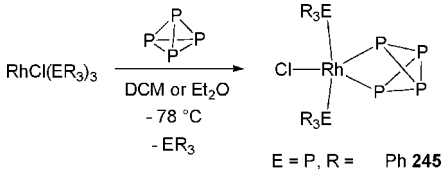

E = P, R = Ph **245**
R = *p*-Tos **247**
R = *o*-Tos **248**
E = As, R = Ph **246**

to −280.3 ppm for the pair of P-atoms coordinated to rhodium, and to −283.3 for the uncoordinated ones, respectively (Figure 49). The dihapto-coordination mode was also inferred from the couplings $^1J_{RhP}$ of 31−34 Hz, as opposed to negligible coupling of ^{103}Rh with P(5) and P(6).

The intact P_4 ligand is η^2-coordinated with the metal-bonded P−P edge perpendicular to the ligand plane, with the triphenylphosphine groups bending away from ligated P_4. The Rh−P(3) and Rh−P(4) bond lengths in **245** are 2.3016 (16) and 2.2849 (16) Å, respectively, and the most important deformation of the P_4 molecule is a lengthening (ca. 0.25 Å) of the P(3)−P(4) bond, compared to the regular tetrahedron (2.21 Å). Shortening of the P(5)−P(6) bond is also observed at 2.1884 (24) Å. EHMO calculations using *trans*-$[RhCl(PH_3)_2(\eta^2\text{-}P_4)]$ as a simplified model showed that in P_4 the six HOMOs are largely sp hybrids and the LUMOs are pd hybrids. The theoretical analysis of the Rh−P_4 bonding in **245** was carried out at a more sophisticated level by Krossing and van Wüllen using DFT methods on the PH_3 model.[174] This study definitely clarified the question of whether the complex should be regarded as a Rh(III) or Rh(I) species, pointing out that the P_4 ligand in **245** is best rationalized as being formally derived from a dianionic P_4^{2-} tetraphosphabicylclobutane structure.

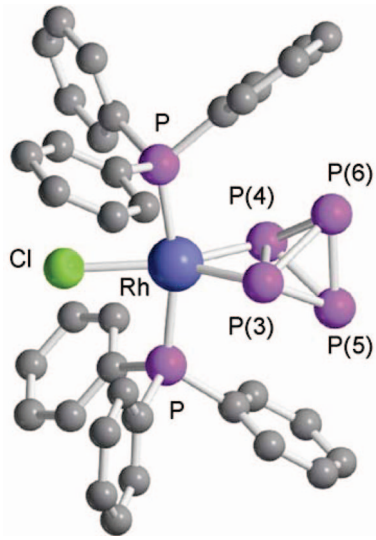

Figure 49. X-ray crystal structure of $[RhCl(PPh_3)_2(\eta^2\text{-}P_4)]$ (**245**). Adapted from ref 173.

As described in section 4.1, the reactivity of group 9 transition metal complexes stabilized by tripodal polyphosphines with white phosphorus was largely explored mainly by Sacconi et al. starting from 1978. The first article describing Rh and Ir complexes having a *cyclo*-P_3 moiety, i.e., $[(triphos)M(\eta^3\text{-}cyclo\text{-}P_3)]$ (M = Rh, **144**; Ir, **145**) was published soon after.[175] Complex **144** was synthezised by reacting a mixture of $[Rh(C_2H_4)_2Cl]_2$ and triphos with an excess of P_4 in THF/EtOH, whereas **145** was obtained under the same conditions, choosing as metal precursor Vaska's compound $[Ir(PPh_3)(CO)Cl]$. Both complexes were crystallized and the corresponding X-ray crystal structures are isomorphous to that of $[(triphos)Co(\eta^3\text{-}cyclo\text{-}P_3)]$ (**44**) described in section 4.1, with M−P bond lengths longer than for **44** (2.294 and 2.418 Å for **144**; 2.277 and 2.436 Å for **145**, respectively). The P−P distances in the *cyclo*-P_3 unit increase from Co (2.141) to Rh (2.152) to Ir (2.159 Å), due to a decrease in charge delocalization on passing from 3d to 4d and 5d metal orbitals. Further reactivity of these mononuclear *cyclo*-P_3 derivatives is similar to that shown by **44**. Thus, for example, bimetallic "triple-decker" complexes[125,126] $[\{(triphos)M_1(\mu,\eta^{3:3}\text{-}cyclo\text{-}P_3)M_2(triphos)\}]Y_n$ (M_1 = Co, Ni, Rh; M_2 = Rh, Ir; Y = BF_4, BPh_4; n = 1, 2) could be prepared in which the *cyclo*-P_3 fragment behaves as central bridging *trihapto* ligand, as described in section 4.1 and in Scheme 56, including remarks on the magnetic properties of such complexes. Worth mentioning here is the X-ray crystal structure of $[\{(triphos)Rh(\mu,\eta^{3:3}\text{-}cyclo\text{-}P_3)Ni(triphos)\}](BF_4)_2\cdot C_4H_8O$ (**249**). The structure of the dication is grossly similar to those of the Co congeners, although it differs in a way that the *cyclo*-P_3 group is shifted away from the intermetallic vector, along a plane perpendicular to it. This loss of C_3 symmetry is reflected by the P−P distances in the ring, namely, P(7)−P(8) 2.31 Å being much larger than the other two (average 2.15 Å). Other variations include the $M-P_{(triphos)}$ and $M-P_{(cyclo\text{-}P3)}$ bond lengths (2.28 and 2.40 Å, respectively), which are longer than those of the Co−Rh analogue **152** (see Table 1), and the M−M distance of 4.041(3) Å, which is larger than the value found for **152** (3.869(6) Å); all differences are mainly due to electronic factors.

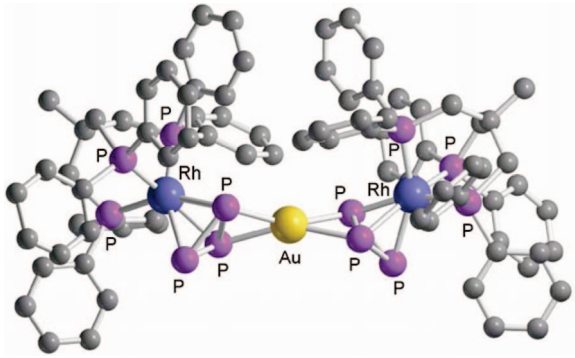

Figure 50. Molecular structure of the [{(triphos)M($\mu,\eta^{3:2}$-*cyclo*-P_3)}$_2$Au]PF_6 cation in **167**; adapted from ref 133.

The synthesis of the methyltriphosphirene complexes [(triphos)M(η^3-MeP_3)]Y (M = Rh, **170**; Ir, **171**; Y = BF_4, OTf) from the reaction of [(triphos)M(η^3-*cyclo*-P_3)] (M = Rh, **144**; Ir, **145**) at 0 °C with either methyl triflate or the Meerwin's salt, $(Me_3O)BF_4$, in CH_2Cl_2 has already been described[135] in section 4.1 and Scheme 59. The trimetallic complex [{(triphos)Rh($\mu,\eta^{3:2}$-*cyclo*-P_3)}$_2$Ag]Y, [Y = OTf, PF_6; (**165**)], obtained by treatment of **144** with either AgOTf or $[AgCl(PPh_3)_2]_4$ in 2:1 ratios followed by anion metathesis as well as their gold analogues [{(triphos)M($\mu,\eta^{3:2}$-*cyclo*-P_3)}$_2$Au]PF_6 [M = Rh (**167**), Ir (**168**)], prepared from **144** and **145** by reaction with [AuCl(PR_3)] (R = Me, Ph) or $[AuCl(L_2)]_2$ (L_2 = dppm, dppe) in the presence of $TlPF_6$, have been briefly described above (see Scheme 58).[133] These products belong to the class of trinuclear compounds of formula [{(triphos)M($\mu,\eta^{3:2}$-*cyclo*-P_3)}$_2$M′]$^+$ where two {(triphos)M(η^3-*cyclo*-P_3)} units are bridged by a coinage metal atom. X-ray crystal structures were obtained for some of these complexes, and that corresponding to **167** is shown in Figure 50. The {$Rh_2(\mu,\eta^{3:2}$-$P_3)_2$}Au core closely resembles that of [{(triphos)Co($\mu,\eta^{3:2}$-P_3)}$_2$Cu]PF_6 (**163**) shown in Figure 33 (section 4.1),[133] except for the Rh−P bond of each RhP_3 unit lying opposite to the perturbated P−P bond, which is slightly lengthened compared to those opposite the other two P−P bonds (2.431 vs 2.374 and 2.371 Å).

Organometallic fragments such as {$CpRu(PPh_3)$} were also coordinated to the *cyclo*-P_3 unit of [(triphos)M(η^3-P_3)] (M = Co, **44**; Rh, **144**).[176] The reaction between complexes **44** and **144** and $[CpRu(PR_3)(MeCN)_2]PF_6$ (R = Ph, Me, Cy) in 1:1 ratios in DCM in the presence of MeCN gave the bimetallic adducts [{(triphos)M}($\mu,\eta^{3:1}$-P_3){$CpRu(PR_3)$(MeCN)}]PF_6 [M = Co, R = Ph, (**250**); Me, (**251**); Cy, (**252**); M = Rh, R = Ph, (**253**); Me, (**254**); Cy, (**255**)]. When Rh complexes **253** and **255** were treated with PMe_3, complexes [{(triphos)Rh}($\mu,\eta^{3:1}$-P_3){$CpRu(PR_3)(PMe_3)$}]PF_6 (R = Ph, **256**; Cy, **257**) were obtained. Interestingly, complexes **253** and **255** lose acetonitrile on standing in dichloromethane solutions, while the $CpRu(PR_3)$ moiety rearranges, coordinating further to *cyclo*-P_3 in a $\eta^{3:1,1'}$-P_3 fashion, yielding complexes [{(triphos)Rh}($\mu,\eta^{3:1,1'}$-*cyclo*-P_3){$CpRu(PR_3)$}]PF_6 (R = Ph, **258**; Me, **259**) (Scheme 78).

Similarly to **44**, the reaction of [(triphos)Rh(η^3-*cyclo*-P_3)] with $W(CO)_5$ or $[W(CO)_4(PPh_3)(THF)]$ in THF at RT gives the carbonyl adducts [{(triphos)Rh}($\mu,\eta^{3:1}$-*cyclo*-P_3){$W(CO)_5$}] (**260**) and [{(triphos)Rh}($\mu,\eta^{3:1}$-*cyclo*-P_3){$W(CO)_4(PPh_3)$}] (**261**), respectively.[131] These compounds, like the analogous cobalt derivatives, are fluxional in solution, as demonstrated by variable-temperature NMR studies, suggesting that the {(triphos)M} fragment rotates about its

Scheme 78

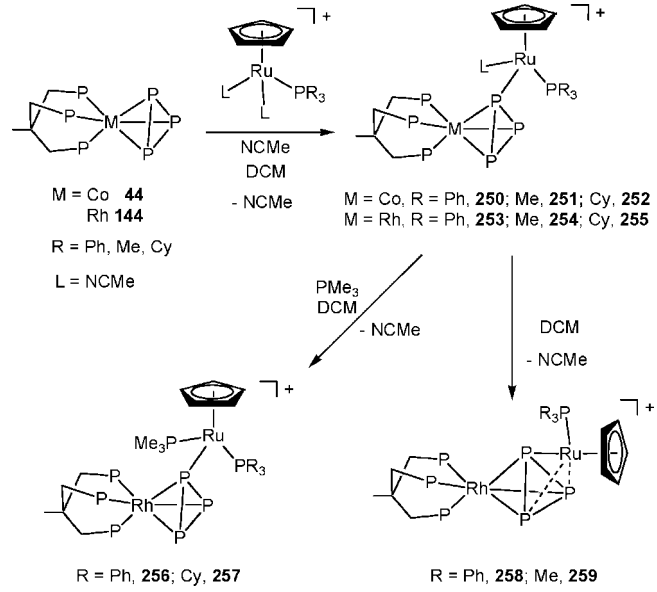

C_3 axis and {$W(CO)_5$} or {$W(CO)_4(PPh_3)$} scramble over the P_3 cycle. A view of the molecular structure of **261** is shown in Figure 51.

A rhodium complex featuring the intact *tetrahedro*-tetraphosphorus ligand was prepared by Stoppioni and coworkers using tetrapodal polyphosphine and aminophosphines as bulky ancillary coligands.[140] This chemistry has been briefly mentioned in section 4.1 when the related $[(PP_3)Co(\eta^1\text{-}P_4)]^+$ species was illustrated.

The presence of different donor atoms (P vs N) in the tetrapodal ligands (L) such as PP_3 or NP_3 (see section 4.1) has a profound effect on the topology of the η^1-P_4 coordinated unit in $[(L)M(\eta^1\text{-}P_4)]^+$. Whereas in the presence of PP_3 the trigonal bipyramidal complex $[(PP_3)Rh(\eta^1\text{-}P_4)]^+$ (**179**) containing the intact P_4 molecule coordinated in a end-on fashion is formed, the octahedral Rh(III) complex $[(NP_3)Rh(\eta^2\text{-}P_4)]^+$ (**180**) is obtained when replacing PP_3 by NP_3. In the latter derivative, a *dihapto*-coordinated mode, resulting from oxidative addition to Rh(I) precursor and switch from η^1 to η^2-coordination, is evident on the basis of NMR analysis. The reactions were carried out starting from [(L)MH] (L = PP_3, M = Co, Rh; L = NP_3, M = Rh),

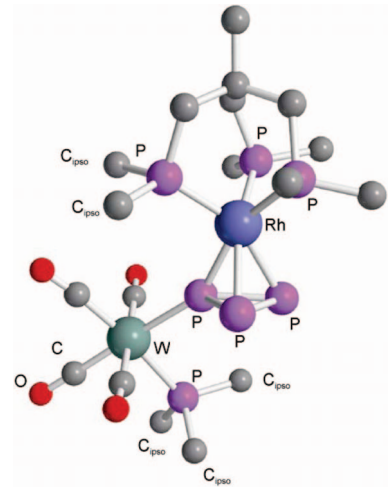

Figure 51. X-ray crystal structure of [{(triphos)Rh}($\mu,\eta^{3:1}$-P_3){$W(CO)_4(PPh_3)$}] (**261**); only *ipso*-carbons shown. Adapted from ref 131.

Scheme 79

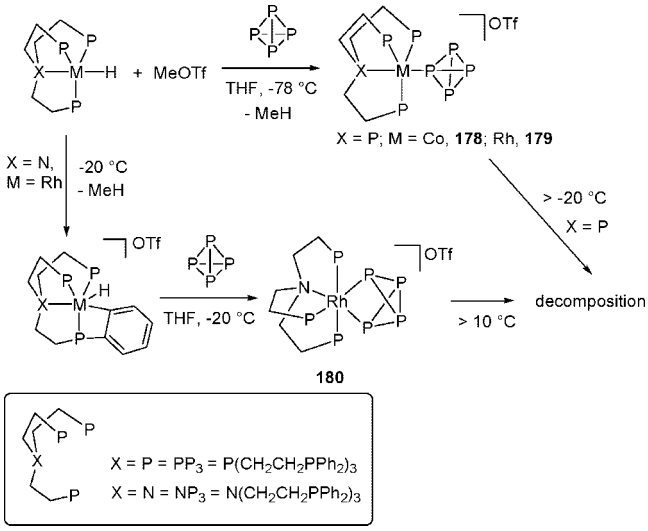

followed by addition of methyl triflate at room temperature in THF. The solutions obtained were cooled to −70 °C, and P_4 dissolved in THF was added (for L = NP_3, $NaBPh_4$ was also added). The reaction involving [(NP_3)RhH] was found to proceed via an *ortho*-metalated intermediate stable at −20 °C (Scheme 79).

Hydrido complexes [(triphos)RhH_3] and [(triphos)IrH_3] were also used as starting materials for the reactions with P_4. Irrespective of the rhodium(I) or iridium(I) precursor, the reactions gave the air- and moisture-stable complexes [(triphos)M(η^3-*cyclo*-P_3)] as lemon-yellow (M = Rh, **144**) or off-white (M = Ir, **145**) crystalline materials in moderate yields as final products.[177] The reactions proceed via thermal reductive elimination of dihydrogen to produce the highly reactive intermediate [(triphos)MH]. The reaction of the 16-electron fragment [(triphos)RhH] with white phosphorus in THF at about 70 °C under nitrogen does not produce directly the *cyclo*-triphosphorus species **144**; instead it yields an orange solution from which dark orange microcrystals of the novel complex [(triphos)Rh($\eta^{1:2}$-HP_4)] (**262**) are obtained after solvent removal under reduced pressure. Complex **262** reacts with H_2 at atmospheric pressure, forming PH_3 in high yield together with **144**. In a similar way, when the reaction between [(triphos)RhH_3] and phosphorus was carried out in a closed system such as a sealed NMR tube, it afforded quantitatively PH_3 and the *cyclo*-triphosphorus complex **144** (Scheme 80) via the intermediacy of **262**. The presence of a P−H bond in **262** was confirmed by a combination of ^{31}P DEPT and ^{1}H−^{31}P HMQC NMR experiments, showing a strong one-bond correlation peak between a P-resonance at −280.33 ppm and a ^{1}H NMR signal at 0.01 ppm (doublet of multiplets), with a $^1J_{HP}$ coupling constant of ca. 120 Hz. PH_3 is produced only in stoichiometric amount, i.e., only one P atom of P_4 is hydrogenated, with the remaining three forming the *cyclo*-P_3 unit, as demonstrated by sapphire-tube NMR experiments under a pressure or atmosphere of hydrogen gas.

Transition metal mediated P−C bond-forming reactions are quite rare. An example of such reactivity was demonstrated by Peruzzini and co-workers.[178] Ethylene labilization in the alkyl and aryl rhodium complexes [(triphos)RhR(η^2-C_2H_4)] (R = H, Me, Et, Ph) by white phosphorus under extremely mild conditions (THF, −20 °C) affords the unprecedented rhodium(III) complexes [(triphos)Rh($\eta^{2:1}$-

Scheme 80

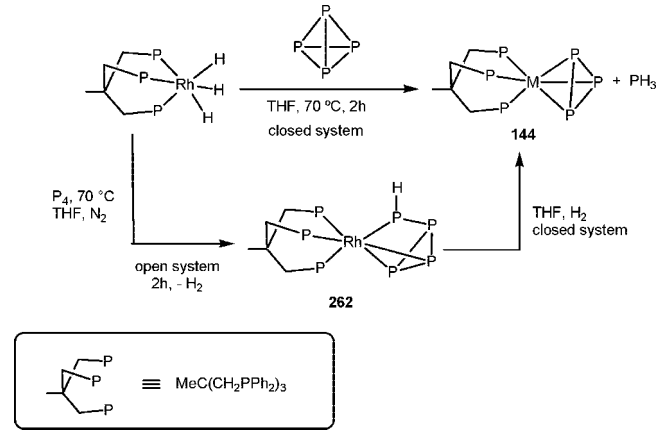

Scheme 81

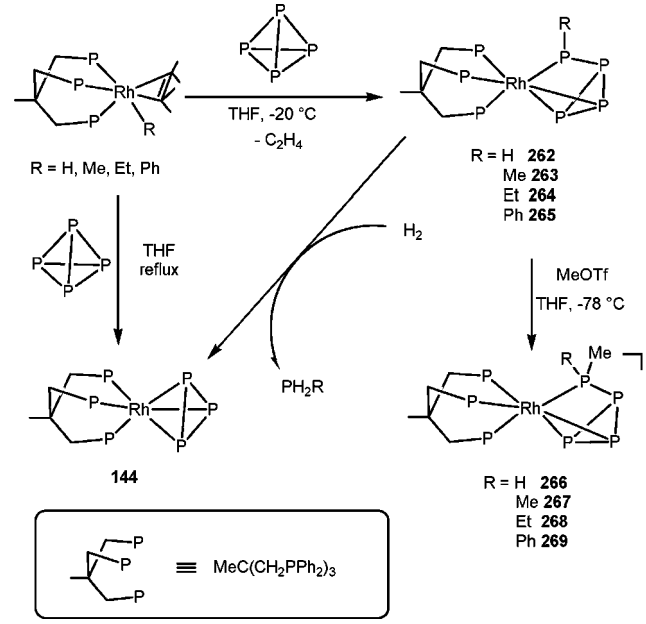

P_4R)] [R = Me, (**263**); Et, (**264**); Ph, (**265**)] where an alkyl or aryl tetraphosphido group is coordinated to the metal as a six-electron ligand (Scheme 81). The reaction with the hydrido−ethylene complex [(triphos)RhH(η^2-C_2H_4)] does not give **262**, instead resulting in the ethylphosphido derivative **264** via a double-insertion process occurring at first by insertion of the ethylene ligand in the Rh−H bond followed by a migratory step transferring the ethyl ligand obtained to the activated P_4 unit. These organyltetraphosphido derivatives are stable and can be isolated in the solid state, but they are highly reactive toward electrophilic reagents and other simple molecules.

The electrophilic attack of MeOTf or HBF_4 to the P_4R ligand in the complexes **262**−**265** is regioselective and yields cationic products of formula [(triphos)Rh($\eta^{1:2}$-P_4RR′)]$^+$ [R′ = H; R = Me, (**266**); R′ = Me; R = Me, (**267**); Et, (**268**); Ph, (**269**)].[179] The direct attack to the substituted P−R phosphorus atom is demonstrated by crossing experiments. Complexes of the latter type have been isolated in the solid state for the combinations R = H and R′ = Me or R = Ph and R′ = Me.

Multinuclear and multidimensional NMR analyses carried out for [(triphos)Rh($\eta^{1:2}$-P_4RR′)]$^+$ complex cations confirm the solid-state structure determined by X-ray diffractometry

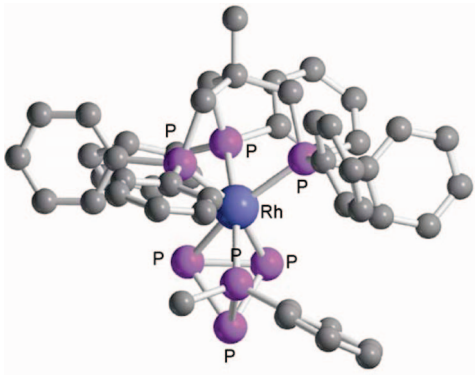

Figure 52. Molecular structure of the [(triphos)Rh{$\eta^{2:1}$-P_3PPh(Me)}]$^+$ cation in (**269**). H atoms are omitted for sake of clarity; adapted from ref 179.

Scheme 82

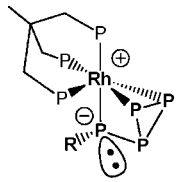

(vide infra).[180] 2D ^{1}H NOESY and ^{31}P{^{1}H} exchange NMR spectroscopy (EXSY) show that these complexes are flexible on the NMR time scale over the temperature range 253−318 K, experiencing a dynamic process between the PPh_2 groups of triphos. The NMR data indicate a slow scrambling motion in which the P_4R unit tumbles with respect to the (triphos)Rh moiety. DFT calculations suggest the presence of a turnstile mechanism involving the 3- and 2-fold rotors in which the complex is subdivided.

The X-ray crystal structure of the doubly alkylated [(triphos)Rh{($\eta^{2:1}$-P_3PPh(Me)}]OTf (**269**) has been determined, and a view of the cation is shown in Figure 52. The geometry at the metal is better described as trigonal bipyramidal rather than pseudo-octahedral. This is due to the P_4RR' group that behaves as bidentate through the exocyclic PR_2 donor group and the endocyclic dihapto-P═P bond. This assignment was confirmed by NMR experiments and DFT calculations (Scheme 82).

Of particular relevance is the reaction taking place when a solution of **262**−**265** is exposed to a hydrogen atmosphere, resulting in the formation of alkyl or arylphosphines PH_2R in moderate yields (Scheme 81). The stoichiometric functionalization reaction involves one phosphorus atom while the three remaining P atoms are scavenged to give the known *cyclo*-P_3 complex [(triphos)Rh(η^3-*cyclo*-P_3)] (**144**).

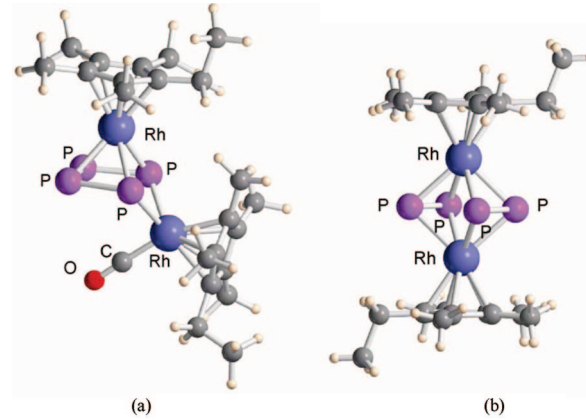

Figure 53. Molecular structures of (a) [(Cp^{Et}Rh)($\mu,\eta^{4:2}$-P═P−P═P){Rh(CO)Cp^{Et}}] (**270**) and (b) [{Cp^{Et}Rh}$_2$($\mu,\eta^{2:2}$-P_2)$_2$] (**271**); adapted from refs 181 and 182.

Substituted cyclopentadienyl Rh fragments were successfully reacted with white phosphorus causing P−P bond activation and reaggregation toward novel polyphosphorus topologies. Reaction of [Cp^{Et}Rh(CO)$_2$] with P_4 in a Schlenk-type pressure tube in xylene at 200 °C for 30 min caused the tetraphosphorus incorporation into a metallatetraphosphacyclopentadiene unit, which functions as a $\mu,\eta^{4:2}$-ligand in the sandwich complex [(Cp^{Et}Rh)($\mu,\eta^{4:2}$-P═P−P═P){Rh(CO)Cp^{Et}}] (**270**) (Scheme 83).[181] After chromatographic workup and recrystallization, **270** is recovered as red crystals that are stable in the air only for a short time, sufficient enough to allow for the X-ray data collection (Figure 53a). Complex **270** loses CO upon heating and rearranges, giving the more stable [{Cp^{Et}Rh}$_2$($\mu,\eta^{2:2}$-P_2)$_2$] (**271**), which accompanies **270** as byproduct and can be recovered after chromatographic column separation. The molecular structure of **270** shows a planar configuration of the tetraphosphorus square with nearly identical P−P distances ($d_{(P-P)ave}$ = 2.154 Å), which are shorter than those for the Midollini's Co complex containing an opened tetraphosphabutadiene chain [Co{$Ph_2PCH_2P(Ph)_2$*PPPP*$(Ph)_2CH_2PPh_2$}]BF_4 (**181**) described in section 4.1.[141]

Complexes [{Cp^{Et}Rh}$_2$($\mu,\eta^{2:2}$-P_2)$_2$] (**271**) and [{Cp*Rh}$_2$-($\mu,\eta^{2:2}$-P_2)$_2$] (**272**) were independently synthesized by refluxing the mixture in xylene for 8 h.[182] After chromatography and recrystallization, compound **271** was recovered as crystals suitable for X-ray analysis (Figure 53b). The solid-state structure of **271** should be regarded as a binuclear sandwich complex bearing two 4-electron $\mu,\eta^{2:2}$-P_2 donors, with long Rh···Rh nonbonding distance (3.324 Å), P(1)−P(2) distance at 2.052 Å, and P(1)···P(2′) at 2.845 Å.

Scheme 83

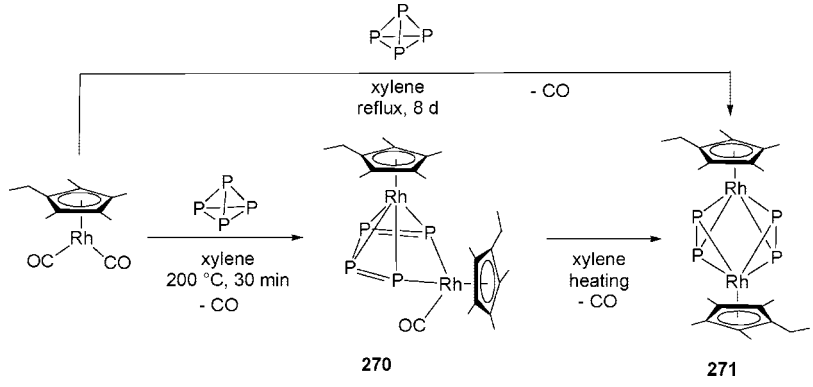

Scheme 84

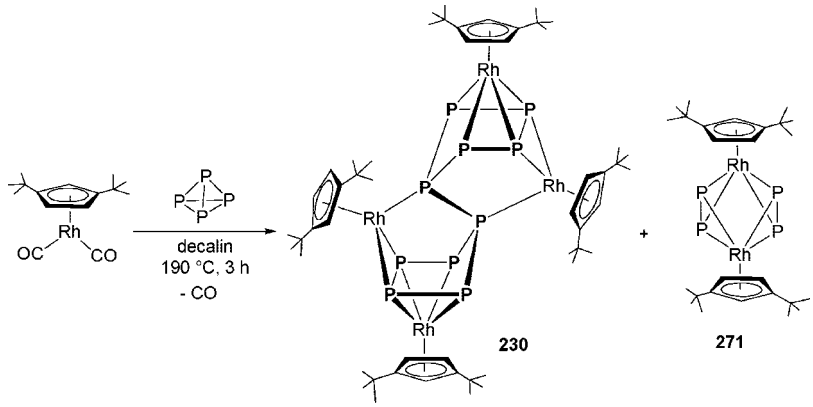

The effect of bulky substituents on the Cp ring has been tested also in the case of Rh complexes. The reaction of [Cp″Rh(CO)$_2$] with white phosphorus in decalin at 190 °C for 3 h gave a mixture of [(Cp″Rh)$_4$P$_{10}$] (**230**) and [{Cp″Rh}$_2$-(μ,$\eta^{2:2}$-P$_2$)$_2$] (**273**) (Scheme 84).[161]

In complex **230**, the X-ray crystal structure confirms the existence of the polycyclic Rh$_4$P$_{10}$ framework, formally analogue of all-phosphorus dihydrofulvalene with P$_{10}$ acting as a 16-electron donor ligand (see Scheme 74). The structure shares with **229** and **237**[162] the unusual decaphosphorus topology and may be alternatively seen as the "doubled version" of **270**, with two P$_5$ units connected by the out-of-plane P atoms. The average P−P distance (2.17 Å) is significantly shorter than that for the chromium decaphosphorus complex [{CpCr(CO)$_2$}$_5$P$_{10}$] (2.22 Å), which, however, displays a different arrangement of the 10 P atoms.[183]

The reaction of white phosphorus with [Cp^{Bu}Rh(CO)$_2$] in the presence of [Cr(CO)$_5$(THF)] at 50−60 °C in toluene gives a mixture of [{Cp^{Bu}Rh(CO)}(μ_5,$\eta^{2:1:1:1:1}$-P$_4$){Cr(CO)$_5$}$_4$] (**274**) and [{Cp^{Bu}Rh}(μ_5,$\eta^{4:1:1:1:1}$-P$_4$){Cr(CO)$_5$}$_4$] (**275**) as air-stable complexes.[154] Moreover, **275** can be formed exclusively either by using a large excess of [Cr(CO)$_5$(THF)] or by thermolysis of **274**. The reaction is reminiscent of the chemistry described in Scheme 67. The crystal strucutre of **274** (Figure 54) shows a RhP$_4$ core with an open-edged phosphorus tetrahedron in butterly conformation, isostructural with the Co complex [Cp*Co(CO)(η^2-P$_4$)] (**202**), with the main difference being in the P···P distance of the open edge, which is larger for **274** (2.808 Å) than for **202** (2.606 Å). In the case of **275**, the RhP$_4$ core consists of a tetraphosphorus planar square capped by Cp^{Bu}Rh, with a slight kitelike distortion, and all P atoms also coordinate to a Cr(CO)$_5$ fragment. While the P−P bond lengths are similar ($d_{(P-P)ave}$ = 2.149 Å) and shorter than single-bond distances, the P−P distance belonging to the edge opposite to the *tert*-butyl group is slightly lengthened (2.160 Å). The topology change was rationalized by assuming an initial P−P edge opening from the P$_4$ tetrahedron upon coordination to Rh, followed by sequestration of each P lone pair to Cr. The attack of the second Rh fragment to the P−P edge being blocked by Cr capping and CO abstraction is favored and, in turn, causes the opening of a second P−P edge to obtain the final kitelike conformation and η^4-P$_4$ coordination.

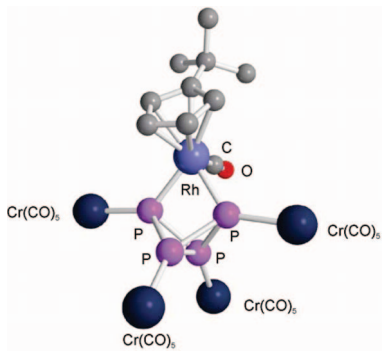

Figure 54. Molecular structure of [{Cp^{Bu}Rh(CO)}(μ_5,$\eta^{2:1:1:1:1}$-P$_4$){Cr(CO)$_5$}$_4$] (**274**); carbonyl ligands on Cr omitted for clarity. Adapted from ref 154.

The presence of two *tert*-butyl groups on the Cp ring forces lability of one Cr(CO)$_5$ group, resulting in the formation of [{Cp″Rh}(μ_4,$\eta^{4:1:1:1}$-P$_4$){Cr(CO)$_5$}$_3$] (**276**).[184] The X-ray crystal structure of [{Cp″Rh(CO)}(μ_5,$\eta^{2:1:1:1:1}$-P$_4$){Cr(CO)$_5$}$_4$] (**277**) was also obtained, confirming the stepwise P−P bond cleavage in passing from the tetrahedron to square planar, also in the case of Cp″Rh complexes. The study was substantiated by variable-temperature ^{31}P{^{1}H}NMR data, which allowed for the evaluation of the activation energy for conversion $\Delta G^{\ddagger}$ = 36 kJ mol^{-1} by freezing the Cp″ rotation at low temperature.[185]

4.3. Iridium

Iridium complexes resulting from the activation of white phosphorus are the least represented among group 9 metals. Usually the main advantage in the use of Ir vs Rh is the higher kinetic stability of the former, which can help in the detection and isolation of short-lived reaction intermediates in the case of Rh chemistry.

The chemistry of [(triphos)Ir(*cyclo*-η^3-P$_3$)] (**145**) has been briefly outlined in sections 4.1 and 4.2, where the synthesis and the reactivity of the more investigated cobalt and rhodium cyclotriphosphorus complexes have been detailed. Worth being mentioned here is the reaction with gold(I) precursors that provides access to the structurally authenticated[{(triphos)Ir(μ,$\eta^{3:2}$-*cyclo*-P$_3$)}$_2$Au]PF$_6$(**168**).[134][(triphos)-Ir(*cyclo*-η^3-P$_3$)] has been also used to prepare triple-decker sandwich complexes including [{(triphos)Ir(μ,$\eta^{3:3}$-*cyclo*-P$_3$)Co(triphos)}]Y$_2$ (Y = BF$_4$, BPh$_4$), **153**.[125]

An Ir analogue of the "super sandwich" [{(triphos)Co(η^3-*cyclo*-P$_3$)}$_2$(CuBr)$_6$] (**162**)[132] was obtained by Midollini et al. by reacting CuBr in DCM with [(triphos)Ir(*cyclo*-η^3-P$_3$)] (**145**) at RT for 30 min.[186] The orange crystals of [{(triphos)-Ir(η^3-*cyclo*-P$_3$)}$_3$Cu$_5$Br$_4$](CuBr$_2$) (**278**) were recrystallized from nitroethane/*n*-BuOH, and the corresponding X-ray crystal structure is shown in Figure 55.

In the structure of the complex cation, three (triphos)Ir(η^3-*cyclo*-P$_3$) units are held together by the central Cu$_5$Br$_4$ core

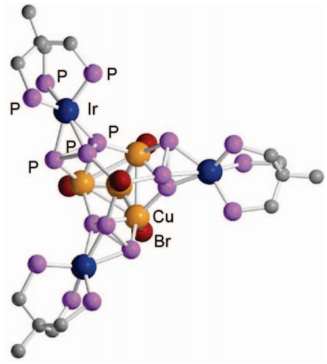

Figure 55. View of the molecular structure of the cation $[\{(triphos)Ir(\eta^3\text{-}P_3)\}_3Cu_5Br_4]^+$ (**278**). Phenyl groups on triphos omitted for clarity; adapted from ref 186.

Scheme 85

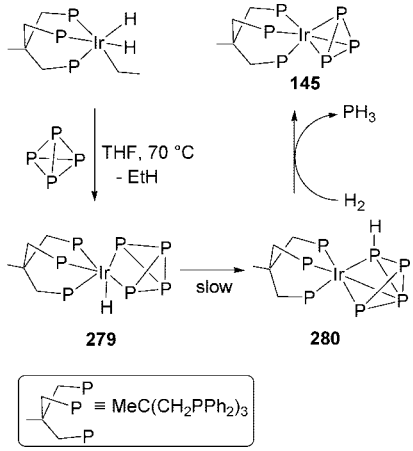

cluster via the P_3 fragment connected edge-on. The upper edge of the distorted trigonal bipyramid made of the five Cu atoms is much longer (4.637 Å) than the equatorial edges (avg. 2.795 and 3.017 Å). The Ir−P_3 distances are at 2.427 Å, at values comparable to the parent compound **145**.

The reaction of $[(triphos)IrH_3]$ with white phosphorus parallels that of the rhodium congener, yielding, upon elimination of phosphine, the *cyclo*-P_3 complex **145** as the thermodynamic sink of the reaction.[177] The mechanism of white phosphorus functionalization reactions mediated by $[(triphos)RhH_3]$ (section 4.2) has been investigated in depth by studying the behavior of the kinetically more stable iridium complexes, $[(triphos)IrH_3]$ and $[(triphos)IrH_2(Et)]$. In particular, the dihydride−ethyl derivative, when heated to 70 °C in THF, releases ethane rather than H_2, providing a simple way to the coordinatively unsaturated fragment [(triphos)IrH]. Thus, the reaction of $[(triphos)IrH_2(Et)]$ with elemental phosphorus in refluxing THF allowed for the isolation of the hydrido−tetraphosphido species $[(triphos)Ir(H)(\eta^2\text{-}P_4)]$ (**279**), which slowly isomerizes in solution to $[(triphos)Ir(\eta^{1:2}\text{-}P_4H)]$ (**280**) by transfer of the metal-bonded hydride to one of the metalated phosphorus atom of the P_4^{2-} ligand (Scheme 85). Addition of H_2 to **280** completes the reaction, affording PH_3 and $[(triphos)Ir(cyclo\text{-}\eta^3\text{-}P_3)]$ (**145**).[178]

The reaction of $[Cp^*Ir(CO)_2]$ with P_4 under photolytic (UV light, 15 °C) or thermolytic (70 °C, THF) activation conditions in the presence of $[Cr(CO)_5(THF)]$ was studied by Scheer et al.[187] At variance with the reactivity observed in the case of Co (section 4.1) and Rh analogues (section 4.2), the reactions described above yield, together with the expected

Scheme 86

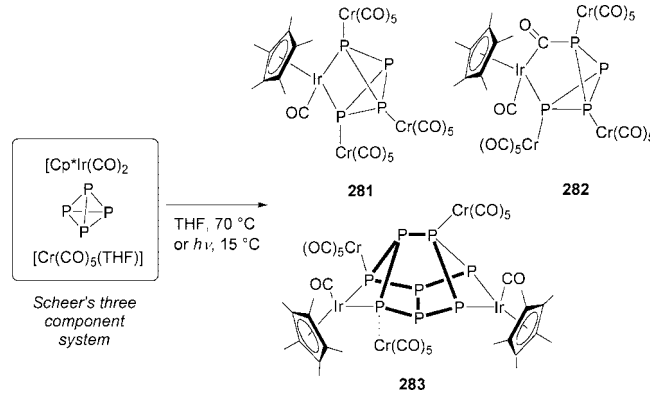

$[\{Cp^*Ir(CO)\}(\mu_4,\eta^{2:1:1:1}\text{-}P_4)\{Cr(CO)_5\}_3]$ (**281**), complex $[\{Cp^*Ir(CO)\}(\mu_4,\eta^{2:1:1:1}\text{-}\{(CO)P_4\})\{Cr(CO)_5\}_3]$ (**282**), where a CO group has undergone insertion into the Ir−P bond, and the cuneane-type complex $[\{Cp^*Ir(CO)\}_2(\eta^{2:2:1:1:1}\text{-}P_8)\{Cr(CO)_5\}_3]$ (**283**), formally deriving from the coupling of two molecules of **282** via a P−P edge of the η^2-P_4 unit, as shown in Scheme 86. The complexes were also characterized by X-ray crystallographic methods, and the molecular structure of **282** is shown in Figure 56. The structure of **283** contains the cuneane P_8-topology, which was previously determined in Dahl's tetrairon species $[Cp^{Me}{}_4Fe_4(CO)_6P_8]$ (**36**).[41]

Although already discussed in section 3.1.2 dedicated to iron, we recall here that Scherer's pentaphosphaferrocene derivative, $[Cp^*Fe(\eta^5\text{-}P_5)]$ (**14**), undergoes a thermal reaction with the iridium carbonyls $[\{Cp^*Ir(CO)\}_2]$[83] and $[Cp^*Ir(CO)_2]$,[86] yielding a variety of mixed Fe/Ir derivatives in which the *cyclo*-P_5 topology may also be lost (see Schemes 34 and 35).

Highly reactive Rh and Ir complexes stabilized by diphosphines such as $[M(dppm)_2]OTf$ (M = Rh, Ir; dppm = $PPh_2CH_2PPh_2$) were reacted with white phosphorus in DCM at RT under nitrogen. Subsequent workup allowed for the isolation of $[M(dppm)(Ph_2PCH_2PPh_2\textit{PPPP})]OTf$ as either orange (M = Rh, **284**) or light yellow microcrystals (M = Ir, **285**) (Scheme 87).[188] In these complexes, a new P_4 topology formed by a *cyclo*-P_3 ring and a dangling functionalized P atom is present. This bonding situation can be seen as the intermediate key structural motif leading to the tetraphosphabutadiene moiety $Ph_2PCH_2PPh_2\textit{PPPP}Ph_2PCH_2PPh_2$ observed in $[Co\{Ph_2PCH_2P(Ph)_2\textit{PPPP}(Ph)_2CH_2PPh_2\}]BF_4$ (**181**),[141] which in principle can be obtained by

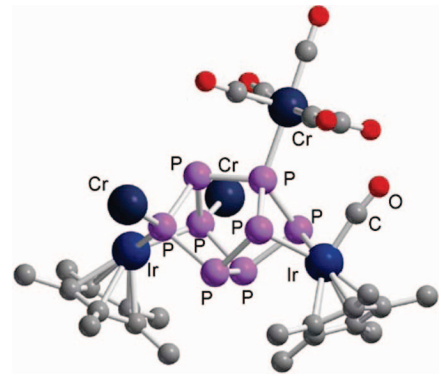

Figure 56. View of the molecular structure of **283**. The carbonyl ligands of two $Cr(CO)_5$ units are omitted for clarity; adapted from ref 187.

Scheme 87

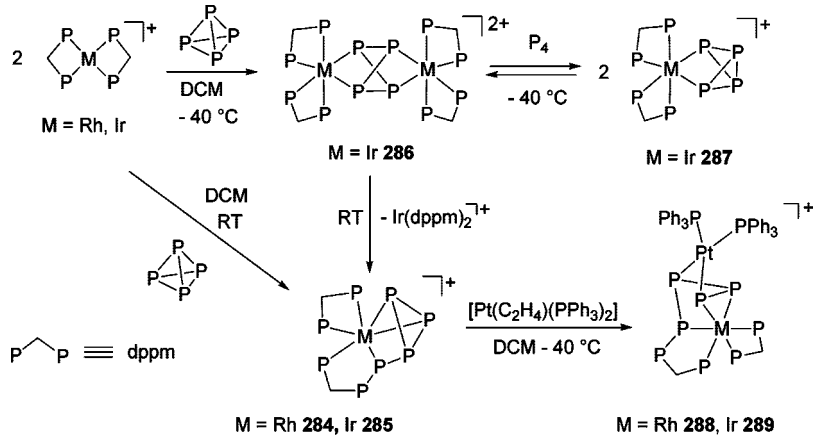

further cleavage of P7−P8 bond, followed by attack to a PPh_2 group of chelating dppm. The reaction was monitored by VT $^{31}P\{^1H\}$ NMR spectroscopy using the less reactive [Ir(dppm)$_2$]OTf precursor. White phosphorus immediately reacts with the iridium educt already at −40 °C, giving a highly fluxional intermediate whose NMR spectrum suggests to be the dimer [{Ir(dppm)$_2$}$_2$(μ,$\eta^{2:2}$-P$_4$)]$^{2+}$ (**286**). Increasing the temperature to 25 °C slowly gives the final compound **285** in almost quantitative yield after ca. 4 days (Scheme 87). In a separate experiment, on standing at −40 °C, a set of resonances ascribable to [Ir(dppm)$_2$(η^2-P$_4$)]OTf (**287**) appeared in the spectrum within 20 min. After a week at −20 °C, brown crystals of **287** precipitated. The structure of the complex cation in **285** is presented in Figure 57a, and the complex consists of the [Ir(dppm)($Ph_2PCH_2PPh_2PPPP$)]$^+$ cation and a triflate anion. In the complex cation, the metal is pseudo-octahedrally coordinated by a dppm and by the new $Ph_2PCH_2PPh_2PPPP$ ligand, which originates from the attack of one terminal dppm Ph_2P group to the P_4 molecule. The structure of **287** contains [(dppm)$_2$Ir(η^2-P$_4$)]$^+$ complex cations (Figure 57b) with the metal center hexacoordinated by the four phosphorus donors of two dppm ligands and by an η^2-P_4 tetraphosphabicyclobutadienide ligand. The distances in η^2-P_4^{2-} moiety are comparable with those of other reported butterfly P_4 ligands. The whole activation process results in the rupture of two P−P edges (P5−P7 and P5−P8) followed by attack of P5 to one dppm PPh_2 terminal group.

Both complexes **284** and **285** are electrochemically active at cathodic potentials and undergo a two-electron reduction at the cathodic peak $\mathbf{C_1}$ (two-electron process, see Figure 58).[189]

Thus, complexes **284** and **285** can be activated electrochemically by irreversible transfer of two electrons or by interaction with nucleophiles by reaction with [Pt(C_2H_4)(PPh_3)$_2$], as clearly identified by ^1H and $^{31}P\{^1H\}$ NMR experiments.[190] Regioselective insertion of the {Pt(PPh_3)$_2$} moiety into one of the P−P edges of the P_5 unit in DCM at −40 °C results in the formation of the novel heterobimetallic complexes [Rh(dppm)($Ph_2PCH_2PPh_2PPPP$){Pt(PPh_3)$_2$}]OTf (**288**) and [Ir(dppm)($Ph_2PCH_2PPh_2PPPP$){Pt(PPh_3)$_2$}]OTf (**289**). The heterobimetallic complexes obtained are unstable both in solution and in the solid state at room temperature due to loss of triphenylphosphine. The $^{31}P\{^1H\}$ NMR spectrum of **289** consists of a temperature-invariant, 10-resonance spin system, indicating the chemical nonequivalence of all phosphorus nuclei. A new pentaphosphorus topology can be assumed to be present in the new complexes, in agreement with a phosphonium(+)−tetraphosphabutadienide(2−) ligand $^{(-)}P_8{=}P_7{-}P_6{}^{(-)}{=}P_5{}^{(-)}{-}P_3{}^{(+)}Ph_2R$.

The tetrahedral triiridium cluster, [{Ir(PF_3)$_3$}$_3$(μ_3-P)] (**290**), was obtained in poor yield as an orange crystalline material from the high pressure (80−200 atm) reaction of $IrCl_3$ and PF_3. The product was characterized by MS analysis only.[191]

5. Group 10 Metals

5.1. Nickel

The first complex containing the *tetrahedro*-P_4 ligand was published in 1979 by Sacconi and co-workers, with an organonickel fragment containing the tripodal aminophospine

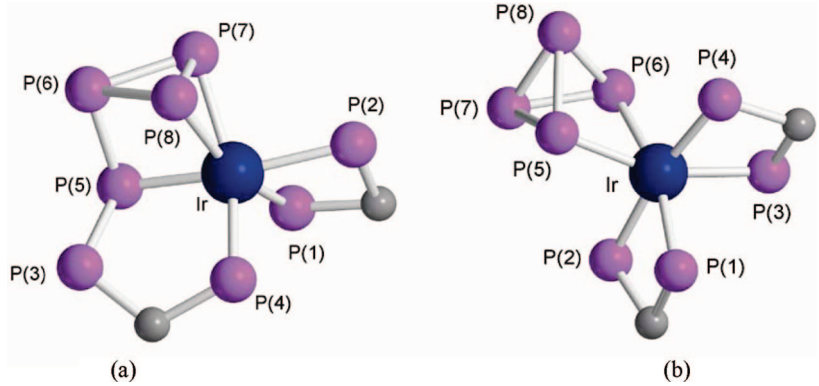

Figure 57. Molecular structure of the complex cations [Ir(dppm)($Ph_2PCH_2PPh_2PPPP$)]$^+$ in **285** (a) and [(dppm)$_2$Ir(η^2-P$_4$)]$^+$ in **287** (b). Hydrogen atoms and phenyl ligands are omitted; adapted from ref 188.

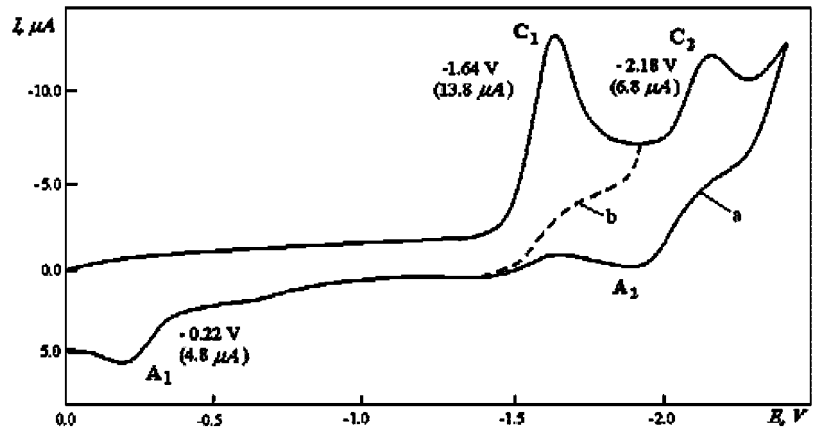

Figure 58. Cyclic voltammogram (CV; cathodic part) in DMF of complex **285** (1.0×10^{-2} M) on glassy carbon (GC) electrode in the presence of 0.1 M $(NBu_4)BF_4$ [CV curve was recorded at the first scan: (a) from 0.00 to −2.50 V and back to 0.00 V; (b) from 0.00 to −1.90 V and back to 0.00 V; vs $Ag/AgNO_3$ 1.0×10^{-2} M in CH_3CN; 50 mV s^{-1}]. Reproduced with permission from Figure 2 in ref 189. Copyright 2008 Taylor and Francis Ltd.

Scheme 88

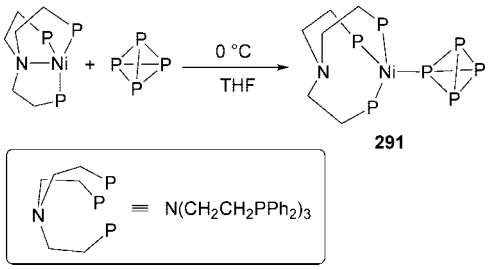

tris(2-diphenylphosphinoethyl)amine (NP_3). The new complex, $[(\kappa^3\text{-}P,P,P\text{-}NP_3)Ni(\eta^1\text{-}P_4)]$ (**291**), was prepared from the trigonal pyramidal Ni(0) species $[(\kappa^4\text{-}NP_3)Ni]$ and P_4 in cold THF (Scheme 88).[5] The reaction proceeds via white phosphorus coordination following NP_3−nitrogen decoordination so that the overall coordination geometry at nickel in **291** is tetrahedral with the metal atom bound to the three P atoms of the ancillary ligand and to one P atom from the P_4 molecule. The flexibility of NP_3 backbone allows for a facile κ^4-κ^3 switch in its coordination hapticity. The complete insolubility of **291** in all the common organic solvents did not allow for the characterization of the species in solution and to develop any reactivity on this intriguing compound.

The reaction of P_4S_3 dissolved in benzene and $[Ni(H_2O)_6](BF_4)_2$ in EtOH/THF, in the presence of triphos (Scheme 89), gave lemon yellow crystals of $[(triphos)Ni(\eta^3\text{-}cyclo\text{-}P_3)]BF_4$ (**150b**),[127] isoelectronic and isostructural with the homologous neutral compounds of the cobalt triad $[(triphos)M(\eta^3\text{-}cyclo\text{-}P_3)]$ [M = Co (**44**), Rh (**144**), Ir (**145**)] (vide supra).[6,125] The crystal structure is also similar, with the triphos P atoms and those of the planar *cyclo*-P_3 unit coordinated to the metal center, in a distorted octahedral environment. The crystal structure of the triodide salt $[(triphos)Ni(\eta^3\text{-}cyclo\text{-}P_3)]I_3$ was also reported.[192]

Scheme 89

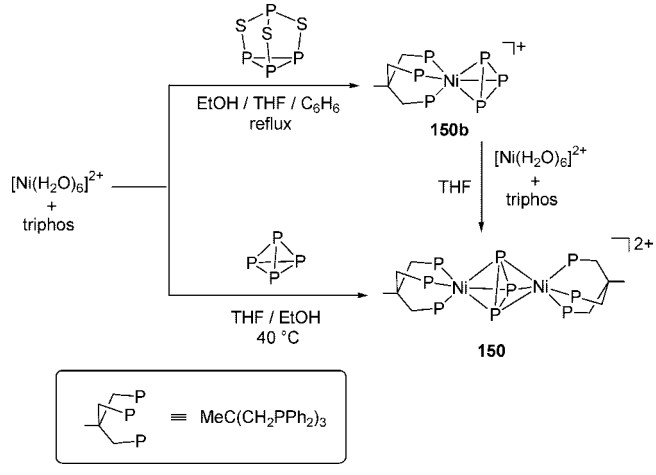

Remarkably, the same reaction performed using white phosphorus instead of P_4S_3 gives only the "triple-decker" sandwich compound $[\{(triphos)Ni\}_2(\mu,\eta^{3:3}\text{-}cyclo\text{-}P_3)](BF_4)_2$ (**150**, Figure 59) where the triangular ligand acts like a 3π system.[6,121] Later studies on the mechanism of formation of these three-membered cyclic units revealed that the presence of triphos is important.[167] The dinuclear complex **150** can be obtained, apart from the straightforward addition of $[Ni(H_2O)_6]^{2+}$/triphos, also when using other P-containing starting materials such as tris(trimethylsilyl)heptaphosphanotricyclene, $P_7(SiMe_3)_3$, despite its very different chemical behavior, molecular arrangement, and mass fragmentation pattern from P_4S_3 or P_4. Reduction of **150** with $NaBH_4$ affords the 34 VE diamagnetic dimer $[\{(triphos)Ni\}_2(\mu,\eta^{3:3}\text{-}cyclo\text{-}P_3)]BF_4$ (**292**). A few mixed triple sandwich complexes of the type $[\{(triphos)M\}(\mu,\eta^{3:3}\text{-}cyclo\text{-}P_3)\{Ni(triphos)\}]^{2+}$ [M = Co (**151**),[121,122] Rh (**249**)][126] have been synthesized and structurally characterized (see sections 4.1 and 4.2, respectively).

The cationic *cyclo*-P_3 complex **150b** was also used as starting material to prepare bimetallic derivatives by reaction with $[Pt(C_2H_4)(PPh_3)_2]$ from which the carbene-like $Pt(PPh_3)_2$ fragment is easily generated. Thus, **150b** undergoes insertion of the PtL_2 moiety into one P−P bond of the *cyclo*-P_3 unit under smooth conditions to give $[\{(triphos)Ni(\mu,\eta^{3:2}\text{-}cyclo\text{-}P_3)\}\{Pt(PPh_3)_2\}]^+$ (**176**) (Scheme 90).[139] The dinuclear Ni/Pt compound exhibits a dynamic behavior in solution, which has been rationalized in terms of a whizzing motion of the

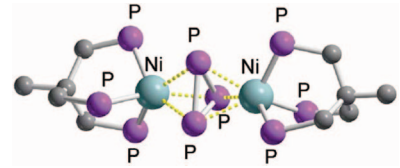

Figure 59. X-ray crystal structure of the cation $[\{(triphos)Ni\}_2(\mu,\eta^{3:3}\text{-}cyclo\text{-}P_3)]^{2+}$ in **150**. Hydrogen atoms and phenyl rings omitted for clarity; adapted from ref 121.

Scheme 90

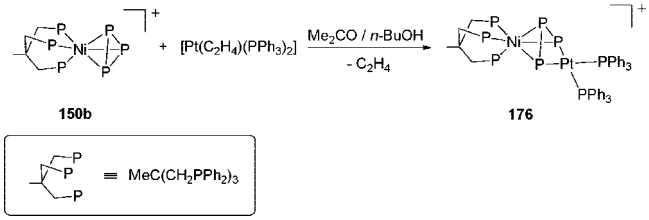

platinum fragment over the three phosphorus atoms. The structure of **176** was determined (Figure 60), resembling that of related complexes [(triphos)Co($\mu,\eta^{3:2}$-*cyclo*-E_2S){Pt(PPh_3)$_2$}]$^+$ (E = P, As). The two P-atoms where the insertion has occurred are set apart at 2.527 Å, while the other P−P bond separation averages 2.174 Å.

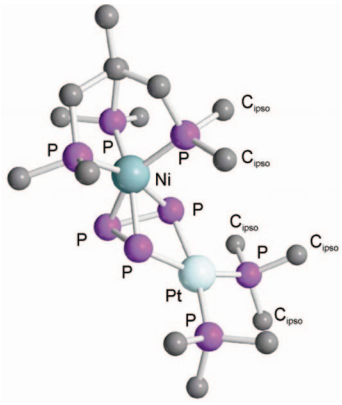

Figure 60. X-ray crystal structure of the cation [{(triphos)Ni-($\mu,\eta^{3:2}$-*cyclo*-P_3)}{Pt(PPh_3)$_2$}]$^+$ in **176**. Only *ipso*-carbons of each phenyl ring of triphos are shown; adapted from ref 139.

Scheme 91

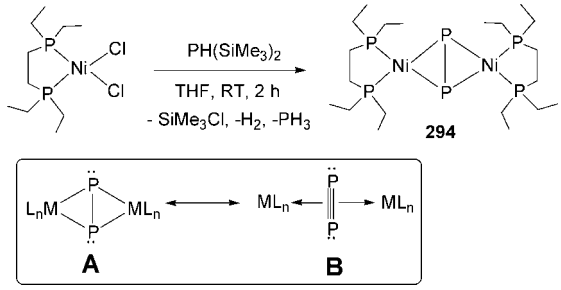

Interest in diphosphenes as olefin analogues stems from their ability to undergo coupling reactions forming metallaphosphacyclopentane species, $M(PR)_4$, which recalls the formation of metallacyclopentadiene from alkene coupling.[193] The intense research in this area led to the unexpected synthesis of [{Ni(depe)}$_2$($\mu,\eta^{2:2}$-P_2)] (**292**) by Schäfer and co-workers from the reaction of [(depe)$NiCl_2$] and different silylated phosphines. The best yield of **292** was obtained by using $PH(SiMe_3)_2$, as illustrated in Scheme 91.[194] The complexes [{Ni(dcpe)}$_2$($\mu,\eta^{2:2}$-P_2)] (**293**) and [{Ni(dppe)}$_2$($\mu,\eta^{2:2}$-P_2)] (**294**) were also briefly mentioned.

In **294** the P−P distance of the P_2 group (2.12 Å) lies in between the typical values for a single (2.20−2.25 Å) and a double (2.00−2.05 Å) bond. This strongly supports a significant contribution of the resonance structure **B** (Scheme 91) in representing the dinuclear complex, which is also in agreement with the observed high downfield shift of the ^{31}P NMR resonance of complex (133 ppm).

Thermolysis of [$Cp^RNi(\mu$-CO)]$_2$ and white phosphorus in high-boiling hydrocarbons has been the subject of a complete study by Scherer and co-workers. Once again, a clear dependence of the reaction outcome from the bulkiness of the Cp substituents was observed. Thus, heating [Cp*Ni(μ-CO)]$_2$ in toluene at 120 °C in the presence of P_4 generates the nickelaphosphacubanes [{Cp*Ni}$_3$($\mu_3,\eta^{2:2:2}$-P_4)(μ_3-P)] (**295**) and [{$Cp^RNi(\mu_3$-P)}$_4$] [Cp^R = Cp* (**296**), Cp″ (**297**)] together with the sandwich complexes [$Cp^RNi(\eta^3$-*cyclo*-P_3)] [Cp^R = Cp* (**298**), Cp″ (**299**)] (Scheme 92).[195,196] Complex **295** exhibits the structural motif already found in **86**,[85] and also the cubanes **296** and **297** have structural precedents in the chemistry of cobalt (**143**, see section 4.1). Addition of coordinatively unsaturated group 6 metal fragments, {$M(CO)_5$}, in THF at RT to **295** leads to the bimetallic derivatives [{Cp*Ni}$_3${($\mu_3,\eta^{2:2:2:1}$-P_4)[$M(CO)_5$]}(μ_3-P)] (M = Cr, **300**; Mo, **301**; W, **302**) where the pentacarbonyl metal unit is coordinated to the P-atom of the tetraphosphorus ligand sitting on the nonmetalated vertex of the cubane.[196] Similarly, the reaction of **300** with photolyzed $Cr(CO)_6$ in THF at RT affords the trimetalated [Cp*Ni($\mu_4,\eta^{3:1:1:1}$-*cyclo*-P_3){$Cr(CO)_5$}$_3$] (**303**) where each P-atom of the *cyclo*-P_3 ligand is additionally coordinated to chromium.[196]

The photolytic reaction of [$Cp^{Pr}Ni(\mu$-CO)]$_2$ and P_4 in *n*-hexane, shown in Scheme 93, gave a mixture of the *cyclo*-P_3 derivative [$Cp^{Pr}Ni(\eta^3$-*cyclo*-P_3)] (**304**) together with the

Scheme 92

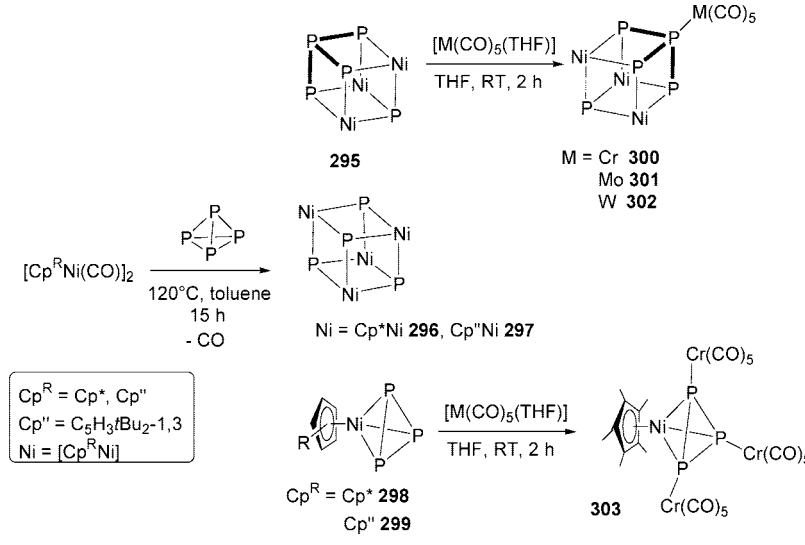

Scheme 93

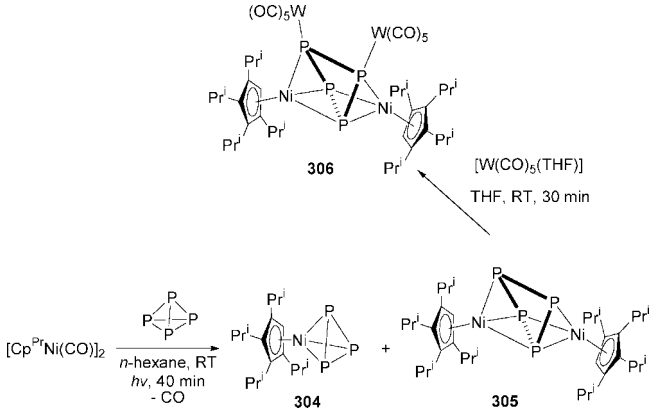

new complex [{$Cp^{Pr}Ni$}$_2$(μ,$\eta^{3:3}$-P_4)] (**305**).[197] Complex **305** exhibits a new prismatic structure with the two nickel atoms occupying the opposite basal vertices of the distorted triangular prism. Further reaction of **305** with [$W(CO)_5$(THF)] produced the bimetallic species [{$Cp^{Pr}Ni$}$_2$(μ,$\eta^{3:3:1:1}$-P_4){$W(CO)_5$}$_2$] (**306**), characterized by a single-crystal X-ray analysis. The molecular structure of **306**, as well as that of [{$Cp^{Pr}Ni$}$_2$(μ,$\eta^{3:3}$-As_4)], the tetrarsenic analogue of **305**, clearly shows that the four P-atoms are distributed along a tetraphosphorus chain with P−P bond distances ranging from 2.182 to 2.216 Å. All the other P−P separations are larger, although d_{P1-P2} is only 2.379 Å, suggesting the existence of a weak interprismatic interaction between these atoms. The intriguing structure of the ditungsten adduct **306** is shown in Figure 61.

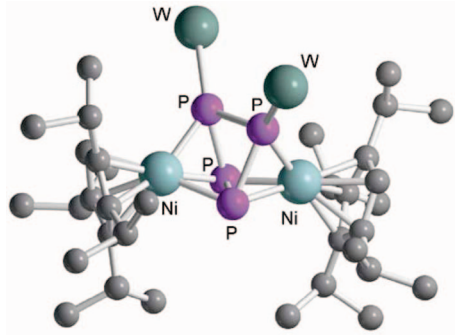

Figure 61. X-ray crystal structure of the cation [{$Cp^{Pr}Ni$}$_2$-(μ,$\eta^{3:3:1:1}$-P_4){$W(CO)_5$}$_2$] (**306**); carbonyl ligands omitted for clarity. Adapted from ref 197.

Soon thereafter, this chemistry was also investigated by Scheer and co-workers, who got intriguing results carrying out the thermal reaction of [Cp*Ni(μ-CO)]$_2$ and P_4 in THF at 70 °C in the presence of freshly photogenerated [$Cr(CO)_5$(THF)]. Performing the reaction under further UV light irradiation gave several novel polyphosphorus species (Scheme 94).[198] Thus, the bent *cyclo*-P_4 complex [{Cp*Ni}{Cp*Ni(CO)}(μ_5,$\eta^{3:1:1:1:1}$-P_4){$Cr(CO)_5$}$_3$] (**307**) and the Ni(II) prismane species [{Cp*Ni}$_2$(μ,$\eta^{3:3:1:1}$-P_4){$Cr(CO)_5$}$_2$] (**308**) were characterized through single-crystal X-ray diffraction besides IR, NMR, and MS analyses. The diphosphorus species, i.e., [{Cp*Ni}$_2$(μ,$\eta^{2:2:1:1}$-P_2){$Cr(CO)_5$}$_2$] (**309**), and the cyclotriphosphorus nickel complex [Cp*Ni(μ_4,$\eta^{3:1:1:1}$-*cyclo*-P_3){$Cr(CO)_5$}$_3$] (**310**) are also obtained (Scheme 94). The observed conversion of **307** into **308** gives evidence for a P_4 transformation pathway taking place via the undetected bicyclotetraphospane intermediate **A** along the formation of **307**. Additional P_3/P_1 fragmentation is observed under photochemical reaction conditions, yielding the stable *cyclo*-P_3 **310** and the transient dimetallaphosphinidene [Cp*Ni≡P{$Cr(CO)_5$}] (**B**). The highly reactive species **B** is stabilized by dimerization, to give the Ni_2P_2 tetrahedral complex **309**, isolated as the main final product.[15] Finally, thermal degradation of **307** in refluxing toluene results in the formation of the trinickelatetraphosphorus cubane [{Cp*Ni}$_3$(μ_3-P_5)] (**311**).

The first example of a coordinated phosphorus monoxide (PO), the heavier analogue of NO, was reported by Scherer

Scheme 94

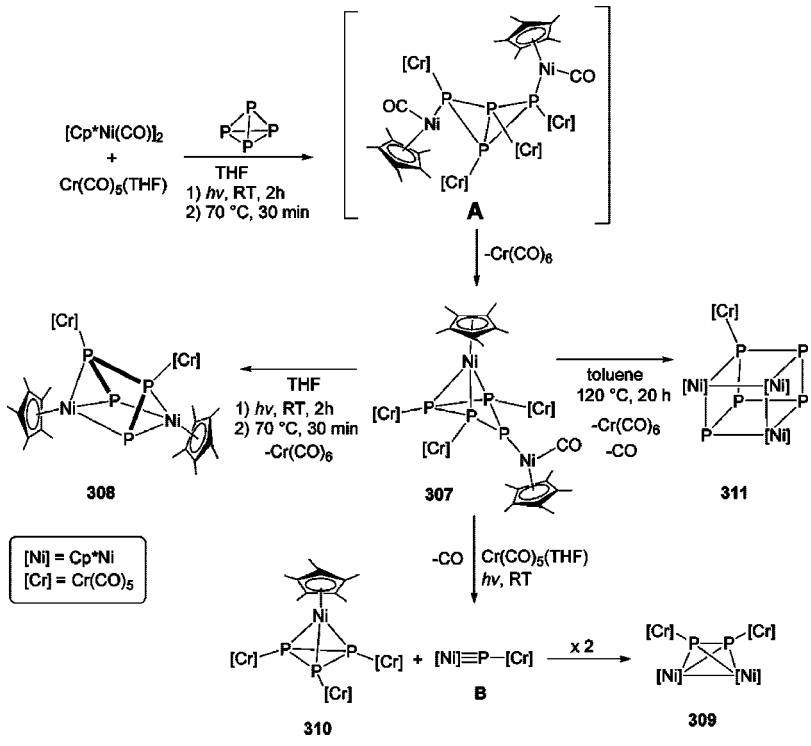

Scheme 95

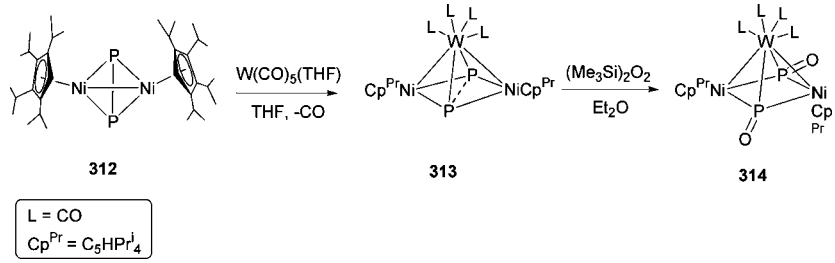

et al. in 1991.[90,199] Thus, reaction of the Ni_2P_2-tetrahedrane $[Cp^{Pr}_2Ni_2(\mu,\eta^{2:2}\text{-}P_2)]$ (**312**), stabilized by bulky Cp^{Pr} coligand, with $[W(CO)_5(THF)]$ in THF led to the unusual $\{Ni_2WP_2\}$ complex $[\{Cp^{Pr}Ni\}_2(\mu_3,\eta^{2:2:1}\text{-}P_2)\{\mu\text{-}W(CO)_4\}]$ (**313**), which was easily oxidized by $(SiMe_3)_2O_2$ to give $[\{Cp^{Pr}Ni\}_2(\mu_3,\eta^{2:2:1}\text{-}PO)_2\{\mu\text{-}W(CO)_4\}]$ (**314**) (Scheme 95). All these species were characterized through single-crystal X-ray diffraction and IR and ^{31}P NMR spectroscopy; they represent illustrative examples of the isolobal principle and are extensively applied in the field of phosphorus organometallic chemistry in that period. In this case, one P atom in the P_4 cage can be replaced either by the $Cp^{Pr}Ni$ fragment or by the $W(CO)_4$ unit.

Compounds with a high phosphorus content occur quite frequently in the inorganic chemistry of nickel in combination with low-valent phosphorus compounds and represent the vast class of polyphosphides.[17a,200] The variety of compositions and structures shown by these molecules is enormous, covering a wide range of physical properties related to their stoichiometry and structure. Among them is worth mentioning the Zintl ion P_7^{3-}, which undergoes reactions with Ni-based metal fragments to give the C_{2v}-symmetrical norbornadiene-like $[(\eta^4\text{-}P_7)Ni(CO)]^{3-}$ (**315**) (Figure 62), which can be subsequently protonated by MeOH at −50 °C to $[(\eta^4\text{-}HP_7)Ni(CO)]^{2-}$ (**316**). The latter can be considered as the conjugate acid of the 18 VE $[P_7ML]^{3-}$ anion (Scheme 96).[201]

Reaction of $Li_3P_7\cdot 3DME$ with $[NiCl_2(PBu^n_3)_2]$ leads to the polyphosphide $[\{Ni(PBu^n_3)_2\}_2P_{14}]$ (**316**, Figure 63).[49] The crystal structure reveals that the P_7 nortricyclane framework does not remain intact, but a P_{14} cage is formed instead, as a result of a sort of "dimerization" process. It contains two linked P_7 units, with a norbornadiene-like structure. Both

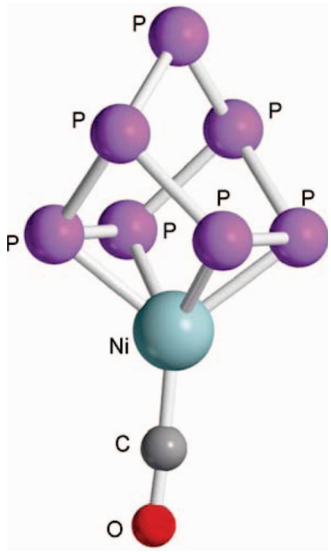

Figure 62. X-ray crystal structure of the trianion $[(\eta^4\text{-}P_7)Ni(CO)]^{3-}$ (**315**); adapted from ref 201.

Scheme 96

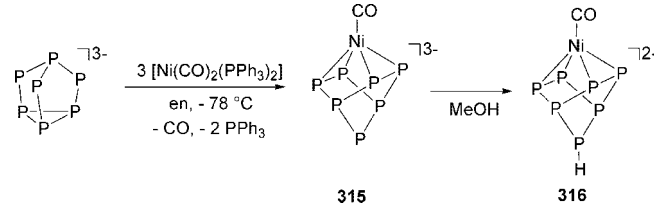

Scheme 97

the XRD data and the electronic structure calculations (DFT// B−P) confirm the presence of delocalized π-electron bond pairs on P(1)−P(2) and P(3)−P(4).

Nickel phosphides are corrosion-resistant, oxidation-resistant, and wearproof materials; they also find a wide range of applications in the fields of catalysis, electronics, and magnetism.[202] Solvothermal reactions in stainless-steel autoclaves with inner Teflon beakers were carried out to prepare nanocrystalline nickel phosphide (Ni_2P) from white phosphorus and $NiCl_2\cdot 6H_2O$ heated in diluted ammonia solution (pH ≥ 10) at 160 °C for 12 h.[203] Powder X-ray peaks indexing in the spectrum of the solid product revealed that the phase obtained is hexagonal, with mean crystallite size of 16 nm; the Ni_2P grains are homogeneously spherical. If the starting material is $Ni(SO_4)\cdot 6H_2O$ and the solvent is changed to a 1:4 ethylene glycol/water mixture, the solvothermal reaction gives dendritic Ni_2P. Temperature and time are fundamental factors that influence both particle size and shape. In particular, the total reaction time seems to be influent for the shape change from spherulites (6 h) to dendrites (12 h), with the other conditions being unchanged.[204] The reaction between zerovalent nickel metallorganic precursor $Ni(COD)_2$ and P_4 affords Ni_2P in a stoichiometric manner (Scheme 97).[205] An alternative is the use of Ni(0) stabilized nanoparticles. The stabilizing agent in the latter case is the tri-*n*-octylphosphine oxide ligand (TOPO).

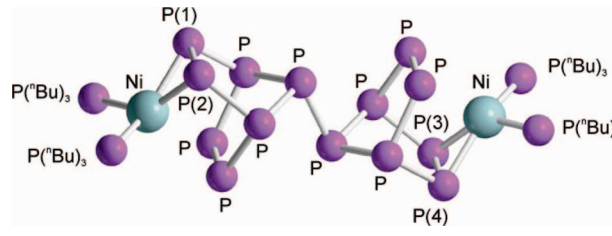

Figure 63. X-ray crystal structure of $[\{Ni(PBu_3)_2\}_2P_{14}]$ (**316**); the *n*-butyl groups of the PBu^n_3 ligands are omitted for clarity. Adapted from ref 49.

Facile, low-temperature solvothermal synthesis of the phosphorus-rich phase NiP_2 from elemental P_4 was achieved in 2008 by Gillan et al., by employing rigorously dry anhydrous $NiCl_2$ and white phosphorus in dry toluene, at 275 °C for two days.[206] The dryness of the salt is fundamental to improve the final reaction yields, which drop dramatically (from 85% to 15%) if the chloride is hydrated. The new phase can be prepared in a more crystalline form by low-temperature annealing. Another nickel polyphosphide obtained in the form of hollow microspheres is $Ni_{12}P_5$,[207] prepared from $Ni(NO_3)_2 \cdot 6H_2O$ and white phosphorus in the presence of HMT as a pH modifier and polyethylene glycol 10000 (PEG-10000) as a "templating" agent.

The environmentally sustainable synthesis of organophosphorus compounds (such as phosphonic acids and esters, phosphines, and phosphine oxides) is much sought for, due to the considerable importance of these derivatives in various branches of medicine, engineering, and agriculture. Growing attention has been paid in recent years to electrochemical chlorine-free production using white phosphorus as the main P source. The Ni(II) 2,2′-bipyridyl complex $Ni(BF_4)_2(bipy)_3$ electrochemically generates Ni(0) species at the electrode, and when the latter interact with R−X species, they are reported to form σ-organyl complexes of general formula Ni(R)(X)(bipy), as a consequence of the oxidative addition of the R−X bond to the metal center. In the presence of P_4 in the reaction medium, the R group is transferred to phosphorus, to generate organophosphorus derivatives depending on the substrates and experimental conditions. Rupture of the P_4 tetrahedron and cleavage of other P−P bonds is reported to occur under the action of the Ni^0(bipy) or the Ni^{II}(bipy) fragments, with formation of nickel phosphides or polyphosphides. For example, the complex $[\{(triphos)Ni\}_2(\mu,\eta^{3:3}\text{-}cyclo\text{-}P_3)](BF_4)_2$ (**150**) mentioned above could be obtained electrochemically via a one-pot reaction from $Ni(BF_4)_2$, white phosphorus, and triphos. The functionalized P_nR_m fragment can itself be a ligand for Ni.[208]

The synthesis of pentaphosphanickelocene species was also attempted by treating $[(\eta^3\text{-}C_3Ph_3)Ni(PPhMe_2)Br]$ with NaP_5 at RT. The reaction did not provide the expected product but gave the unexpected 1,2-diphosphacyclopentadienide anion $[C_3Ph_3P_2]^-$ whose crystal structure was determined as its Na(diglyme)$_2$ salt.[209] Even though the mechanism of formation is unclear, nickel(II) plays an important part in this reaction, as no reaction is observed when starting from the simple $[C_3Ph_3]Br$ salt instead of $[(\eta^3\text{-}C_3Ph_3)Ni(PPhMe_2)Br]$.

5.2. Palladium

The coordination chemistry of palladium toward white phosphorus is largely neglected, and very few reports in this area have been published so far. The structures of the Pd-polyphosphido species generally compare with those of the nickel analogues. Thus, $[(\kappa^3\text{-}P,P,P\text{-}NP_3)Pd(\eta^1\text{-}P_4)]$ (**317**), containing the *tetrahedro*-P_4 ligand similarly to **291**, was reported, although a final crystallographic proof could not be given (vide supra, section 5.1).[210] An extension of the chemistry of the *cyclo*-P_3 ligand to the heavier group 10 metals led to the synthesis of simple and triple-decker sandwich complexes $[(triphos)M(\eta^3\text{-}cyclo\text{-}P_3)]BF_4$ [M = Pd, (**318**); Pt, (**319**)] and to the dinuclear Pd(II) complexes $[\{(tripod)Pd\}_2(\mu,\eta^3\text{-}cyclo\text{-}P_3)]BPh_4$ (tripod = triphos (**320**); $\kappa^3\text{-}P,P,P\text{-}NP_3$ (**321**)], with the former pair being isostructural with the nickel analogue **150b** and the latter being isostructural with the triple-decker species **150** (vide supra, section 5.1) (Scheme 98). Complete XRD and NMR analyses for the three palladium derivatives have been presented.[210]

Scheme 98

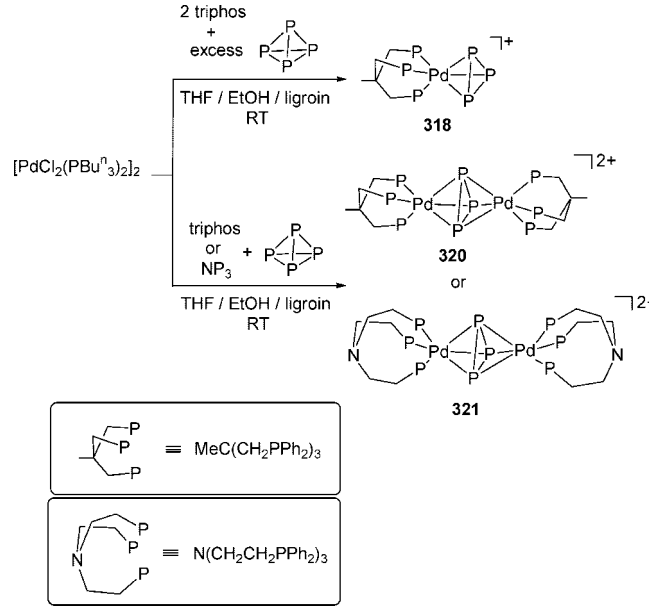

Starting from $Pd(acac)_2$ in DMF at 80 °C under 1 atm of H_2, white phosphorus was also employed as starting reagent to prepare nanosized Pd catalysts after formation of intermediate Pd phosphides of general formula Pd_xP_y, with different compositions. The relative contents of the various phases were determined through powder X-ray diffraction analysis. Styrene hydrogenation was tested using different nanocatalysts, and the results showed catalytic activities in some cases higher than those obtained in the presence of Pd-phosphine single-site materials.[211]

5.3. Platinum

A few complexes containing the platinum(0) carbene-like species $\{Pt(PPh_3)_2\}$ inserted across a P−P bond of a transition metal complexes incorporating a polyphosphorus ligand $L_nM(P_x)$ have been reported in the literature. In most instances, such heterodinuclear compounds have been already mentioned in the appropriate sections related to each specific metal. Examples of such species are $[\{(triphos)Ni(\mu,\eta^{3:2}\text{-}cyclo\text{-}P_3)\}\{Pt(PPh_3)_2\}]^+$ (**176**),[139] $[Co(\mu,\eta^{1:2:1}\text{-}P{=}P{-}PPh_2CH_2PPh_2)_2\{Pt(PPh_3)_2\}]BF_4$ (**185**),[143] $[M(dppm)(Ph_2PCH_2PPh_2PPPP)\{Pt(PPh_3)_2\}]OTf$ [M = Rh (**288**), Ir (**289**)][190] and the related $[\{(triphos)Co\}_2(\mu_3,\eta^{3:3:3}\text{-}P_6H_2)\{Pt(PPh_3)_2\}](OTf)_2$ (**177**) where one PPh_3 ligand has been additionally replaced by the PtL_2 fragment.[139]

The reaction of P_4 with $\{Pt(PPh_3)_2\}$, generated from either $[Pt(C_2H_4)(PPh_3)_2]$ or $[Pt(PPh_3)_4]$, was first investigated by Scheer and Herrmann,[212] but no definitive formulation could be assigned to the amorphous isolated dark-brown reaction product. Taking advantage from the stabilizing effect played by $[Cr(CO)_5(THF)]$ fragments, the same reaction was later reinvestigated by Scheer et al., who obtained the trimetallic derivative $[(PPh_3)_2Pt(\mu_3,\eta^{2:1:1}\text{-}P_4)\{Cr(CO)_5\}_2]$ (**322**) from a Pt/Cr/P_4 mixture (Scheme 99).[213] The compound was characterized by multinuclear NMR spectroscopy (including ^{195}Pt-NMR) and IR and MS spectrometry, which unambiguously supported a butterfly structure of the tetraphosphorus

Scheme 99

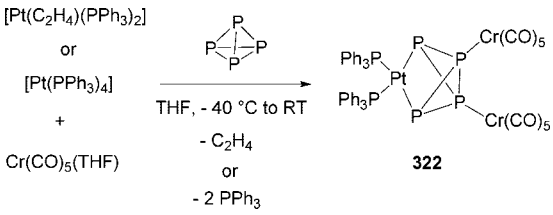

molecule with the two nonactivated P-atoms coordinated by terminal {$Cr(CO)_5$} moieties.

The [$Pt(C_2H_4)(PPh_3)_2$] precursor has been elegantly used by Cummins and co-workers as a trap for the P_2-containing molecule {$W(CO)_5(P_2)$}.[214] This species, which contains the elusive diphosphorus molecule, could be obtained in situ by thermal elimination from the diphosphaazide (Mes*N═P^+═P^-) niobium complex [{Mes*N═P−P[$W(CO)_5$]}Nb{N(Np)-Ar}$_3$], a remarkable P_2 synthon.[215] Thus, thermolysis of the niobium precursor at about 20 °C in the presence of the Pt(0) species [$Pt(C_2H_4)(PPh_3)_2$] afforded the bridging P_2 complex [{$(PPh_3)_2Pt$}$_2$(μ_3,$\eta^{2:2:1}$-P_2){$W(CO)_5$}] (**323**), shown in Scheme 100, via efficient trapping of the tungsten stabilized diphosphorus molecule by two PtL_2 units. The butterfly geometry of **323** was authenticated by X-ray methods (see Figure 64) and confirmed in solution by multinuclear NMR analysis. Remarkably, the P−P bond separation is 2.122 Å, i.e., significantly shorter than a genuine P−P single bond (2.21 Å in white phosphorus), suggesting that a multiple-bond character is still featuring the P_2 ligand in **323** despite its multiple metal coordination. Attempted trapping of the P_2 molecule in the absence of the stabilizing pentacarbonyl metal fragment was unsuccessful, yielding, nonetheless, the interesting phosphinidene species [(Mes*N═P){$Pt(PPh_3)$}$_2$-PNb{N(Np)Ar}$_3$] (**324**). Complex **324** was formed following

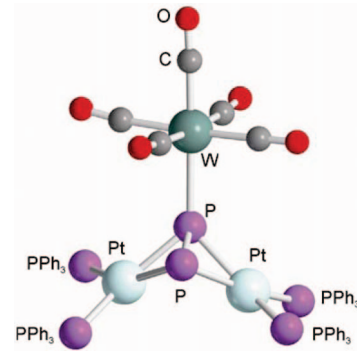

Figure 64. X-ray crystal structure of [{$(PPh_3)_2Pt$}$_2$(μ_3,$\eta^{2:2:1}$-P_2){$W(CO)_5$}] (**323**); adapted from ref 214.

PPh_3 loss and P−P bond cleavage which resulted in the assemblage of the new rhombic Pt_2P_2 core featuring **324** with a direct Pt−Pt bond (d_{Pt-Pt} = 2.6490 Å) in line with the presence of two Pt(I) metal centers (Figure 65).[214]

A complex featuring the Pt_2P_2 core related to **323** was reported by Schäfer and Binder from the reaction of [$PtCl_2(PEt_3)_2$] with $LiP(SiMe_3)_2$ at low temperatures. Initially the substitution product [$(PEt_3)_2PtCl${$P(SiMe_3)_2$}] is formed, which in turn rearranges to the P_2 complex [{$(PEt_3)_2Pt$}$_2$-(μ,$\eta^{2:2}$-P_2)] (**325**) and $SiMe_3Cl$ at 80 °C. NMR and mass spectral data are reported.[216] Interestingly, the synthetic pathway used to make **325** is totally different from that employed for **323**, despite their very similar structures.

The reaction of K_3P_7 with [$Pt(C_2H_4)(PPh_3)_2$] in en/2,2,2-crypt solution was also investigated (Scheme 101).[201] The isolated dark-red compound, [η^2-P_7{$PtH(PPh_3)$}][K(2,2,2-crypy)]$_2$ (**326**), was characterized by spectral and crystallographic methods showing the presence of a practically unperturbed nortricyclene moiety di-*hapto* coordinated by

Scheme 100

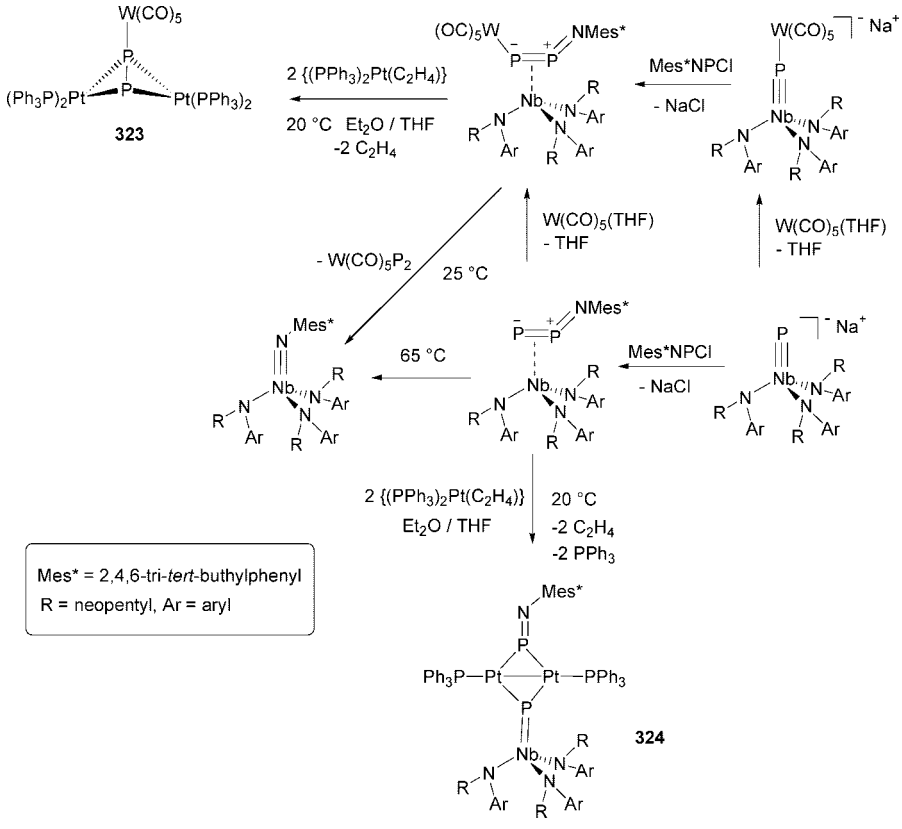

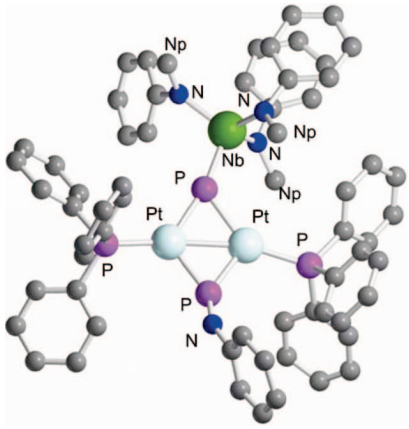

Figure 65. X-ray crystal structure of [(Mes*N=P){Pt(PPh3)}2-PNb{N(Np)Ar}3] (**324**); only the carbon atom of Np group linked to nitrogen is shown. Adapted from ref 214.

Scheme 101

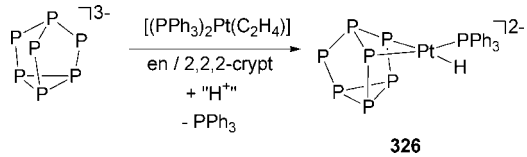

the cation $Pt(H)(PPh_3)^+$. The source of the hydride hydrogen atom coordinated to platinum and determined by NMR methods ($\delta_{Pt-H} = -10.1$, $^1J_{H-Pt} = 1080$ Hz, $^2J_{H-P} = 14$ Hz) was not ascertained.

Finally, as for all the other late transition metals, also for platinum, Sacconi and co-workers were able to prepare the *cyclo*-P_3 sandwich complex. [(triphos)Pt(η^3-*cyclo*-P_3)]BF_4 (**319**) does not differ from the related cationic Ni or Pd sandwich derivatives mentioned above and could be straightforwardly prepared by treating $[PtCl_2(PBu^n_3)_2]$ with an excess of white phosphorus in the presence of triphos. The structure of **319** was determined by X-ray methods showing that only minor structural modifications affect the coordinated η^1-P_4 molecule on going down the triad from [(triphos)Ni(η^3-*cyclo*-P_3)]$^+$ (**150b**) to [(triphos)Pt(η^3-*cyclo*-P_3)]BF_4 (**319**).

6. Group 11 Metals

The coordination chemistry of white phosphorus toward coinage metals, copper, silver, and gold, is not much developed, and generally discrete complexes of formula $[L_nM(P_x)]^{m+}$ of such metals are extremely scarce and often associated with polymeric species. Copper and silver cations or their halide complexes have been largely used as electrophilic reagents to stabilize dinuclear or polynuclear complexes either as discrete molecules or 2D- and 3D-coordination polymers. These bimetallic complexes, which encompass cobalt,[132] rhodium, iridium,[186] and iron[93,96,98−102] derivatives, have been already described in the appropriate sections of this review. Gold species are even less documented and, to the best of our knowledge, limited to the Stoppioni's family of trimetallic cations [{(triphos)M($\mu,\eta^{3:2}$-*cyclo*-P_3)}$_2$Au]PF_6 [M = Co (**166**), Rh (**167**), Ir (**168**)].[134]

6.1. Copper

In 2007, the homoleptic Cu−P complex, [Cu(η^2-P_4)$_2$][Al(pftb)$_4$] (**327**), containing the extremely weak coordinating anion perfluoro-*tert*-buthoxyaluminate, was synthesized by Krossing et al.[217] The product was obtained in

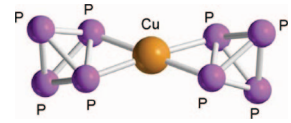

Figure 66. X-ray crystal structure of the complex cation [Cu(η^2-P_4)$_2$]$^+$ in the homoleptic complex **327**; adapted from ref 217.

Scheme 102

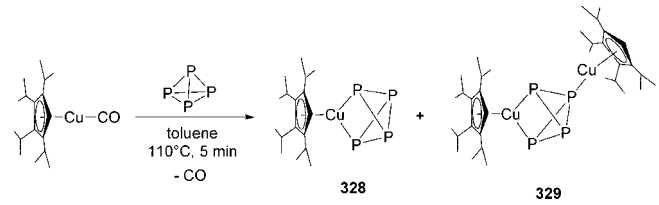

quantitative yield by sonication of a mixture of excess CuI, Ag[Al(pftb)$_4$], and P_4. From the XRD analysis, the local copper coordination is nearly planar and the cation approaches D_{2h} symmetry (Figure 66). ^{31}P NMR gives a sharp singlet at −460 ppm, even at low temperature (−90 °C), indicating fast dynamical rotation of the P_4 ligands on the NMR time scale. The existence of **327** had been somehow "predicted" three years before by a computational screening of the bonding properties of P_4 and ethylene in the "isolobal" species [M(η^2-P_4)$_2$]$^+$ and [M(η^2-C_2H_4)]$^+$ (M = Cu, Ag, Au).[218] From this study, the Cu−L bond was found to be even stronger than the Ag−L one (counterintuitively), due to the increased interactions involving 3d with respect to 4d metal orbitals. In the case of gold, the bond would have been further stabilized by relativistic effects.

Activation of P_4 takes place upon reaction with the half-sandwich Cu(I) carbonyl complex [Cp^{Pr}Cu(CO)] to yield an approximately 1:1 mixture of mono- and bimetallic complexes **328** and **329**, with different P_4 hapticity (Scheme 102).[219] The strong ^{31}P NMR analogy between **328**, **329**, and [(PPh$_3$)$_2$RhCl(η^2-P_4)] (**245**) strongly supports an interpretation of the P_4 ligand as an edge-opened P_4^{2-} moiety resulting from the oxidative addition of a P−P bond to the Cu(I) fragment, to give Cu(III) products. In **329**, a second equivalent of {Cp^{Pr}Cu} coordinates to a phosphorus atom, likely binding one of the distal unmetalated P-atoms.

Copper halides can be used as useful and versatile synthetic tools to get new phosphorus-based structures (polyanions, phosphorus chalcogenide cages, etc.).[220] Treatment of the red allotrope of elemental phosphorus with the stoichiometric amount of CuI at high temperature led to the formation of crystalline polymers of formula [(CuI)$_8$P$_{12}$] (**330**),[221] [(CuI)$_3$P$_{12}$] (**331**),[222] and [(CuI)$_2$P$_{14}$] (**332**).[223] Treating solid **330** or **331** with an excess of aqueous KCN at low temperature under prolonged stirring quantitatively extracts the copper ion in water and leaves a polymeric inorganic matrix formed by $[P_{12}]_\infty$ chains as crystalline nanorods. These may be considered as a new allotropic form of phosphorus.[224]

Anions $[Cu_xS_y]^-$ ($x = 1-6$; $y = 2-4$), obtained via laser ablation from Cu_2S, were found to react with P_4 in the gas phase to form P_2S_m ligands ($m = 1, 2$) coordinated to copper. The most likely structures of the products were determined through DFT//BLYP calculations and collisional induced dissociation techniques, and they were found to be the new species $[Cu_2S_2P_2]^-$ and $[Cu_2S_3P_2]$.[225]

Several copper/phosphorus-containing intermetallic compounds and Zintl phases have been synthesized since 1979.[226] A recent example of ternary copper phosphide with metallic

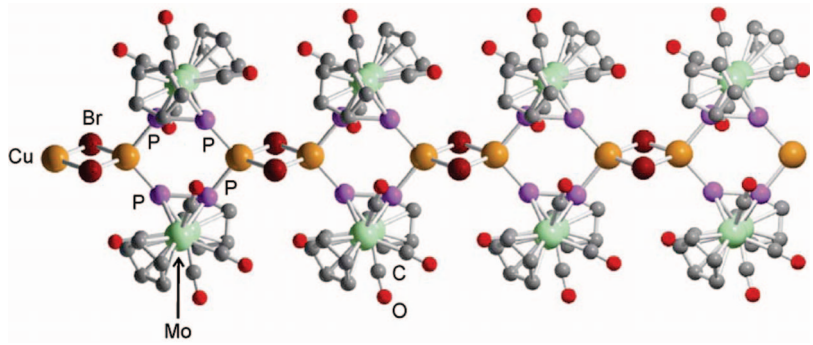

Figure 67. 1D polymer constituting the crystal lattice of **334**, where the six-membered $[Cu_2P_4]$ and the four-membered $[Cu_2Br_2]$ rings are clearly visible; adapted from ref 94. Atom color code: gray, C; red, O; purple, P; aquamarine, Mo; light brown, Cu; dark brown, Br.

character $BaCu_{10}P_4$ (**333**) was obtained by mixing stoichiometric amounts of the bare elements at 1200 °C for 24 h.[227] In the structure, chains of edge-shared Cu_4 tetrahedral prisms are knitted together by P atoms (P^{3-} anions). Extended Hückel bond calculations are consistent with the hypothesis of a strong Cu−Cu interaction, through extensive Cu−Cu bonding orbital overlap at the Fermi level.

P_n ligand complexes can be used as connecting moieties between Cu(I) cations to form discrete polymetallic species or well-oriented 1D or 2D coordination polymers. Examples already discussed in previous sections of this review are the [(triphos)M(η^3-*cyclo*-P_3)] compounds (M = Co, Rh, Ir).[132] These represent suitable platforms to build metal-bridged dimers and trimers in the presence of Cu(I) salts and complexes. In order to generate well-defined polymers, P_2-ligand complex precursors seem to be the best starting materials. The first 1D polymer of Cu(I) containing a P_2-ligand complex was published by Scheer et al. who described [{Cu(μ-Br)[$Cp_2Mo_2(CO)_4$($\mu,\eta^{2:1:1}$-P_2)]}$_\infty$] (**334**) from the reaction of [$CpMo(CO)_2$($\mu,\eta^{2:2}$-P_2)] with CuBr in MeCN.[94] The linear chain consists of planar six-membered Cu_2P_4 and four-membered Cu_2Br_2 rings, alternately disposed in an orthogonal manner. The coordination geometry at copper is tetrahedral (Figure 67).

6.2. Silver

Silver salts of the superweak coordinating anion $Al(pftb)_4$ have been used as key reagent by Krossing to access the first homoleptic tetraphosphorus species, i.e., the silver diphosphorus cation [Ag(η^2-P_4)$_2$][$Al(pftb)_4$] (**335**), showing the same structural and spectroscopic features of the copper analogue **327**. The pyrophoric silver complex was prepared by the straightforward reaction of elemental phosphorus dissolved in CS_2 with Ag[$Al(pftb)_4$] at RT after careful workup (Scheme 103).[228] Depending on the Ag/P_4 ratio, the molecular species [{Ag(η^2-P_4)}{$Al(pftb)_4$}] (**336**) and the dimer [{Ag(η^2-P_4)$Al(pftb)_4$}] (**337**) could be obtained.

The local silver coordination sphere is nearly planar, and the Ag^+ ion binds two tetrahedral P_4 ligands in an η^2 fashion. An additional proof of the weak Ag−P interaction is the slight elongation of the P−P distances of the coordinated edges compared with those of free P_4 (from 2.21 to 2.33 Å). The square-planar coordination geometry for Ag^+ is induced by a $d_{x2\text{-}y2}$(Ag) → σ^*(P−P) interaction, according to the calculated MO scheme. The question whether η^2 complexes are derived from neutral *tetrahedro*-P_4 or from P_4^{2-} in a tetraphosphacyclobutane structure has been a matter of debate. The results of an accurate analysis based on ^{31}P NMR CPMAS/Raman spectroscopy, X-ray diffraction, and MOs/

Scheme 103

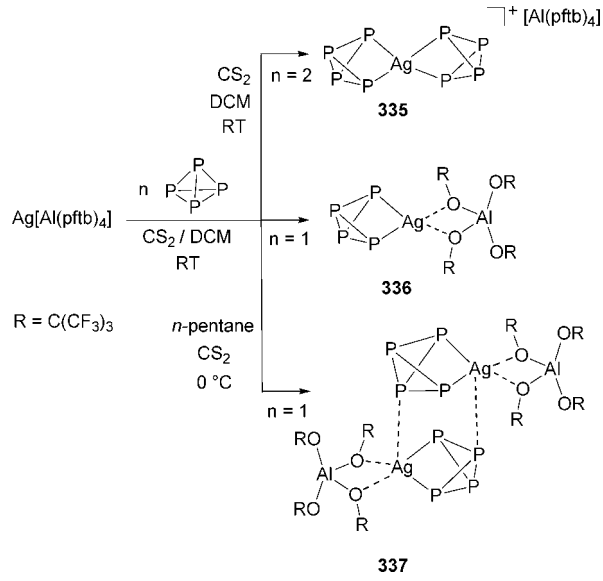

charge density calculations led to the unquestionable assignment of **335** to the former class of compounds, while the rhodium analogue [$RhCl(PPh_3)_2(P_4)$] (**245**) belongs to the latter.[174] In order to corroborate this assignment, DFT//BLYP and ab initio MP2 methods, in addition to the energy-decomposition scheme of Ziegler and Rauk, were employed to carry out a thorough theoretical study of **335** and its comparison with its ethylene counterpart $[Ag(C_2H_4)_2]^+$.[229] In **335**, the D_{2h} isomer, with a square planar Ag coordination geometry, is at lower energy (also confirmed by the XRD data), while in $[Ag(C_2H_4)_2]^+$ the D_{2d} "staggered" tetrahedral geometry is slightly favored. The reason for this difference is attributed to the lack of an occupied symmetry-suitable linear combination of the ligands' frontier orbitals that can interact with the $5p_x$ orbital of silver in the case of Krossing's cation. The use of the least coordinating anion [$(pftb)_3Al$−F−$Al(pftb)_3$]$^-$ by the same group allowed for the preparation of the corresponding [Ag(η^2-P_4)$_2$]$^+$ salt.[230] Its solid-state structure was compared with that of the [$Al(pftb)_4$]$^-$ derivative: the rotation along the Ag−(P−P centroid) bond is barrierless, and the structure adopted in the solid state merely depends on packing effects. The more symmetrical the counterion {[$Al(pftb)_4$]$^-$ vs [$(pftb)_3Al$−F−$Al(pftb)_3$]$^-$}, the more symmetrical the final solid-state cation structure (D_{2h} vs D_2). In Figure 68, the crystal structure of [{Ag(η^2-P_4)}{$Al(pftb)_4$}] (**336**) is presented.

The use of the weakly basic anion [$Al(pftb)_4$]$^-$, essential for the isolation of **335**−**337** as a stable species, was also

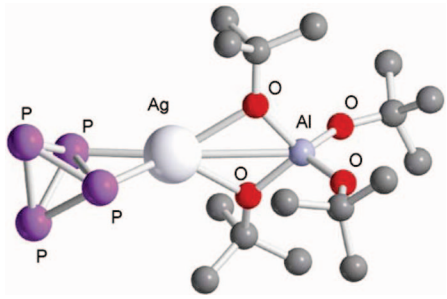

Figure 68. X-ray crystal structure of complex [{Ag(η^2-P_4)}{Al(pftb)$_4$}] (**336**); fluorine atoms omitted for clarity. Adapted from ref 174.

Scheme 104

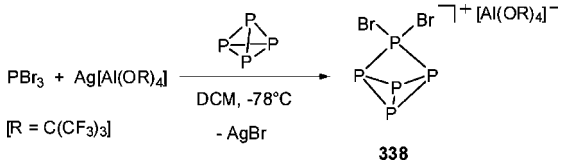

exploited to avoid decomposition of the highly reactive carbene analogues PX_2^+ cations (X = Br, I), obtained via silver salt metathesis from Ag[Al(OR)$_4$] and PX_3.[231] Thus, their insertion chemistry into P_4 is feasible; the reaction product of the mixture of P_4, PBr_3, and Ag[Al(OR)$_4$] in dichloromethane at −78 °C is the intriguing salt $[P_5Br_2]^+$-[Al(OR)$_4$]$^-$ (**338**) (Scheme 104). Formation of a P_5 cage was unprecedented, and the range of the P−P bond lengths in **338** (2.15/2.26 Å) is close to the values found in isolated P_4. Detailed IR/Raman/^{31}P NMR spectroscopic analyses and thermochemical calculations completed the characterization.

The first supramolecular aggregates incorporating a *cyclo*-P_3 ligand present in complexes [Cp^{R}Mo(CO)$_2$(η^3-P_3)] [Cp^R = Cp (**339**), Cp* (**340**)] as linking units to Ag(I) were described recently by Scheer et al.[232] The reaction of **339** with AgX [X = OTf, Al(pftb)$_4$] gave the 1D-coordination polymers [Ag{CpMo(CO)$_2$(μ,$\eta^{3:1:1}$-P_3)}$_2$]$_n$[Al(pftb)$_4$]$_n$ (**341**) and [Ag{CpMo(CO)$_2$(μ,$\eta^{3:1:1}$-P_3)}$_3$]$_n$[X]$_n$ [X = OTf (**342**), Al(pftb)$_4$ (**343**)]. The solid-state structures of these polymers were obtained by X-ray crystallography, showing polycationic chains well-separated from the weakly coordinating anions. Polymers **342** and **343** are the first examples of homoleptic silver complexes in which Ag centers are found octahedrally coordinated to six phosphorus atoms. Conversely, **340** reacts with Ag(pftb)$_4$ to yield the 1D polymer [Ag{Cp*Mo(CO)$_2$(μ,$\eta^{3:2:1}$-P_3)}$_2$]$_n$[Al(pftb)$_4$]$_n$ (**344**). Interestingly, the crystal structure of **344** differs from that of **341** in the coordination mode of the *cyclo*-P_3 ligands. Whereas in **341** the Ag^+ cations are edge-bridged by the *cyclo*-P_3 ligands in a $\eta^{1:1}$ fashion, in **344** they are linked in a $\eta^{2:1}$ face-bridging mode (Scheme 105).

6.3. Gold

Gold compounds resulting from the activation of elemental phosphorus have not yet been reported. The only species worth being mentioned here are the multiple-decker species [{(triphos)M(μ,$\eta^{3:2}$-*cyclo*-P_3)}$_2$Au]PF_6 [M = Co (**166**), Rh (**167**), Ir (**168**)] already described in section 4 of this review.[134]

For many main group elements, including phosphorus, hypercoordination with electron-deficient bonding and nonclassical coordination geometries are typical features when reacted with Au(I) species. Treatment of bis(pivaloyl)phosphine, PH(OCBu^t)$_2$ (or PH_3), with the strong aurating agent tris{(triphenylphosphine)gold}oxonium tetrafluoborate, [(PPh$_3$-

Scheme 106

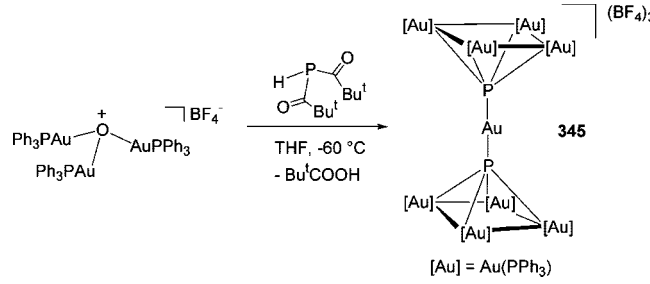

Scheme 105

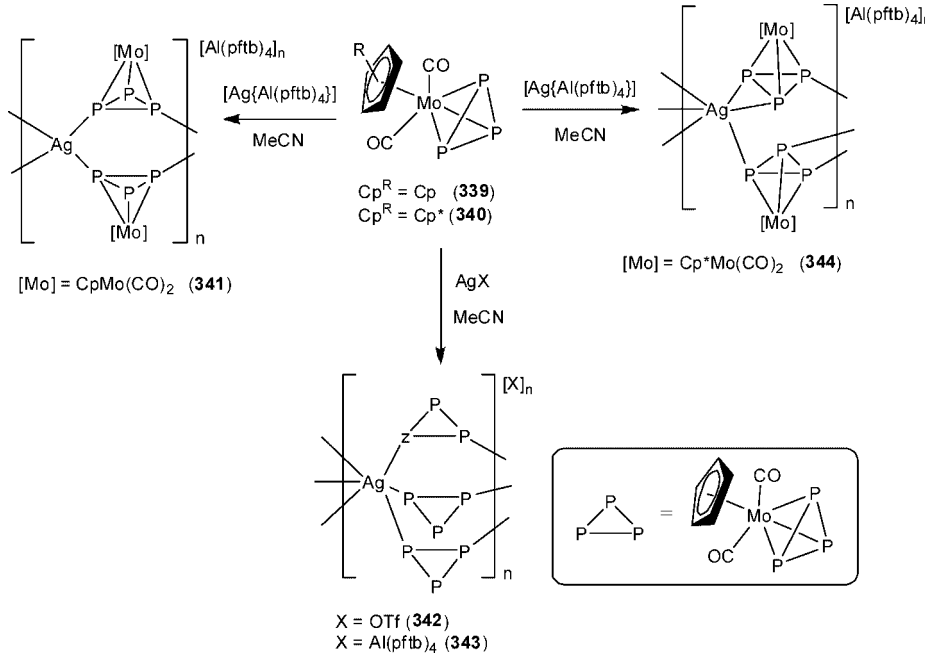

$Au)_3O]^+BF_4^-$, in THF at −60 °C afforded small amounts of the enneanuclear complex $[Au\{\mu_5\text{-}P(AuPPh_3)_4\}_2](BF_4)_3$ (**345**), Scheme 106).[233]

The crystal structure analysis indicates that the overall cation symmetry in **345** is D_{4h}, and it recalls an hourglass. The two peripheral Au_4 rings are almost planar and eclipsed with respect to the central Au atom. The trication contains, at both ends, two square pyramidal $\{P(AuPPh_3)_4\}$ units P-coordinated to the central gold atom featuring an almost planar P−Au−P interatomic vector.

7. Abbreviations

acac	acetylacetonate, $[CH_3COCHCOCH_3]^-$
Bu	butyl
Bz	benzyl
CAAC	cyclic alkyl(amino)carbene
COD	1,5-*cyclo*-octadiene
Cp	cyclopentadienyl, C_5H_5
Cp*	pentamethylcyclopentadienyl, C_5Me_5
Cp″	1,3-di-*tert*-butylcyclopentadienyl,1,3-$C_5H_3Bu^t_2$
Cp‴	1,2,4-tris-*tert*-butylcyclopentadienyl,1,2,4-$C_5H_2Bu^t_3$
Cp^{bz}	pentabenzylcyclopentadienyl, $C_5(CH_2Ph)_5$
Cp^{Bu}	*tert*-butylcyclopentadienyl, $C_5H_4Bu^t$
Cp^{Et}	ethyltetramethylcyclopentadienyl, C_5Me_4Et
Cp^{Me}	methylcyclopentadienyl, C_5H_4Me
Cp^{Ph}	pentaphenylcyclopentadienyl, C_5Ph_5
Cp^{Pr}	tetra-isopropylcyclopentadienyl, $C_5HPr^i_4$
Cp^{Pr5}	penta-isopropylcyclopentadienyl, $C_5Pr^i_5$
Cp^R	generic substituted cyclopentadienyl ring
Cp^S	(β-thiomethylethyl)tetramethylcyclopentadienyl, $C_5Me_4(C_2H_4SMe)$
Cp^{Si_2}	1,3-bistrimethylsilylcyclopentadienyl,1,2,4-C_5H_2-$(SiMe_3)_3$
Cp^{Si_3}	1,2,4-tristrimethylsilylcyclopentadienyl,1,2,4-C_5H_2-$(SiMe_3)_3$
CP-MAS	cross-polarization magic angle spinning
crypt	2,2,2-cryptate
Cy	cyclohexyl
DCM	dichloromethane
DFT	density functional theory
DMF	dimethylformamide
DMO	dimethoxyethane
dcpe	1,2-(dicyclohexylphosphino)ethane, $Cy_2PCH_2CH_2PCy_2$
depe	1,2-(diethylphosphino)ethane, $Et_2PCH_2CH_2PEt_2$
dppe	1,2-bis(diphenylphosphino)ethane, $Ph_2PCH_2CH_2PPh_2$
dppm	bis(diphenylphosphino)methane, $Ph_2PCH_2PPh_2$
DMSO	dimethylsulfoxide
EHMO	extended Hückel molecular orbital
EHT	extended Hückel theory
en	ethylenediamine
ESI	electrospray ionization
ESR	electron spin resonance spectroscopy
Et	ethyl etriphos 1,1,1-tris(diethylphosphinomethyl)ethane, $MeC(CH_2PEt_2)_3$
FMO	Frontier Molecular Orbital
FT	Fourier transform
GED	gas electron diffraction
HMT	hexamethylenetetramine (urotropine)
L	generic two-electron donor ligand
LT	low temperature
Me	methyl
Mes*	(2,4,6-tris-*tert*-butyl)phenyl,$C_6H_2Bu^t_3$
MO	molecular orbital
MS	mass spectrometry
NHC	*N*-heterocyclic carbene
Np	neopentyl, CH_2Bu^t
NP_3	tris(2-diphenylphosphinoethyl)amine, $N(CH_2CH_2PPh_2)$
OTf	triflate, trifluoromethanesulfonate, OSO_2CF_3
PEG	polyetheleneglycol
$Al(pftb)_4$	perfluoro-*tert*-butoxyaluminate, $[Al\{OC(CF_3)_3\}_4]$
Ph	phenyl
PP_3	tris(2-diphenylphosphinoethyl)phosphine, $P(CH_2CH_2PPh_2)$
Pr	propyl
RT	room temperature
THF	tetrahydrofuran
TOPO	tris-*n*-octylphosphine oxide
triphos	1,1,1-tris(diphenylphosphinomethyl)ethane, $MeC(CH_2PPh_2)_3$
tripod	generic tripodal ligand
UV	ultraviolet
VE	valence electrons
VPO	vapor pressure osmometric
XRD	X-ray diffraction analysis

8. Acknowledgments

This work was supported by MIUR (Rome) through PRIN project 2007X2RLL2: *Nuove strategie per il controllo delle reazioni metallo assistite: interazioni non convenzionali di frammenti molecolari*, and NATO (Brussels) through project CPB.NR.NRCLG 983375. Special thanks go to THERMPHOS International B. V. for supporting this research activity and useful discussions. Thanks are also expressed to COST Action CM0802 (*PhoSciNet*) for financial support.

9. References

(1) (a) Ginsberg, A. P.; Lindsell, W. E.; Silverthorn, W. E. *Trans. Acad. Sci. N. Y.* **1970**, 303. (b) Ginsberg, A. P.; Lindsell, W. E. *J. Am. Chem. Soc.* **1971**, *93*, 2082.

(2) Curiously, the first pnictido complexes ever reported were the cobalt complexes $[Co(CO)_3(cyclo\text{-}As_3)]$, $[Co_2(CO)_6(\mu,\eta^{2:2}\text{-}As_2)]$, and $[\{Co_2(CO)_5(PPh_3)\}(\mu,\eta^{2:2}\text{-}As_3)]$, which contained naked arsenic units as ligands. See: (a) Foust, A. S.; Foster, M. S.; Dahl, L. F. *J. Am. Chem. Soc.* **1969**, *91*, 5631. (b) Foust, A. S.; Foster, M. S.; Dahl, L. F. *J. Am. Chem. Soc.* **1969**, *91*, 5633.

(3) Vizi-Orosz, A.; Pályi, G.; Markó, L. *J. Organomet. Chem.* **1973**, *60*, C25.

(4) Simon, G. L.; Dahl, L. F. *J. Am. Chem. Soc.* **1973**, *95*, 2175.

(5) Dapporto, S.; Midollini, S.; Sacconi, L. *Angew. Chem., Int. Ed. Engl.* **1979**, *18*, 469.

(6) Di Vaira, M.; Ghilardi, C. A.; Midollini, S.; Sacconi, L. *J. Am. Chem. Soc.* **1978**, *100*, 2550.

(7) The Roald Hoffmann's Nobel lecture 1981 on the isolobal concept, "Building Bridges between Inorganic and Organic Chemistry", is available at http://nobelprize.org/nobel_prizes/chemistry/ laureates/ 1981/hoffman-lecture.pdf. See also Hoffmann, R. *Angew. Chem., Int. Ed.* **1982**, *21*, 711.

(8) Scherer, O. J.; Sitzmann, H.; Wolmershäuser, G. *Angew. Chem., Int. Ed. Engl.* **1985**, *24*, 351.

(9) Scherer, O. J.; Brück, T. *Angew. Chem., Int. Ed. Engl.* **1987**, *26*, 59.

(10) Dillon, K. B.; Mathey, F.; Nixon, J. F. *Phosphorus: The Carbon Copy*; Wiley: Chichester, U.K., 1998.

(11) Peruzzini, M.; de los Rios, I.; Romerosa, A.; Vizza, F. *Eur. J. Inorg. Chem.* **2001**, 593.

(12) Peruzzini, M.; Abdreimova, R. R.; Budnikova, Y.; Romerosa, A.; Scherer, O. J.; Sitzmann, H. *J. Organomet. Chem.* **2004**, *689*, 4319.

(13) (a) Scherer, O. J. *Angew. Chem., Int. Ed. Engl.* **1985**, *24*, 924. (b) Scherer, O. J. *Comments Inorg. Chem.* **1987**, *6*, 1. (c) Scherer, O. J. *Angew. Chem., Int. Ed. Engl.* **1990**, *29*, 1104. (d) Scherer, O. J. *Acc. Chem. Res.* **1999**, *32*, 751. (e) Scherer, O. J. *Chem. Unserer Zeit* **2000**, *34*, 374.

(14) (a) Di Vaira, M.; Stoppioni, P.; Peruzzini, M. *Polyhedron* **1987**, *6*, 351. (b) Ehses, M.; Romerosa, A.; Peruzzini, M. *Top. Curr. Chem.* **2002**, *220*, 107. (c) Peruzzini, M.; Gonsalvi, L.; Romerosa, A. *Chem. Soc. Rev.* **2005**, *34*, 1038.

(15) (a) Scheer, M. *Coord. Chem. Rev.* **1997**, *163*, 271. (b) Johnson, B. P.; Balazs, G.; Scheer, M. *Top. Curr. Chem.* **2004**, *232*, 1. (c) Balázs, G.; Gregoriades, L. J.; Scheer, M. *Organometallics* **2007**, *26*, 3058. (d) Johnson, B. P.; Balázs, G.; Scheer, M. *Coord. Chem. Rev.* **2006**, *250*, 1178.

(16) (a) Figueroa, J. S.; Cummins, C. C. *Dalton. Trans.* **2006**, 2161. (b) Cummins, C. C. *Angew. Chem., Int. Ed.* **2006**, *45*, 862. For recent examples of Cummins' contributions to this research field, see also (c) Cossairt, B. M.; Cummins, C. C. *J. Am. Chem. Soc.* **2009**, *131*,

15501, and references therein. (d) Curley, J. J.; Piro, N. A.; Cummins, C. C. *Inorg. Chem.* **2009**, *48*, 9599. (e) Piro, N. A.; Cummins, C. C. *J. Am. Chem. Soc.* **2008**, *130*, 9524. (f) Cossairt, B. M.; Cummins, C. C. *Inorg. Chem.* **2008**, *47*, 9363.
(17) (a) von Schnering, H.-G.; Hönle, W. *Chem. Rev.* **1988**, *88*, 243. (b) Whitmire, K. H. *Adv. Organomet. Chem.* **1998**, *42*, 2. (c) Schlesinger, M. E. *Chem. Rev.* **2002**, *102*, 4267. (d) Milyukov, V. A.; Budnikova, Yu. H.; Sinyashin, O. G. *Russ. Chem. Rev.* **2005**, *74*, 781. (e) Lynam, J. F. *Angew. Chem., Int. Ed.* **2007**, *46*, 2. (f) Dyker, C. A.; Burford, N. *Chem. Asian J.* **2008**, *3*, 28.
(18) (a) Corbridge, D. E. C. *Phosphorus: An Outline of its Chemistry, Biochemistry and Technology*, 5th ed.; Elsevier SA: Amsterdam, NL, 1995. (b) Gleason, W. An Introduction to Phosphorus: History, Production, and Application. *JOM*; **2007**, *59*, http://www.tms.org/pubs/journals/JOM/JOMbyIssue.asp?issue=JOM\2007\June.
(19) (a) Masuda, J. D.; Schöller, W. W.; Donnadieu, B.; Bertrand, G. *Angew. Chem., Int. Ed.* **2007**, *46*, 7052. (b) Masuda, J. D.; Schöller, W. W.; Donnadieu, B.; Bertrand, G. *J. Am. Chem. Soc.* **2007**, *129*, 14180. (c) Back, O.; Kuchenbeiser, G.; Donnadieu, B.; Bertrand, G. *Angew. Chem., Int. Ed.* **2009**, *48*, 5530.
(20) A few examples of f-block elements containing phosphorus units have been described. These include Scherer's thorium complex [{Cp''_2Th}$_2$(*bicycle*-$\mu,\eta^{3:3}$-P_6)], see: Scherer, O. J.; Werner, B.; Heckmann, G.; Wolmershäuser, G. *Angew. Chem., Int. Ed. Engl.* **1991**, *30*, 553. For the recently described samarium derivative, [{Cp^*_2Sm}$_4P_8$], a molecular octaphosphide showing a regular core structure, see: Konchenko, S. N.; Pushkarevsky, N. A.; Gamer, M. T.; Köppe, R.; Schnöckel, H.; Roesky, P. W. *J. Am. Chem. Soc.* **2009**, *131*, 5740.
(21) Strube, A.; Heuser, J.; Huttner, G.; Lang, H. *J. Organomet. Chem.* **1988**, *356*, C9.
(22) Li, Z.; Zhao, C.; Chen, L. *THEOCHEM* **2007**, *810*, 1.
(23) Baudler, M.; Etzbach, T. *Angew. Chem., Int. Ed. Engl.* **1991**, *30*, 580.
(24) Peruzzini, M.; Marvelli, L.; Romerosa, A.; Rossi, A.; Vizza, F.; Zanobini, F. *Eur. J. Inorg. Chem.* **1999**, 931.
(25) Scherer, O. J.; Ehses, M.; Wolmershäuser, G. *J. Organomet. Chem.* **1997**, *531*, 217.
(26) Scherer, O. J.; Ehses, M.; Wolmershäuser, G. *Angew. Chem., Int. Ed.* **1998**, *37*, 507.
(27) Ehses, M.; Schmitt, G.; Wolmershäuser, G.; Scherer, O. J. *Z. Anorg. Allg. Chem.* **1999**, *625*, 382.
(28) Schmitt, G.; Ullrich, D.; Wolmershäuser, G.; Regitz, M.; Scherer, O. J. *Z. Anorg. Allg. Chem.* **1999**, *625*, 702.
(29) Schmid, G.; Kempny, H. P. *Z. Anorg. Allg. Chem.* **1977**, *432*, 160.
(30) Scheer, M.; Dargatz, M.; Schenzel, K.; Jones, P. G. *J. Organomet. Chem.* **1992**, *435*, 123.
(31) de los Ríos, I.; Hamon, J.-R.; Hamon, P.; Lapinte, C.; Toupet, L.; Romerosa, A.; Peruzzini, M. *Angew. Chem., Int. Ed. Engl.* **2001**, *40*, 3910.
(32) Lorenzo Luis, P.; de los Ríos, I.; Peruzzini, M. *Phosphorus Res. Bull.* **2001**, *12*, 167.
(33) Scherer, O. J.; Schwarz, G.; Wolmershäuser, G. *Z. Anorg. Allg. Chem.* **1996**, *622*, 951.
(34) Jutzi, P.; Opiela, S. *J. Organomet. Chem.* **1992**, *431*, C29.
(35) Weber, L.; Sonnenberg, U. *Chem. Ber.* **1991**, *124*, 725.
(36) Brück, T. Ph.D. Thesis, Universität Kaiserslautern, Germany, 1989.
(37) Scherer, O. J.; Hilt, T.; Wolmershäuser, G. *Organometallics* **1998**, *17*, 4110.
(38) Eichhorn, C.; Scherer, O. J.; Sögding, T.; Wolmershäuser, G. *Angew. Chem., Int. Ed. Engl.* **2001**, *40*, 2859.
(39) Scherer, O. J.; Hilt, T.; Wolmershäuser, G. *Angew. Chem., Int. Ed. Engl.* **2000**, *39*, 1425.
(40) Pfitzner, A. *Angew. Chem., Int. Ed. Engl.* **2006**, *45*, 699.
(41) Barr, M. E.; Adams, B. R.; Weller, R. R.; Dahl, L. F. *J. Am. Chem. Soc.* **1991**, *113*, 3052.
(42) The violet allotrope of phosphorus (Hittorf's phosphorus) contains alternating P_8 and P_9 units held together by chelating P_2 junctions. See: (a) Thurn, H.; Krebs, H. *Angew. Chem., Int. Ed. Engl.* **1966**, *5*, 1047. (b) Thurn, H.; Krebs, H. *Acta Crystallogr.* **1969**, *B25*, 125.
(43) Baudler, M.; Koll, B.; Adamek, C.; Gleiter, R. *Angew. Chem., Int. Ed. Engl.* **1987**, *26*, 347. (a) Baudler, M.; Arndt, V. *Z. Naturforsch.* **1984**, *B39*, 275.
(44) Baudler, M.; Standeke, H.; Borgardt, M.; Strabel, H.; Dobbers, J. *Naturwissenschaften* **1966**, *53*, 106.
(45) (a) Mathey, F. *Coord. Chem. Rev.* **1994**, *137*, 1. (b) Nixon, J. H. *Coord. Chem. Rev.* **1995**, *145*, 201. (c) Mathey, F. *Angew. Chem., Int. Ed. Engl.* **2003**, *42*, 1578.
(46) Maigrot, N.; Avarvari, N.; Charrier, C.; Mathey, F. *Angew. Chem.* **1995**, *107*, 623. Angew. Chem., Int. Ed. Engl. 1995, *34*, 590.
(47) (a) Müller, C.; Bartsch, R.; Fischer, A.; Jones, P. G.; Schmutzler, R. *J. Organomet. Chem.* **1996**, *512*, 141. (b) Bartsch, R.; Hitchcock, P. B.; Nixon, J. F. *J. Organomet. Chem.* **1988**, *340*, C37. (c) Bartsch, R.; Hichcock, P. B.; Nixon, J. F. *J. Chem. Soc., Chem. Commun.* **1987**, 1146. (d) Müller, C.; Bartsch, R.; Fischer, A.; Jones, P. G. *J. Organomet. Chem.* **1993**, *453*, C16.
(48) Scheer, M.; Deng, S.; Scherer, O. J.; Sierka, M. *Angew. Chem., Int. Ed.* **2005**, *44*, 3755.
(49) Ahlrichs, R.; Fenske, D.; Fromm, K.; Krautscheid, H.; Krautscheid, U.; Treutler, O. *Chem.—Eur. J.* **1996**, *2*, 238.
(50) Bianchini, C.; Meli, A.; Di Vaira, M.; Sacconi, L. *Inorg. Chem.* **1981**, *20*, 1169.
(51) For a review on triple-decker *cyclo*-triphosphorus complexes, see: Di Vaira, M.; Sacconi, L. *Angew. Chem., Int. Engl. Ed.* **1982**, *21*, 130.
(52) Barr, M. E.; Dahl, L. F. *Organometallics* **1991**, *10*, 3991.
(53) Mal, P.; Breiner, B.; Rissanen, K.; Nitschke, J. R. *Science* **2009**, *324*, 1697.
(54) Mal, P.; Schultz, D.; Beyeh, K.; Rissanen, K.; Nitschke, J. R. *Angew. Chem., Int. Ed.* **2008**, *47*, 8297.
(55) Baudler, M. *Angew. Chem., Int. Ed. Engl.* **1987**, *26*, 419.
(56) Baudler, M.; Duester, D.; Ouzounis, D. *Z. Anorg. Allg. Chem.* **1987**, *544*, 87.
(57) Baudler, M.; Akpapoglou, S.; Ouzounis, D.; Wasgestian, F.; Meinigke, B.; Budzikiewicz, H.; Muenster, H. *Angew. Chem., Int. Ed. Engl.* **1988**, *27*, 280.
(58) (a) Miluykov, V.; Sinyashin, O. Russ. Patent 200106504/12 (006673). (b) Miluykov, V.; Kataev, A. V.; Sinyashin, O.; Hey-Hawkins, E. *Russ. Chem. Bull. Int. Ed.* **2006**, *55*, 1297.
(59) Scherer, O. J.; Schwalb, J.; Wolmershäuser, G.; Kaim, W.; Gross, R. *Angew. Chem., Int. Ed. Engl.* **1986**, *25*, 363.
(60) Scherer, O. J.; Brück, T.; Wolmershäuser, G. *Chem. Ber.* **1988**, *121*, 935.
(61) In the experimental part of ref 83, it has been briefly mentioned that prolonged reflux (3 h) in a higher boiling solvent like decalin followed by chromatographic work-up could increase significantly the yield of **14** to ca. 60%.
(62) Dielmann, F.; Merkle, R.; Heinl, S.; Scheer, M. *Z. Naturforsch.* **2009**, *64B*, 3.
(63) The volatility of **14** is confirmed by the observation that it can be purified by sublimation (90−110 °C/0.01 Torr) as green needles. See ref 9.
(64) Blom, R.; Brück, T.; Scherer, O. J. *Acta Chem. Scand.* **1989**, *43*, 458.
(65) (a) Chamizo, J. A.; Ruiz-Mazon, M.; Salcedo, R.; Toscano, R. A. *Inorg. Chem.* **1990**, *29*, 879. (b) Kerins, M. C.; Fitzpatrick, N. J.; Nguyen, M. T. *Polyhedron* **1989**, *8*, 1135.
(66) Frunkze, J.; Lein, M.; Frenking, G. *Organometallics* **2002**, *21*, 3351.
(67) Urnezius, E.; Brenessel, W. W.; Cramer, C. J.; Ellis, J. E.; Schleyer, P. R. *Science* **2002**, *295*, 832.
(68) Miluykov, V.; Sinyashin, O.; Scherer, O. J.; Hey-Hawkins, E. *Mendeleev Commun.* **2002**, *12*, 1.
(69) Miluykov, V.; Sinyashin, O.; Lönnecke, P.; Hey-Hawkins, E. *Mendeleev Commun.* **2003**, *13*, 212.
(70) Scheer, M.; Friedrich, G.; Schuster, K. *Angew. Chem., Int. Ed. Engl.* **1993**, *32*, 593.
(71) Scheer, M.; Schuster, K.; Krug, A.; Hartung, H. *Chem. Ber.* **1997**, *130*, 1299. The versatility of [$Cr(CO)_5(PCl_3)$] as starting material for phosphorus-rich P_x species has been confirmed by the synthesis of molybdenum derivatives containing *cyclo*-P_3 and $\mu,\eta^{2:2}$-P_2 ligands by reaction with suitable K[$Cp^RMo(CO)_3$].
(72) Winter, R. F.; Geiger, W. E. *Organometallics* **1999**, *18*, 1827.
(73) Scherer, O. J.; Brück, T.; Wolmershäuser, G. *Chem. Ber.* **1989**, *122*, 2049.
(74) Callaghan, C. S. J.; Hitchcock, P. B.; Nixon, J. F. *J. Organomet. Chem.* **1999**, *584*, 87.
(75) Deng, S.; Schwarzmaier, C.; Zabel, M.; Nixon, J. F.; Timoshkin, A. Y.; Scheer, M. *Organometallics* **2009**, *28*, 1075, and references therein.
(76) (a) Kudinov, A. R.; Loginov, D. A.; Starikova, Z. A.; Petrovskii, P. V.; Corsini, M.; Zanello, P. *Eur. J. Inorg. Chem.* **2002**, 3018.
(77) For a review of the stacking reactions to synthesize triple-decker complexes, see: Kudinov, A. R.; Rybinskaya, M. I. *Russ. Chem. Bull.* **1999**, *48*, 1615.
(78) Kudinov, A. R.; Petrovskii, P. V.; Rybinskaya, M. I. *Russ. Chem. Bull.* **1999**, *48*, 1362.
(79) Rink, B.; Scherer, O. J.; Heckmann, G.; Wolmershäuser, G. *Chem. Ber.* **1992**, *125*, 1011.
(80) Rink, B.; Scherer, O. J.; Wolmershäuser, G. *Chem. Ber.* **1995**, *128*, 71.
(81) Koch, B.; Scherer, O. J.; Wolmershäuser, G. *Z. Anorg. Allg. Chem.* **2000**, *626*, 1797.
(82) Scherer, O. J.; Kemény, G.; Wolmershäuser, G. *Chem. Ber.* **1995**, *128*, 1145.
(83) Detzel, M.; Mohr, T.; Scherer, O. J.; Wolmershäuser, G. *Angew. Chem., Int. Ed. Engl.* **1994**, *33*, 1110.

(84) Scherer, O. J.; Winter, R. T.; Wolmershäuser, G. *J. Chem. Soc., Chem. Commun.* **1993**, 313.
(85) Scherer, O. J.; Mohr, T.; Wolmershäuser, G. *J. Organomet. Chem.* **1997**, *529*, 379.
(86) Detzel, M.; Friedrich, G.; Scherer, O. J.; Wolmershäuser, G. *Angew. Chem., Int. Ed. Engl.* **1995**, *34*, 1321.
(87) Hofmann, C.; Scherer, O. J.; Wolmershäuser, G. *J. Organomet. Chem.* **1998**, *559*, 219.
(88) Scherer, O. J.; Weigel, S.; Wolmershäuser, G. *Chem.—Eur. J.* **1998**, *4*, 1910.
(89) Scherer, O. J.; Weigel, S.; Wolmershäuser, G. *Angew. Chem., Int. Ed. Engl.* **1999**, *38*, 3688.
(90) Another example for stabilization of PO is the nickel−tungsten complex $[\{Cp^RNi\}_2\{W(CO)_4\}(\mu_3\text{-}PO)_2]$ (**314**, see section 5.1): Scherer, O. J.; Braun, J.; Walther, P.; Heckmann, G.; Wolmershäuser, G. *Angew. Chem., Int. Ed. Engl.* **1991**, *30*, 852.
(91) (a) Mielke, Z.; McCluskey, M.; Andrews, L. *Chem. Phys. Lett.* **1990**, *165*, 146. (b) McCluskey, M.; Andrews, L. *J. Phys. Chem.* **1991**, *95*, 2988.
(92) Jarrett-Sprague, I.; Hillier, H.; Gould, I. R. *Chem. Phys.* **1990**, *140*, 27.
(93) Bai, J.; Virovets, A. V.; Scheer, M. *Angew. Chem., Int. Ed. Engl.* **2002**, *41*, 1737.
(94) The first 1D coordination polymer ever reported was based on the Mo_2P_2 tetrahedrane unit, see: Bai, J.; Leiner, E.; Scheer, M. *Angew. Chem., Int. Ed. Engl.* **2002**, *41*, 783.
(95) Krossing, I. *Chem.—Eur. J.* **2001**, *7*, 490.
(96) Scheer, M.; Gregoriades, L. J.; Virovets, A.; Kunz, W.; Neueder, R.; Krossing, I. *Angew. Chem., Int. Ed.* **2006**, *45*, 5689.
(97) Deng, S.; Schwarzmaier, C.; Vogel, U.; Zabel, M.; Nixon, J. F.; Scheer, M. *Eur. J. Inorg. Chem.* **2008**, 4870.
(98) Bai, J.; Virovets, A. V.; Scheer, M. *Science* **2003**, *300*, 781.
(99) Scheer, M.; Bai, J.; Johnson, B. P.; Merkle, R.; Virovets, A. V.; Anson, C. E. *Eur. J. Inorg. Chem.* **2005**, 4023.
(100) The inclusion of a molecule of **14** into the inner cavity of the *inorganic fullerene* **110** was suggested by ^{31}P CP-MAS NMR experiments, but could not be substantiated by X-ray diffraction analysis. See refs 98 and 99.
(101) Scheer, M.; Schindler, A.; Merkle, R.; Johnson, B. P.; Linseis, M.; Winter, R.; Anson, C. E.; Virovets, A. V. *J. Am. Chem. Soc.* **2007**, *129*, 13386.
(102) Scheer, M.; Schindler, A.; Gröger, C.; Virovets, A. V.; Peresypkina, E. V. *Angew. Chem., Int. Ed. Engl.* **2009**, *48*, 5046. For recent reviews about the formation of supramolecular assemblies based on P_n-ligands, see: Scheer, M.; Gregoriades, L.; Laurence, J.; Merkle, R.; Johnson, B. P.; Dielmann, F. *Phosphorus, Sulfur Silicon* **2008**, *183*, 504. Scheer, M. *Dalton Trans.* **2008**, 4372.
(103) (a) Fritz, G.; Schneider, H. W.; Hoenle, W.; von Schnering, H. G. *Z. Anorg. Allg. Chem.* **1990**, *584*, 21. (b) Fritz, G.; Schneider, H. W.; Hoenle, W.; von Schnering, H. G. *Z. Anorg. Allg. Chem.* **1990**, *585*, 51.
(104) Peruzzini, M.; Mañas, S.; Romerosa, A.; Vacca, A. *Mendeleev Commun.* **2000**, *10*, 134.
(105) Di Vaira, M.; Frediani, P.; Seniori Costantini, S.; Peruzzini, M.; Stoppioni, P. *Dalton Trans.* **2005**, 2234.
(106) Di Vaira, M.; Peruzzini, M.; Seniori Costantini, S.; Stoppioni, P. *J. Organomet. Chem.* **2006**, *691*, 3931.
(107) Compound **123** was independently prepared, see: Nagaraja, C. M.; Nethaji, M.; Jagirdar, B. R. *Inorg. Chem.* **2005**, *44*, 4145.
(108) Akbayeva, D. N.; Di Vaira, M.; Seniori Costantini, S.; Peruzzini, M.; Stoppioni, P. *Dalton Trans.* **2006**, 389.
(109) Sokolov, M. N.; Hernández-Molina, R.; Clegg, W.; Fedin, V. P.; Mederos, A. *Chem. Commun.* **2003**, 140.
(110) Sokolov, M. N.; Virovets, A. V.; Dybtsev, D. N.; Chubarova, E. V.; Fedin, V. P.; Fenske, D. *Inorg. Chem.* **2001**, *40*, 4816.
(111) Barbaro, P.; Di Vaira, M.; Peruzzini, M.; Seniori Costantini, S.; Stoppioni, P. *Chem.—Eur. J.* **2007**, *13*, 6682.
(112) Baudler, M. *Chem. Rev.* **1994**, *94*, 1273.
(113) Barbaro, P.; Di Vaira, M.; Peruzzini, M.; Seniori Costantini, S.; Stoppioni, P. *Angew. Chem., Int. Ed. Engl.* **2008**, *47*, 4425.
(114) A species having the same formula P_5H_5O of **133** was detected by mass spectrometry analyzing the mixture from the hydrolysis of calcium phosphide, see: Baudler, M.; Staendecke, H.; Dobbers, J.; Borgardt, M.; Strabel, H. *Naturwissenschaften* **1966**, *53*, 251.
(115) Barbaro, P.; Di Vaira, M.; Peruzzini, M.; Seniori Costantini, S.; Stoppioni, P. *Inorg. Chem.* **2009**, *48*, 1091.
(116) Wang, W.; Enright, G. D.; Carty, A. R. *J. Am. Chem. Soc.* **1997**, *119*, 12370.
(117) Corrigan, J. F.; Doherty, S.; Taylor, N. J.; Carty, A. J. *J. Am. Chem. Soc.* **1994**, *116*, 9799.
(118) Caporali, M.; Di Vaira, M.; Peruzzini, M.; Seniori Costantini, S.; Stoppioni, P.; Zanobini, F. *Eur. J. Inorg. Chem.* **2010**, 152–158.
(119) Cecconi, F.; Dapporto, P.; Midollini, S.; Sacconi, L. *Inorg. Chem.* **1978**, *17*, 3292.
(120) (a) Di Vaira, M.; Peruzzini, M.; Stoppioni, P. *J. Chem. Soc., Chem. Commun.* **1982**, 894. (b) Di Vaira, M.; Peruzzini, M.; Stoppioni, P. *J. Chem. Soc., Dalton Trans.* **1984**, 359.
(121) Di Vaira, M.; Midollini, S.; Sacconi, L. *J. Am. Chem. Soc.* **1979**, *101*, 1757.
(122) The dinuclear CoNi species **151** can be also prepared by the straightforward reaction of $[(triphos)Ni(\eta^3\text{-}cyclo\text{-}P_3)]^+$ in THF/EtOH with Co^{2+} hydrated salts and triphos.
(123) Mealli, C.; Costanzo, F.; Ienco, A.; Perez-Carreño, E.; Peruzzini, M. *Inorg. Chim. Acta* **1998**, *275/276*, 366.
(124) Fabbrizzi, L.; Sacconi, L. *Inorg. Chim. Acta* **1979**, *36*, L407.
(125) Bianchini, C.; Di Vaira, M.; Meli, A.; Sacconi, L. *Angew. Chem., Int. Ed. Engl.* **1980**, *19*, 405.
(126) Bianchini, C.; Di Vaira, M.; Meli, A.; Sacconi, L. *J. Am. Chem. Soc.* **1981**, *103*, 1448.
(127) Di Vaira, M.; Sacconi, L.; Stoppioni, P. *J. Organomet. Chem.* **1983**, *250*, 183.
(128) (a) Midollini, S.; Orlandini, A.; Sacconi, L. *Angew. Chem., Int. Ed. Engl.* **1979**, *18*, 81. (b) Ghilardi, C. A.; Midollini, S.; Orlandini, A.; Sacconi, L. *Inorg. Chem.* **1980**, *19*, 301.
(129) Plastas, H. J.; Stewart, J. M.; Grim, S. O. *Inorg. Chem.* **1973**, *12*, 265.
(130) Mealli, C.; Midollini, S.; Moneti, S.; Sacconi, L. *Cryst. Struct. Commun.* **1980**, *9*, 1017.
(131) Di Vaira, M.; Eshes, M. P.; Stoppioni, P.; Peruzzini, M. *Inorg. Chem.* **2000**, *39*, 2199.
(132) Cecconi, F.; Ghilardi, C. A.; Midollini, S.; Orlandini, A. *J. Chem. Soc., Chem. Commun* **1982**, 229.
(133) Di Vaira, M.; Ehses, M. P.; Peruzzini, M.; Stoppioni, P. *Polyhedron* **1999**, *18*, 2331.
(134) Di Vaira, M.; Stoppioni, P.; Peruzzini, M. *J. Chem. Soc., Dalton Trans.* **1990**, 109.
(135) Capozzi, G.; Chiti, L.; Di Vaira, M.; Peruzzini, M.; Stoppioni, P. *J. Chem. Soc., Chem. Commun* **1986**, 1799.
(136) Barth, A.; Huttner, G.; Fritz, M.; Zsolnai, L. *Angew. Chem., Int. Ed. Engl.* **1990**, *29*, 929.
(137) Di Vaira, M.; Stoppioni, P.; Midollini, S.; Laschi, F.; Zanello, P. *Polyhedron* **1991**, *10*, 2123.
(138) Di Vaira, M.; Stoppioni, P. *C. R. Chimie* **2005**, *8*, 1535.
(139) Di Vaira, M.; Stoppioni, P. *Polyhedron* **1994**, *13*, 3045.
(140) Di Vaira, M.; Ehses, M. P.; Peruzzini, M.; Stoppioni, P. *Eur. J. Inorg. Chem.* **2000**, 2193.
(141) Cecconi, F.; Ghilardi, C. A.; Midollini, S.; Orlandini, A. *J. Am. Chem. Soc.* **1984**, *106*, 3667.
(142) Cecconi, F.; Ghilardi, C. A.; Midollini, S.; Orlandini, A. *Inorg. Chem.* **1986**, *25*, 1766.
(143) Caporali, M.; Barbaro, P.; Gonsalvi, L.; Ienco, A.; Yakhvarov, D.; Peruzzini, M. *Angew. Chem., Int. Ed.* **2008**, *47*, 3766.
(144) Vizi-Orosz, A. *J. Organomet. Chem.* **1976**, *111*, 61.
(145) Vizi-Orosz, A.; Galamb, V.; Pályi, G.; Markó, L. *J. Organomet. Chem.* **1981**, *216*, 105.
(146) Campana, C. F.; Vizi-Orosz, A.; Pályi, G.; Markó, L.; Dahl, L. F. *Inorg. Chem.* **1979**, *18*, 3054.
(147) (a) Maxwell, L. R.; Hendricks, S. R.; Mosley, V. M. *J. Chem. Phys.* **1935**, *3*, 699. (b) Interatomic distances. Spec. Publ. Chem. Soc. 1965, No. 18.
(148) Douglas, A. E.; Rao, K. S. *Can. J. Phys.* **1958**, *36*, 565.
(149) Vizi-Orosz, A.; Galamb, V.; Pályi, G.; Markó, L.; Boese, R.; Schmid, G. *J. Organomet. Chem.* **1985**, *288*, 179.
(150) Lang, H.; Huttner, G.; Sigwarth, B.; Jibril, I.; Zsolnai, L.; Orama, O. *J. Organomet. Chem.* **1986**, *304*, 137.
(151) Scherer, O. J.; Swarowsky, M.; Wolmershäuser, G. *Organometallics* **1989**, *8*, 841.
(152) Bjarnason, A.; Des Enfants, R. E., II; Barr, M. E.; Dahl, L. F. *Organometallics* **1990**, *9*, 657.
(153) Scheer, M.; Becker, U.; Huffman, J. C.; Chisholm, M. H. *J. Organomet. Chem.* **1993**, *461*, C1.
(154) Scheer, M.; Troitzsch, C.; Jones, P. G. *Angew. Chem., Int. Ed. Engl.* **1992**, *31*, 1377.
(155) Scheer, M.; Becker, U. *Phosphorus, Sulfur Silicon* **1994**, *93−94*, 391.
(156) Scheer, M.; Becker, U.; Chisholm, M. H.; Huffman, J. C.; Lemoigno, F.; Eisenstein, O. *Inorg. Chem.* **1995**, *34*, 3117.
(157) Scheer, M.; Becker, U. *J. Organomet. Chem.* **1997**, *545−546*, 451.
(158) Scherer, O. J.; Berg, G.; Wolmershäuser, G. *Chem. Ber.* **1995**, *128*, 635.
(159) Friederich, G.; Scherer, O. J.; Wolmershäuser, G. *Z. Anorg. Allg. Chem.* **1996**, *622*, 1478.
(160) Scherer, O. J.; Berg, G.; Wolmershäuser, G. *Chem. Ber.* **1996**, *129*, 53.
(161) Scherer, O. J.; Höbel, B.; Wolmershäuser, G. *Angew. Chem., Int. Ed. Engl.* **1992**, *31*, 1027.

(162) Scherer, O. J.; Völmecke, T.; Wolmershäuser, G. *Eur. J. Inorg. Chem.* **1999**, 945.
(163) Weigel, S.; Wolmershäuser, G.; Scherer, O. J. *Z. Anorg. Allg. Chem.* **1998**, *624*, 559.
(164) Complex **224** obtained initially by cothermolysis of of [Cp″Co(CO)$_2$] with complex [Cp*Fe(η^5-P$_5$)] (**14**) may be better prepared by the thermal reaction of [Cp″Co(μ-CO)]$_2$ with white phosphorus in boiling decalin (see ref 168). The known clusters [{Cp″Co(μ_3-P)}$_4$] (**222**) and [{Cp″Co(μ,$\eta^{2:2}$-P$_2$)}$_2$] (**211**) (see Schemes 68 and 37) are also formed in the reaction.
(165) Scherer, O. J.; Weigel, S.; Wolmershäuser, G. *Heteroatom Chem.* **1999**, *10*, 622.
(166) For the reaction of Li$_3$P$_7$·DME with [CpFe(CO)$_2$Br] see ref 103. The reaction gave the trinuclear cluster [{CpFe(CO)$_2$}$_3$P$_7$] (**114**, see section 3.3).
(167) The reaction of P$_7$(SiMe$_3$)$_3$ with Co(BF$_4$)$_2$ and triphos in refluxing THF/EtOH mixture was briefly studied to give [(triphos)Co(η^3-*cyclo*-P$_3$)] (**44**). See: Peruzzini, M.; Stoppioni, P. *J. Organomet. Chem.* **1985**, *288*, C44.
(168) Scherer, O. J.; Pfeiffer, K.; Heckmann, G.; Wolmershäuser, G. *J. Organomet. Chem.* **1992**, *425*, 141.
(169) Scheer, M.; Vogel, U.; Becker, U.; Balazs, G.; Scheer, P.; Hönle, C.; Becker, M.; Jansen, M. *Eur. J. Inorg. Chem.* **2005**, 135.
(170) (a) Lang, H.; Zsolnai, L.; Huttner, G. *Angew. Chem. Suppl.* **1983**, 1463. (b) De Lal, R.; Vahrenkamp, H. *Z. Naturforsch.* **1985**, *40B*, 1250.
(171) Scheer, M.; Hermann, E.; Sieler, J.; Oehme, M. *Angew. Chem., Int. Ed. Engl.* **1991**, *30*, 969.
(172) Lindsell, W. E. *J. Chem. Soc., Chem. Commun.* **1982**, 1422.
(173) (a) Lindsell, W. E.; McCullough, K. J.; Welch, A. J. *J. Am. Chem. Soc.* **1983**, *105*, 4487. (b) Ginsberg, A. P.; Lindsell, W. E.; McCullough, K. J.; Sprinkle, C. R.; Welch, A. J. *J. Am. Chem. Soc.* **1986**, *108*, 403.
(174) Krossing, I.; van Wüllen, L. *Chem.—Eur. J.* **2002**, *8*, 700.
(175) Bianchini, C.; Mealli, C.; Meli, A.; Sacconi, L. *Inorg. Chim. Acta* **1979**, *37*, L543.
(176) Barbaro, P.; Di Vaira, M.; Peruzzini, M.; Seniori Costantini, S.; Stoppioni, P. *Eur. J. Inorg. Chem.* **2005**, 1360.
(177) Peruzzini, M.; Ramirez, J. A.; Vizza, F. *Angew. Chem., Int. Ed. Engl.* **1998**, *37*, 2255.
(178) Barbaro, P.; Peruzzini, M.; Ramirez, J. A.; Vizza, F. *Organometallics* **1999**, *18*, 4237.
(179) Barbaro, P.; Ienco, A.; Mealli, C.; Peruzzini, M.; Scherer, O. J.; Schmitt, G.; Vizza, F.; Wolmershäuser, G. *Chem.—Eur. J.* **2003**, *9*, 5195.
(180) Barbaro, P.; Caporali, M.; Ienco, A.; Mealli, C.; Peruzzini, M.; Vizza, F. *Eur. J. Inorg. Chem.* **2008**, 1392.
(181) Scherer, O. J.; Swarowsky, M.; Swarowsky, H.; Wolmershäuser, G. *Angew. Chem., Int. Ed. Engl.* **1988**, *27*, 694.
(182) Scherer, O. J.; Swarowsky, M.; Wolmershäuser, G. *Angew. Chem., Int. Ed. Engl.* **1988**, *27*, 405.
(183) Goh, L. Y.; Wong, R. C. S.; Sinn, E. *J. Chem. Soc., Chem. Commun.* **1990**, 1484.
(184) (a) Scheer, M.; Becker, U. *Phosphorus, Sulfur Silicon* **1994**, *93*−*94*, 257. (b) Scheer, M.; Schuster, K.; Becker, U. *Phosphorus, Sulfur Silicon* **1996**, *109*−*110*, 141.
(185) Scheer, M.; Troitzsch, C.; Hilfert, L.; Dargatz, M.; Kleinpeter, E.; Jones, P. G.; Sieler, J. *Chem. Ber.* **1995**, *128*, 251.
(186) (a) Cecconi, F.; Ghilardi, C. A.; Midollini, S.; Orlandini, A. *Angew. Chem., Int. Ed. Engl.* **1983**, *22*, 554. (b) Cecconi, F.; Ghilardi, C. A.; Midollini, S.; Orlandini, A. *Angew. Chem. Suppl.* **1983**, 718.
(187) Scheer, M.; Becker, U.; Matern, E. *Chem. Ber.* **1996**, *129*, 721.
(188) Yakhvarov, D.; Barbaro, P.; Gonsalvi, L.; Mañas Carpio, S.; Midollini, S.; Orlandini, A.; Peruzzini, M.; Sinyashin, O.; Zanobini, F. *Angew. Chem., Int. Ed.* **2006**, *45*, 4182.
(189) Yakhvarov, D.; Peruzzini, M.; Caporali, M.; Gonsalvi, L.; Midollini, S.; Orlandini, A.; Ganushevich, Y.; Sinyashin, O. *Phosphorus, Sulfur Silicon* **2008**, *183*, 487.
(190) Caporali, M.; Barbaro, P.; Bolaño, S.; Gonsalvi, L.; Mañas Carpio, S.; Peruzzini, M. *Magn. Reson. Chem.* **2008**, *46*, S120.
(191) Kruck, T.; Sylvester, G.; Kunau, I. P. *Z. Naturforsch.* **1973**, *28B*, 38.
(192) Di Vaira, M.; Peruzzini, M.; Stoppioni, P. *Acta Crystallogr.* **1983**, *C39*, 1210.
(193) For a nice example of diphosphene coupling, see: Jones, R. A.; Seeberger, M. H.; Whittlesey, B. R. *J. Am. Chem. Soc.* **1985**, *107*, 6424.
(194) Schäfer, H.; Binder, D.; Fenske, D. *Angew. Chem., Int. Ed.* **1985**, *24*, 522.
(195) Scherer, O. J.; Dave, T.; Braun, J.; Wolmershäuser, G. *J. Organomet. Chem.* **1988**, *350*, C21.
(196) Scherer, O. J.; Braun, J.; Wolmerhäuser, G. *Chem. Ber.* **1990**, *123*, 471.
(197) Scherer, O. J.; Braun, J.; Walther, P.; Wolmershäuser, G. *Chem. Ber.* **1992**, *125*, 2661.
(198) Scheer, M.; Becker, U. *Chem. Ber.* **1996**, *129*, 1307.
(199) Herrmann, W. A. *Angew. Chem., Int. Ed.* **1991**, *30*, 818.
(200) Bailer, J. C., Emelus, H. I., Nyholin, R., Trotman-Dichenson, A. F., Eds. *Comprehensive Inorganic Chemistry*, Vol. 2; Pergamon Press: Oxford, U.K., 1973.
(201) Charles, S.; Fettinger, J. C.; Bott, S. G.; Eichhorn, B. W. *J. Am. Chem. Soc.* **1996**, *118*, 4713.
(202) Some examples: (a) Shu, Y.; Oyama, S. T. *Chem. Commun.* **2005**, 1143. (b) Brock, S. L.; Perera, S. C.; Stamm, K. L. *Chem.—Eur. J.* **2004**, *10*, 3364. (c) Oyama, S. T. *J. Catal.* **2003**, *216*, 343.
(203) Su, H. L.; Xie, Y.; Li, B.; Liu, X. M.; Qian, Y. T. *Solid State Ionics* **1999**, *122*, 157.
(204) Liu, S.; Liu, X.; Xu, L.; Qian, Y.; Ma, X. *J. Cryst. Growth* **2007**, *304*, 427.
(205) Carenco, S.; Resa, I.; Le Goff, X.; Le Floch, P.; Mézailles, N. *Chem. Commun.* **2008**, 2568.
(206) Barry, B. M.; Gillan, E. G. *Chem. Mater.* **2008**, *20*, 2618.
(207) Li, J.; Ni, Y.; Liao, K.; Hong, S.-K. *J. Colloid Interface Sci.* **2009**, *332*, 231.
(208) (a) Kargin, Y. M.; Budnikova, Y. H.; Martynov, B. I.; Turygin, V. V.; Tomilov, A. P. *J. Electroanal. Chem.* **2001**, *507*, 157. (b) Yakhvarov, D. G.; Budnikova, Y. H.; Tazeev, D. I.; Sinyashin, O. G. *Russ. Chem. B* **2002**, *51*, 2059. (c) Yakhvarov, D. G.; Budnikova, Y. G.; Sinyashin, O. G. *Russ. J. Electrochem.* **2003**, *39*, 1261. (d) Budnikova, Y. H.; Kafiyatullina, A. G.; Balueva, A. S.; Kuznetsov, R. M.; Morozov, V. I.; Sinyashin, O. G. *Russ. Chem. B* **2003**, *52*, 2419. (e) Budnikova, Y. G.; Tazeev, D. I.; Kafiyatullina, A. G.; Yakhvarov, D. G.; Morozov, V. I.; Gusarova, N. K.; Trofimov, B. A.; Sinyashin, O. G. *Russ. Chem. B* **2005**, *54*, 942.
(209) Miluykov, V.; Kataev, A.; Sinyashin, O.; Lonnecke, P.; Hey-Hawkins, E. *Organometallics* **2005**, *24*, 2233.
(210) Dapporto, P.; Sacconi, L.; Stoppioni, P.; Zanobini, F. *Inorg. Chem.* **1981**, *20*, 3834.
(211) Belykh, L. B.; Skripov, N. I.; Belonogova, L. N.; Umanets, V. A.; Shmidt, F. K. *Russ. J. Appl. Chem.* **2007**, *80*, 1523.
(212) Scheer, M.; Herrmann, E. *Z. Chem.* **1990**, *30*, 41.
(213) Scheer, M.; Dargatz, M.; Rufinska, A. *J. Organomet. Chem.* **1992**, *440*, 327.
(214) Piro, N. A.; Cummins, C. C. *Inorg. Chem.* **2007**, *46*, 7387.
(215) Piro, N.; Figueroa, J. S.; McKellar, J. T.; Cummins, C. C. *Science* **2006**, *313*, 1276.
(216) Schäfer, H.; Binder, D. *Z. Anorg. Allg. Chem.* **1988**, *560*, 65.
(217) Santiso-Quiñones, G.; Reisinger, A.; Slattery, J.; Krossing, I. *Chem. Commun.* **2007**, 5046.
(218) Tai, H.-C.; Krossing, I.; Seth, M.; Deubel, D. V. *Organometallics* **2004**, *23*, 2343.
(219) Akbayeva, D.; Scherer, O. J. *Z. Anorg. Allg. Chem.* **2001**, *627*, 1429.
(220) (a) Pfitzner, A. *Chem.—Eur. J.* **2000**, *6*, 1891. (b) Pfitzner, A.; Reiser, S.; Nilges, T. *Angew. Chem., Int. Ed.* **2000**, *39*, 4160. (c) Reiser, S.; Brunklaus, G.; Hong, H. J.; Chan, J. C. C.; Eckert, H.; Pfitzner, A. *Chem.—Eur. J.* **2002**, *8*, 4228.
(221) Möller, M. H.; Jeitschko, W. J. *J. Solid State Chem.* **1986**, *65*, 178.
(222) Pfitzner, A.; Freudenthaler, E. *Angew. Chem., Int. Ed. Engl.* **1995**, *34*, 1647.
(223) Pfitzner, A.; Freudenthaler, E. *Z. Naturforsch.* **1997**, *B52*, 199.
(224) Pfitzner, A.; Bräu, M. F.; Zweck, J.; Brunklaus, G.; Eckert, H. *Angew. Chem., Int. Ed.* **2004**, *43*, 4228.
(225) Fisher, K.; Dance, I. *J. Chem. Soc., Dalton Trans.* **1997**, 2381.
(226) Some examples are: (a) *BaCuP* : Mewis, A. *Z. Naturforsch., B* **1979**, *34*, 1373. (b) Dünner, J.; Mewis, A. *J. Less-Common Metals* **1990**, *167*, 127. (c) Pilchowsky, I.; Mewis, A.; Wenzel, M.; Gruehn, R. *Z. Anorg. Allg. Chem.* **1990**, *588*, 109. (d) Dünner, J.; Mewis, A. *J. Alloys Compd.* **1995**, *221*, 65.
(227) Young, D. M.; Charlton, J.; Olmstead, M. M.; Kauzlarich, S. M.; Lee, C.-S.; Miller, G. J. *Inorg. Chem.* **1997**, *36*, 2539.
(228) Krossing, I. *J. Am. Chem. Soc.* **2001**, *123*, 4603.
(229) Deubel, D. V. *J. Am. Chem. Soc.* **2002**, *124*, 12312.
(230) Bihlmeier, A.; Gonsior, M.; Raabe, I.; Trapp, N.; Krossing, I. *Chem.—Eur. J.* **2004**, *10*, 5041.
(231) Gonsior, M.; Krossing, I.; Müller, L.; Raabe, I.; Jansen, M.; van Wüllen, L. *Chem.—Eur. J.* **2002**, *8*, 4475.
(232) Gregoriades, L. J.; Wegley, B. K.; Sierka, M.; Brunner, E.; Gröger, C.; Peresypkina, E. V.; Virovets, A. V.; Zabel, M.; Scheer, M. *Chem. Asian J.* **2009**, *4*, 1578.
(233) Schmidbaur, H.; Beruda, H.; Zeller, E. *Phosporus, Sulfur Silicon* **1994**, *87*, 245.

CR900349U